The
GEOLOGICAL BULLETIN
of the
PUNJAB UNIVERSITY

Number 43 *2008*

CONTENTS

Geol. Bull. Punjab Univ. 43, 2008.

SHALLOW SHELF SEDIMENTATION OF THE JURASSIC SAMANA SUK LIMESTONE, KALA CHITTA RANGE, LESSER HIMALAYAS, PAKISTAN

BY

KALEEM AKHTAR QURESHI
Department of Botany, University of the Punjab, Quaid-e-Azam Campus, Lahore-54590, Pakistan
E-mail: mkaleemakhter@yahoo.com

SHAHID GHAZI AND AFTAB AHMAD BUTT
Institute of Geology, University of the Punjab, Quaid-e-Azam Campus,
Lahore-54590, Pakistan.

Abstract: -*Detailed sedimentological studies of the Samana Suk Limestone (type section Samana Suk Peak, Samana Range, Pakistan) have been carried out from the Kala Chitta Range, Pakistan as the first comprehensive contribution of its kind. Two lithologs from Surg and Chapra have been extensively studied to elaborate the sedimentological details. The stratigraphic name refers to the Upper Triassic to Liassic Kioto Limestone of earlier literature, which has now been differentiated into the Triassic Mianwali Formation, the Chak Jabbi Limestone, the Kingriali Formation and the Jurassic Datta Formation, and the Samana Suk Limestone.*

The Samana Suk Limestone is well-bedded limestone and can be identified in the field into oyster bearing beds, micritic beds, shelly limestone composed of gastropods and pelecypods, sandy limestone and the oolitic limestone. These observations are indicative of shallow shelf deposits. The microscopic studies have identified most common microfacies into the mudstone (micritic facies), bioclastic wackestone, packstone where the skeletal elements are the oysters, gastropods and the pelecypods, while the grainstone is non skeletal represented by the oolitic grains. Apart from the microfacies analysis, the diagenetic imprints have also been elucidated. All these features also substantiate its shallow shelf sedimentation. In other words, it represents a carbonate platform deposition.

INTRODUCTION

The Kala Chitta Range is a part of the foreland-fold and thrust belt, which forms the northern border of the adjoining hydrocarbon bearing Potwar Basin (Fig. 1)

The stratigraphic name Samana Suk Limestone was introduced by Davies (1930) for his Upper Jurassic Limestone Unit from the Samana Range, the type locality being Samana Suk Peak in the Samana Range.

In the Kala Chitta Range, this formation formed part of the Upper Triassic – Liassic Kioto Limestone of Cotter (1933) which is now formalized by the Stratigraphic Committee of Pakistan (Fatmi, 1973) into the Triassic Mianwali Formation, the Chak Jabbi Limestone and the Kingriali Formation, the Lower Jurassic bauxite bearing Datta Formation and the Middle Jurassic Samana Suk Limestone. This terminology has also been extended to the Salt Range, Potwar and the Hazara Mountains of northern Pakistan.

The Samana Suk Limestone comprises thin to thick-bedded limestone, dolomitic limestones and dolomites alternating with marls and marlstone. Occasional sandy limestone beds are also present. Cyclic or rhythmic bedding has also been observed.

The Samana Suk Limestone is light grey, yellowish grey, olive grey to grayish orange in colour. The weathering colour is usually medium dark grey to grayish brown. These are predominantly bioclasts bearing wackestone to packstone or pure lime mudstone (the calcisiltites). However, peloidal, oolitic and intraclastic packstone and grainstone are also commonly repeated. The individual bed varies in thickness from 3 cm to 30 cm. However, thick

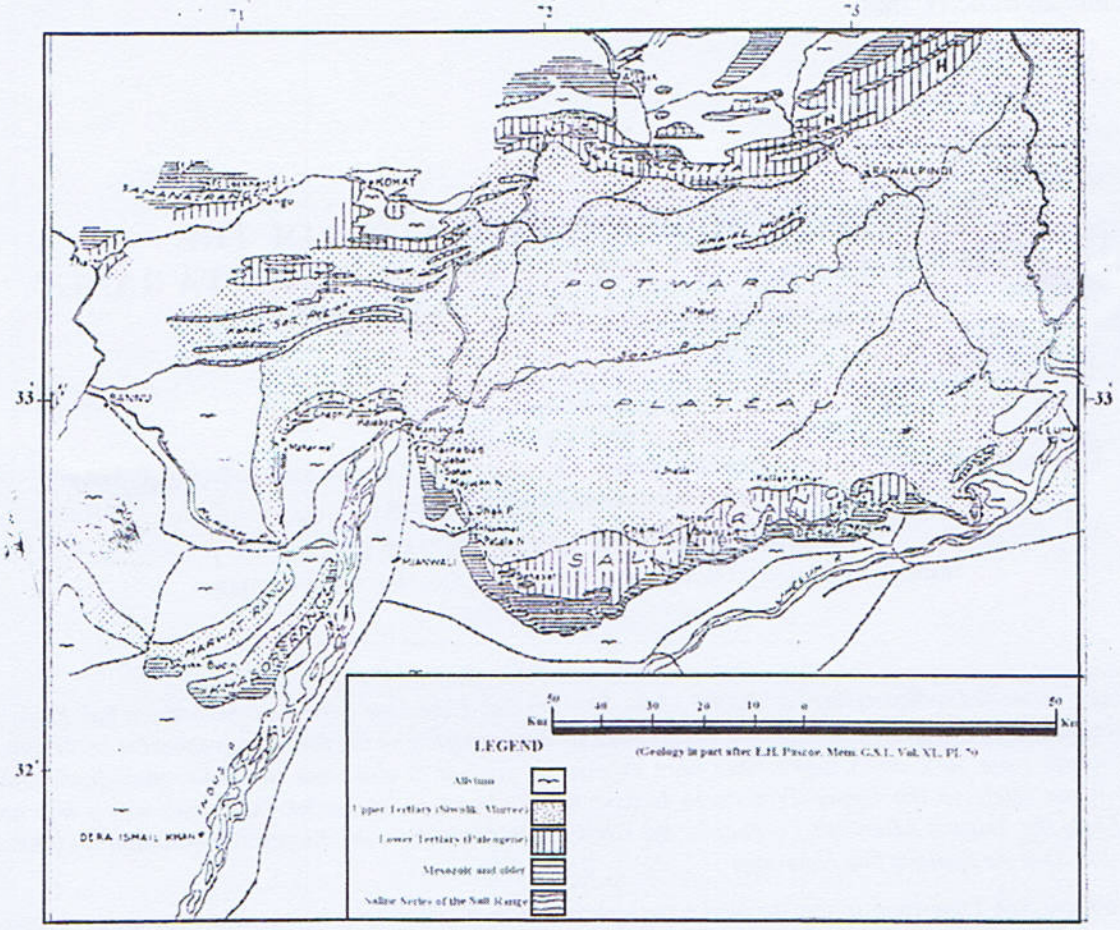

Fig. 1. Location map of the Kala Chitta and Samana Ranges (after Davies and Pinfold,1937)

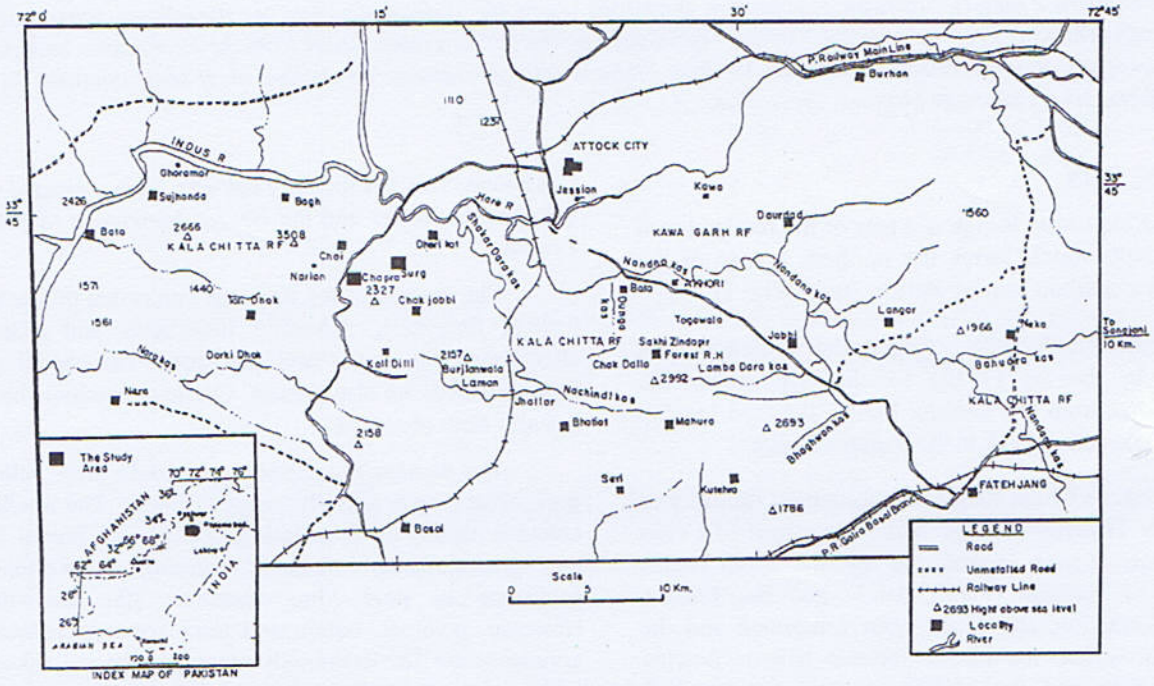

Fig. 2. Location map of the study area of Surg and Chapra Kala Chitta Range.

beds (over 50-cm thickness) are also frequent. Massive beds (over 2 meter thickness) are not uncommon especially in the upper part of the formation.

The marls are usually compact, nodular, yellowish grey to light grayish yellow and vary in thickness from 5 cm to 1 meter. The marls being soft are mostly squeezed between compact limestone beds. In the upper part of the formation, well developed marlstone zone of 25 meters thickness (125 meters above the base of the formation) in Surg section and of 12 meters thickness (130 meters above the base) at Chapra Section are found.

Dolomitization of varying intensity has been observed at various levels in the formation and has been described in detail. Troughs cross bedding and parallel lamination, flaser bedding, ripple marks and bioturbation are common sedimentary structures observed in the field. Stylolitization is also very frequently present.

The lower contact with the underlying Datta Formation is gradational, whereas the upper contact with the overlying Chichali Formation is unconformable. Apart from the skolithos type burrows and residual lateretized film over the top surface of the Samana Suk Limestone, the presence of abrupt and non gradational change from limestone to pyritic, glauconitic sandstone and shale accompanied with limestone clasts at shale-limesotne interface, the irregular topography of the limestone surface and small scale banking of shale against such relief are the strong evidences of the erosional upper surface of the Samana Suk Limestone.

The Mesozoic succession of the Kala Chitta Range as formalized by the Stratigraphic Committee of Pakistan (Fatmi, 1973) has been tabulated here as follows.

	Nomenclature of the Stratigraphic Committee of Pakistan (Fatmi 1973)	**Nomenclature after Cotter (1933)**
Upper Paleocene	Lockhart Limestone (Thanetian) Sequence Boundary (Absence of Maastrichtian-Danian)	Hill Limestone
Upper Cretaceous	Kawagarh Formation (Coniacian to Campanian) Sequence Boundary (Absence of Cenomanian-Turonian)	Kawagarh shales
Lower Cretaceous	Lumshiwal Formation	Giumal sandstone
Upper Jurassic	Chichali Formation Sequence Boundary (Latritic Crust)	Spiti shale
Middle Jurassic	Samana Suk Limestone	Kioti Limestone
Lower Jurassic	Datta Formation	Ferruginous beds in the kiotos
Triassic	Kingriali Formation Chak Jabbi Limestone Mianwali Formation	Kioto Limestone

Base n[illegible]osed by virtue of the Thrust Fault

Detailed sedimentological and digenetic framework of Chapra and Surg (Fig. 2) have been carried out as the first comprehensive research of this kind. Various microfacies have been illustrated (Plates 1-3) Two lithologs of Chapra and Surg (Figs. 3-4) are presented here.

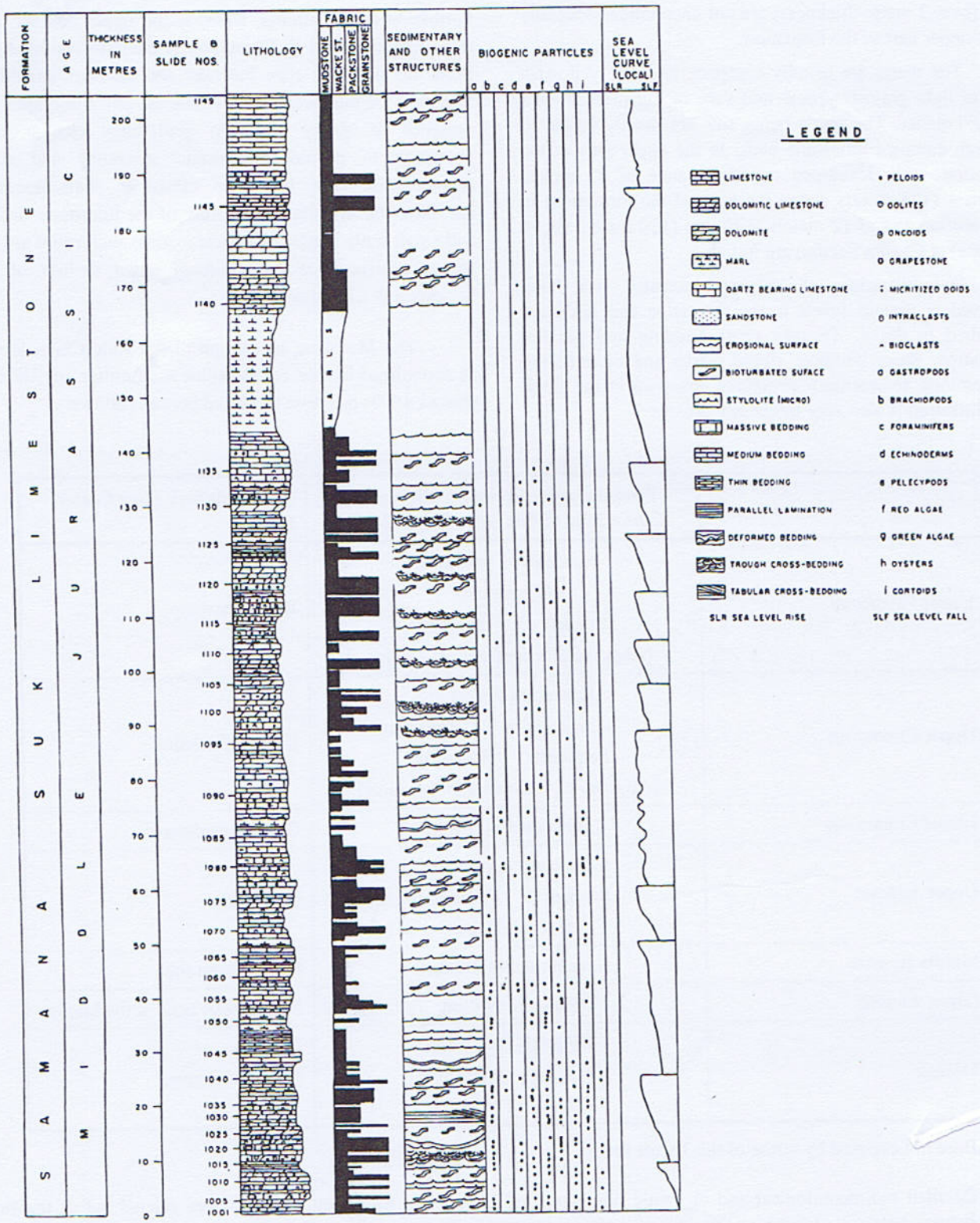

Fig. 3.. Lithostratigraphic section of the Samana Suk Limestone at Surg, Kala Chitta Range.

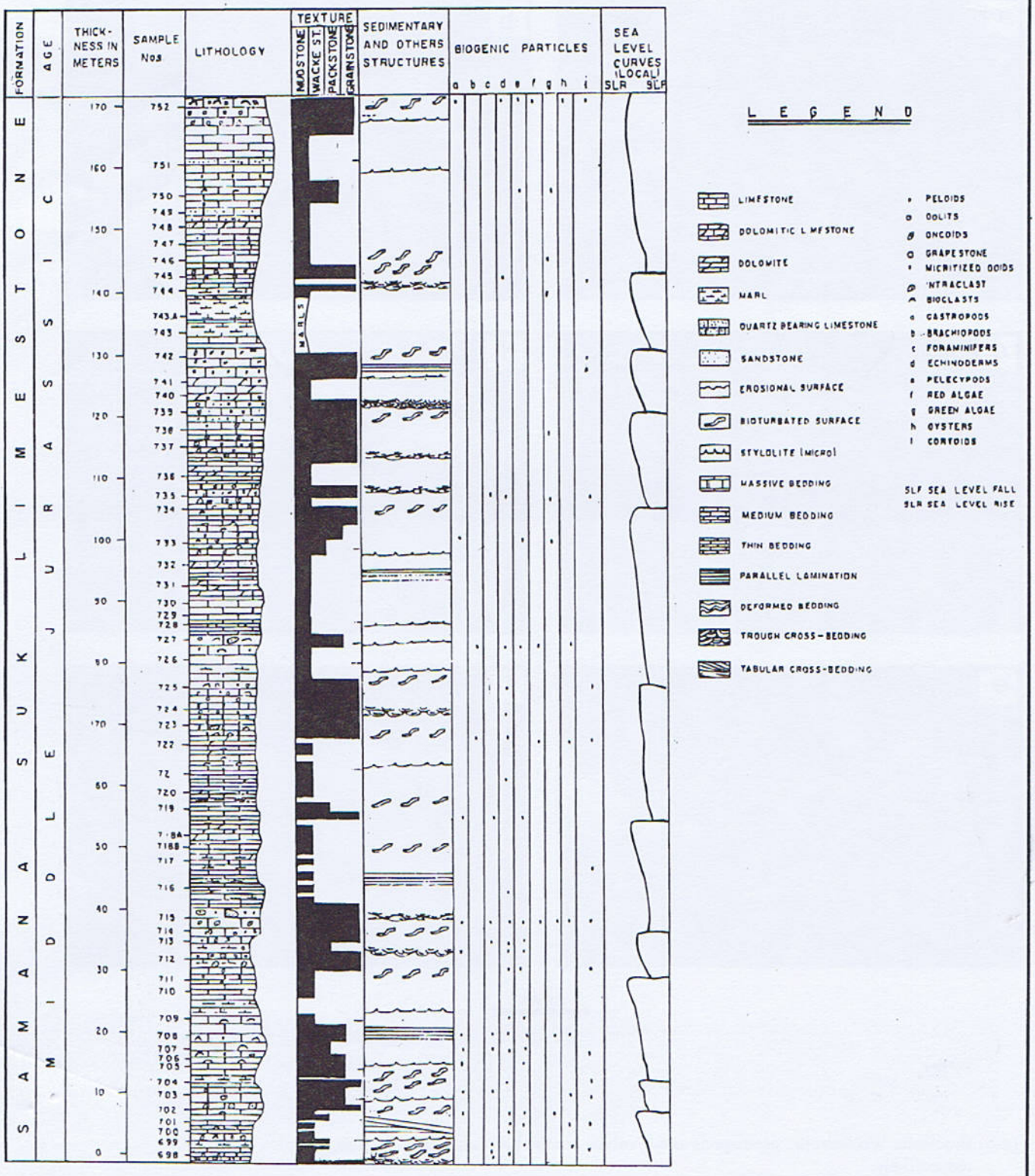

Fig. 4. Lithostratigraphic section of the Samana Suk Limestone at Chapra, Kala Chitta Range.

PLATE 1

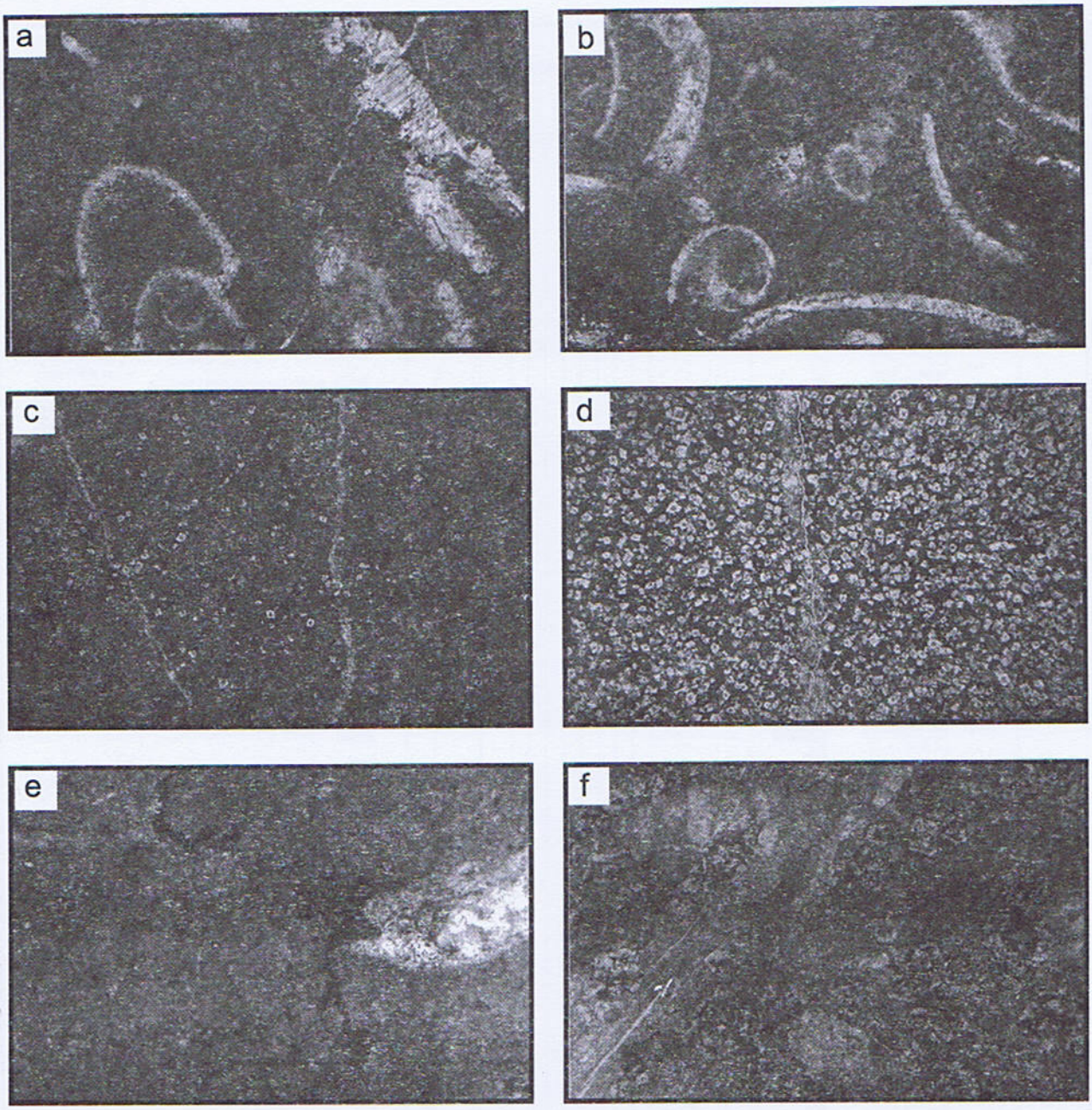

(a-b) Bioclastic Wackestone. gastropods and bivalves are the bioclasts. Surg Section, samples 1050, 1005 respectively.
(c-d) Dolomicrite. scattered small sized (c) and closely packed small sized dolomite crystals (d). Surg Section, samples 1121, 1093 respectively.
(e) Mudstone showing high amplitude stylolite. Surg Section, sample 1090

PLATE 2

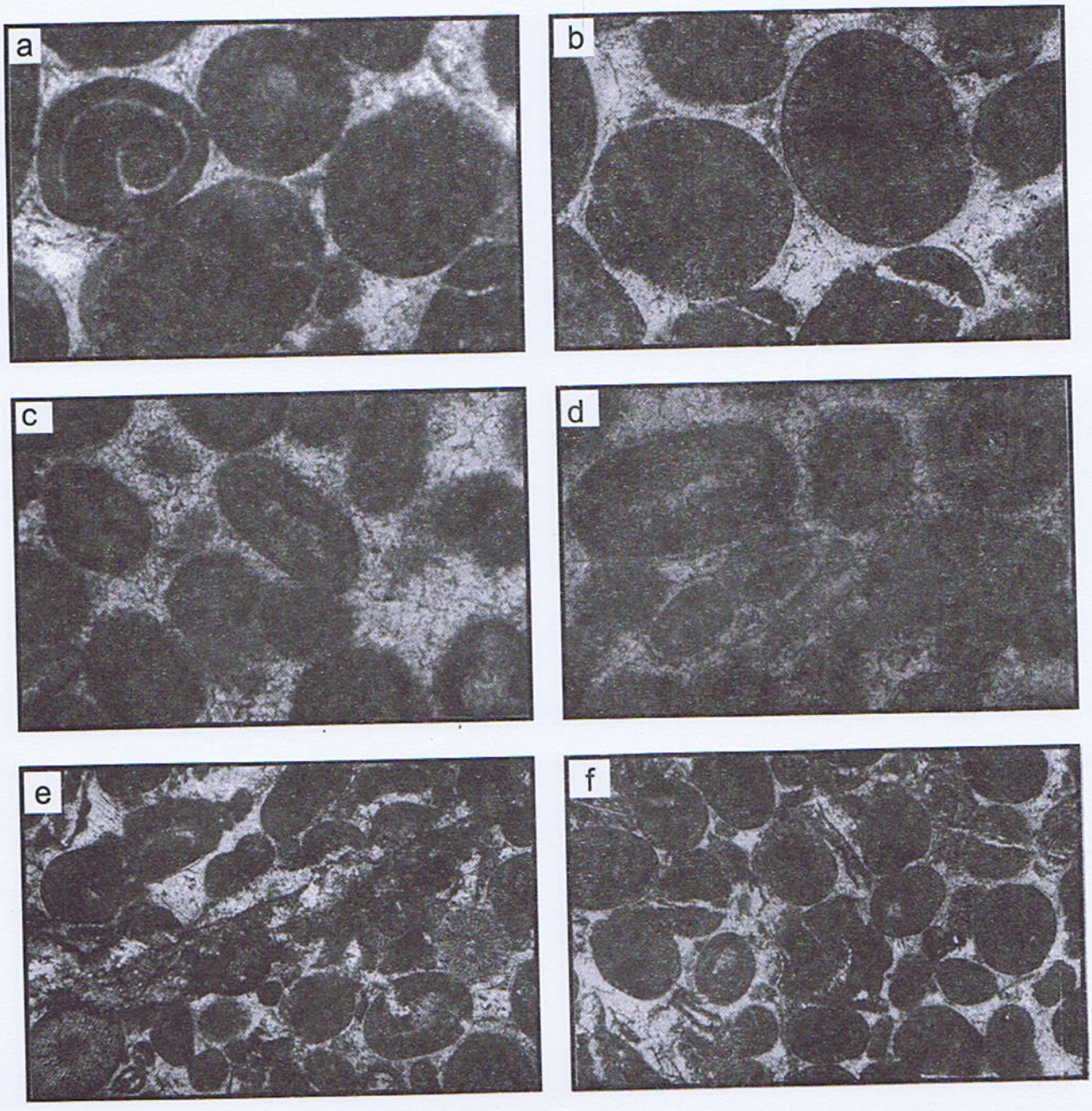

(a-f) Oolitic Grainstone.
(a) a gastropod shell forming the nucleus in the ooid. Surg Section, sample 1128
(b) Ooids showing columnar cement. Surg Section, sample 1017
(c) stretched ooids. a molluscan shell seen in the centre (d) Chapra Section, sample 737
(e) Echinoderms grains, one in the right extremity and the other at the bottom left corner. Surg Section, sample 1017
(f) Spar filled fracture in few ooids, one even extending into the echinodetm grain upper right corner Surg Section, sample 1017

PLATE 3

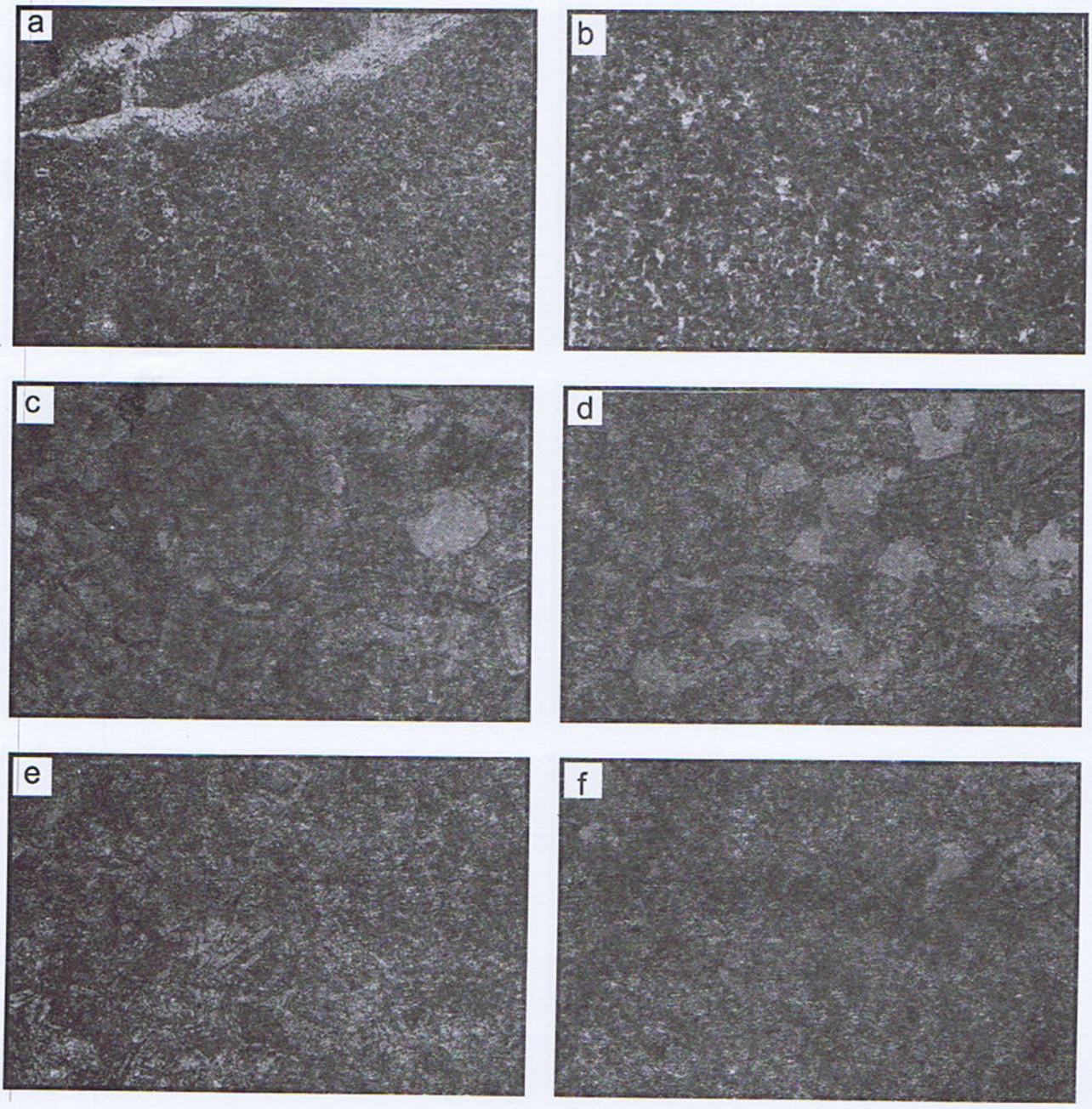

(a-b) Peloidal Grainstone. Surg Section, samples 1097, 1094 respectively
(c) Dolospar showing large size dolomite crystals. Surg Section, sample 1111
(d) Dolospar showing large size dolomite crystals. Surg Section, sample 1129 The voids are the result of plucking During the thin Section preparation
(e) Dolospar showing zoned dolomite crystals. Chapra Section, sample 740
(f) Calcitization of the Dolospar. Surg Section, sample 1023

DIAGENETIC FEATURES

A series of diagenetic events were recognised within the Samana Suk Limestone, which described below.

Micritic Envelopes

The micritization of grains by endolithic algae and fungi is commonly observed in the Samana Suk Limestone. In this process the bioclasts are altered by boring around the grain margin and holes filled by fine-grained sediment or cement. If the activity is intense the grain is completely micritized. The micritic envelopes are generally associated with the packstones/grainstones. Furthermore, where the mineralogy was originally aragonitic, the fragment/shell is more susceptible to the formation of the micritic envelopes than if it were calcitic. However, there are evidences of 0-micritic envelope formation where the fragment was originally calcite.

Cements

The precipitation of the cements in the carbonate rocks is a major diagenetic process and takes place when pore fluids are supersaturated with respect to cement phase and there is no kinetic factor inhibiting the precipitation (Sandberg, 1985). The cements are reasonably good indicators of the diagenetic events. However, on the other hand a similar type of cement can be precipitated in different diagenetic environment. The cements types distinguished in the Samana Suk Limestone at Surg and Chapra sections are as follows:

Circumgranular Cements

a. Isopachus acicular fibrous cement: When the nucleation sites on the grain surface are many and the crystals are fine needles like growing at right angle to the surface. This isopachus acicular fibrous cement might be of marine origin and is found just above the middle part of the Samana Suk Limestone.

b. Columnar or bladed cement Cleaved crystals growing at right angle to the grain margin: The fibrous nature of these cements is the main criterion for their possible formation in marine phreatic zone, which refers to warm shallow seas (less than 100 m) with sediments in which all pores are filled by marine waters. Marine aragonite cement is typically present as fibrous crystals and the textures depend upon the nature of substrate, nature of vugs and rate of crystallization (Tucker and Wright 1992)

Intergranular Cements

The intergranular calcite spar is characterized by crystal sizes generally larger than 10 micron and by light coloured translucent crystals, in plane polarized light.

a. The drusy calcite spar: The sparry calcite cement with drusy mosaic constitutes spar crystals filling a cavity or void. The size of the crystals increase towards the centre of the cavity. This mosaic is called drusy mosaic and is characteristic of meteoric phreatic environments, but may also continue into burial environments.

b. Equant spar: When the equicrystalline mosaics of spar or the size of the crystal remains almost constant the fabric is termed as equant spar equicrystalline mosaic. The equant cement may be related to burial phreatic or meteoric phreatic environments when it does not surround the particle. However, the circumgranular equant cement might be related to the meteoric phreatic environments (Tucker and Wright, 1992).

c. Ferroan calcite spar: The calcite spar containing ferrous iron is considered to be probably precipitation in the phreatic zone where the interstitial waters has low Eh. (Tucker and Wright, 1992). The vadose waters are oxidizing and most iron is present in ferric form, which does not substitute for calcium.

d. Syntaxiaal overgrowth cement: These are developed as an overgrowth on existing grains within a sediment, in many places growing in optical continuity of the grain or the substrate usually abundant on echinoderms. These cements are interpreted to be of meteoric origin in burial environments (Walker, 1990). This cement is repeatedly found on the echinoderms grains in many horizons of the Samana Suk Limestone.

e. Poikilotopic cement: These are also disconformable cements in which crystal grow from few nucleation points on the grain and enclose the grain. These are interpreted as precipitated in burial environments that postdate pervasive dolomitization and intergranular cements.

Texture preserving dolomitization

The texture preserving non-mimic dolomitization is restricted to matrix and is commonly seen throughout the Samana Suk Limestone. This dolomitization where increased, becomes texture destroying and only minor original features are visible.

HARD GROUND SURFACES

Prominent hard ground surfaces have been observed, in the Samana Suk Limestone, Kala Chitta Range. Each surface marks the culmination of a local depositional cycle caused by regression. According to Bathurst (1986), "A limestone bed is regarded as hard ground if its upper surface has been bored, corroded or eroded (by abrasion). If encrusting or other sessile organisms are attached to the surface and/or if the clasts or pebbles derived from a bed occur in the overlying sediment". Other features which have been recognized from various parts of the world (Garrison and Fisher, 1969; Flugel, 1982; Tucker and Wright 1992) include impregnation by glauconite and phosphate, iron or manganese salts. Commonly the upper surface of hard ground coincides with paleontological non-sequence.

A hardground surface represents an early lithification and consolidation before the deposition of the overlying sediment (Purser, 1969). Various features confirming hardground surfaces in the Samana Suk Formation are as under:

Field observations: The presence of hardground surfaces has been observed in the field. The important features observed include:

Cyclic thick bedded peloidal/aggregate grain/lithoclastic or ooids bearing packstone/grainstone with bored, corroded or iron leached surfaces invariably marking the top underlain by thin bedded argillaceous lime mudstones and thicker middle unit of peloidal bioclastic wackestone/packstone.

Surfaces having ferruginous pits, spots and films on uneven beds.

Bioturbated and burrowed beds, burrows filled by secondary yellow coloured dolomitized material forming patchy look.

Oyster encrusted surfaces repeatedly present in the formation marking the hard lithified substrate for the oyster to attach.

Hardground surfaces followed by reworked intraclasts bearing horizons. These intraclastic horizons just over hardground suggest a transgressive phase during which the rudstone broken by storm current have been incorporated in the over lying fine sediment.

COMPACTION

Due to progressive increase in the overburden, the sediments in the Samana Suk Limestone are subjected to compaction. Both mechanical compaction and chemical compaction has been observed, resulting into fracturing and stylolitisation. These are described as under:

a. Mechanical compaction: More overburden pressure resulted in denser confirguration the sediments resulting into point, planer and interfering grain contacts. Shelter porosity is created when a larger grain forms bridge between smaller grains. Increased overburden pressure results in the destruction of shelter porosity by brittle fracture. Several phases of fracturing with one or more episode of calcite fracture fill can be observed in the Samana Suk Limestone.

b. Chemical Compaction: According to Tucker (1990) the chemical compaction takes place in two ways (i) is an uncemented sediment by dissolution at isolated stressed grain to grain contact, (ii) within cemented sediment by dissolution being concentrated along a particular surface, usually irregular, termed as stylolite. The dissolutioning of grain contacts due to chemical compaction has commonly been observed in the Samana Suk Limestone. Progressive solution compaction leads to alteration of grain to grain contacts from original point contact to interfering or sutured contacts.

STYLOLITES

A variety of stylolites and stylocumulates have been observed in the Samana Suk Limestone, representing dissolution within cemented sediments along a particular surface. High peak stylolite horse tail stylolite and stylocumulate horse tail stylolite and stylocumulate have been observed during the thin section study. These solution seams also represent considerable amount of dissolutioning in the subsurface and may locally source cementation, lessening the permeability of the zone surrounding the solution seams (Park and Schot, 1968). Various phases of chemical compaction has been observed as calcite filled vein being cut by younger veins and stylolites. There appear to be two distinct periods of stylolitization. Firstly, the stylolitization prior to dolomitization, thus resulting into stylocumulate. In the post-dolomitization phase the stylolites are cutting the dolomite crystals. The stylolite may act as barriers to fluid migration or when have little insoluble residue and high amplitude may become pathways of preferential fluid migration that may later be filled by cements.

EXTENSIVE DOLOMITIZATION

Extensively dolomitized limestones and dolomite beds are frequently present within the Samana Suk Limestone and a large variety of modes of crystallization have been observed during thin section study. Evidences of both early and late stage dolomitizations are present. In general at least two (may be more) phases of dolomitization have been established from the close association of zones and unzones dolomite crystal in some individual samples.

The various dolomite fabric and facies observed are described as under:

a. Dolomicrite: It is fine grained dolomite that resulted from the dolomitization of micrite which provide nucleation point for the development of scattered or closely packed euhedral dolomite crystals. The dolomitization is not intense enough to completely recrystallize the rock rather the original fabric of the limestone is still easily recognized. In some cases the small subhedral-anhedral dolomite crystals have haphazardly affected the bioclasts and the matrix. The dolomite crystal size is essentially less than 20 Um.

a. Dolospar: This facies is composed of brownish yellow to pinkish coloured dolomites beds in the Samana Suk Limestone. These are composed of 90 – 100% large size dolomite rhombohedron. The crystals are in every case more than 20 Um in size. The facies commonly exhibits porphyrotopic texture with large crystals surrounded by small crystals. Poikilotopic texture is also present in the

facies. Other components including bioclasts, lithoclast constitute less than 5% of the rock.

The following four types of dolospar are recognizable in the Samana Suk Limestone. Oolospar with scrosic mosaic: These have euhedral dolomite rhombs with a porous mosaic.

Dolospar with xenotopic mosaic: These dolomites have large size anhydral dolomite crystals with curved inter-crystalline boundaries.

Dolospar with hypidiotopic masaic: The dolomite crystals with subhedral rhombs constitute this facies. The inter-crystalline boundaries are planer and in most of the cases, the crystals are cloudy and unzones.

Dolospar with idiotopic mosaic: Dolospar with euhedral dolomite crystals texture.

Gregg and Sibley (1984) experimentally showed that in the occurrence of xenotopic and idiotopic dolomite mosaics, the temperature at which the crystals were growing was the major factor. At low temperatures a smooth crystal surface is energetically favoured so that crystal mosaics consists of euhedral-subhedral crystals, whereas above a critical roughening temperature (CRT) a rough surface is favoured leading to mosaic of anhedral crystals. Some idiotopic texture can form at high temperature where crystals grow into cavities or are affected by impurities such as clay and aragonite matter.

In addition to temperature affecting dolomite textur, the saturation stage of dolomitizing fluid also plays an important role. Where saturation rate in high then dolomitization is likely to be persvasive and all components, whatever their mineralogy and crystal size will be replaced. Where it is low only more susceptible components (aragonite, high Mg-calcite and finely crystalline low Mg-calcite) will be dolomitized.

Dedolomitization

When calcite spar replaces dolomite rhombs, the process is termed as dedolomitization or more accurately as calcitization. In the Samana Suk Limestone calcitization has been frequently observed. In some cases moulds and relics of dolomite rhombs are identifiable, whereas in others fabric destruction takes place.

COMPARISON WITH OTHER AREAS

Trans Indus Range

Mensink et al. (1991) measured and described Jurassic sequence and facies from localities in the Trans Indus Range (Lat. 32°55′; Long. 71°10′). A total of nine microfacies have been described in the Shinawari/Samana Suk Limestone. The details of the section is as follows:

Facies of the Jurassic rocks in the Surghar Range (Mensink et al., 1991)

Chichali Formation (Upper Oxfordian to Valanginian)	Glauconitic sandstone facies
----------Disconformity ----------	
Samanak Suk Limesotne (Middle Jurassic)	• Palletal sparitic limestone facies • Pelletal limestone facies • Micrite facies • Bioclastic-pelletal limestone facies • Biogenic-Pelletal limestone facies • Oolithic limestone facies • Intraclastic limestone facies • Sandy limestone facies • Fe oolithic limestone facies
Datta Formation (Lower Jurassic)	• Sandstone facies
----------Gradational contact ----------	
Kingriali Formation (Triassic)	• Dolomite facies

The paleoenvironments during the deposition of the Shinawari/Samana Suk Limesotne are interpreted as to be ranging between carbonate platform phase to open marine subtidal phase in the upper part with a number of internal cycles punctuated by various firm grounds/hard grounds and mud cracks of local interest.

Hazara

Sangargali Section (Latitude 34°12′50″; Long. 73°19′).

A section of the Samana Suk Limestone in the vicinity of Sangargali area, District Abbottabad, Hazara has

been recently studied and described (Sheikh et al. 2001, Qureshi et al. 1997, Masood, 1989). A total of fourteen microfacies types have been identified. These include seven oosparitic (or ooidal grainstone) four lime-mudstones, one cortoid bearing biosparite (or bioclastic grainstone) one lag unit and one oncoid bearing oosparite (or the oncoidal-ooidal grainstone). A number of diagenetic cements including acicular, bladed, equant granular, drusy, syntaxial overgrowth has been observed and are interpreted to be formed in meteoric-phreatic environments. Dolomitization and dedolomitization is significantly seen and include unzoned and zoned dolomite crystals. The depositional environments are interpreted to range from facies zofne 6 to facies zone 9 of the middle shelf environments as explained by Wilson (1975).

The abundance of ooidal horizon in the Samana Suk Limestone at Sangargali and the presence of sandy limestone and intraclastic grainstone in the Surghar Range show more shallower body of water with high energy conditions at both sites as compared with the Samana Suk Limesotne at Kala Chitta Range where the dominance of pure lime mudstone and aggregate grain/graphestone bearing packstones/grainstone indicates common prevalence of more restricted and relatively low energy environments.

Balochistan: In the Balochistan Basin, the equivalent rocks are named as the Chiltan Limestone and Zidi Formation. The microfacies analyses from these areas are not available; thus it is not possible to draw precise environmental inferences from these areas. In general, however, shallow marine shelf environments are considered to be prevailing during the deposition of Jurassic sequences in those areas (Fatmi, 1986; Bender and Raza, 1995).

DIAGENETIC HISTORY

The presence of micritic envelopes and circumgranular acicular cements suggest an early phase of marine diagenesis. The presence of early diagenesis is also supported by the occurrence of peloids produced by the complete micritization of the skeletal partices and non-skeletal grains. Following the burial, the meteoric fluids lead to the formation of syntaxial overgrowth cements on echinoid/crinoids grains in the grainstones. This was followed by the precipitation of outer zones of zoned dolomite crystals and also the poikilotopic cements.

The late diagenetic features including the formation of fractures, might be related to the uplift as a result of weathering and erosion following a break in deposition and also afterwards due to tectonic overburdening resulting from the emplacement of various thrust sheets. Some sparry cements postdate the fractures. The dolomitization was probably the last phase of the diagenesis.

DEPOSITIONAL ENVIRONMENT

The Jurassic marine transgression reached Kala Chitta Range area during early Toarican with the deposition of *Bauleiceras* bearing transgressive beds of sandy limestones. The presence of concentric ooids with quartz grains constituting the core in the basal beds of the Samana Suk Limestone at Chapra Section indicates the presence of extensive terrigenous (sand) material on the shore face which served as the rolling nucleus for the precipitation of calcium carbonate ring during the advent of the early currents.

In the studied sections, the biogenic particles are frequent and diverse in the lower part, less common in the middle and sparse to completely absent in the upper part of the Samana Suk Limestone. The biogenic particles are dominated by echinoderm with substantial amount of pelecypods, gastropods, benthic foraminiferas brachiopods and oysters shell. Variety of red and green algae has also been recorded at various levels in both the sections. The abundances of organisms in the lower part and scarcity to total absence in the upper part suggests that initially the conditions were more conducive and favourable for life which include open marine, well oxygenated water with normal salinity. During the later part of its depositional history, however, more varied and changing conditions prevailed creating stress environment for the organisms to survive, these conditions may include waters with restricted circulations and higher to variable salinities, such conditions may exist in cut off ponds and protected shelf lagoons.

The ooidal grainstones are surprisingly limited at both the sections are compared with the reported and observed ooidal horizons in other areas like Trans Indus Range, Kohat and Hazara. However, peloidal grainstone/grapstone bearing grainstones are quite frequent. All these facies suggest variation in the shallow shelf areas from high energy shoal beaches and tidal bars, changing to more restricted water circulations in possible tidal flats, with warm water with normal to slightly higher salinity, essentially above normal wave base, where the activity of the currents continuously kept winnowing the mud.

The relatively deeper water environments prevailed in certain segments of the outer shelf where the deposition of packstone/wackestone with gravel sized bioclasts derived from shallow shelf areas are accumulated in wavy beds of depositional slopes shifted down flank, where finer sediments are infiltrated in the frame work with common geopetals and indicate slope or toe of slope depositional settings.

Cyclic marls/clays are persistently present in both the sections and in the upper part a well developed nodular marl zone (20 metes thick at Surg and 10 metes thick at Chapra Section) is present. The marls/clays are considered to be the periodic influxes from land followed by some

distant uplift and erosion. This may also be due to the periodic climatic change in the adjoining landmass. The dolomitic limestone are persistently encountered in the Samana Suk Limestone, however, below marls horizons the dolomite horizons are more frequent. The presence or zoned dolomite crystals, with inclusion rich internal zone and clear outer zone and the clacitization are very prominent evidences based on which Sheikh (1992) proposed a mixed meteoric-marine water dolomitization model as to be most suitable for the dolomitization in the Samana Suk Limestone. The dolomitized zones underlying marls/shales might have been dolomitized to some extent due to the release of Mg-rich fluids from these rocks, as a result of burial compaction.

The detailed depositional environmental interpretations are given in section 3.2.3.2 under the Microfacies encountered and described from both the sections. All these condition, accompanied with features like varying bedding thicknesses, shoaling upward cycles, hard ground surfaces strongly indicate shallow marine shelf environments during the deposition of the Samana Suk Limestone at Kala Chitta Range.

SHOALING UPWARD CYCLES

Shoaling upward cycles with lime mudstone at the base followed by bioclastic grainstone with rounded, worn and coated bioclasts grainstone and some well formed oolites and/or peloids grainstones are repeatedly present in the Samana Suk Limestone. These cycles have been observed during field and microscopic studies. According to Wilson (1975) these carbonate shelf cycles represent a general regressive earth history. They tend to multiply upward, becoming thinner, more restricted marine in character and less regular. In the Samana Suk Limestone interestingly, the upward shoaling lithologic cycles have close similarity with the Middle Jurassic deposits of Paris Basin (Wilson, 1975). The description of these cycles is as follows:

A lower argillaceous thin bedded bioclastic lime mudstone (or marl unit) overlain by thicker middle unit of bioclastic or cortoid bearing packstone/grainstone followed by thick bedded, light coloured peloidal/aggregate grains bearing grainstone units and occasional ooidal grainstone unit. Hardground surfaces begin to appear in the upper showing oxidized layers with large oyster plastering along it. In places evidences of bored and corroded surfaces are commonly associated.

The microfacies types through each cycle, generally illustrate the regressive sequence of events, these are:

Well-bedded, argillaceous lime mudstones / wackestone, off bank on the shelf.

Well bedded bioclastic peloidal wackestone / packstone off bank on the shelf.

Bioclastic peloidal packstone/grainstone with coated grains edge of the bank.

Cortoid bearing grainstone or ooidal grainstone at the edge of the bank.

Bioclastic-oncoid and/or coated particles packstone / grainstone.

Peloidal/aggregate grainstone.

The formation represents shelf facies with pure carbonate deposition and is hardly affected by terrigenous influx thus the variation in clastic sedimentation is not the cause for the cyclicity rather the sea level changes or the shoreline fluctuations has been the only cause of these shoaling upward sequences in the Samana Suk Limestone. The shoaling upward cycles are fairly well defined in the Surg section, whereas in the Chapra Section these cycles are not so clearly distinctive. As the two sections are close to each other, this change may be due to the location of the section either more within the shelf or near its landward side where exposure surfaces are prominent and cycle members are incomplete through non deposition. It can also be slightly on the outer edges of shelves, where subsidence is continuous and water is deep enough for the effect of sea level fluctuation to be reflected in the sedimentary record on a local basis. The idea is also supported by limited microfacies variations in the Chapra Section. There are other factors for the break in a complete cycle, like changes in degree of restriction of water circulation over the shelf, tidal variation, degree and frequency of periodic drop of sea level (Wilson, 1975).

These upward shoaling cycles show as if a relatively rapid rise of sea level occurred repeatedly on a steadily subsiding shelf and was followed by sedimentary progradation and fill-in of the inundated area over some period of time. The sea level rise and fall as depicted during the deposition of the Samana Suk Limestone is considered to be the local transgressions and regressions of the shore line and thus cannot be equated with the global eustatic sea level rises and falls. Vail et al. (1984) have cautioned for such curves to be correlated with the global eustatic curves and suggested that differing local and regional subsidence and sediment supply rates can produce apparent transgressions or regressions that may not be synchronous with the global cycles.

CONCLUSIONS

The Samana Suk Limestone represents a variety of shallow marine shelf environments from high energy to low energy environment.

The sea level fluctuations represented by the Shoaling Upward Shelf Cycles terminated by hardground surfaces are well defined in the Surg Section in contrast to the Chapra Section.

Extensive post depositional dolomitization overprints is prominent. This dolomitization is of multigenetic origin.

Various cements including marine and fresh water are suggestive of different diagenetic environments.

The overprints of physical and chemical compactions are evident.

REFERENCES

Bathurst, R.G.C. 1986. Carbonate Sediments and their Diagenesis; Developments in Sedimentology. 12, Elsevier, New York pp. 1-658.

Bender, F.K. and Reza, H.A. 1995. Geology of Pakistan. Gebruder Borntraeger, Berlin 1-414.

Cotter, G. de. P. 1933. The geology of the part of the Attock District, west of longitude 72 45'E. *Mem. Geol. Surv. India,* **55,** 63-161.

Davies, L.M. 1930. The fossil fauna of the Samana Range and some neighbouring areas; Part I. An introductory note: *Mem. Geol. Surv. India, Pal. Indica, New Series,* **15,** 1-15.

Fatmi, A.N. 1973. Lithostratigraphic units of Kohat-Potwar Province, Indus Basin, Pakistan. *Mem. Geol. Surv. Pakistan,* **10,** 1-80.

Fatmi, A.N., Hydari, I. Anwer, M. Mengal, J.M. 1986. Stratigraphy of "Zidi Formation" (Ferozabad Group) and "Parh Group" (Monajhal Group) Khuzdar District, Balochistan, Pakistan. *Recs Geol. Surv. Pakistan* **75.** 1-32.

Flugel, E., 1982. Microfacies analysis of carbonate rocks. Springer-Verlage. 1-633.

Garrison, R.E. and Fisher, A.G. 1969. Deep water limestones and radiolarites of the Alpine Jurassic. In: Depositional environments in carbonate rocks. (ed. Friedman, G.M.) A symposium. *Soc. Econ. Pal. Min. Spec. Publ.* **14,** 20-55.

Gregg, J.M. and Sibley, D.F. 1984. Epigenetic dolomitization and the origin of xenotopic dolomite texture, *jour. Sed. Pet.* **54,** 908-931.

Masood, H. 1989. Samana Suk Formation depositional and diagenetic history, *Kashmir Jour. Geol* **6 & 7:** 151-161.

Mensink, H., Mertmann, D., Ahmed, S. and Shams, F.A. 1991. Facies of Jurassic rocks in Surghar Range, Pakistan. *Acta Mineralogica Pakistanica* **5**: 109-120.

Park, W.C. and Schot, E.H. 1968. Stylolitization in carbonate rocks. In: Recent developments in sedimentology in Central Europe (ed. Muller, G. and Friedman, G.M.).

Purser, B.H. 1969. Synsedimentary marine lithification of Middle Jurassic limestone of Paris Basin, France. Sedimentology 12 (3/4).

Qureshi, M.A., Baig, S. and Munir, M.H. 1997. Reconnaissance microfacies analysis of the Upper Jurassic Samana Suk Formation, Northern Hazara Pakistan. *Geol. Bull. Punjab Univ.* **31 & 32,** 145-151.

Qureshi, M.K.A. 1997. Stratigraphical and Sedimentological Studfies of the Mesozoic Rocks of the Kala Chitta Range, Northern Pakistan. Ph.D. Thesis, Punjab Univ., Lahore, 1-552.

Sandberg, P.A. 1985. Aragonite cements and their occurrence in ancient limestones. In: Carbonate Cements (Eds. Schneideremann, N. and Harris, P.M.). *Soc. Econ. Pal. Min. Spec. Publ.,* **36,** 33-57.

Sheikh, R. 1992. Deposition and Diagenesis of Mesozoic Rocks, Kala Chitta Range, Northern Pakistan. Ph.D. Thesis. Imperial College, London.

Sheikh, R.A., Qureshi, M.K.A, Ghazi, S. and Masood, K.R. 2001. Jurassic carbonate shelf deposition Abbottabad District Northern Pakistan. *Geol. Bull. Punjab Univ.* **36:** 49-62.

Tucker, M.E. 1990. Techniques in Sedimentology. Blackwell Scientific Publications, London. 1-394.

Tucker, M.E. and Wright, V.P. 1992. Carbonate Sedimentology. Blakwell Scientific Publications, London. 1-482.

Vail, P.R., Todd, R.G. and Hardenbol, J. 1982. Jurassic unconformities, chronostratigraphy and sea level changes from seismic stratigraphy and biostratigraphy. In: Interregional unconformities and hydrocarbon accumulation: (ed. J.S. Schlee) *Amer. Assoc. Petrol. Geol. Mem.* **36:** 129-144.

Vail, P.R., Todd. R.G. and Hardenbol J. 1984. Jurassic unconformities, chronostratigraphy and sea level changes from seismic stratigraphy and biostratigraphy. *Soc. Econ. Pal. Min. Found. Proc. 3rd Annual Res. Conf.* 347-364.

Walker, K.R. 1990. Petrographic ctiteria for the recognition of marine syntaxial overgrowth and their distribution in geologic time. Carbonates and evaporates, 5/2: 141-151.

Wilson, J.L. 1975. Carbonate Facies in Geologic History. Springer-Verlage. New York. 1-472.

Geol. Bull. Punjab Univ. 43, 2008.

MINERALOGY AND THE TEXTURES OF THE VOLCANIC ROCKS OF THE HARRAH AL-HAMAD OF SAUDI ARABIA

BY

SYED MAHMOOD ALI SHAH

Institute of Geology, University of the Punjab, Quaid-i-Azam Campus, Lahore-54590 Pakistan
shah061@gmail.com

Abstract:- *In the Arabian peninsula, Cenozoic basalts occur in the form of isolated, but vast lava fields which are called harrahs. A total of 13 volcanic fields exist in Saudi Arabia covering an area of about 100,000 sq. km with variable locations relative to the Red Sea. The nearest volcanic field occurs at the coastal plain, whereas the farthest is about 500 km east of the eastern coast of the Red Sea (Arno et al. 1980). The volcanic field of Harrah Al-Hamad lies in the northwest of Saudi Arabia out of the Arabian Shield boundaries (Fig 1a, 1b). A total of 215 thin sections and 20 polished sections were studied, where the mineralogical composition as well as the textural features of the volcanic rocks were identified and described. An excellent section is exposed in the vicinity of Kaf area where 4 distinguishing successive volcanic episodes of Harrah Al-Hamad are exposed with interlayered sedimentary rocks composed of chalky, silicified, phosphatic limestones, chert and calcareous sandstone of Eocene, Miocene and Pliocene age (Ell. Naggar et al. 1982). Based on sample locations and rock types of these basaltic rocks, five episodes can be grouped in the study area. Mineralogically the oldest to youngest volcanic rocks of Episode 1-5 are composed essentially of plagioclase laths (40-60%), olivine phenocrysts partially to completely replaced by secondary mineral (iddingsite) and clinopyroxene crystals. The accessory minerals are calcite and epidote. Euhedral to subhedral crystals of olivine, pyroxene and plagioclase are more developed in Older Episodes (1-3) and are fine-grained in Younger Episodes (4-5). Groundrnass is normally cryptocrystalline. Polished sections study indicates that opaques occur as disseminated triangular, square and rhombic grains of haematite, magnetite and ilmenite. Geochemically (using APL program of Glazner, 1984) volcanic rocks of Episode 1-3 are found as Alkali Olivine Basalts with normative Ne. &/or Hy and Ol (Ne<5%); Episode 4 as Basanite with normative Ol, Ne & Ab (Ne >5%); and Episode 5 as olivine Nephelinite with normative Ol, Ne and Lc.*

INTRODUCTION

The volcanic field of Harrah Al-Hamad covers an area of about 15000 sq.Km. in the form of isolated patches of volcanic rocks. Previous geological work on the volcanic rocks of Harrah Al-Hamad is minimal, but sedimentary rocks in the area have been investigated to explore the sedimentary phosphate deposits, the underground water, and brines in the region mainly by Riofinex Geological Mission (1979). Powers et al. (1966) distinguished three types of basalts in this region: (a) older highly weathered basalts, exposed at Quryyat Al-Milh, (b) middle basalts without amygdaloidal phase, at places; and (c) a younger lava at Umm Mu'al resting directly on the Eocene surface.

The occurrence of interstratified sedimentary rocks with the volcanics has been found to be of significance in distinguishing successive volcanic episodes.

An excellent section for this is exposed in the vicinity of Kaf (Fig. 2). Based on this section, as well as other observations, a general sequence for the volcanic and interlayered sedimentary rocks of Harrah Al-Hamad has identified (Section A).

SECTION A (FROM YOUNGEST TO OLDEST)

- Post-Volcanicity Sediments
- Fifth Outcrdpping Cinder-cones. And Other Volcanic Rocks (Episode 5)
- Fourth Outcropping Volcanic Rock Layer (Episode 4).
- Third Intelayered Sedimentary Rocks
- Third Outcropping Volcanic Rock Layer (Episode 3)
- Second Interlayered Sedimentary Rocks
- Second Outcropping Volcanic Rock Layer (Episode 2)
- First Interlayered Sedimentary Rocks
- First Outcropping Volcanic Rock Layer (Episode 1)
- Pre-volcanicity (Older) sedimentary Rocks

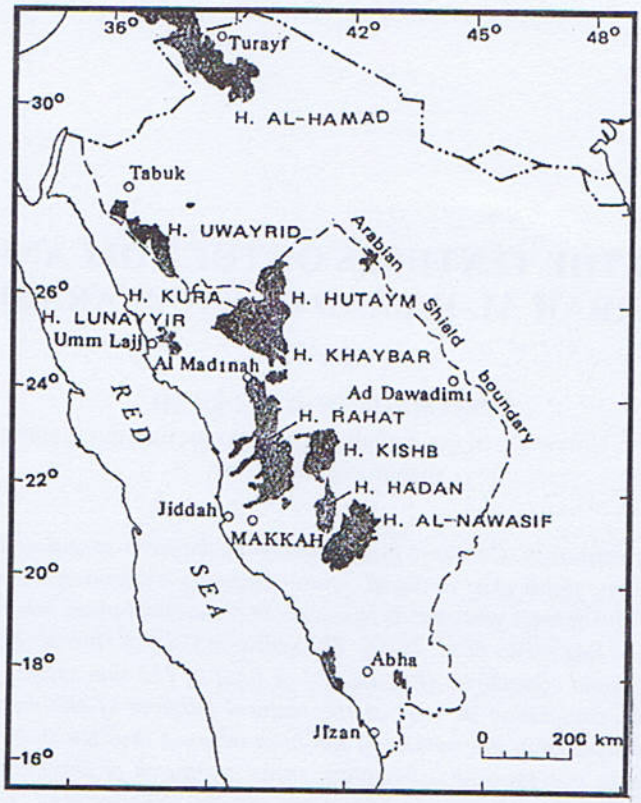

Fig. 1. Index map of western Saudi Arabia showing cenozoic volcanic fields referred to in this report (After Coleman and otheers, 1983, and SAMRAR, 1980-1981).

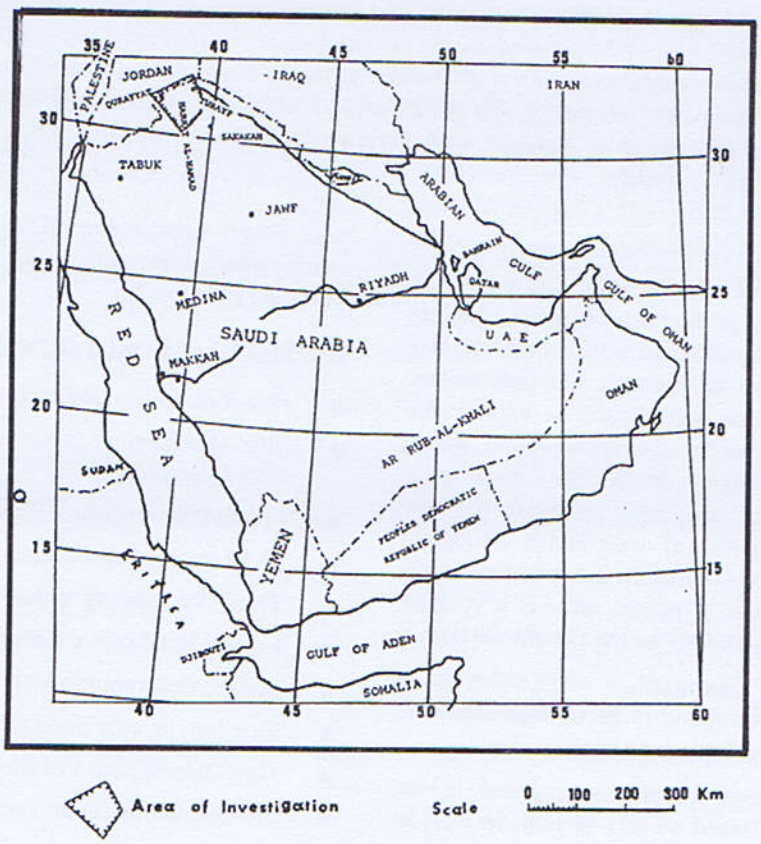

Fig. 2. Location map showing the area of investigation (Harrah al-Hamad).

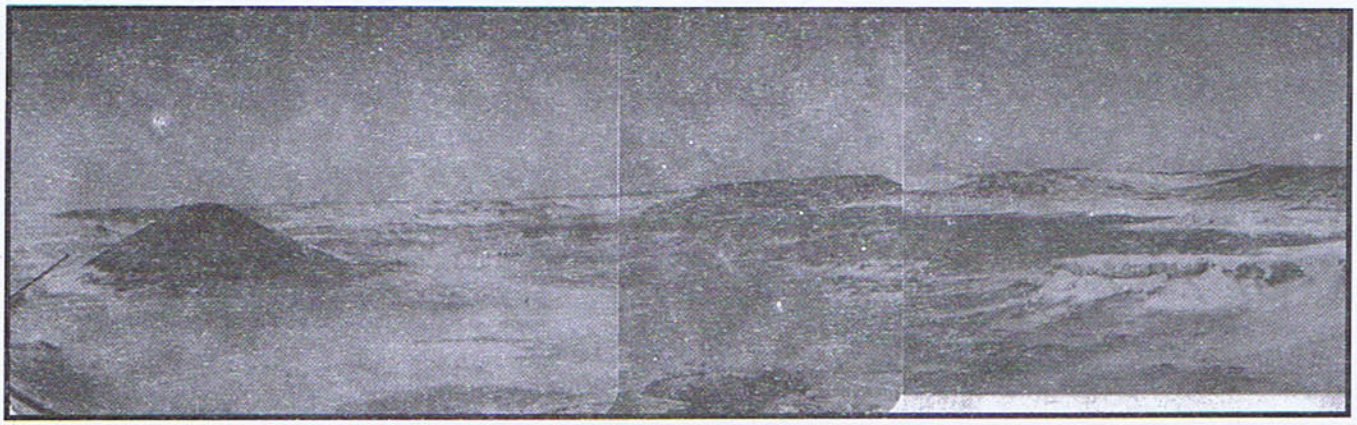

Fig. 2: A panoramic view showing the First, Second, Third and Fourth Outcropping Volcanic Rock Layers exposed near Kaf, in northern partjof Wadi as-Sirhan. The paved meandering road leads north westward to al-Hadithah.

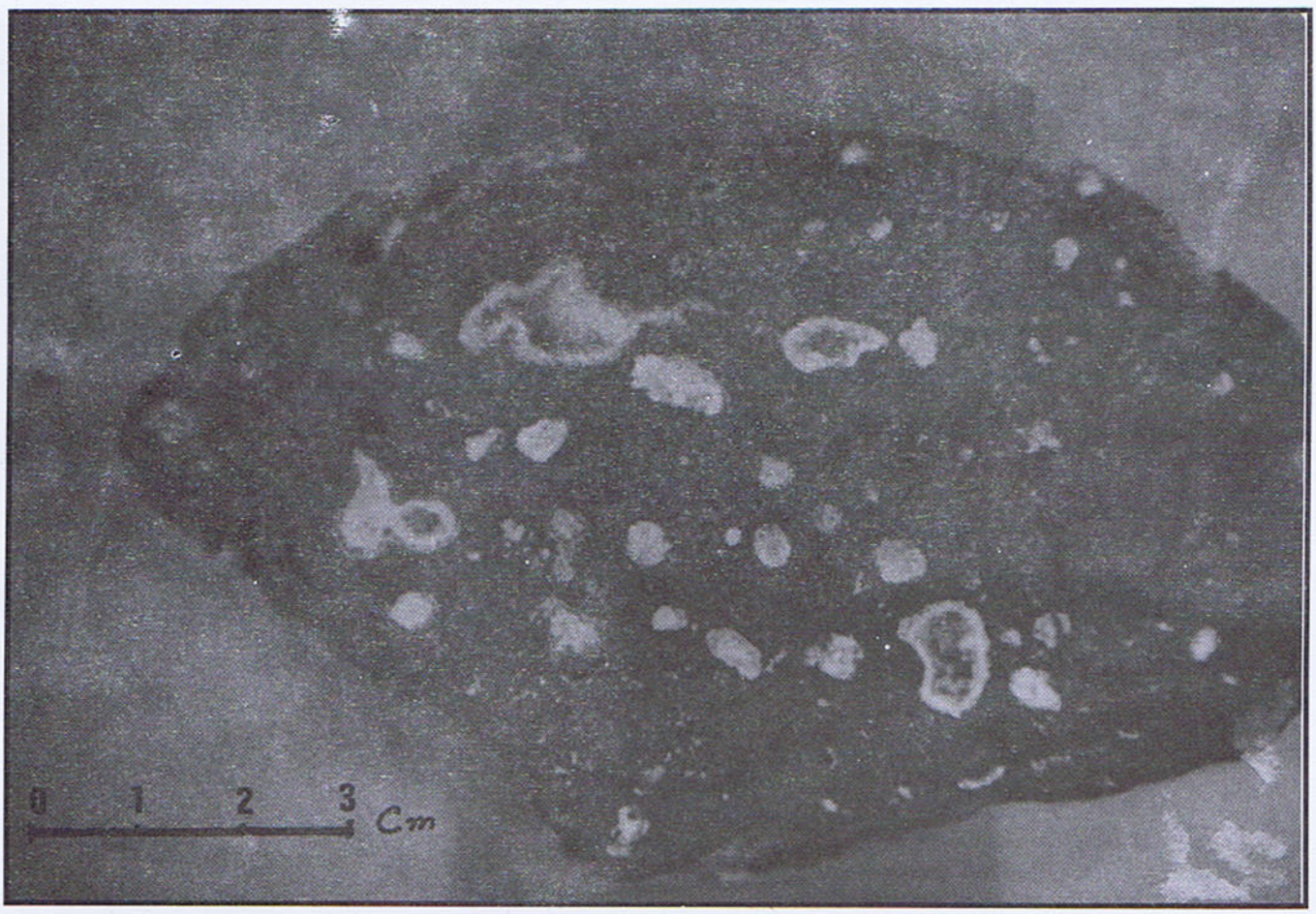

Fig. 3a. Photograph of hand-specimen showing weathered nature of the First Outcropping Volcanic Rock Layer (Episode 1), collected from road-side exposure in the vicinity of Kaf. Amygdales are completely to partially filled with calcite (Sample 170).

MINERALOGY AND THE TEXTURE OF THE VOLCANIC ROCKS

A total of 215 volcanic rock sample collected from all the outcropping volcanic layers and interlayered sedimentary rocks have been investigated for their mineralogical and textural characteristics. Twenty semis polished slabs have been studied for opaque minerals.

The First Outcropping Volcanic Rock Layer (Episode 1)

The thin-section study of samples from the first layer reveals that the volcanic rocks are composed essentially of plagioclase laths (40-50%), phenocrysts of olivine (20-25%) and clinopyroxene (10-15%). The extinction angle of plagioclase laths is between 32 to 36 , indicating a labradorite variety showing poor albite twinning (Fig. 3b). The clinopyroxene is mostly masked by yellow palagonite/limonite (Fig. 3b). Olivine is completely replaced by dull brown weakly pleochroic occurs as pherocrysts and interstitial matrixs. Numerous vesicles are partially or completely filled with calcite producing amygdales (Fig. 3c, 3d). The opaque accurs as grains and specks of steel gray black hematite, black magnetite, and the minralogy and texture of these rocks revealed that they are highly altered and weathered fine-grained basalts (Fig 3a).

The Second Outcropping Volcanic Rock Layer (Episode 2).

Under microscope the samples indicate that these volcanic rocks are composed essentially of plagioclase laths (50-60%), olivine (20-25%), pyroxene crystals (10-15%), opaques (3-5%) and accessories (about 2%). The plagioclase laths exhibit lamellar and Carlsbad twining (Fig. 4a) and extinguish between 32 and 38 , indicating presence of labradorite as well as bytownite varieties. Electron microprobe analysis carried out on some laths (shown in table I) records the composition of plagioclase to be An 67-73. The Olivine is present as phenocrysts as well as fine crystals in the matrix, and partially to completely altered to iddingsite. Some grains show corroded outline due to resorption (Fig. 4b, 4c). The clinopyroxene occurs as parted crystals displaying a pinkish-voilet, blue, and strong green interference colour. Calcite and apatite are present as necessary minerals. Opaques including hematite, magnetite and ilmenite occur as disseminated triangular, square; and rhombic grains.

The Third Outcropping Volcanic Rock Layer (Episode 3).

The microscopic study of the rocks from the third volcanic layer indicates that they are composed essentially of plagioclase laths (59-60%), olivine phenocrysts (20-25%), pyroxene crystals (10-15%), opaques (about 4%) and accessories (about 2%). The plagioclase laths are quite fresh and well developed showing both albite and Carlsbad twining. Extinguishing angle is between 29 and 35 , indicating labradorite composition (Fig. 5a, 5b). Olivine occurs as phenocrysts and fine crystals in the matrix. These are partially to completely replaced by iddingsite. The fresher olivine shows olive-green and pink interference colours. The interference colour of clinopyroxene are pinkish-voilet, yellow and purple (Fig. 5a, 5b). The accessories are calcite and epidote while opaques are hematite, magnetite and ilmenite.

The Fourth Outcropping Volcanic Rock Layer (Episode 4).

The fourth volcanic rock layer is composed essentially of microlites of plagioclase and clinopyroxene (40-50%), phenocrysts of olivine (25-30%), opaques about (10%) and accessories (5%). The plagioclase microlites extinct between 22 and 30 , indicating andesine-labradorite varieties of plagioclase. Olivine phenocrysts and granules are replaced by iddingsite which form narrow irregular external rind along partially altered olivine phenocrysts (Fig. 6a). Some phenocrysts have been resorbed to amoeba-form (Fig. 6b) and skeletal-form. The atomic percentage of Mg dominates over Fe as detected by electron microprobe for several olivine phenocrysts.

Occasionally olivines (at places irregularly fractured) are surrounded by reaction rims (Fig. 7a, 7b). Epidote and granules of olivine and pyroxene? May be the main constituents of reaction. rims. The size of grains in the reaction rims increases towards the inner margin of the rims.

Cryptocrystalline calcite which fills the vesicles and fractures, is strongly bi refringent. Other filling material includes feldspar and epidote. Feldspar crystals display grey birefringence. Zeolite (picotite?) is rarely present as crystals displaying deep yellow color with opaque margins in plane-polarized light (Fig. 8a). Under cross nicols, however, zeolite (picotite?) crystals appear dark brown (Fig. 8b). Electron microprobe analysis carried out on zeolite (picotite?) grains detects an increase in Fe and Ti elements from the center to the rim (table II).

In reflected light, the metallic luster is steel-grey black for hematite, black for magnetite, and blue-black fbr ilmenite. Groundmass glass, occasionally, makes contrasting black and grey layers, and at places displays flow texture around olivine phenocrysts.

Euhedral to subhedral phenocrysts of olivine are embedded in glassy groundmass. Olivine is also present as hexagonal to polygonal phenocrysts. Texturally these are amygdaloidal, vesicular, and porphyritic fine-grained basalts.

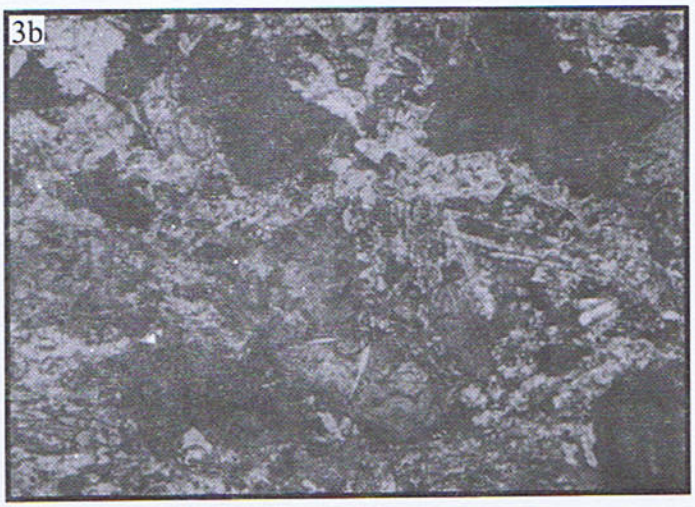

Fig. 3b. Photomicrograph of the First Outcropping Volcanic Rock Layer (Episode 1) showing glomerocryate of pseudomorphic hexagonal to polygonal olivine an pyroxene, both are completely replaced respectively by iddingsite and palagonite (?). Plagioclase laths are completely to partially replaced by sericite and iron oxide

Figure 3c: Photomicrograph of the First Outcropping Volcanic Rock Layer (Episode 1) showing partial to complete replacement of phenocrysts as well as groundmass olivine. Pyroxene crystals and plagioclase laths are present; weathering product is more pronounced (Sample 161, 165x, x-polars).

Fig. 3d. Another photomicrographic view showing the mineralogical features as observed in Fig. 3c except complete

Fig. 4a. Photomicrograph showing cluster of well developed plagioclase (labradorite) laths in the second Outcropping Volcanic Rock Layer (Episode 2). Bright orange and pale small grains are of olivine (Sample 184, 165x, x-polars)

Fig. 4b. Photomicrograph of the Second Outcropping Volcanic Layer (Episode 2) showing reddish brown iddingsite replacing olivine phenocrysts at margins. Proxene (diopside on top centre) side showspartially preserved two cleavage directions. Plagioclase (labradorite-bytownite) laths are quite clear here. Epidote grains showing characteristic green interference color are seen in the lower half of the picture (Sample 160, 175x, x-polars).

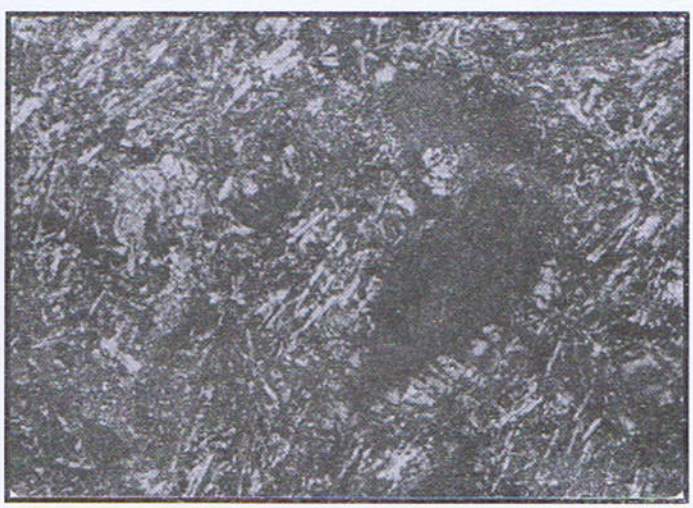

Fig. 4c. Photomicrograph of the Second Volcanic Rock Layer (Episode 2). Fractured olivine phenocrysts are mostly replaced by iddingsite. Plagioclase (labradorite) laths and hematite, magnetite and ilmenite (black grains) are also seen (Sample 142, 185x, x-polars).

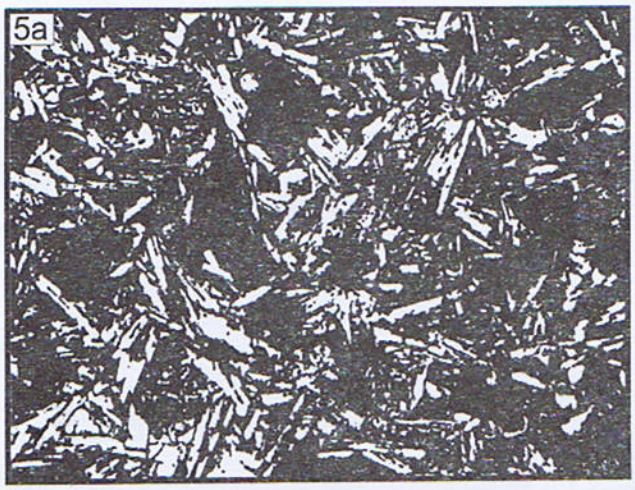

Fig. 5a, 5b. Photomicrographic views showing the subophitic textgures in the Third Outcropping Volcanic Rock Layer (Episode 3). It consists of olivine and pyroxene crystals with interpenetrated plagioclase laths. Iddingsite makes pseudomorphs by completely or partially replacing olivine phenocrysts. (Sample 16a, 32x, xpolar

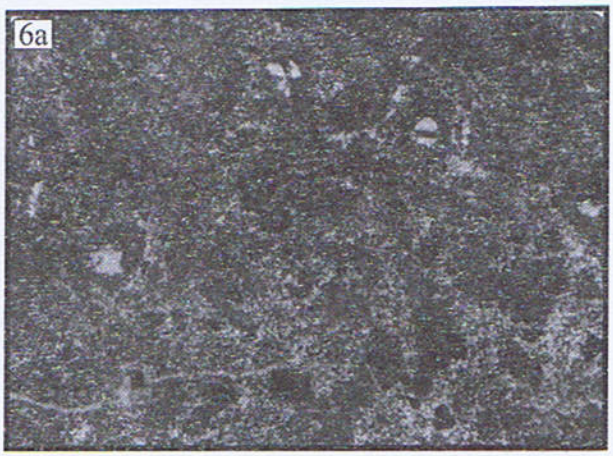

Fig. 6a. Photomicrograph of the Fourth Outcropping Volcanic Rock Layer (Episode 4) showing yellowish, and brown iddingsite after altering subhedral to anhedral olivine crystals. Groundmass is composed of black hematite, magnetite, ilmenite grains and glass (Sample 20, 100x, x-polars).

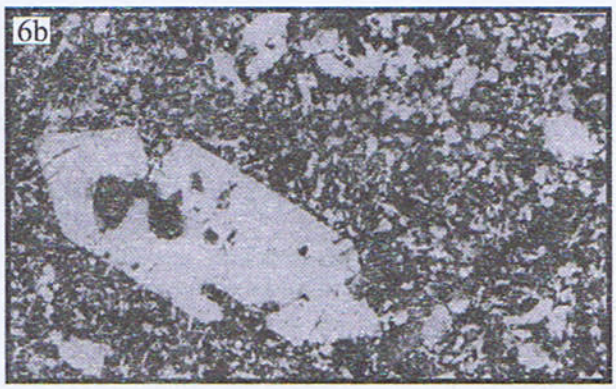

Fig. 6b. Photomicrograph of porphyritic basalt (The Fourth Outcropping Volcanic Rock Layer). Amoeba-from olivine occupies most of the area. Olivine is also present as fine-grained crystals. Groundmass consists of microlites of plagioclase and pyroxene. Opaques are hematite, magnetite, and ilmenite to (Sample 59, 175x, x-polars).

Fig. 7a. Photomicrograph of basalt (The Fourth Outcropping Volcanic Rock Layer). Large olivinephenocrysts, (having irregular fractures) are surrounded by reaction rim which is composed of minute olivine,epidote granules and opaque grains (Sample 82, 200x, x-polars).

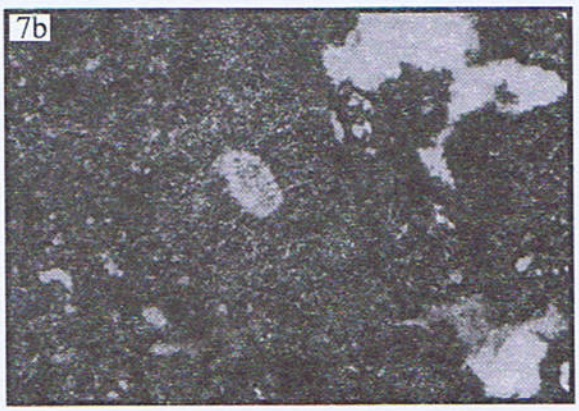

Fig. 7b. Photomicrograph of the Fourth Outcropping Volcanic Rock Layer (Episode 4) showing a large mixed, zoned phenocrysts consisting of olivine, pyroxene? And opaques (mostly iron oxides). Smaller olivine phenocrysts are present in the fine-grained groundmass, (Sample 32, 200x, x-polars).

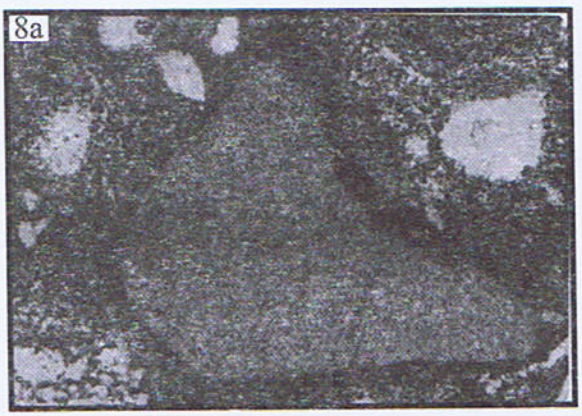

Fig. 8a. Photomicrographs of basalt (The Fourth Outcropping Volcanic Rock Layer) showing zeolite (picotite?) Crystal which is yellow with black margin in plane-polarized light (38a), and dark brown with black margin under cross-nicols (38b), (Sample 59, 185x, PP Light & x-polars)

Fig. 8b. Photomicrographs of basalt (The Fourth Outcropping Volcanic Rock Layer) showing zeolite (picotite?) Crystal which is yellow with black margin in plane-polarized light (38a), and dark brown with black margin under cross-nicols (38b), (Sample 59, 185x, PP Light & x-polars).

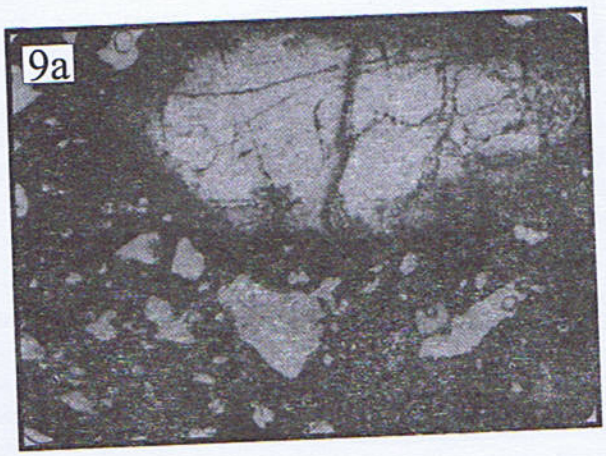

Fig. 9a. Photomicrograph of a scoriaceous Cinder-cone (Episode 5) pyroclastic material showing porphyritic texture. Corroded olivine phenocrysts are embedded in a reddish glass. Vesicles arewithout filling material, (Sample 23, 200x, PP Light).

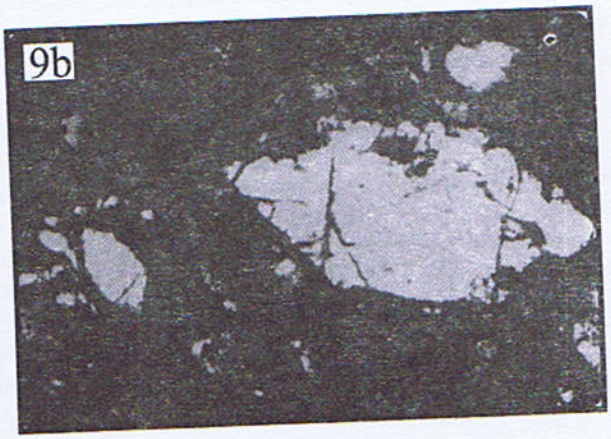

Fig. 9b. Photomicrograph of Rock from Cinder-cone (Volcanic Episode 5). Excellent hexagonal, fractured olivine phenocrysts are generally corroded as well as embayed by resorbtion. Groundmass is totally composed of black glass and opaques (Sample 8A, 200x, x-polars).

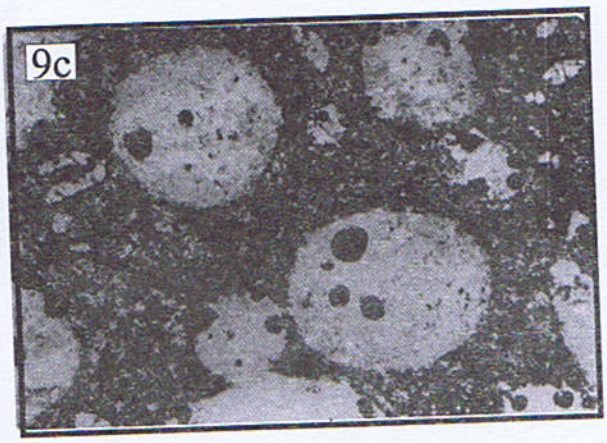

Fig. 9c. Photomicrograph of Rock from Outcropping Cinder-cones (Volcanic Episode 5)showing circular amygdales (generally filled with calcite) as well as hexagonal and birefringence in a fine-grained groundmass (Sample 2, 200x, x-polars).

The Fifth Outcropping Cinder-Cones and Other Volcanic Rocks (Episode 5)

The microscopic study of the samples from cinder-cone material reveals that these rocks are extremely fine-grained with olivine phenocrysts (Fig. 9a, 9b). The phenocrysts are also replaced by secondary minerals. So their visual modal estimation is totally difficult.

The plagioclase and pyroxene occasionally occur as microlites, generally camouflaged by finely disseminated opaques and glass. Olivine occurs as completely to partially replaced phenocrysts, which are commonly resorbed and corroded. Numerous vesicles are completely or partially filled with cryptocrystalline calcite producing spherical, ovoid, and coalesced amygdales (Fig. 9c). Granular opaques as well as brownish red and black glass are present in groundrmass.

Euhedral to subhedral, hexagonal to polygonal, olivine phenocrysts are embedded in glassy groundmass. Texturally these are amygdaloidal, scoriaceous, porphyritic, fine-grained basaltic rocks.

CONCLUSION

The petrographic study reveals that the basaltic rocks are essentially composed of plagioclase (labradorite mostly) laths, clinopyroxene (diopside) crystals, and olivine phenocrysts. The olivines mostly show resorption, and are abundant in the groundmass. Alkali-feldspar is also present in young volcanic rocks (Episode 4 & 5). Quartz is totally absent. Presence of olivine as phenocrysts as well as in the groundmass (more iron rich, similar to one described by Brown, (1968), Nagao and Sakaguchi (1990) and Shoji and Natsue (1995) is a common feature of alkali olivine basalts. Based on these salient petrographic features, these volcanic rocks are considered as alkali olivine basalts. The work of Iizumi et al., (1975) Nagao and Sakaguchi, (1990) also showed that alkali olivine basalt containing upto 12% normative nepheline (Shozi and Natsu, 1995) is also in accordance with the normative nepheline value of episode 5 basalt of the research project area. According to Graham et al., (2003) secondary mineral assembelages are enriched in Ca, Na, K and $(CO_3)^2$. They are divided into three distinct varieties.

The Older Alkali Olivine Basalts (Episode 1,2,3)

These are exposed at Kaf and characterized by plagioclage (40-60%), olivine (20-30%), and pyroxene (15-20%). The opaques and accessory minerals are also in considerable amount. These rocks display amygdaloidal, vesicular, porphyritic, fine-grained texture. These layers are limited to the vicinity of Kaf area. Microscopically the volcanic rocks exposed at Tall al-Hibr display similar mineralogical and textural featuters as those of second volcanic rock layer present at kaf.

The Younger, Fragmental Basalts (Episode 4)

These are characterized by replaced plagioclase and pyroxene, and olivine phenocrysts. Texturally these are compact, partially amygdaloidal, porphyritic, fine-grained rocks with olivine phenocrysts in cryptocrystalline groundmass.

The Youngest, Cinder- cone and other Basaltic Rocks (Episode 5)

These are composed of pyroclastic, amygdaloidal, scoriaceous, porphyritic fine-grained rocks. Although absent at kaf, they are exposed over all Harrah Al-Hamad.

ACKNOWLEDGEMENT

The writer would like to express his gratitude to the Academic Management of King Fahd University of Petroleum and Minerals, Dhahran, Saudi Arabia, for providing me invaluable research facilities and imparting knowledge in my thesis work.

Dr. M.N. Chaudhry and Dr.M. Ashraf are also acknowledged for discussions and critical reading of this paper.

REFERENCES

Arno, V., Bakashwin, M.A. Bakor, A.Y., Barberi, F., Basahel, A., Dipaola, G.M., Ferrara, G. Gazzaz, M.A., Guiliani. A., Heikel, M., Marinelli, G., Nassief, A.O., Rosi, M. and Santacroce, R., (1980) Recent Volcanism within the Arabian Plate. Preliminary Data from the Harrats Hadan and Nassief-al-Buqum, In Geodynamic Evolution of the Afro-Arabian Rift System, *Inter. Meet. Rome, vol. 47,* pp.629-643.

Augustithis, S.S., (1978) Atlas of the Textural Patterns of Basalts and their Genetic Significance, *Elsevier Scientific Publishing Company, New York, pp.6-60, 103-305.*

Bindagji, H.H., (1979) Atlas of Saudi Arabia *Oxford University Press,* 34p.

Brown, G.M., (1971) Tectonic Map of Arabian Peninsula, *U.S. Arabian Project Report, SA (IR)-134, Jeddah, Saudi Arabia*

Brown, G.M., (1968) Mineralogy of Basaltic Rocks, In Basalts, vol., I., Hess, H.H. and Poldervaart, A. (Editors), 482p, *Interscience, John Willey and sons, New York,* pp.103 16-162.

Cross, W.; Iddings, J.P.; Pirson, L.V. and Washington, H.S., (1902) The Texture of Igneous Rocks, *Jour. Geol.*, **14**, pp. 697-707.

El-Naggar, Z.R., Saif, S.I., and Abdennabi, A., (1982) Stratigraphical Analysis of the Phosphate Deposit in Northwestern Saudi Arabia, *Progress Report 1-4 submitted to SANCT, Riyadh,* 120p.

Glazner, A.F., (1984) A Short CIPW Norm Program, *Computers and Geosciences,* **10,** *No. 4,* pp.449-450,

Graham I.T., R.E. Pogson, D.M. Colchester and A. Baines, (2003) Zeolite crystal habits, compositions, and paragenesis; Blackhead Quarry, Dunedin, New Zealand. *Mineralogical Magezine,* pp. 625-637

Kerr, P.F., (1977) Optical Mineralogy *MaGraw-Hill Book Co., 4th Ed.,* 485p

Nagao T. and Sakaguchi Y. (1990) Ultramafic xenoliths in the Cenozoic Kawashimo alkali basalt from Masuda, Shimane Prefecture SW Japan. *Journal of Mineralogy, Petrology and Economic* **17** pp. 21-27

Powers, R, W., Ramirez, L.F., Redmond, C.D., and Elberg, Jr., E.L., (1966) Geology of Saudi Arabia, *U.S.G.S. Prof Paper 650-D, Washington,* 147p.

Riofinex (1979.) Geological Mission, Investigation of The Upper Cretaceous and Tertiary phosphate Sedimentary Rocks of Northern Saudi Arabia, Open-File Rep. DGMR, Jiddah, Sandi Arabia, pp10-17

Saudi Arabian Mineral Resources Annual Report, Ministry of Petroleum and Mineral Resources, Kingdom of Saudi Arabia, (1980-81) pp.6-8.

Shoji A., and Natsue A. (1995) Reaction of orthopyroxene in peridotite xenoliths with alkali basalt melt and its implication of genesis of alpine type chromitite, *American Mineralogist,*. **80**. pp 1041-1047

Geol. Bull. Punjab Univ. 43, 2008.

FRACTURE ANALYSIS OF THE DHOK PATHAN FORMATION AT THE EASTERN LIMB OF THE JABBAR ANTICLINE, NORTHEASTERN POTWAR, DISTRICT RAWALPINDI

BY

SYED MAHMOOD ALI SHAH, AMER HAFEEZ AND RANA NAEEM KHAN
Institute of Geology, University of the Punjab, Quaid-i-Azam Campus, Lahore-54590 Pakistan
shah061@gmail.com

Abstract: *The fracture system was comprehensively studied and analyzed around the eastern limb of the Jabbar Anticline in the Dhok Pathan Formation of the Siwalik sediments located in the northeastern part of the Potwar Plateau. The Jabbar Anticline is a non plunging fold and a short structure with a box fold termination on its southern edge and to the north this fold is truncated by the Jhelum Fault. The sandstone beds of the Dhok Pathan Formation exposed in the eastern limb of the anticline are fractured. In-situ length, width and strike of fractures were measured from seven stations located in the Dhok Pathan Formation by using circle inventory method. The data is combined and calculated to measure the fracture density, porosity and permeability of the Dhok Pathan Formation.The Rose diagram is also plotted for stress analysis of the Dhok Pathan Formation.*

INTRODUCTION

The Potwar Plateau is constituted by a less internally deformed fold and thrust belt having a width of approximately 150 km in N–S direction. It is bounded to the south by the Salt Range and to the north by the Kala Chitta–Margalla Hill Range. Indus River forms its western limit whereas the Jhelum River marks its eastern boundary. There is a marked difference in the tectonic style of Potwar. The northern part of the Potwar Plateau, also referred to as the Northern Potwar Deformed Zone (NPDZ) lies between the Main Boundary Thrust and the Soan Syncline (Jaswal et al., 1997). It is more intensely deformed than the southern part, which is known as the Southern Potwar Deformed Zone (SPDZ) (Fig. 1).

The Jabbar Anticline is located in the northeastern Potwar. This part of the Potwar Plateau, situated to the east of Chakri–Balkasar up to the Jhelum River, is the north eastern Potwar which is bounded to the north by MBT and to the south by Domeli–Diljabba Thrust. It is a land of tight anticlines separated by broad open synclines. Anticlines represent folding phenomena while synclines are not true folds and represent undeformed area between anticlines. The dips in the axial zones of most anticlines are steep to overturned. Fold structures mostly trend NE–SW, which is in sharp contrast to EW trending folds in the central western Potwar Plateau, and NW–SE trending folds on the eastern side across Jhelum River. NE–SW structural trends in eastern Potwar may be explained by drag induced 30° rotation under the influence of left lateral Jhelum Fault and Hazara Kashmir Syntaxis relative to the Salt Range and western Potwar.

JABBAR ANTICLINE

The Jabbar Anticline is a NE–SW trending short structure which forms part of SPDZ. It is a non plunging asymmetric fold which is located in the northeast of the Gujar Khan at a distance of 15 Km. The structure is covered in the Survey of Pakistan's toposheet no. 43G/11 and 43G/12. The longitudes and the latitudes of the area are 73°30'00" to 73°35'00" and 33°14'00" to 33°20'00".

The Jabber Village is located on the north western limb of the Jabbar Anticline. The formations exposed in the Jabber Anticline belong to the Siwalik Group. The Siwaliks are of Late Miocene Chinji Formation, Early Pliocene Nagri Formation, Early to Middle Pliocene Dhok Pathan Formation and the Late Pliocene to Early Pleistocene Soan Formation (Shah, 1977). Which are mainly composed of sandstone, shale, clay and conglomerate and pebbles. The Chinji Formation is in the core of the Jabbar Anticline (Fig.2). The dips are very steep in the axial part and ranges from 50° to 60°. The axial part is low lying area due to soft lithology of the Chinji Formation comprising thick shale and thin friable sandstone as compared to the more resistant thick sandstone of the Nagri Formation with relatively

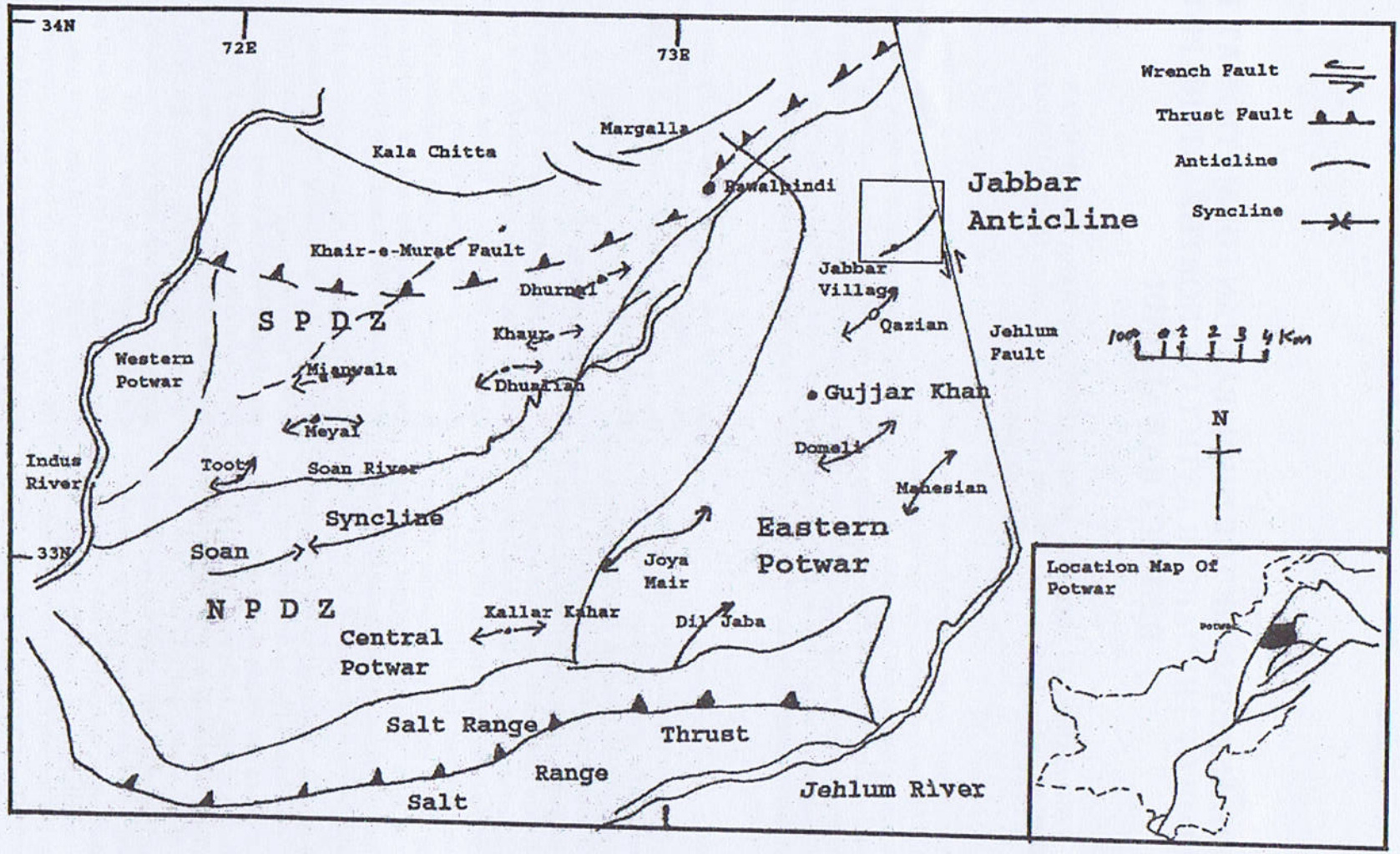

Fig. 1. Location map of the Potwar Plateau showing in the Jabbar Anticline

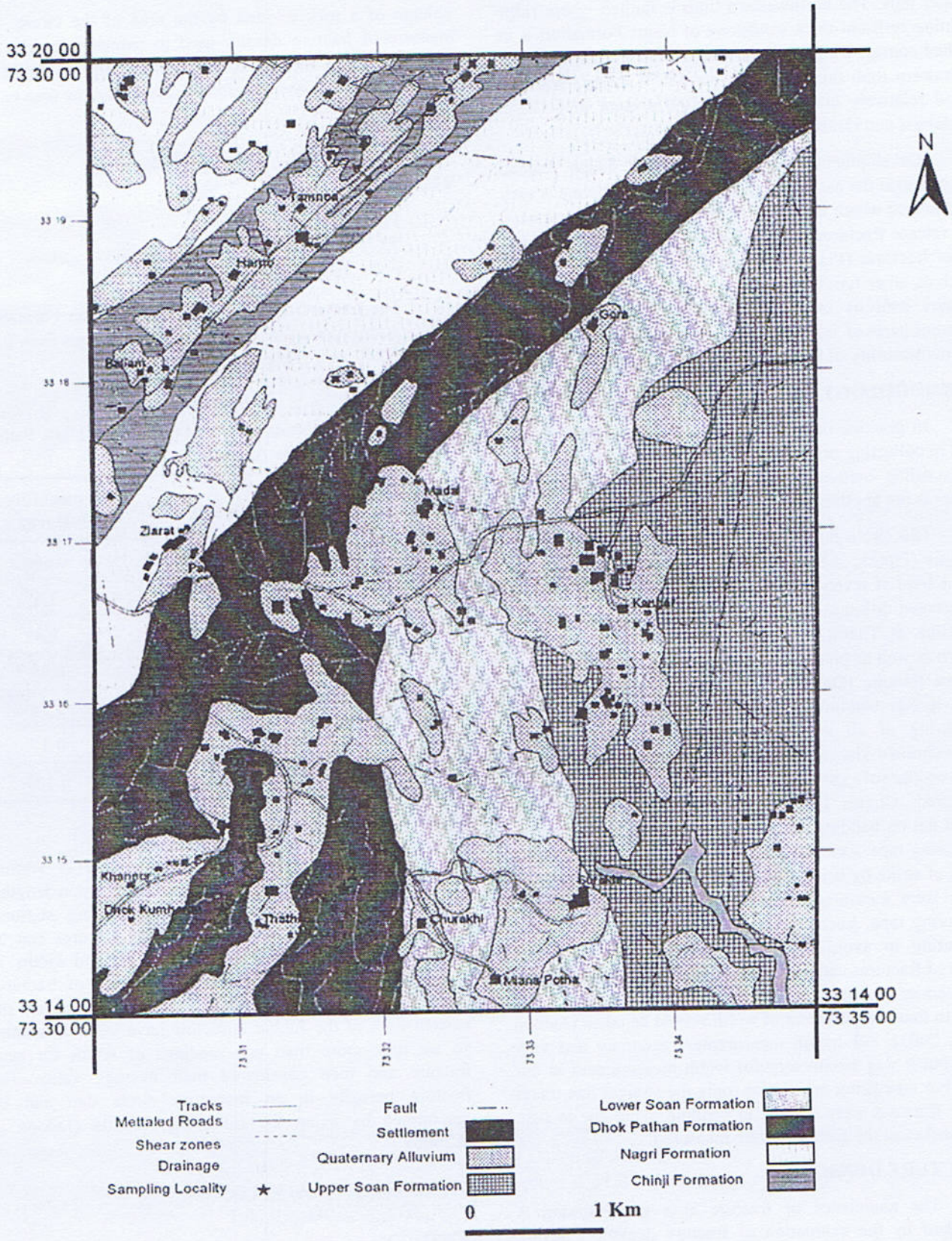

Fig. 2. Location map of eastern limb of Jabbar Anticline

gentler dips. The northwestern limb is faulted where ridge forming resistant thick sandstone of Nagri Formation is in faulted contact with the underlying Chinji Formation while on eastern limb this contact is normal. It merges with the broad relatively undeformed syncline present in between the Jabbar and Qazian Anticlines.

Development of fractures in the Dhok Pathan Formation at the eastern limb of the Jabbar Anticline is very pronounced which form part of the present study. Extension and release fractures are mostly developed while conjugate set of fractures (Plate 1, b.) are also developed but not so much as other types of fractures. The main purpose of the fracture analysis is to calculate the fracture density at different parts of fold and to estimate the fracture porosity and permeability of Dhok Pathan Formation.

METHODOLOGY

In practice there are two basic approaches that are used in collecting orientation data at sample stations. These are scanline method and circle inventory method, .the former is not applied in the present study.

The circle inventory method was used for fracture analysis (Plate1,. a.) because it is easy and convenient to use. A total of seven sampling stations were selected which represented different parts of the eastern limb of the Jabbar Anticline at Thathi Village. In this method a circle of known as well as predetermined radius is traced. On hosting surface fracture (Davis and Reynolds, S.J., 1996) in our case, it was bedding plane all the time and it required measuring of all the fractures that were occupied by predetermined size of the circle. The orientations, lengths and widths of each fracture within the circle were measured. Circles having radius of 50cm-100cm were traced out on bedding plane with the help of chalk and the measuring tape. Orientation of fractures were measured in terms of strike by using Brunton type compass. Length and width were measured with the help of simple ruler and measuring tape. Each fracture was traced with chalk after measuring to avoid repetition. Accuracy for measuring width of fractures can be enhanced by using advanced tools like vernier– calliper and for a fracture of variable width three to four measurement of width should be taken (Jadoon et. al, 2003). For length measurement accuracy was very good but it was satisfactory for width measurement in our case. For measuring orientation, only the straight line traces of the fractures were evident at bedding plane due to that, only strikes of the fractures were measured.

FRACTURE DENSITY

The abundance of fracture at a given station is described by the evaluation of fracture density. Fracture density can be measured and described in a number of ways; total cumulative length of fracture within a given volume of a rock divided by the area of the circle. The measure of fracture density used in conjunction with the circle inventory method is the summed up length of all fractures within inventory circles, divided by the area of the circle (Davis,1996).

$$FD=\sum L / \pi r^2$$

Where

FD = Fracture density
$\sum L$ = cumulative length of all fractures
r = radius of inventory circle

The fracture density of the Dhok Pathan Formation at the eastern limb of the Jabbar Anticline ranges from 0.01 cm^{-1} to 0.042cm^{-1}(Table 1)

Table 1

Fracture density, permeability and porosity of Dhok Pathan Formation at the Jabbar Anticline

Sr. No.	Circle No.	Density cm^{-1}	Porosity %	Permeability 10^7 Darcy
01	01	0.028	1.3	0.266
02	02	0.03	1.73	3.6
03	03	0.028	02	2.4
04	04	0.042	1.33	0.38
05	05	0.014	0.68	0.25
06	06	0.025	1.12	0.17
07	07	0.039	1.13	0.104

FRACTURE POROSITY

There is variation in fracture density at various places in the project area. Porosity depends upon lengths, widths, and density of fractures at sampling stations. Through Monte Carlo techniques, these fractures can be combined to yield fracture porosity. Lengths and widths, in fact are the lengths and widths of segments of fractures captured in an inventory circle. As the fractures on the eastern limb of the Jabbar Anticline have variable widths, so we took more than one readings of width for each fracture and then considered their average value. The fracture porosity in an inventory circle that can be determined by using the following formula (Jadoon et al.2003)

$$\text{Porosity} = (1/A) \sum_{i=1}^{N} (Li \times Wi)$$

Where

i = index to designate each fracture in an inventory circle

PLATE 1

a. Circle- inventory method for fracture analysis of the Dhok Pathan Formation (Long 73 31'17", Lat.30 19'17")

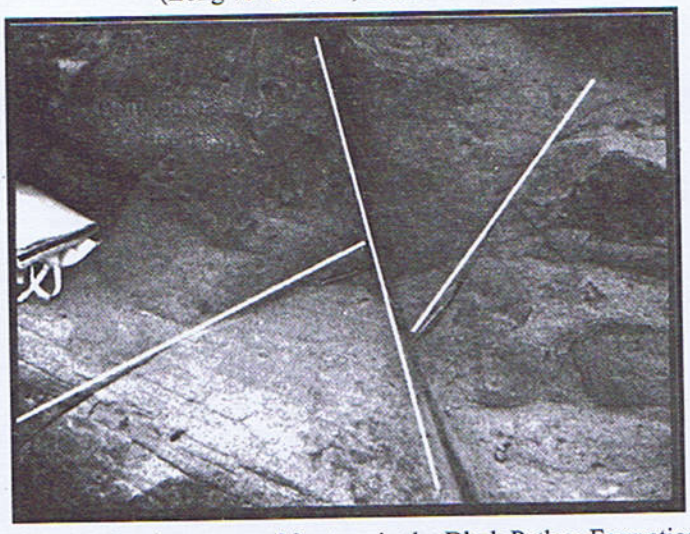

b. Circle- Conjugate set of fracture in the Dhok Pathan Formation (Long 73 30'17", Lat.30 17'05")

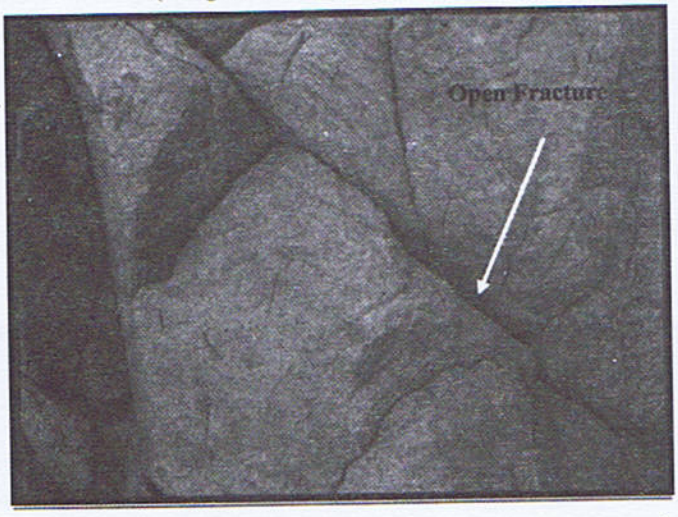

c. Circle- Conjugate set of fracture in the Dhok Pathan Formation (Long 73 31'17", Lat.30 19'17")

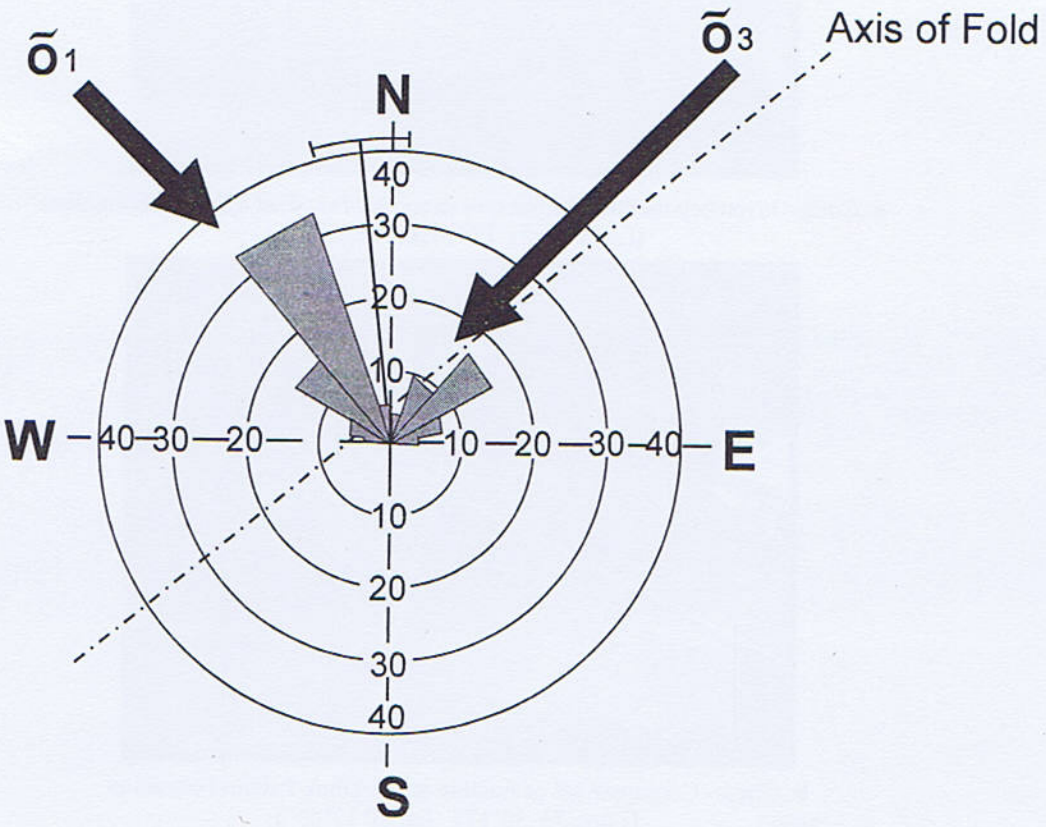

Fig. 3. Rose Diagram showing orientation of fractures and stress analysis of the Dhok Pathan Formation At the Jabbar Anticline

Li = Length of the i^{th} fracture
Wi = width of the i^{th} fracture
N = Number of fractures in the inventory circle
A = area of the inventory circle.

The fracture porosity for the Dhok Pathan Formation at the eastern limb of the Jabbar Anticline ranges from 0.6% to 2% (Table 1).

FRACTURE PERMEABILITY

The permeability within individual inventory circle, assuming no matrix, is estimated from the following equation (Muskat M.,1949);

$$K = (3.5 \times 10^{8}) (1/A) \sum_{i=1}^{N} (Li \times Wi^{3})$$

Where

K = Permeability in darcy,
I = Index to designate each fracture in a inventory circle,
N = Number of fractures in the inventory circle,
Wi = Width of the i^{th} fracture,
A = Area of the inventory circle, and
3.35×10^{8} = Factor to convert cm^2 to darcy

This calculation is also based on a Monte Carlo approach and is similar to that carried out for estimating fracture porosity. The fracture permeability for the Dhok Pathan Formation on the eastern limb of the Jabbar Anticline ranges from 0.1×10^{7} to 3.6×10^{7} darcy (Table 1).

STRESS ANALYSIS

In situ stresses are the current day natural stresses present in the Earth's crust. They are the result of a few components: (1) Gravitational stresses due to the weight of the overburden, (2) Crustal tectonic stresses related to present day tectonic forces such as those resulting from the active collision, (3) Residual stresses locked in the rocks during the past episodes of tectonic and gravitational stresses.

The fracture orientation data can be presented on the Rose Diagram. The Rose Diagram provides an immediate visual estimate regarding any orientation data. A standard Rose Diagram is constructed on a grid, composed of concentric circles superimposed on a set of radial lines.

A fault is passing near the sampling stations, whose strike was NW. Rose Diagrams of the fractures shows that maximum numbers of fractures have NW strike. The principal stress direction is always parallel to the extensional fracture set and normal to the release/longitudinal fractures (Marland P. Billings, 1972) (Davis, G. H. and Reynolds, S. J., 1984, 1996) (Twiss, R.J. and Moores, E. M., 1992).

The general behavior of fractures in study area is as:

- Release fractures have orientation NW-SE (N34W)
- Extension fractures have orientation NE-SW(N65E)

Nearly orthogonal relationship of cross fractures and release fractures suggests that tensile force is normal to the principal stress õ1 direction, whereas compressive force is parallel to the principal stress direction. Hence on the basis of orientation of release and extension fractures, we can say that principal stress direction is from NNW-SSE, while the direction of minimum stress õ3 is NE and the fractures are formed due to the stress related to the formation of the Jabbar Anticline (Fig. 3).

DISCUSSIONS

Extension and release fractures are well developed while conjugate set of fractures are also developed at the eastern limb of the Jabbar Anticline. The data collected from field observations of study area is used to measure the fracture density, porosity and permeability and rose diagram is plotted for interpretation of stress analysis.

Totally seven sampling stations at different parts of the eastern limb of the Jabbar Anticline at Thathi Village were used for fracture analysis. The measurements of fractures were made at bedding plane all the time. Fracture analysis of Dhok Pahtan Formation was carried out by using circle inventory method.

In-situ fracture length, width measurement, the fracture density of Dhok Pahtan Formation of the eastern limb of the Jabbar Anticline ranges from 0.01 cm^{-1} to 0.042 cm^{-1}; the fracture porosity ranges from 0.6% to 2%; and permeability ranges from 0.1×10^{-7} to 3.6×10^{7} darcy.

In-situ stress analysis near the sampling stations showed the presence of a fault trending northwest. Most of the fractures are extension fractures because their strike is perpendicular to the axis of the Jabbar Anticline.

CONCLUSIONS

Only open fractures (Plate 1, c.) were measured in the Dhok Pathan Formation along the eastern limb of the Jabbar Anticline for the estimation of the fracture density, porosity, permeability and stress analysis.

The value of the fracture density, porosity and permeability is 0.01 cm^{-1} to 0.042cm^{-1}, 0.6% to 2% and 0.1×10^{-7} to 3.6×10^{7} darcy respectively

The Rose diagram is plotted for stress analysis and fracture orientation. This shows the generalized direction of principal stress (õ1) is NNW whereas the direction of minimum stress (õ3) is NE.

The measurement of the fracture analysis was applied to further support the already given trend of the Jabbar Anticline.

ACKNOWLEDGEMENTS

The authors express their gratitude to Dr. Khurshid Alam Butt, Director General Atomic Energy Mineral Centre, Lahore for permission to carry out their study in the area under the professional guidance of Mr. Abdul Qadir, Director P and D and Mr. Mumtaz Farooq, Principal Scientist, Atomic Energy Mineral Centre, Lahore, as well as authorizing to publish this paper. The authors are also thankful to Dr. Mohammad Ashraf and Dr. Aftab Ahmad Butt for their critical review of the manuscript. Thanks are also due to Professor Dr. Nasir Ahmad, Director of the Institute of Geology, Punjab University, Lahore for moral encouragement and support. Special thanks are due to Mr. Nadeem Younas for his assistance.

REFERENCES

Billing, M. P., (1972), @Structural Geology@, 3rd ed., Prentice-Hall. Inc., New Jersey 606

Kazmi, A.H., Jan, M.Q (1997), "Geology and Tectonics of Pakistan" Graphic Publishers 139p

Davis, G.H. and Reynolds, (1984), "Structural Geology of Rocks and RegionsJohn Wiley & Sons, Inc," New York, 325-352

Davis, G.H. and Reynolds, S.J., (1996), "Structural Geology of Rocks and Regions" John Wiley & Sons, Inc., " New York 1-737p

Jaswal, T.M., Lillie, R.J. and Lawrence, R.D., (1997), "Structure and Evolution of the Northern Potwar Deformed Zone, Pakistan" *Amer. Assoc. Petrol Geol. Bull.* **81**, 308-352

Jaswal, T.M. & Willian S. (2003), "Kinematics of Eastern Salt Range and Southern Potwar Basin" Pakistan.

Jadoon, (2003) "Fracture analysis of Khaur Anticline and its Implications on Subsurface Fracture System" *Ann. Tech. Conf. Isl. Pakistan.* 235-249

Kazmi, A.H., Jan, M.Q (1997), "Geology and Tectonics of Pakistan" Graphic Publishers. 139p

Muskat M., (1949), "Physical Principal of Oil Production" McGraw Hill, New York 922p.

S.M. Ibrahim Shah "Stratigraphy of Pakistan" *Mem. Geol. Surv. Pakistan.* **12** 89-94

Twiss, R.J., and Moores, E.M., (1992), "Structural Geology" W.H. Freeman and Company.

Geol. Bull. Punjab Univ. 43, 2008.

DIAGENETIC SEQUENCE AND MICROFACIES ASSEMBLAGES OF THE UPPER EOCENE NISAI FORMATION, PISHIN BASIN, BALOCHISTAN, PAKISTAN

BY

ABDUR RAUF NIZAMI
Institute of Geology, University of the Punjab, Quaid-i-Azam Campus, Lahore-54590 Pakistan
Email: raufnizami@yahoo.com

MOHAMMAD ASHRAF
179-B, PCSIR ECHS, Canal Road, Lahore-54590 Pakistan

MUHAMMAD NASIR MAHMOOD
Pakistan Institute of Engineering and Applied Sciences, Nilore, Islamabad Pakistan

MOHAMMAD IMRAN, AAMIR SOHAIL RANDHAWA
Mari Gas Company Limited, Mauve Area, G-10/4, Islamabad Pakistan

AND

MUHAMMAD IMRAN RAFIQUE
Institute of Geology, University of the Punjab, Quaid-i-Azam Campus, Lahore-54590 Pakistan

Abstract: *A detailed study on the diagenetic sequence and microfacies assemblages of the Upper Eocene Nisai Formation exposed at Nisai-Murgha Faqirzai Rud Section, Pishin Basin, Pakistan, was carried out for microfacies and diagenetic framework. The Nisai Formation is widely distributed in the Pishin Basin and is present in the subsurface also. The formation, predominantly a carbonate sequence, is highly fossiliferous at certain stratigraphic levels containing benthonic larger foraminifera belonging to different genera. At these levels the formation grades to a massive reefoid limestone. The microfacies identified are bioclastic rudstone, bioclastic floatstones, bioclastic grainstones, intraclastic grainstones, pelloidal grainstones, bioclastic packstones, bioclastic wackestones and bioclastic mudstones. The signatures of tectonic deformation have, also, been noted which resulted in the development of stylolites and fractures at certain horizons. The bioclastic rudstone, bioclastic floatstone, bioclastic grainstone and bioclastic wackestone microfacies are mainly containing larger foraminifera. Based on these analytical studies it is infered that the Nisai Formation was deposited in the open marine environments of shallow (outer and inner) shelf and the age of Nisai Formation at this section extends up to Upper Eocene.*

INTRODUCTION

The Upper Eocene Nisai Formation is exposed in the Nisai-Murgha Faqirzai Rud, northwest of Muslim Bagh, Pishin Basin, NE Balochistan, Pakistan (Fig. 1). The formation is widely exposed in the Pishin Basin, Axial Belt and Balochistan. The Nisai Formation is predominantly a massive reefoid limestone, along with shale and minor local development of sandstone, siltstone and conglomerate. Although various lithological components of the formation become significant in different areas, yet reefoid limestone of grey, grayish brown, sometimes dark brown to black in color, occasionally nodular, with variable texture constitutes the dominant lithology in studied area and in many other areas. The shale is light gray to yellowish gray, however, mainly gray in colour. The sandstone is thinly bedded, light brownish gray in color and is rarely fossiliferous. The conglomerate is a poorly sorted mass of angular to rounded grains and pebbles of limestone, siltstone and sandstone. The field geological features, like, bed forms, solution weathering and presence of calcite veins were observed at different horizons of this formation.

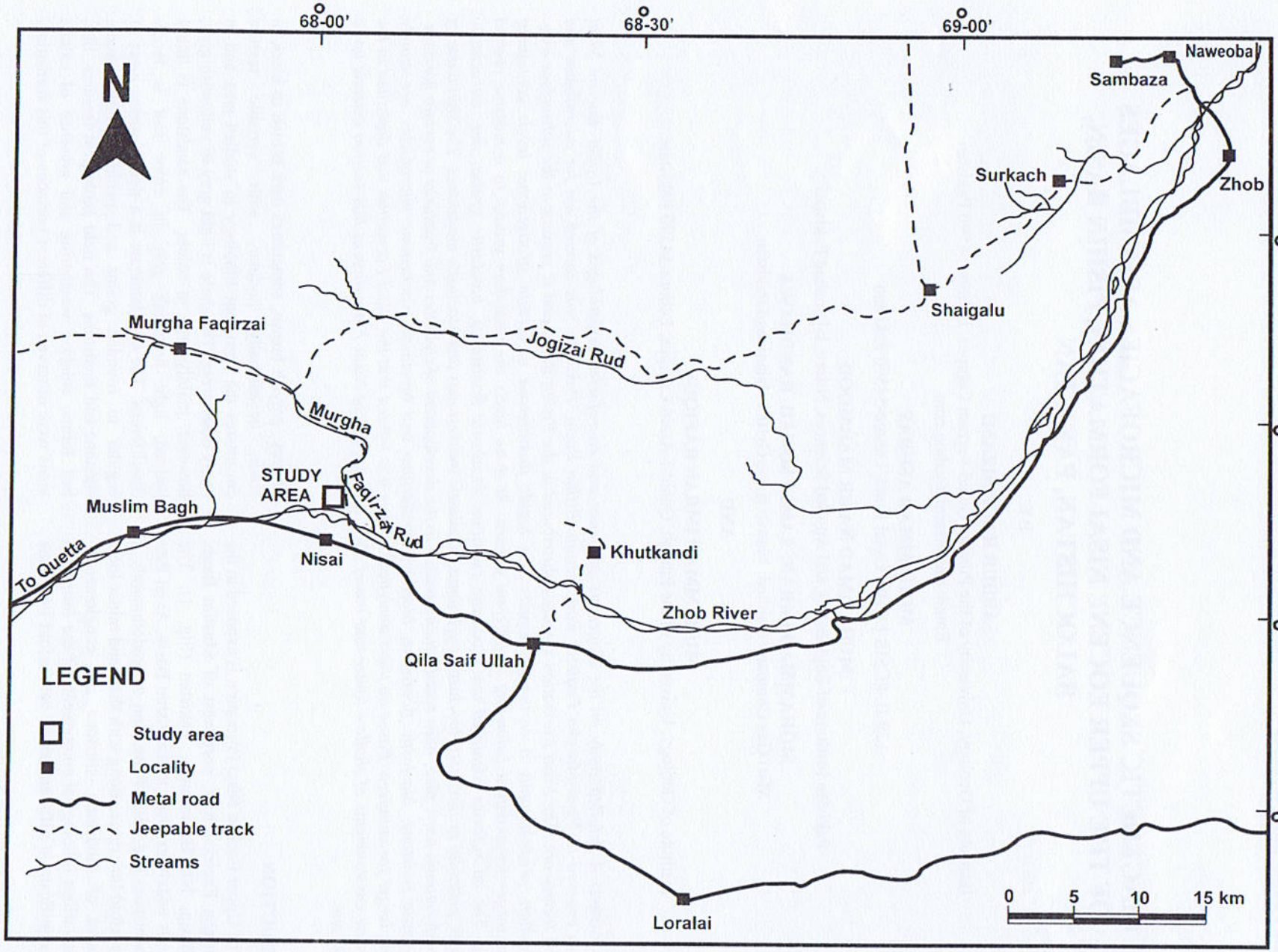

Fig. 1. Location map showing the studied Upper Eocene Nisai Formation, Nisai-Murgha Faqirzai Rud Section,NW of Muslim Bagh, Pishin Basin, Pakistan.
(Modified after Ahmad & Afzal, 2002)

The present authors investigated the sedimentology of reefoid limestone of Nisai Formation in detail and measured its Nisai-Murgha Faqirzai Rud Section. Here the thickness of Nisai Formation is 1027m. A total of 50 samples were collected representing various microfacies, while 28 samples were selected for petrographic studies. The Nisai-Murgha Faqirzai Rud Section (Latitude 31° 55′ 49 N and Longitude 68° 04′ 13 E, falling in Toposheet No. 34 M/16 of Survey of Pakistan, Scale 1: 50,000), could be approached from Muslim Bagh through Nisai on Quetta-Zhob Road and from Nisai via a shingle/jeepable road at a distance of 12km towards north (Fig. 1).

The host area is sandwiched between two major tectonic features, i.e., Chaman Transform Fault and Zhob Valley Thrust. The oldest formation exposed in Pishin Basin is the Upper Eocene Nisai Formation and rests on mélange rocks. The contact between Nisai Formation and Murgha Faqirzai Formation of Oligocene age is unconformable. According to Shah (1977) on the basis of faunal assemblage recorded from the Nisai Formation Eocene to Oligocene age has been assigned to it. However, no Late Eocene fossils have been reported from any area, except the one between Sheikh Wasil and Gidar area and where an Early to Middle Eocene age has been assigned to the formation. Ahmad and Afzal (2002) and Iqbal (2004) reported an Early Eocene age for the Nisai Formation. The authors of present research contribution recorded an age designating species of Nummulites (Plate 2c), the Nummulites *perforates* (Monfort). Hence the age of Nisai Formation at this section extends upto Upper Eocene age on the basis of this documented age diagnostic species of Nummulites and its higher frequency of presence in the investigated section.

First of all reconnaissance survey was carried out to get familiarize with the geology, stratigraphy, and general structural style of the area, hosting Nisai Formation. Field studies were conducted during the month of July, 2006. The field work comprised of outcrop observations, section measurement and representative sampling of various facies of the Nisai Formation. Taking into consideration the lithological character of section sampling was primarily done in the lower and upper reefoid limestone units. By keenly observing the differences in physical appearance of outcrop and lithological variations the representative sampling was carried out.

PREVIOUS INVESTIGATIONS

The name "Nisai Group" was proposed for the Nisai Formation by Hunting Survey Corporation, 1961. The "Nisai Group" represented the "Black Nummulitic Limestone" and conglomerates at the base of "Khojak Shales" of Vrendenburg (1906) and "Ghazij Shales and Older Nummulitic Beds" of Davies (1930). Different packages of lithology, which were previously named differently by various workers, (Vrendenburg, 1904 and 1909 and Blandford, 1879), were redefined by Shah (1977) as Nisai Formation. The availability of information regarding the investigations on various aspects the Nisai Formation and those of geology of Pishin Basin are not encouraging and it is still relatively less investigated basin in Pakistan (Iqbal, 2004). The regional reconnaissance work of Hunting Survey Corporation (HSC, 1961) provides basic information about the stratigraphy of basin. According to Beck (1995) the Kabul Block is a corner of Indo Pakistani Plate which was broken away during the Late Paleocene and Eocene epochs. The oblique convergence of the irregular Indo-Pakistani and Eurasian plates' margins resulted in the formation of Pishin Basin. Ahmad and Afzal (2002) gave detail account of the petroleum prospectivity of the Pishin Basin, where the Nisai Formation is present as an important stratigraphic unit. According to Ahmad and Afzal (2002) the basal black shale of Nisai Formation shows similarity in facies and organic richness with shale in the upper part of Paleocene/Eocene Patala Formation of the oil producing Potwar Depression. The dark brown/black limestone of Nisai Formation resembles in physical character and microfacies with oil shale of Habib Rahi Limestone of Sulaiman Range, while the upper nodular limestone of the Nisai Formation exhibits similarities with oil producing Early Eocene Sakesar Limestone of the Potwar Depression. The present authors carried out detailed field work and produced a lot of field and laboratory data on lithostratigraphy and sedimentology of the Nisai Formation and investigated the diagenetic sequence and microfacies assemblages of its limestones.

LITHOSTRATIGRAPHY

The detailed lithological characteristics of this formation are presented here. Generally the Nisai Formation could be divided into following four units.

The lower shale unit

This unit with 320m thickness is composed of thick shales, laminated sandstones and siltstones and thinly bedded, unfossiliferous limestones. This lower part mainly consists of shales with thin bands of sandstones, siltstones and limestones. The limestone bands are fine to medium grained with 30% Milliolids, and pelloids up to 50% and 10% intraclasts. The shaly material is dark grey to light grey with fragments of bioclasts at places.

The lower limestone unit

It is 120m thick and is composed of highly fossiliferous (faunal assemblages of foraminiferal tests) limestones. It is mainly limestone with some alternating beds of sandstone and shale. The limestone is brownish grey, grey to light grey. The sandstones are sometimes

calcareous (micrite and sparite bearing), and with sparse mudstone clasts. The limestone beds are highly fossiliferous having foraminiferal genera (up to 60%), Nummulites, Assilina, Ranikothalia, Lockhartia, Discocylina, Alveolina and Milliolids.

The upper shale unit

This unit consists of shale of mainly light grey color with intercalations of siltstones and micritic limestones. It is 260m thick. Its upper part is predominantly limestone having some intercalations of shale (25m) and sandstone (about 30m). The limestone is characterized by coquinal texture and is studded with foraminiferal whole tests and shells and fragments, which range from 20 to 70%.

The upper limestone unit

It is comprised of richly fossiliferous and nodular limestones grading in to coquinal/reefoid limestone. Its thickness is 327m. This reefoid limestone of grey, greyish brown, sometimes dark brown to black in color, occasionally nodular, with variable texture constitutes the dominant lithology in the studied area and in many other areas. The limestone is massive reefoid and richly fossiliferous. At certain levels it grades into coquinal limestone comprised predominantly of large shells and tests of various genera of foraminifera.

MICROFACIES ANALYSIS

Petrographic studies of stained and unstained thin sections were made by using the Olympus DX-50 light microscope with attached Olympus DP-12 digital camera. For identification and interpretation of limestone microfacies the classifications proposed by Dunham (1962) and Embry and Klovan (1971) were used.

The Nisai Formation is dominated with bioclastic microfacies from bioclastic mudstones to bioclastic grainstones and floatstones/rudstones facies. The dominant bioclasts belong to different genera of foraminifera, such as, Milliolid (Plates 5b and Plate 4d), and other skeletal grains, such as, Sponges (Plate 4c). For microfacies classification the scheme suggested by Dunham (1962) has been followed for the present research work. To interpret reefoid limestone facies extanded scheme of Embry and Klovan (1971) has been adopted, who further subdivided the boundstone microfacies of Dunham into two categories: Autochthonous (in place) limestone and allochthonous (derived) limestone. Allochthonous reefoid limestones are classified as floatstones, in which more than 10% bioclasts are larger than 2mm and are matrix-supported, and rudstones, which are grain-supported (Scoffin, 1987). In the studied section microfacies, identified and compared with the Dunham classification and Embry and Klovan scheme, include bioclastic mudstones, bioclastic wackestones, bioclastic floatstones, bioclastic packstones, bioclastic grainstones, bioclastic rudstones intraclastic grainstones and pelloidal grainstones.

Grainstones

The petrographic analysis revealed the following sub-microfacies of grainstones. Diversity of bioclastic grains has commonly been observed in all grainstones:

Bioclastic grainstones: Bioclastic grainstones consist of skeletal shells, tests and fragments of different organisms. However, these shells and grains, mostly belong to foraminifera. Bioclastic grainstone with different faunal assemblage are also present (Plates 1a and 2a).Sometimes a few quartz grains are also found (Plate 2a).

Pelloidal grainstones: The pelloidal grainstones are found only at one horizon in this section. This microfacies is comprised of pelloids, having micritic composition. A few bioclastic grains are also found along with pelloids (Plate 4a).

Intraclastic grainstones: The intraclastic grainstone have also been recorded at only one level (Plates 3d and 6b). However, intraclasts are present in other microfacies as component grains. The frequency of their appearance in other microfacies is relatively low.

Bioclastic rudstones

According to Embry and Kalovan (1971) rudstone is a grain supported sub-microfacies of allochthonous (derived) limestones, mainly composed of more than 2mm larger shells and grains of organisms. The rudstones found in the Nisai Formation are composed predominantly of bioclasts of foraminiferal shells, tests and their fragments with more than 6mm in length and 2 to 4mm in width. This microfacies has been recorded at a number of horizons in the reefoid limestone of studied formation (Plates 1c, 4d, 5a, and 6a). Faunal diversity is also observed in these rudstones. The bioclastic shells and fragments present in this microfacies belong to foraminifera, sponges, mollusks, algae and echinoderm.

Bioclastic floatstones

Floatstone, a matrix supported microfacies of allochthonous (derived) limestones, comprised of shells and grains of organisms lesser than 2mm in size (Embry and Kalovan, 1971), is found frequently in studied limestones of the Nisai Formation. Shells and fragments of foraminifera have, mostly, been recorded in this microfacies (Plates 1b and 1d).

Bioclastic packstones

The packstone microfacies is commonly composed of different skeletal shells and grains, mostly belonging to foraminifera. The frequency of occurrence of various skeletal shells/grains shows a range of component skeletal

grains belonging mostly to foraminifera, and less frequently to other organisms (Plate 2b).

Bioclastic wackestones

Dunham (1962) categorized the carbonate microfacies with more than 10% component grains as wackestone. The wackestones interpreted from the Nisai Formation are bioclastic wackestones (Plates 3a and 5b) and some are composed of bioclasts of mainly foraminifera (Plates 2d and 3c) other skeletal grains have been recorded. Stylolites and fractures are also found in this microfacies (Plates 5c).

Bioclastic mudstones

These mudstones are present only at one horizon of Nisai Formation. The interpreted mudstones are bioclastic mudstone with few skeletal grains and fractures, which are filled with calcite (Plate 3b). A medium amplitude stylolite, cross cutting this fracture, postdates the fracture.

DIAGENESIS

The petrographic studies, supplemented with chemical staining techniques, were conducted to decipher the diagenetic settings of the Nisai Formation from the studied section. The nature of diagenetic processes operating in carbonate sediments is predominantly of chemical nature and can be grouped into isochemical (processes rendering sediment into a rock without any drastic chemical change) and allochemical (processes with notable change in chemical composition). As it is common for carbonate rocks diagenetic overprinting has greatly affected the lower and upper limestone units of Nisai Formation. Formation is micritized, dolomitized and calcitized in places, sometimes along with incorporation of iron. Sparite in the micro fractures/structures, stylolites and interstices at different levels, filled and open fractures, development of a variety of cement types, alteration of primary porosity, precipitation of sparite with and without incorporation of iron and development of dissolution fabric are important diagenetic characters recorded in present research work. Chemical compaction and dissolution have caused the point contacts, intergrain embayments, sutured grain boundaries and stylolites. Under the effect of mechanical compaction the brittle deformation caused by over burden pressure and tectonic stresses a fair number of bioclasts is noted broken, sometimes these grains are found highly broken. The diagenetic features, identified and interpreted, are cements, micritic envelopes, compaction and stylolite formation, fractures, dolomitization and dissolution porosity.

Micritic envelopes

These envelopes develop as a result of microbial boring of skeletal/nonskeletal grains and serve to protect the outline and morphology of affected grain. These envelopes are commonly found on grains with original aragonitic mineral composition. Aragonite, being metastable among carbonate minerals, is dissolved in the first phase of diagenesis of carbonate sediments and is replaced by micrite, hence the name micritic envelopes. These micritic envelopes are found on skeletal and non-skeletal grains in different microfacies of this formation (Plate 4d).

Cements

Cement is an important diagenetic feature of the carbonate sediments, which endows strength and stability to the sediment. The well developed cement, always, resists physical, as well as, chemical compaction and fracturing episodes, if any. It is a major and must-occurring diagenetic process and takes place as per provision of favorable PT and kinematic conditions and in the presence of super saturated pore fluids with even geochemical composition in the prevailing diagenetic setting (Scofin, 1987). The cement phases, which happen to be there in the geologic past of Nisai Formation, produced a diverse range of cement types. The identified types of cements in various microfacies of this formation are: cavity and pore filling, circumgranular and syntaxial rim cements. Morphologically these cements are blocky/equant, dog tooth and overgrowth rims, while chemically these are calcitic, ferroan calcitic, dolomitic and ferroan dolomitic cements. Early cements precipitate as fibrous/acicular cement from decomposition of aragonite, while dog tooth cement (circumgranular equent cement), dolomite cement, pore filling calcite cement and syntaxial rim cements precipitate as later diagenetic cements. The microspar precipitates immediately after the deposition of carbonate sediments and is formed by the alteration/recrystallization of metastable aragonite and micritic matrix and signatures as an icon of shallow marine depositional settings (Bathurst, 1964). The following cement types have been noted at different levels and in different microfacies of the Nisai Formation from Pishin Basin:

Circumgranular dog tooth cement: The dog tooth cement is circumgranular equant cement which precipitates as later diagenetic cement. Its examples is given in Plate 2a.

Intergranular cements: The intergranular cements, mostly equent in texture, are found at a number of horizons of Nisai Formation. According to Sheikh (1992) it is the next phase of carbonate diagenesis. The following types of this cement have been observed:

a). Pore filling dolomite cement: The pore filling drusy mosaic dolomite cement resembles with the sparry calcite cement, which is actually cavity filling cement with respect to characteristic drusy mosaic of crystals. It has been found in different microfacies represented in Plates 3d and 4a. In due course of diagenesis at some later stage the

PLATE 1

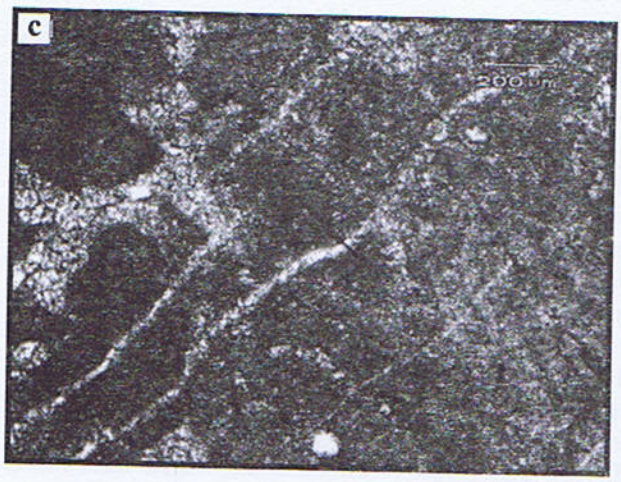

a. Photomicrograph showing pervasive dolomitization in bioclastic grainstone with cavity filling dolomite cement and dolomite filled fracture. (PPL, stained) **Sample No. NS-1**

b. Photomicrograph showing a bioclastic floatstone, composed of large (more than 5mm long) tests of foraminifers and an indeterminate shell in the centre of slide. Point, planar and sutured grain contacts **(all arrowed)** are present due to chemical compaction. (PPL, unstained) Sample **No. NS-3**

c. Photomicrograph showing a bioclastic rudstone along with intergrain multi fractures filled with dolomite (white) and slightly ferroan dolomite. The pink stained bioclasts are of Nummulites **(NM)** tests. Embayments **(EM)** are present along compacted grains as signatures of chemical compaction. Slightly ferroan dolomite **(FD)** has filled the interstices as cement. (PPL, stained) **Sample No. NS-5**

d. Photomicrograph showing an equatoriqal view **(EW)** of Nummulites in bioclastic floatstone. (PPL, unstained) **Sample No. NS-5**

PLATE 2

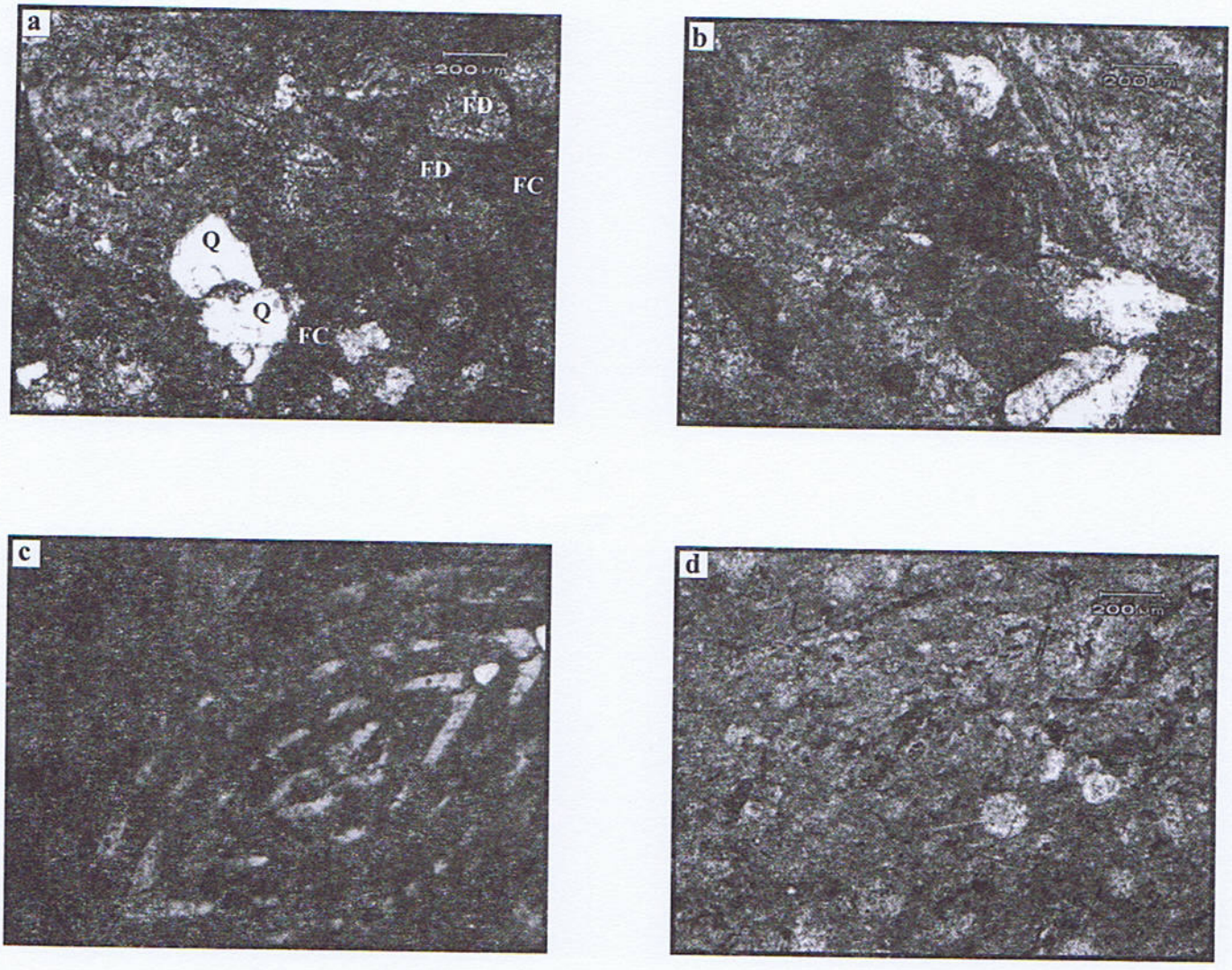

a. Photomicrograph showing a bioclastic grainstone. The dog tooth cement **(arrowed)** has developed on a foram test. The foram shells with original calcitic compostion have altered partially to ferroan calcitie **(FC)** with mauve stain colour and ferroan dolomite **(FD)** with light and deep turquoise stain colour. Quartz **(Q)** grains (clear white) are present also. (PPL, stained) **Sample No. NS-6**

b. Photomicrograph showing a bioclastic packstone. Bioclasts of foraminifera along with intraclasts are present. (PPL, unstained) **Sample No. NS-6**

c. Photomicrograph displays an age diagnostic foraminifera, Nummulites perforates (Monfort), indicating the Upper Eocene age. (PPL, unstained, 20 X) **Sample No. Bio-1**

PLATE 3

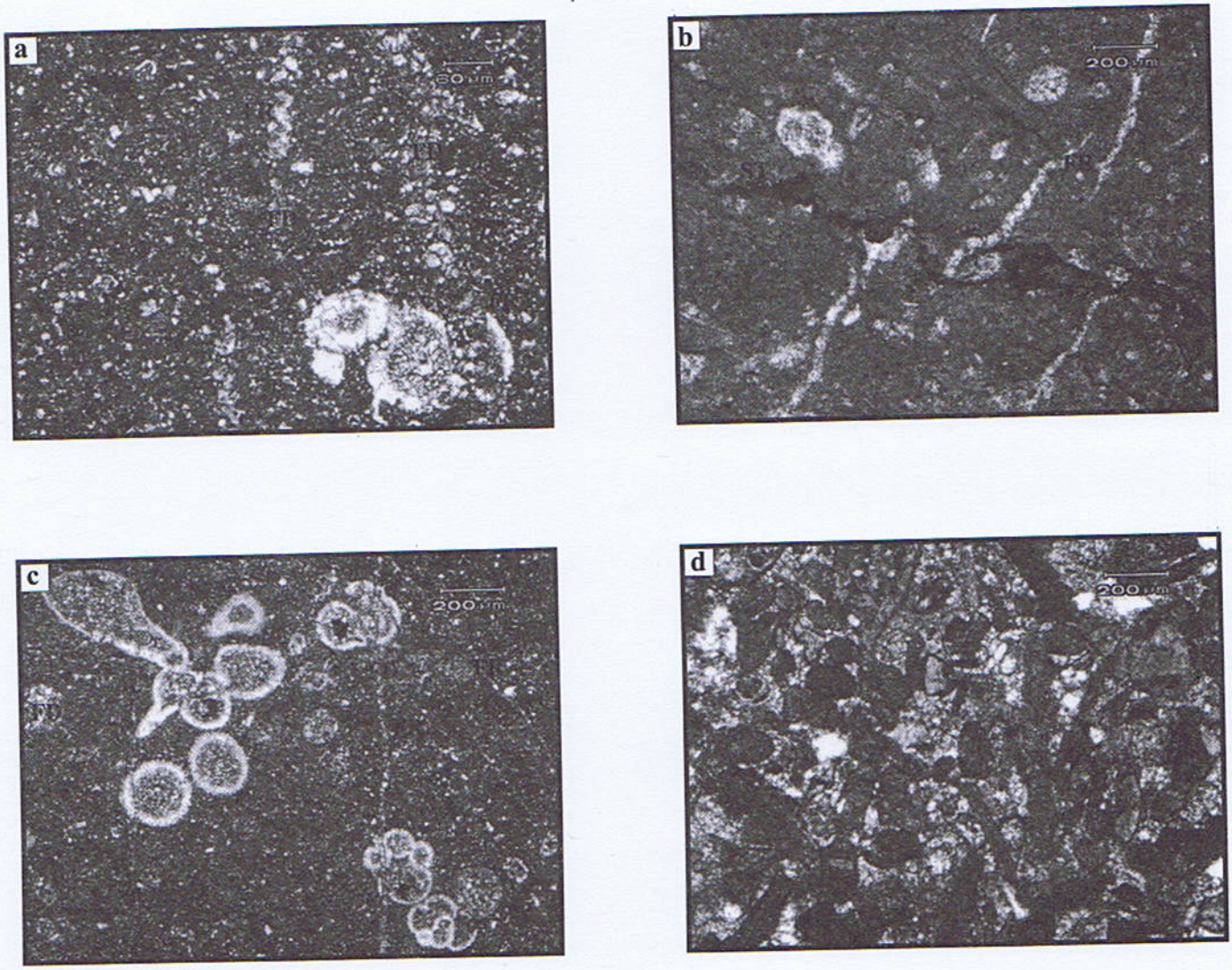

a. Photomicrograph showing pervasive dolomitization (microdolomite) in bioclastic wackestone. Two ferroan dolomite (FD) filled fractures (FR) with turquoise stain color are cutting across the slide. (PPL, stained) **Sample No. NS-10**

b. Photomicrograph showing a low amplitude stylolite **(ST)** in a bioclastic mudstone. The stylolite postdates present fractures (FR) as it is cross cutting these fractures. (PPL, unstained) **Sample No. NS-11L**

c. Photomicrograph showing a microdolomitized bioclastic wackestone. The foram shells are most probably planktons with original composition calcite (pink), altered first to dolomite and then to ferroan dolomite **(FD)** with turquoise stain colour on incorporation of iron. Ferroan dolomite **(FD)** filled fractures are also present. (PPL, stained) **Sample No. NS-11L**

PLATE 4

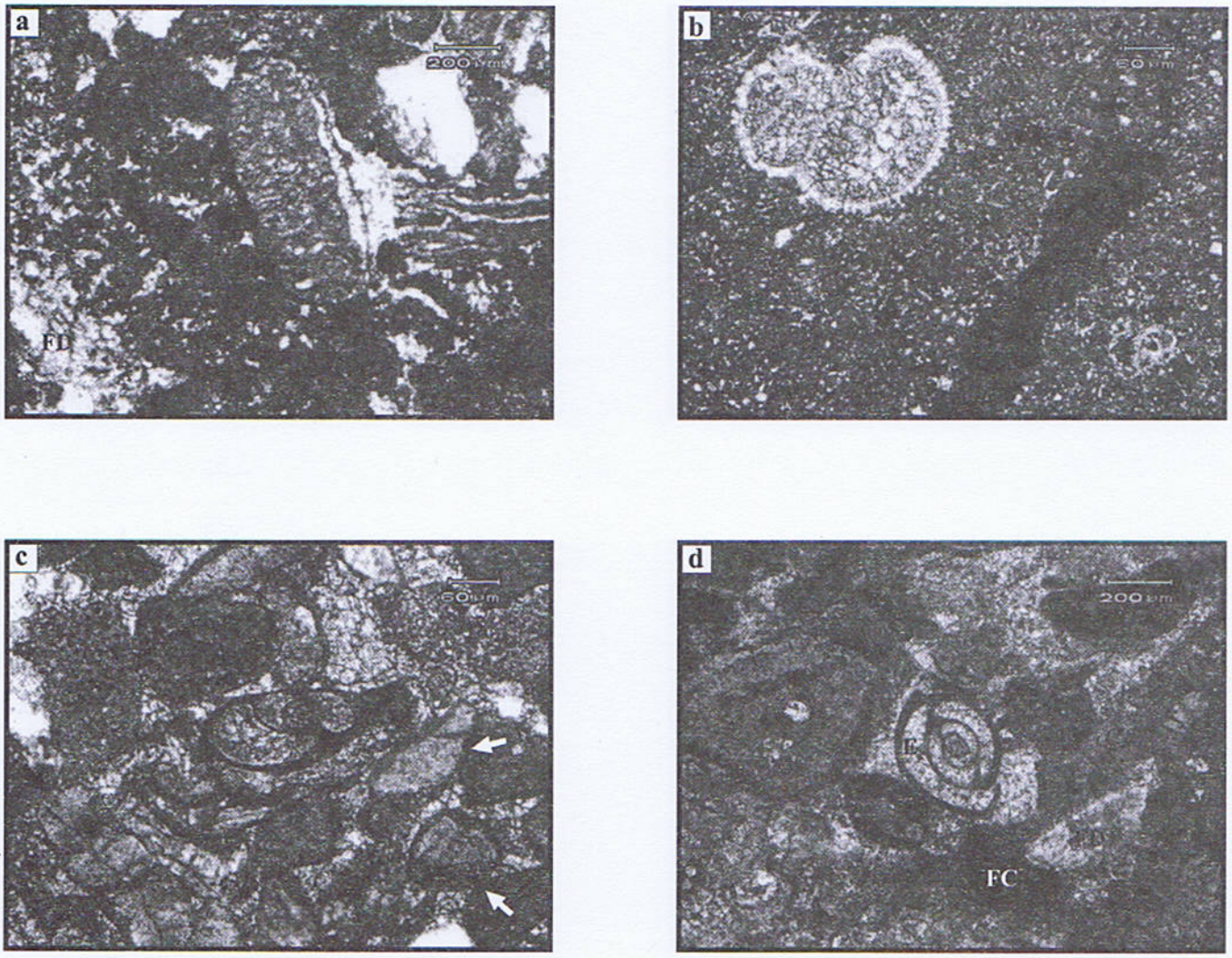

a. Photomicrograph showing a pelloidal grainstone cemented with ferroan dolomite **(FD)** cement. (PPL, stained) **Sample No. NS-34B**

b. Photomicrograph showing a pervasively dolomitized bioclastic wackestone. A large test of indeterminate planktonic foram has undergone two phases of alteration, which is now partially composed of calcite (pink) ferroan calcite (mauve) and ferroan dolomite (turquoise). (PPL, stained) **Sample No. NS-11U**

c. Photomicrograph showing a tightly compacted bioclastic grainstone with sutured grain contacts and embayments (arrowed). A sponge fragment (specked) is present near upper left corner. Slightly ferroan calcite cement with equant crystals is filling pore spaces. Micritic envelopes are present. (PPL, stained) **Sample No. NS-12L**

d. Photomicrograph showing a bioclastic rudstone cemented with cavity filling equent calcite cement. A Milliolid test with micritic envelope **(E)** is present in the centre of slide. Multi phases of alteration and replacement through dissolution are well

PLATE 5

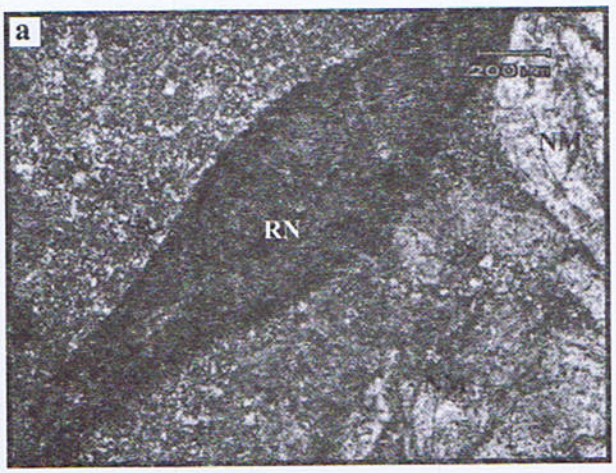

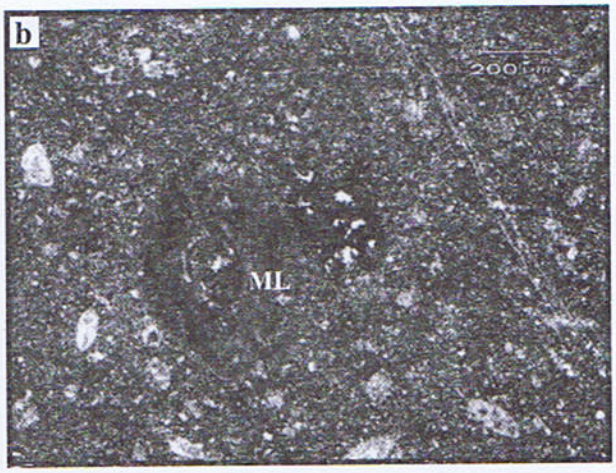

a. Photomicrograph showing Ranikothalia **(RN)** foram test in a bioclastic rudestone with intragrain fractures and solution porosity in. Another foram Nummulites **(NM)** shell, highly broken is also present. The brittle deformantion of bioclasts indicates the postdating of cementation of sediment. (PPL, stained) **Sample No. NS-16**

b. Photomicrograph showing a bioclastic wackestone. A large Milliolid **(ML)** shell (pink) is present. Ferroan. Dolomite filled fractures are also present. (PPL, stained) **Sample No. NS-11L**

c. Photomicrograph showing a low amplitude stylolite **(ST)** in a bioclastic wackestone. Fractures **(FR)** are predating stylolite and are disrupted by it. (PPL, unstained) **Sample No. NS-11U**

PLATE 6

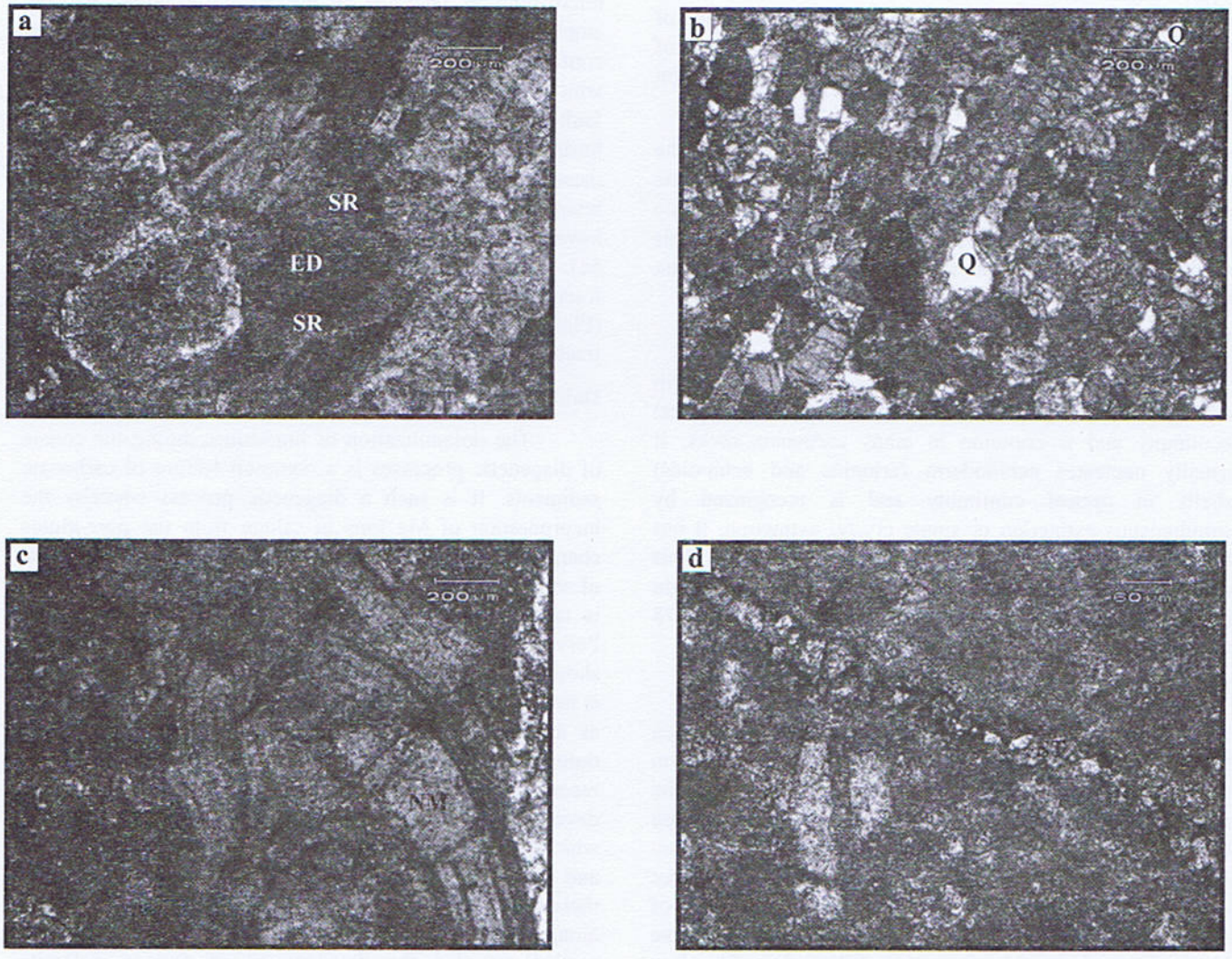

a. Photomicrograph showing a tightly packed bioclastic rudstone. Syntaxial rim **(SR)** cement has nucleated echinoderm **(ED)** grain. The shells and grains of echinoderm are frequent found at this level. (PPL, stained) **Sample No. NS-24**

b. Photomicrograph showing an intraclastic grinstone. A few quartz **(Q)** grains (clear white) are present. (PPL, stained) **Sample No. NS-12L**

c. Photomicrograph showing a broken thick walled Nummulites **(NM)** affected by mechanical compaction, indicating compaction prior to cementation of the sediment. (PPL, stained) **Sample No. NS-16**

d. Photomicrograph showing stylolite **(ST)** and dolomite as stylo-cummulate. (PPL, unstained) **Sample No. NS-1**

incorporation of iron changes its composition as ferroan dolomite (Plates 3c and 4a).

b).Equent cavity filling calcite cement: The cavity filling equent calcite cement has also been recorded from this section. This cement has been identified at a number of levels of the Nisai Formation (Plate 4c). The composition of this calcite cement changes to ferroan calcite on incorporation of iron at some later stage.

c). Cavity filling dolomite cement: It resembles with the cavity filling sparry calcite cement with its characteristic drusy mosaic of crystals. The only difference is of dolomite composition. It is also found at a number of horizons in this section (Plate 1a). The incorporation of iron into dolomite at certain later stage alters it as ferroan dolomite.

Syntaxial rim cement

The syntaxial rim cement is called overgrowth cement also. It grows over the host grain in optical continuity and is common in many carbonate rocks. It usually nucleates echinoderm (crinoids and echinoids) shells in optical continuity and is recognized by simultaneous extinction or single crystal extinction. It has been indentified at only a few horizons (Plate 6a). This cement is mostly considered to be of meteoric origin (Lohmann and Mayres, 1977; Mayres and Lohmann, 1978 and Kaufman, et al., 1988).

Mechanical compaction and fractures

The signatures of mechanical compaction have been recognized in the studie formation. The brittle deformation of various grains (Plates 6c, 5a and 5d) results from the mechanical compaction of sediments. Fractures are commonly found at various levels in the measured section. Lime mudstones particularly bear fractures, which at places are highly fractured (Plate 3b). Various phases of fracturing, sometimes along with stylolite formation, have been observed in this formation (Plate 5c). The low amplitude stylolites developed in the lime mudstone facies have disrupted these calcite filled fractures (Plate 3b). Fractures are also found in other microfacies (Plate 5c). Fractures, filled with calcite (Plates 1c and 5c), dolomite (Plate 1a) and ferroan dolomite (Plates 3a and 5b) have been recorded, which are indicative of different episodes of diagenetic overprinting and changes in the geochemistry of percolating pore fluids.

Chemical compaction and stylolite formation

The signatures of chemical compaction and stylolite formation have been recognized as close packing (Plates 1b and 4c) and deformed morphology of component grains in various microfacies (Plate 1d). Point (Plate 1b), planner (Plate 1b) and sutured grain contacts (Plates 1b and 5d) and inter-grain embayments (Plates 1c and 4c) are produced as a result of compaction. Increased tectonic stresses and/or thousands meters overburden pressure (commonly more than 2000m) produce ultimately pressure solution seams, known as microstylolites in thin section study. The microstylolites recorded in the Nisai formation are low amplitude and are shown in Plate 3b. The features are in conformity with the action of pronounced tectonic stresses, which is also confirmed by the presence of folding and faulting, from small scale to regional scale, in the area hosting studied formation. The frequency of presence of these microstylolites is noted relatively lower. The microstylolites are found mostly in mudstones (Plate 3b), however, these are, also, present in other microfacies (Plate 5c). Some of the microstylolites are found cross cutting the fractures and thus postdate the fracturing of that microfacies (Plate 5c). While some pre-date these fractures as these fractures are cutting across these microstylolites.

Dolomitization

The dolomitization of limestones during the course of diagenetic processes is a common feature of carbonate sediments. It is such a diagenetic process whereby the incorporation of Mg ions in calcite from the pore fluids charged with these ions results in the formation of dolomite of secondary nature. In the Nisai Formation dolomitization is fairly extensive and has developed at various levels. Pervasive dolomitization has been observed in microfacies shown in Plates 1a, 3a and 4b. This type of dolomitization is not texture selective and attacks the whole fabric of rock as a result of which the wholly or partially rock gets dolomitized. The pervasive dolomitization has been recorded in the studied section mainly in the form of development of microdolomite (Plates 1a, 3c and 4b), in which the crystals of dolomite develop in a very small size and sometimes larger magnification is required to observe these crystals. Dolomite is also present as stylocummulate along microstylolites (Plate 6d). Study of stained thin section revealed the development of ferroan dolomite (Plates 4b and 5b). Dolomite has also been recorded at various levels in the measured section as cement (Plates 1a; 2a and 4a).

DISCUSSION

The Nisai Formation is deposited in the form of alternating litho-packages of siliciclastic and carbonate sediments. Its lower most part is predominantly composed of siliciclastic sediments (mainly shale along with a few interbeds of sandstone and siltstone) and miner development of carbonates (a few intercalated beds of unfossiliferous limestone). Package of sediments overlying this part is a sequence of carbonate sediments represented by highly fossiliferous limestone strata with sandwiched 20m thick shale beds. This limestone sequence contains very large faunal tests, shells and bioclasts and is very near

to coquinal lithofacies possessing reservoir characteristics. Bioclasts larger than 6mm are frequently found in it. The next package is again of siliciclastic sediments, which is predominantly a shale sequence with a few intercalated beds of limestone and siltstone. The upper most part, and thickest of all, represents deposition of almost carbonate sediments. This part of Nisai Formation is limestone, very rich in fossils, exhibiting the characteristics of a reefoid limestone at certain stratigraphic levels with well developed and highly enhanced solution porosity fabric like that of lower coquina limestone and is effectively interconnected with open fractures and stylolitic conduits. The bioclastic rudstones, bioclastic floatstones and bioclastic and other grainstones microfacies containing very large skeletal shells and fragments are present in the limestones of Nisai Formation as predominant component.

CONCLUSIONS

The conclusions drawn from the detailed field observations, laboratory and petrographic studies on limestone of Nisai Formation are given as under:

The age of Nisai Formation at this section extends upto Upper Eocene age on the basis of documented age diagnostic species of Nummulites and its higher frequency of presence in the investigated section.

The Nisai Formation is divisible into four lithologic packages regarding its lithostratigraphic succession. However, it is composed of two lithofacies, siliciclastics and carbonates, well recognized in the studied section.

The petrographic studies reveal eight types of microfacies which are: Bioclastic rudstones, bioclastic floatstones, bioclastic grainstones, pelloidal grainstones, intraclastic grainstones, bioclastic packstones, bioclastic wackestones, bioclastic mudstones. The analytical studies of these microfacies lead towards the inference that the Nisai Formation deposited in the open marine environments of shallow (outer and inner) shelf.

The allochemical component grains are predominantly bioclastic shells, tests and particles, which mostly belongs to benthonic foraminifers. Other skeletal grains show a diversity of species, which include echinoderms, sponges, bryozoa and algae.

The diagenetic settings favored the production of a variety of features, which include cements from early marine to late cements, micritization, different types and phases of dolomitization, compaction features and dissolution fabric.

REFERENCES

Ahmad, R. and Jamil Afzal, 2002, "Sequence Stratigraphy of the Mixed Carbonate-Siliciclastic System of Eocene Nisai Formation, Pishin Basin-Distribution of Source Rocks and Reservoir Facies", *PAPG-SPE Annual Technical Conference, Special Publication*, 64-87 Pakistan

Bathurst, R.G.C., 1964, "The Replacement of Aragonite to Calcite in the Molluscan Shell Wall", In: Approaches to Palaeoecology (Ed. J. Imbrie, and N. D. Newell), John Wiley and Sons, New York 357-376, USA

Beck, R. A., 1995,"Late Cretaceous Ophiolite Obduction and Paleocene India-Asia collision in the Western most Himalaya", *Ph.D. dissertation*, Faculty of the Graduate School, Univ. South California, USA

Blanford, W.T., 1879, "The Geology of Western Sind" ", *India Geol. Surv., Mem.*, **17**, 1-196 India

Davies, L. M., 1930, "The Genus Dictyoconus and its Allies: A Review of the Group together with a Description of Three New Species from Lower Eocene Beds of Northern Balochistan": *Royal Soc., Edinburgh, Trans.* **56**, pt. 2, 20, 485-506 UK

Dunham, R.J., 1962, "Classification of Carbonate Rocks According to the Depositional Texture", In: Classification of Carbonate Rocks, *Amer. Assoc. Petrol. Geol. Mem.* **1**, 108-121 USA

Embry, A.F. and Klovan, J.E., 1971, "A Late Devonian Reef Tract on North Eastern Banks Island, North West Territories", (In: Scoffin, P.T. (1987), "An Introduction to Carbonate Sediments and Rocks", Chapman and Hall, New York) 9-10 USA

Hunting Survey Corporation, 1961, "Reconnaissance Geology of Part of West Pakistan-A Colombo Plan Co-operative Project", Toronto, Canada

Iqbal, M., 2004, "Integration of Satellite Data and Field Observations in Pishin Basin, Balochistan", *Pakistan Jour. Hydrocarbon Res.*, **14**, 1-17 Pakistan

Kaufman, J., H. S. Cander, L. D. Daniels and W. J. Meyres, 1988, "Calcite Cement Stratigraphy and Cementation History of the Burlington-Keokuk Formation (Mississipian), Illinois and Missouri", *J. Sed. Pet.* **58**, 312-326, USA

Lohmann, K. C. and W. J. Meyers, 1977, "Macrodolomite Inclusions in Cloudy Prismatic Calcites: A Proposed Criterion for Former High-Magnesium Calcites", *J. Sed. Petrol.* **47**, 1078-1088 USA

Mayers, W.J. and K. C. Lohmann, 1978, "Micro-dolomite Rich Syntaxial Cements: Proposed Meteoric-marine Mixing Zone Phreatic Cements from Mississippian limestones, New Mexico", *J. Sed. Petrol.* **48**, 475-488 USA

Scoffin, P.T., 1987, "An Introduction to Carbonate Sediments and Rocks", Chapman and Hall, New York, USA, 274p USA

Shah, S M I., 1977, "Stratigraphy of Pakistan", *Mem. Geol. Surv. Pakistan*, **12**, 1-138

Sheikh, R. A., 1992, "Deposition and Diagenesis of Mesozoic Rocks, Kala Chitta Range, Northern Pakistan", *Ph.D. dissertation*, Imperial College, London, 360p UK

Vrendenburg, E.W, 1904,"On the Occurrence of a Species of Halorites in Trias of Balochistan", *India Geol. Surv., Mem., Recs.*, **31**, pt. 3 162-166 India

Vrendenburg, E.W, 1906, "The Classification of Tertiary System in Sind with Reference to Zonal Distribution of Eocene Echinoidea described by Duncan and Sladen", *India Geol. Surv., Mem., Recs,* **34**, 172-198 India

Vrendenburg, E.W., 1909,"Mollusca of Ranikot Series, Introductory Note on the Stratigraphy of Ranikot Series", *India Geol. Surv., Mem., Palaeont. Indica*, New Series, **3**, No. 1, 5-19 India

Geol. Bull. Punjab Univ. 43, 2008.

KIRANA VOLCANICS, PAKISTAN-GEOCHEMICAL CHARACTERIZATION AND ORIGIN

BY

SYED ALIM AHMAD

Institute of Geology, University of the Punjab, Quaid-i-Azam Campus, Lahore-54590 Pakistan
Email: syedalim@hotmail.com

AND

MUHAMMAD NAWAZ CHAUDHRY

Postgraduate Centre for Earth Sciences, University of the Punjab, Quaid-a-Azam Campus, Lahore, Pakistan.

Abstract: *Kirana Volcanics are a part of the isolated hillocks of the post-Aravalli sequence, called "MIP" (Malani Igneous Province) in India and "Kirana-Malani Basin" in Pakistan.50 samples of rhyolitic lavas have been analysed geochemically from the Neoproterozoic (870±40) Kirana Complex, district Sargodha, Pakistan. These rocks are intercalated with their mafic counterparts. Geochemically the rhyolites have high-K and are sub-alkaline in character. "Within plate" and "A-type affinity has been proposed for these rocks on the basis of geochemistry. A general LFS vs HFS element fractionation alongwith a positive Ta anomaly similar to A- type granites is clearly observed. As a result of existence of compositional gap between the silicic and mafic magmas in the MIP and KMB the formation of silicic lavas is attributed to anataxis of an intermediate crust. The REE fractionation implies a marginally lower degree of melting for the lava forming magma.*

On the basis of geochemical data the rhyolitic rocks have been divided in to two groups, each derived from a different protolith from within an intermediate crust. Eu correlates negatively with the crystal abundance of each rhyolitic facies.

INTRODUCTION

Kirana Volcanics are a part of the Neoproterozoic Kirana Complex (Ahmad et al., 2000, 2004). The outcrops of this complex occur as isolated hillocks around Sargodha, covering toposheet no 44A/9 and 41A/3 and lie between longitudes 72°-38′-48" to 72°-48′-00" and latitudes 31°-51′ 00" to 32°-15′-00" (Fig.1). The whole complex of hillocks now represented by isolated groups on the Post-Aravalli sequence has been designated as Kirana-Malani Basin (Ahmad et al., 2000). These isolated hillocks (called Malani Igneous Suites in Indian literature) occur as hillocks and scattered hummocks covering areal extent of around 162000 sq. km (including area below cover sediments) in Rajasthan, Thar and Punjab Plain covering parts of Jaisalmer, Barmer, Jodhpur, Kirana, Pali, Jalore, Bikaner, Sirohi and Nagar areas. The whole region is composed of volcanoplutonic association of granite and rhyolite as major rock units along with gabbros and dolerites. Based on field relationships, mode of occurrence, texture and composition, three phases of igneous activity have been identified in the Complex (Ahmad et al., 2004). The first commenced with the eruption of basic flows, followed by voluminous acid flows, which culminated with ash flow deposits. The second phase is represented by intrusion of peraluminous and peralkaline granites as plutons and ring dykes while the third phase is characterized by intrusion of mafic and felsic dyke swarms. The bulk of the volcano-plutonic rocks are overlain by a well-developed sedimentary sequence in Kirana area (Ahmad et al., 2004).

The present study focuses on a Neoproterozoic silicic volcanics with dolerites of the Kirana Complex. The rhyolitic component comprises rhyolitic tuffs, rhyolite porphyries, welded tuffs and ignimbritic sheets associated with silicic lava extrusions, which erupted simultaneously with basaltic lavas. Rocks of andesite composition, though present are rare. This paper is based on the results of field, petrographic and geochemical studies on the rhyolites of the Kirana Complex.

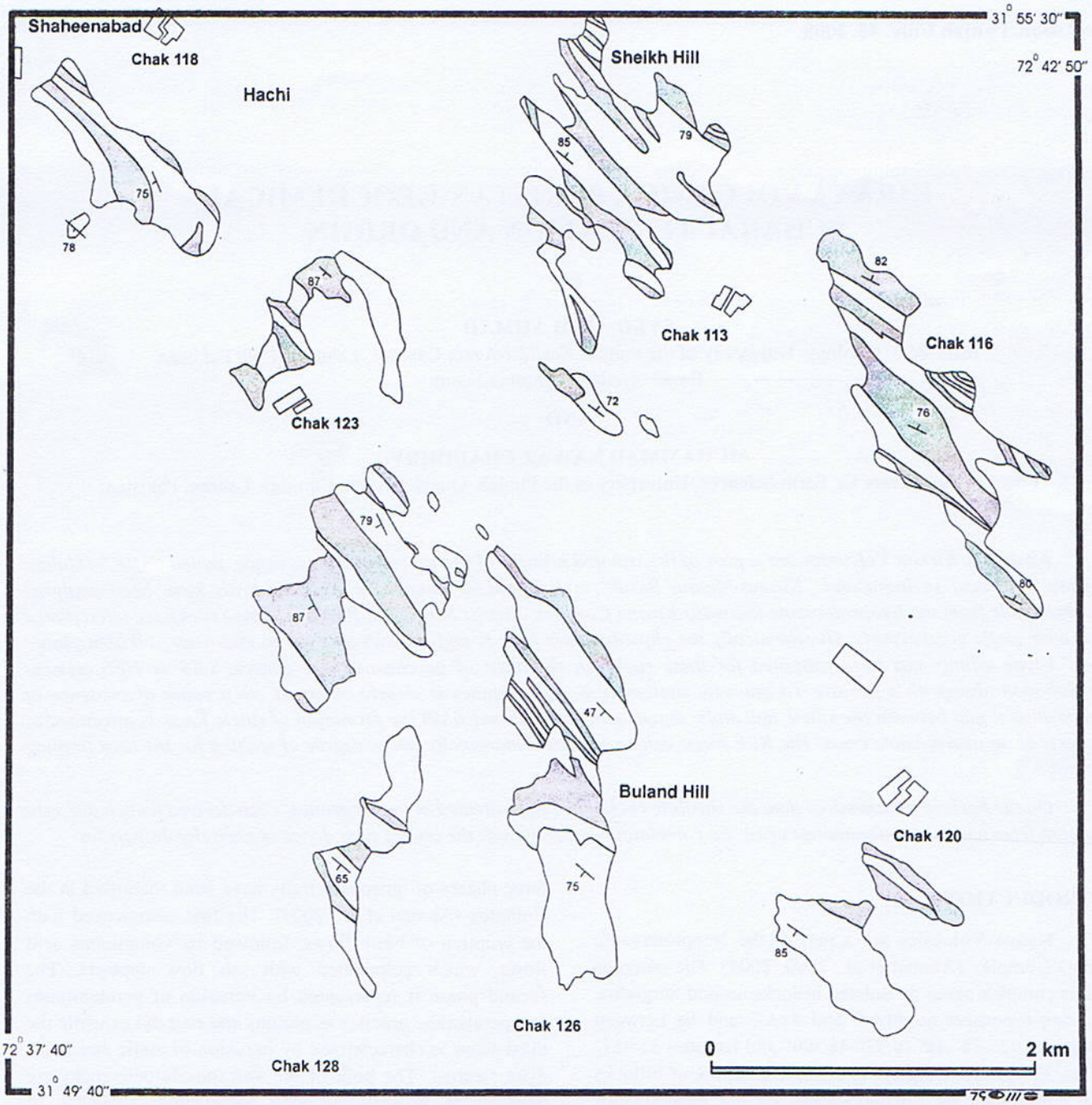

(Amanded after Alam GS., 1987)

LEGEND

Hachi volanics

Rhyolite porphyry, Rhyolite flows

Dolerites (occasionally intercalated, andesites)

Fig. 1. Geological map of Kirana Volcanics

PETROGRAPHY

The volcanics are fine grained and occasionally massive. The rhyolites are characterized by phenocrysts of quartz and feldspar and rarely ferromagnesian mineral phases in microcrystalline or glassy matrix. The rhyolites are generally merrocrystalline, microporphyritic and fluidal. Micro vesicular varieties are also common. The rhyolites, rhyolitic tuffs and rhyolite porphyries are major representatives of silicic volcanic rocks. Generally these rhyolites are merrocrystalline to microcrystalline and rarely holo-hyaline. Notwithstanding physical appearance the volcanics are predominantly rhyolitic in petrographic composition. Generally the rocks are microgranular and composed of minute granules of quartz, altered K-felspar, chlorite and zoisite. Sometimes secondary calcite is present as fracture filling and in the groundmass. Ilmenite/leucoxene occurs as subhedral fine crystals. Occasionally microliths of altered felspar are also seen. Sometimes proportion of microliths increases and the matrix to these microliths is microgranular. The reconstituted texture of the matrix suggests that it represents devitrified and recrystallised glass.

Tuffs are fairly prominent and easy to identify in the field. Generally two textural varieties are identified i.e. lithic felsitic and vitric felsitic. Generally these rocks are typically merrocrystalline i.e. with glassy/spherulitic groundmass and fluidal structure in which are enclosed fragments of K-feldspar/plagioclase and quartz. Hematite/goethite grains may occur along flow foliation. The vitric variety of tuff includes compacted tuff, in which shardy fragments have not been deformed, and also welded tuffs or ignimbrites in which considerable plastic flattening of the original shardy elements has taken place. The presence of later suggests that the deposition of the pile took place under sub-areal conditions. Mineralogical composition of tuffs suggests that they have been derived from magma of acidic composition.

Lava flows are interlayered with slates (often volcanogenic). Lava is of acidic composition and represents typical potassic rhyolites. Lava flows are wide spread in Hachi, Buland, Tuguwali, Shaheenabad, Chak 112, and Chak 128 hills. These are generally greyish, pale green and light brown in colour having quartz and K-feldspar microphenocrysts in glassy/microcrystalline groundmass. In flows the glass to microphenocryst ratio ranges up to 85:15. K-feldspar occurs as subhedral to eumorphic crystals, forming phenocrysts as well as smaller crystals in the groundmass, which are variably sericitized. Some plagioclase laths enclosing chlorite are embedded in microcrystalline/fine grained quartz groundmass. In some cases porphyroblasts of K-felspar (perthite) enclose anhedral quartz and fine laths of albite. Microperthitic texture was also observed in some samples from Chak 123, 128,and 120. Here we find microphenocrysts of quartz and K-felspar are surrounded by very fine anhedral epidote and microcrystalline groundmass composed of quartz and microcrystalline matter. Generally microcrystalline calcite occurs in the groundmass as well as in crystals, filling cracks and other voids. Plagioclase is subhedral to euhedral and occurs as phenocrysts as well as small crystals in the groundmass. It is variably altered to epidote and sericite. Plagioclase laths may enclose chlorite and anhedral epidote. Sometimes laths of plagioclase are embedded in microcrystalline/fine quartz groundmass forming microphenocrystic texture. At places tiny plagioclase laths along with quartz are enclosed by K-felspar perthite phenocrysts. Microphenocrystic texture is common in samples of hills of Chak 123, 128,and 120. Quartz occurs as strained, anhedral grains and microphenocrysts. It may enclose calcite and contain gas and fluids inclusions. Epidote is fine grained and from anhedral to subhedral. Both zoisite and clinozoisite are present. There are secondary minerals formed due to the alteration of plagioclase.

GEOCHEMISTRY

50 rhyolite samples from representative textural varieties were systematically collected across the eruptive sequence of the Kirana Complex. Analyses of the major and trace elements were carried out by wet chemical, AAS, XRF and INAA in the laboratories of the Pakistan Institute of Engineering and Applied Sciences Islamabad and GeoScience laboratories Islamabad. The analyses of the representative samples are given in the Table. 1.

The chemical classification of the Kirana Complex is based on the total alkali-silica diagram (TAS-Fig. 2) of LeBas et al. (1986), LeMaitre (1989) and Middlemost (1991). The SiO_2 boundaries were defined using an equivalent diagram of Ewart (1982). SiO_2 versus Zr/TiO_2 and Nb/Y versus Zr/TiO_2 diagrams (Figs-3, 4 after Winchester and Floyd, 1977) were used as alternate diagrams to check alteration. The igneous rocks of the Kirana Complex exhibit subalkaline trend and range in composition from tholeiite basalt, basaltic andesite, andesite, and dacite to rhyolite. However the intermediate rocks are a minor component and the complex falls into two distinct sets of rocks i.e. mafic suite (dolerite) and felsic rocks (dacite and rhyolite). These rocks represent subalkaline tholeiitic magma activity. The mafic rock suites mostly straddle the low-K (Fig, 5 after Rickwood, 1989) and medium-K boundary; with a few samples showing a trend towards high-K/shoshonites (Fig, 4, 5). With the exception of a few random samples of andesitic composition, a distinct compositional gap exists from 56-wt% SiO_2 to 66 wt% SiO_2. Thus the volcanics show bimodality of dolerite-rhyolite association.

Table. 1.
Major and trace elements analyses of the rhyolites from the Kirana Complex

	TW-613	TW-614	BH-625	FE-630	FE-631	FE-651	FN-669	PD-671	PD-672	T-673	TE-722	SH-731
SiO2	74.15	75.15	77.34	77.18	76.98	76.58	78.46	72.21	79.54	73.67	77.72	77.78
TiO2	0.30	0.50	0.14	0.15	0.16	0.14	0.21	0.26	0.18	0.15	0.65	0.26
Al2O3	13.46	13.14	12.52	11.65	11.33	12.02	12.47	13.55	10.58	11.71	14.70	12.35
Fe2O3(t)	4.02	4.84	1.42	2.72	3.24	4.62	2.23	2.97	1.84	4.21	1.62	3.42
FeO(t)	3.62	4.36	1.28	2.45	2.92	4.16	2.01	2.67	1.66	3.79	1.46	3.08
Fe2O3	1.84	2.23	0.65	1.26	1.49	2.22	1.05	1.36	0.85	2.01	0.74	1.60
FeO	2.03	2.45	0.72	1.38	1.63	2.44	1.15	1.49	0.93	2.21	0.82	1.76
MnO	0.05	0.05	0.05	0.17	0.19	0.51	0.13	0.09	0.11	0.25	0.02	0.05
MgO	0.97	1.37	0.34	0.48	0.40	1.12	0.93	0.46	0.26	1.23	0.53	1.45
CaO	0.56	0.21	2.39	0.82	0.60	1.88	1.90	0.80	1.69	3.35	0.17	1.16
Na2O	2.10	0.04	5.26	1.17	1.39	0.30	0.50	0.04	2.63	0.68	0.04	0.04
K2O	4.53	4.85	0.58	5.74	5.83	2.80	3.19	9.76	3.23	4.73	4.54	3.59
P2O5	0.01	0.05	0.04	0.03	0.04	0.02	0.00	0.01	0.00	0.02	0.10	0.01
Cs	2.56	2.o9	0.94	1.11	1.23	2.24	3.17	3.45	2.45	2.97	2.33	2.38
Rb	192	267	145	148	145	147	157	253	98	139	167	113
Sr	78	51	55	21	24	21	36	52	67	42	14	28
Ba	684	729	448	478	438	479	572	734	326	447	660	428
V	67	57	39	38	44	41	37	55	47	56	78	45
Cr	11	46	28	21	19	16	13	15	9	12	94	17
Co	71	30	29	105	112	99	36	31	44	21	22	21
Ni	4	30	65	7	6	6	6	11	18	8	12	10
Cu	3	12	3	2	2	3	3	1	16	2	7	0
Zn	33	44	35	26	23	26	27	21	45	40	8	50
Ga	31	23	15	26	25	25	19	19	25	26	22	23
Sc	5	11	25	2	6	7	14	17	7	2	6	5
Y	98	90	23	92	87	92	66	84	62	89	44	61
Zr	411	297	118	347	339	348	288	340	300	341	212	394
Hf	11	8	8	13	14	12	9	12	12	11	16	13
Nb	38	24	17	31	36	31	28	29	26	29	15	31
Ta	8.95	6.45	4.38	4.31	4.98	6.09	4.09	2.75	3.66	6.78	4.76	7.74
Th	28.11	20.09	28.11	29.11	30.22	29.12	28.11	24.21	21.41	29.32	16.22	18.32
U	8.34	8.22	8.12	8.34	8.23	8.12	8.32	7.22	7.34	8.12	8.22	6.21
La	79.95	78.77	83.76	93.89	65.98	87.43	66.97	62.98	45.98	90.86	73.77	65.89
Ce	151.33	115.44	145.34	103.45	136.45	155.67	156.78	167.66	85.34	141.44	94.56	117.67
Nd	78.55	65.55	76.77	71.55	75.33	72.54	71.34	68.12	77.34	66.45	67.34	77.45
Sm	16.23	14.34	23.45	16.58	11.34	14.55	12.44	18.29	13.43	17.78	13.44	12.75
Eu	2.54	2.32	5.61	1.87	1.45	1.11	0.69	2.18	2.15	2.05	1.45	1.17
Gd	7.89	8.66	7.88	8.34	9.56	7.55	7.66	7.54	8.67	8.65	7.59	8.87
Tb	4.26	2.55	6.86	2.89	4.56	3.55	3.15	2.81	3.21	3.07	2.34	2.39
Er	5.65	6.09	6.35	6.98	5.98	6.45	4.98	6.66	5.45	5.88	6.09	6.34
Yb	5.76	5.98	5.66	5.88	6.79	4.78	6.76	4.67	6.35	5.74	6.3	5.55
Lu	1.38	0.98	1.05	0.89	0.93	1.06	0.69	0.66	0.87	1.87	0.89	0.77

The geochemical characteristics indicate that the Kirana Volcanics are medium-K-high-K subalkaline rocks (Figs. 5), originated possibly from partial melting of continental crust. The plots of the rhyolites and dolerites on the AFM diagram (Fig. 5, after Irvine and Barager, 1971) straddle the tholeiitic to calcalkaline trend. The plots of dacite and rhyolite on the A/CNK versus A/NK diagram (Fig. 6) exhibit "Peraluminous" character (after Maniar and Piccoli, 1989). This conclusion is supported by geochemical data, petrographic and volumetric features that show that they are not genetically related to mafic rocks by fractional crystallization of mafic magma. The plots of Rb versus Y+Nb (Fig. 7) and Y versus Nb (Fig. 8) of rhyolite exhibit "within plate granite" character (Pearce et al, 1984).

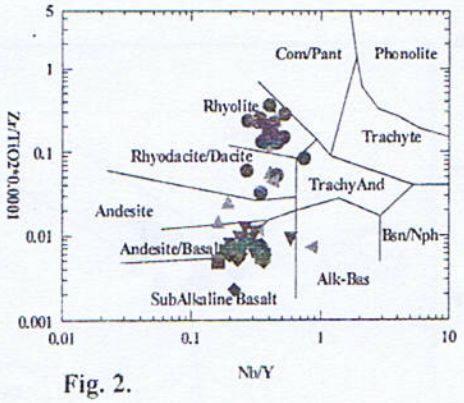

Fig. 2.

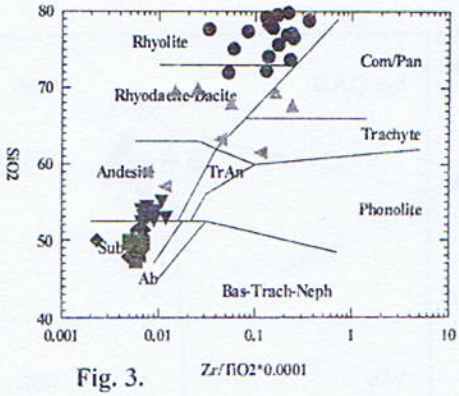

Fig. 3.

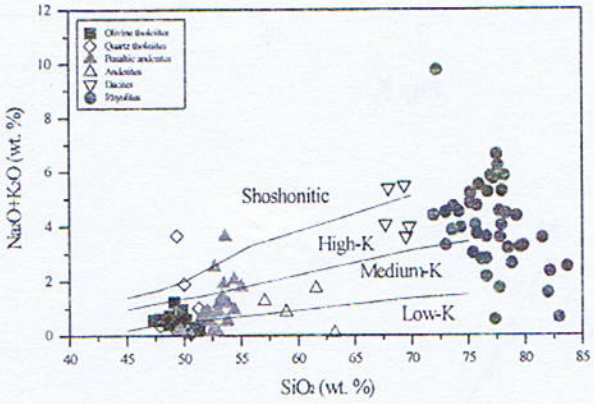

Fig. 4.

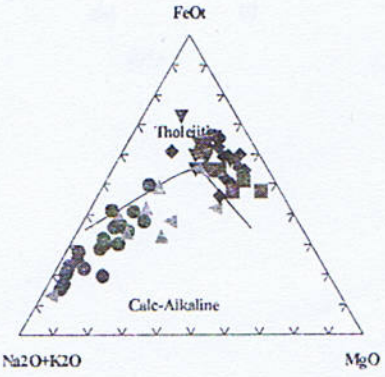

Fig. 5.

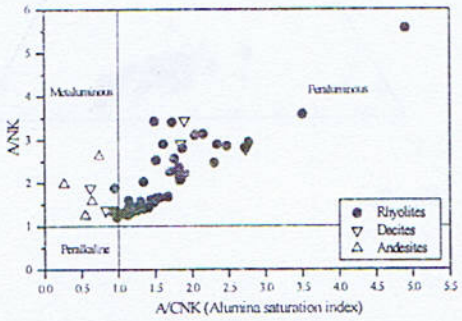

Fig. 6.

Fig. 2. Nb/Y vs Zr/TiO2*0.0001 classification diagram (Winchester and Floyd, 1977), indicating representative rock groups of the Kirana Complex.

Fig. 3. Zr/TiO2 *0.0001 vs SiO2 classification diagram (Winchester and Floyd, 1977). The diagram is indicating representative rock groups of the Kirana Complex

Fig. 4. SiO2 versus K2O (wt%) diagram for the igneous rocks of the Kirana Complex with boundaries for the division into compositional fields of the low-K Tholeiite (low-K), Calc-alkaline (medium-K), high-K Calc-alkaline (High-K) and Shoshonitic suits (after Peccerlillo and Taylor 1976; Rickwood 1989).

Fig. 5. AFM Diagram (based on Irvine and Baragar, (1971) showing the major element compositional diversity in mafic and felsic rocks from the Kirana Complex. All the dolerite/basalt are clearly falling within tholeiitic group.

Fig. 6. Plot of A/NK [mol.%=Al2O3/(Na2O+K2O)] versus A/CNK [mol.%=Al2O3/(CaO+Na2O+K2O)], for felsic rocks of the Kirana Complex (Fields after Maniar and Piccoli, 1989). Peraluminous character is very prominent for the rhyolite of the Kirana Complex.

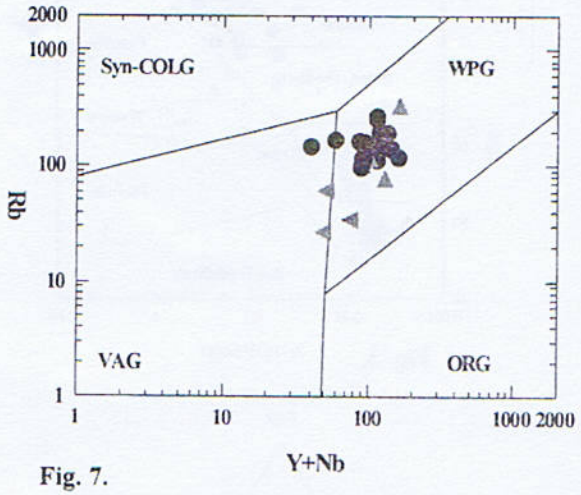

Fig. 7.

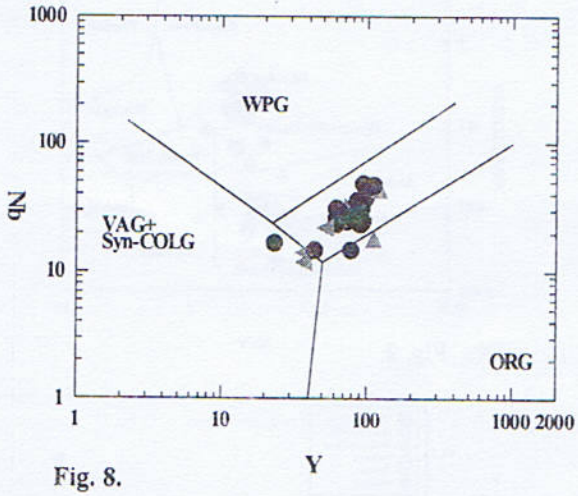

Fig. 8.

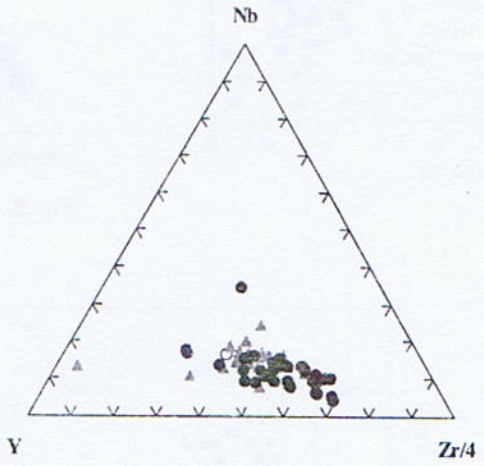

Fig. 9.

Fig. 7. Plots of representative rocks of felsic volcanics from the Kirana Complex on the Y+Nb versus Rb discrimination diagram (after Pearce et al, 1984) indicating "within plate" setting (Rhyolite = filled circle, dacite = filled triangle and andesites = filled angular triangle

Fig. 8. Plots of representative rocks of felsic volcanics from the Kirana Complex on the Y versus Nb discrimination diagram (after Pearce et al, 1984) indicating "within plate setting". Line within the WPG is the approximate boundary between the two groups of A-type granites (after Eby, 1992). Those related to rift, plume, and hot spot plot above and those of post collisional, post-orogenic and anorogenic environments below the line.

Fig.9. Plots of rhyolite and associated felsic volcanics from the Kirana Complex and granite of the Nagarparkar Complex on the Nb-Y-Zr diagram (after Eby, 1992), Almost all the samples fall in "A2" i.e. A-type granites derived from continental crust or underplated crust. "A1" is allocated for A- type granites derived from sources like those of oceanic island basalts (Filled circle = Nagarparkar Granite and Kirana Rhyolite = filled triangle).

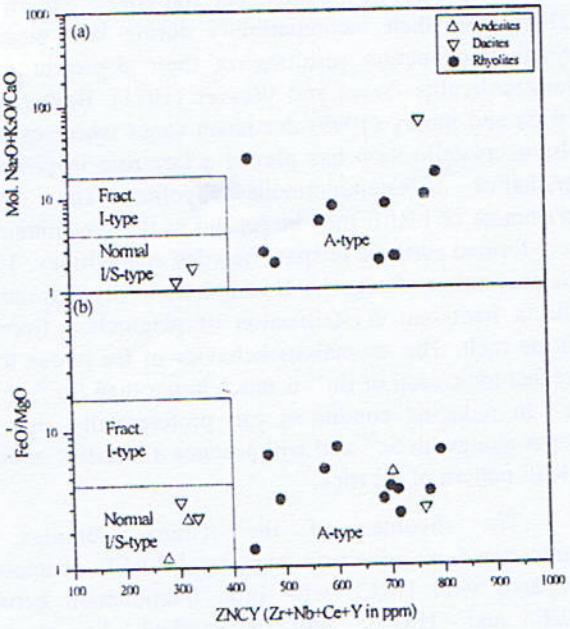

Fig. 10a & 10b

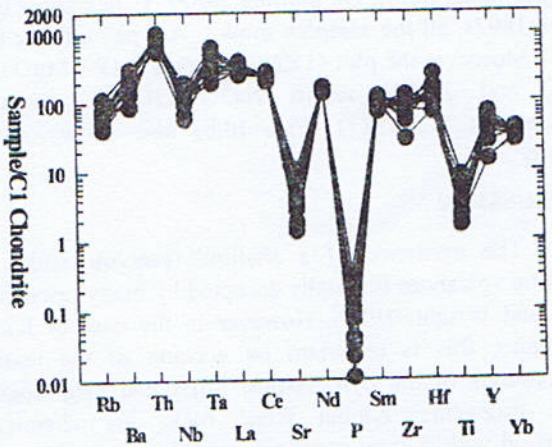

Fig. 11.

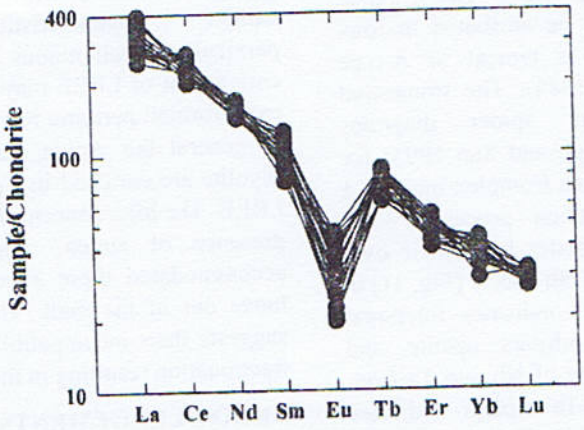

Fig. 12.

Fig. 10,a. Plot of FeOt/MgO and Na2O+K2O/CaO versus Zr+Nb+Ce+Y discrimination diagram (after Whalen et al., 1987) for the Kirana felsic volcanics. All the rhyolite are indicating "A-type" (anorogenic) environment.

Fig. 10,b. Plot of FeO/MgO versus Zr+Nb+Ce+Y discrimination diagram (after Whalen et al.1987) for the Kirana felsic volcanics.

Fig. 11. Chondrite normalized (after McDonough and Sun, 1995) plots of trace pattern of representative rhyolite from the Kirana Complex.

Fig. 12. Chondrite normalized (after McDonough and Sun, 1995) REE plots of the representative Nagarparkar Granite (circle) Kirana Rhyolite (triangle) alongwith Sankara Granite (Pandit and Deep, 1999) (inverted triangle).

The lava flows have a relatively restricted chemical compositional range. On plotting Nb-Zr-Y diagram (Fig. 9) (Eby, 1992), all the samples show " A-type" affinity (Fig. 10,a). Moreover the plot of ZNCY versus FeO^t + MgO (Fig. 10,a) and ZNCY versus Na2O+K2O/CaO diagrams (Whalen et al., 1987) (Fig. 10,b) also show "A-type affinity"

DISCUSSION

The existence of a shallow reservoir under the rhyolitic volcanoes is usually accepted by many researchers (Cas and Wright, 1988). However in the case of Kirana Volcanics, this is uncertain on account of the textural observations of the pyroclastics, Tuffs and their cognate lithic fragments. Kirana felsic rocks are chemically compared with A-type granitoids and rhyolites of bimodal association (Collins et al. 1982; Whalen et al. 1987). The multielement primitive mantle normalized spider gram (Fig. 11) shows that the rhyolites from Kirana Complex are enriched in Rb, Y, U and Zr, a characteristic of A-type granitoids and are strongly depleted in Ti and Sr. Negative Ti anomaly can be interpreted as reflecting ilmenite fractionation. Nb shows low negative anomaly, which is typical of crustal material (Wilson, 1989). The negative anomaly shown by Ba and Sr can be attributed to low-pressure felspar fractionation and is typical of A-type rhyolites/granitoids (Pearce et al., 1984). The Primordial Mantle-normalized, trace element spider diagrams (normalizing values after McDonough and Sun 1995) for representative samples from the Kirana Complex indicate a predominant role of the fractionation processes. The patterns for different magmatic episodes have their own distinct characters. Depletion in Sr, P, Nb and Ti (Fig. 11) in the rhyolite of the Kirana Complex indicates fractional crystallization processes involving felspars, apatite, and ilmenite-magnetite phases. Decoupling of Nb and Ta from other HFSE as a prominent Nb-Ta trough indicates significant crustal incorporation. Significantly, an Nb anomaly has also been reported for other parts of Nagar-Kirana-Malani Basin (Pandit and Deep, 1997; Maheshwari et al., 2001).

The comparatively high concentration of LREE indicates excessive presence of zircon, apatite and sphene, which have accommodated these elements and not allowed them to move out of the melt. The flat HREE pattern (Fig. 12) suggests their incompatibility during later stages of crystal fractionation resulting in their depletion in the granites/rhyolite. Sceal and Weaver (1971), Barberi et al. (1975) and Storey (1995) document cases where extended felspar crystallization has played a key role in producing peralkaline to peraluminous rhyolite. The relative enrichment of LREE may be related to the precipitation of early-formed perthitic felspar (Bowden and Whitley, 1974). The occurrence of negative Eu anomaly in rhyolite samples reflects fractional crystallization of plagioclase from the silicate melt. The anomalous behavior of Eu is due to the fact that ionic radii of Eu^{+2} is much larger than Eu^{+3}, so that Eu^{+2} in reducing conditions can preferentially enter the felspar alongwith Sr^{2+} and will produce a negative anomaly in REE pattern of the rock.

The rhyolites of the Kirana Complex are characterized by relatively high total LREE contents as compared with HREE with little fractionation between LREE and HREE, and a marked Eu anomaly (Eu/Eu*=0.34)(Fig. 12). The rhyolite develop a relative enrichment in Sm with corresponding Eu depletion and exhibit characteristic REE pattern of peralkaline/peraluminous rhyolites/granites. The relative enrichment of LREE may be related to the precipitation of early-formed perthitic felspar (Bowden and Whitley, 1974). In general the within plate A-type peraluminous Kirana rhyolite are enriched in Ce, Sm, Zr, Y, Hf, Ta, Th, Rb and LREE. The high concentration of LREE indicates excessive presence of zircon, apatite and sphene, which have accommodated these elements and not allowed them to move out of the melt. The relatively low HREE pattern suggests their incompatibility during later stage of crystal fractionation resulting in their depletion in the rhyolite.

AKNOWLEDGEMENTS

The authors are highly obliged to Prof. J. P. Burg, Director, Institute of Geology, E. H. Zurich, Switzerland for his guidance during the course of this research project. This research work was carried out under financial support of Punjab University research grant no 211-222-P&D dated 25 6 2002.

REFERENCES

Ahmad, S. A., 2000. Geology and geochemistry of Neoproterozoic Kirana Volcanics, Sargodha district, Pakistan. *Geol. Bull. Punjab Univers.*, **35:** 59-71.

Ahmad, S. A., 2004. Geology, Geochemistry and petrogenesis of the Neoproterozoic Indian Shield extension in Pakistan. *Ph.D thesis, Ins. Geol. Univers. Punjab, Lahore, Pakistan.*,425.

Barberi, Ferrara, G., Santacroce, R., Treuil, M and Varet,J., 1975. A transitional basalt-pantellerite sequence of fractional crystallization, the Bonia Cantre (Afar Rift Ethiopia). *Jour. Petrol.*,.**16:** 22-56.

Bowden, P. and Whitley, J.E., 1974. Rare earth's pattern in peralkaline and associated granites. *Lithos.*,. **7:** 15-23.

Cas, R. A. F., and Wright J. V., 1988. Volcanic Successions Modern and Aricient: A Geological Approach to Processes, Products and Successions *Allen and Unwin*, London.

Collins, W.J., Beam, S. D., White, A. J.R. and Chappel, B.W., 1982. Nature and origin of A-type granites with particular refrence to Southeastern Australia. *Contrib. Min. Pet.*, **80:** 189-200.

Eby, G.N. and Kochhar., 1990. Geochemistry and petrogenesis of the Malani igneous suite,north penisular India.*Jour.Geol.Soc.India.*, **36:** 109-130.

Ewart, A., 1982. The mineralogy and petrology of Tertiary-Recent orogenic volcanic rocks with special refrence to the andesitic basaltic composition range. **In:** Thorpe, *R.S., (ed.). Andesites. Wiley, Chichester.*, 25-87.

Irvine, T.N and Baragar, W.R.A., 1971. A guide to the chemical classification of the common volcanic rocks. *Can.J.Earth. Sci.*,. **8:** 523-548.

Le Bas M.J, Le Maitre,R.W., Streckeisen, A and Zanettin, B., 1986. A chemical classification of volcanic rocks based on the total alkali silica diagram. *Jour Petrol.*, **27:** 745-750.

Le Maitre R .W.,Baterman P.,Dudec A.,Keller J.,Lameyre Le Bas M.J,SabineP.A,Schmid R.,Sorensen H.,Streckeisen A.,Wooley A.Rand Zanettin B.,1989 A classification of igneous rocks and glossary of terms. *Blackwell* ,Oxford.

Maniar, P.D. and Piccoli, P.M., 1989. Tectonic discrimination of granitoids. *Geol. Soc. Amer. Bul.*, **101:** 635-643.

McDonough, W.F. and Sun, S., 1995. The composition of the earth. *Chem. Geol.*,**120:** 223-253.

Maheshwari, A., Sial, A. N., Massimo, C., Chittora, V.K. and Manoel, J.M., 2001. Geochemistry and Petrogenesis of Siwana Peralkaline Granites, West of Barmer, Rajasthan, India. *Gondwana Research.*, **4:** 87-95.

Middlemost, E.A.K., 1991. Towards a comprehensive classification of Igneous rocks and magmas. *Earth Science Reviews.*, **31:** 73-87.*Elsevier Science Publishers, B. V, Amsterdam, Australia.*

Pandit, M and Deep, A., 1997. Geological evolution of the late Proterozoic Sankara suite of rocks, western India. In: Vijayanada, N. P., Cooray, P.G and Mosley, (Eds.), *Geology in South Asia 11. Geological Survey and mines bureau, Sri Lanka*, Prof. Paper **7:** 85-91.

Pearce, J. A., Lippard S.J. and Roberts, S., 1984. Characteristics and tectonic significance of supera-subduction zone ophiolites. In: KoKelaar, B. P and Howells, M. F., (eds.), *Marginal basin geology*. Blackwell, Oxford: 77-94.

Rickwood, P.C., 1989. Boundary lines within petrologic diagrams, which use oxides of major and minor elements. *Lithos.*, **22:** 247-263.

Sceal. J.S.C. and Weaver, S. D., 1971. Trace element data bearing on the origin of sialic rocks from the Quarternary Volcano Paka, Gregory Rift Kenya. *Earth Planet. Sci. Lett.*,**12:** 327-331.

Storey,B.C (1995).The role of mantle plumes in the continental break up: case histories from Gondwanaland .**Nature.,377:** 301-308.

Whalen,J.B.,Currie,K.L and Chappel,B.W., 1987. A-type granites: Geochemical characteristics, discrimination and petrogenesis. *Contrib. Mineral. Petrol.*, **95:** 407-419.

Winchester, J. A. and Floyd, P.A., 1977. Geochemical discrimination of different magma seriesand their differentiation products using immobile elements. *Chem. Geol* **20**: 325-343.

Wilson, M., 1989. Igneous Petrogenesis: A Global Tectonic Approach. *Unwin Hyman*, London, 66-75.

Geol. Bull. Punjab Univ. 43, 2008.

CHARACTERIZATION AND ACTIVATION STUDIES ON AZAD KASHMIR CLAYS

BY

MUSTANSAR NAEEM AND NAZIR AHMAD

Institute of Geology, University of the Punjab, Quaid-i-Azam Campus, Lahore-54590 Pakistan

ABSTRACT:-*Studies were carried out for the evaluation of bleaching capacity of Azad Kashmir clays for edible oils by physical parameters and acid activation process. Minerals were identified by means of XRD, DTA, CEC and other related studies were conducted to explore the activation potential of these clays. The clays are Bentonite in character with subordinate Kaolinite and Illite. Samples were subjected to hydrochloric acid activation by varying the conditions for the optimization of processing parameters. Temperature, solid liquid ratio was kept constant whereas the time and the acid concentration was varied to get optimum values for activation. Efficiency of the process was tested on soybean oil. Study revealed that maximum bleaching value is attained at 80°C, with 2.5 hours treatment at 3N hydrochloric acid concentration.*

INTRODUCTION

Activated clays are used for the decolonization of the vegetable oil in the ghee industry. Vegetable oil contains pigments and various compounds which imparts undesirable colour (Griffiths, 1990). Bentonite has the property to absorb these pigments. The absorption capacity of the bentonite is increased many times by activation process (Christidis et al., 1997). The process considerably increases the absorptive properties of montmorillonite without disturbing the layered crystal structure of these clays (James, et al., 2008). New pores are created by liberation of some ions such as Al, Fe^{+2}, Fe^{+3} and Mg ions from the octahedral layer exposed at edges of smectite, similarly, Si released from tetrahedral layer precipitates in the form of amorphous silica with H ions (Tiwari et al., 1996).Activation process enhances the surface area and pores diameter (Grim, 1962; Srasra et al., 1989; Kaviratna and Pinnavaia, 1994) of the clays thereby absorbing more amount of pigments. Increase in surface area is a function of acid strength and time of treatment of the clay (Zaki et al., 1986; Rhodes and Brown, 1992) along with other parameters. It has been observed (Kardy and Ashraf, 2007) that bleaching capacity of clays is increased more than four times by acid activation process. Tiny pores present in clays contain salts which are removed by the acid treatment thereby increasing the effective absorption area and the bleaching power (Siddiqui, 1968). Salawudeen et al., (2007) showed that activation with hydrochloric acid is more effective as compared with sulphuric acid treatment. Therefore hydrochloric acid was used for the activation of these clays.

Promising deposits of bentonites are available in Pakistan. Bentonite occurs in Dudial and Mirpur of Azad Kashmir is amenable to bleaching process and can be used as decolorizing agents in ghee industry. Detailed mapping and drilling has been conducted by AKMIDC for reserve estimation and to explore the potential of these deposits for ghee industry. Present work deals with the characterization, activation and optimization of processing parameters for these clays. Location of the study area is shown on the map (fig-1).

GEOLOGY

Bentonite deposits of Dudial area are located between Pir Mekal-Sadiqabad and Kathar-Meru gala villages. The Dudial town is located at a distance of about 75 km from Mirpur- Dongali Rawalpindi road, while Sadiqabad village is at a distance of 14 km from Dudial towards north west. These deposits occur in the lower part of Soan formation of Pleistocene age (Shah, 1977) which can be located on survey of Pakistan toposheet no. 43 G/11.Azad Kashmir Mineral Development Corporation (AKMIDC) prepared the geological map on 1:50.000 to 1: 25, 000 scales covering an area from Gora nala in the west to Pir Makal village in the east in a strip of 2.5 kilometers wide and about 10 km long. The geology of the area is described by Hashmi and Pervez (2004).

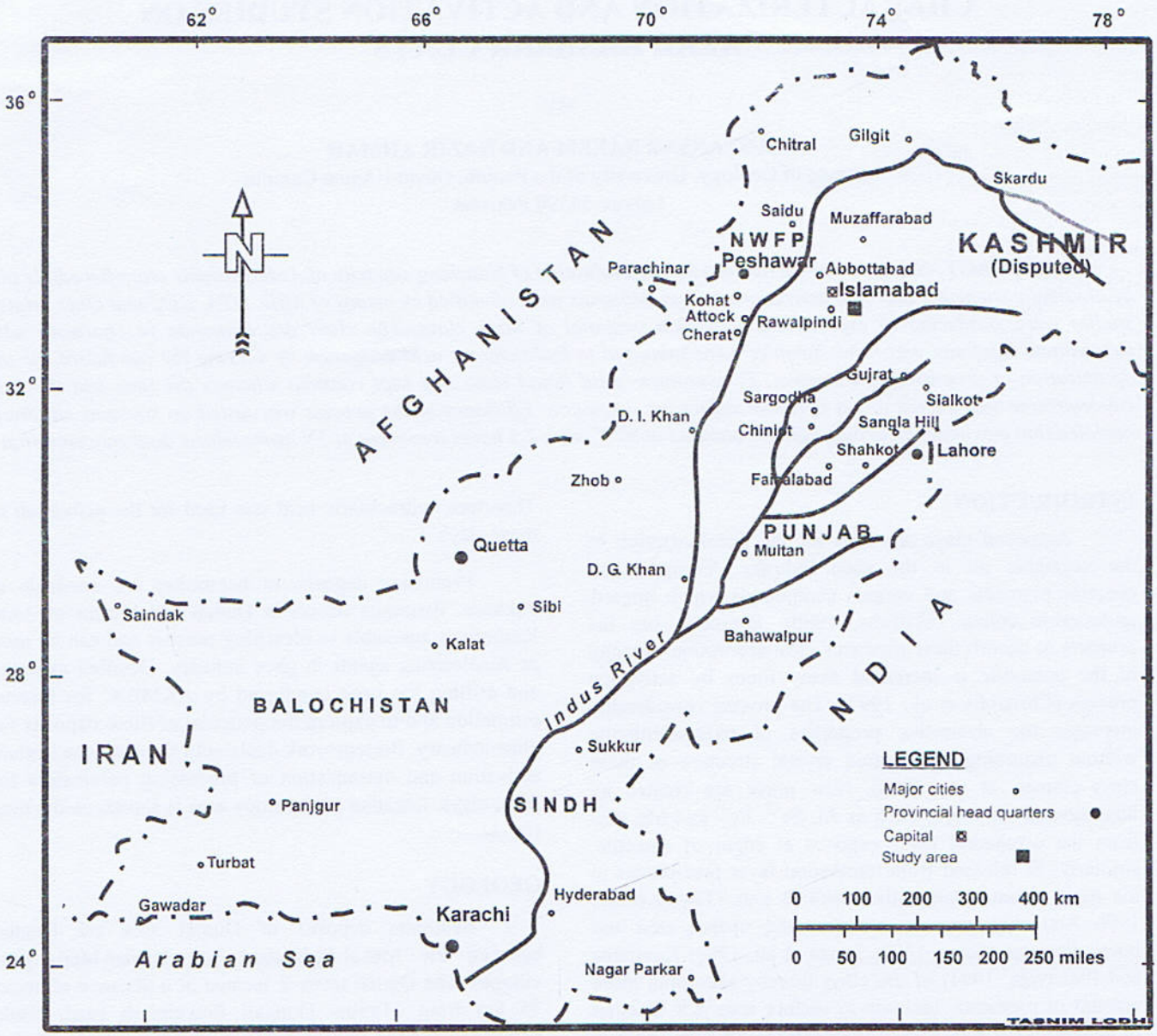

Fig. 1. Location map of the study area.

The area is comprised of sedimentary rocks of Siwaliks group of non-marine origin ranging in age from Late Miocene to Pleistocene. The sequence consists of interbedded sandstone and clay stones with conglomerates and boulder beds. The Bentonite deposits occur in the lower part of the Soan Formation of Pleistocene age. The formation is composed of red maroon clays, green sandstones and loosely cemented beds. Bentonite seams also present on the upper boulder beds of Dhok Pathan Formation. The lower part of Soan Formation is composed of brownish clay stones 0.50 to 18 meters thick, while the thickness of sandstone varies from 2.50 to 10 meters. Silty sandstone, 1-15 meters thick, also occurs in the area.

Bentonite deposits occur as syncline body, the southern limb dips at 45° to 50° to north, whereas the northern limb is gently dipping at 10°-15° due south-west. Trenches, pits, adits and drill holes were used to explore the deposit. Representative samples were collected to carry out study of the deposit for its industrial utilization potential.

MATERIAL AND METHODS

Representative samples of clays were crushed, ground and pulverized in the porcelain pulverizer. Ten samples were prepared by conning and quartering technique for the required studies.

Moisture content, X-ray Diffraction, DTA, pH and acid activation studies were undertaken. A carefully prepared representative sample weighed 2.0 gms was kept in the oven at 105±5°C to a constant weight to determine the moisture content. It is an important property as montmorillonite clays absorb more amount of moisture content. X-ray Diffraction studies were conducted on X-ray Spectrometer System JCX-603 SIEMENS. Powder method was used to determine the 2θ and I values. The results are presented in table 2 and fig-2. pH of the samples were determined with the help of SUNTEX TS-2 pH meter. Clays are hydrated aluminosilicates having extremely small crystalline particles. Therefore, DTA technique is used for the study of these samples DTA studies were conducted with Differential Thermal Analyzer, Schimatzu, Japan (fig-3). Cation Exchange capacity (CEC), Swelling Index and residue on US Sieve No. 200 were also determined to evaluate the percentage of coarser material present in the sample. The results are shown in table No. 1.

For activation process, the sample was passed through 200 US mesh, the clay contents were separated and dried. 10 grams of sample was treated with different concentrations of Hydrochloric acid (HCl) keeping the temperature (80°C) and solid/liquid ratio (1:2.6) constant. The sample was put on hot plate at 80°C with constant stirring varying time and acid concentration for the optimization of processing parameters. The study was conducted on the batch of five samples. The samples after activation were tested for their bleaching capacity. Soybean oil was used to estimate the bleaching characteristics. 100 grams soybean oil was heated to 90 °C on hot plate with constant stirring. The treated clay samples were dried to remove moisture contents. 2.0 grams sample was added to the heated soybean oil for about 30 minutes, with constant stirring and filtered. Bleachability of the oil was evaluated with help of Lovibond Tintometer for colour comparison. Observations were made using 33 mm cell. Original colour of the oil was recorded, the retained colour in the oil was noted, the bleaching value was computed and presented in table Nos. 4a to 4f and fig.-4. Bleaching capacity of untreated samples is shown in table No.3.

Table 1

Sample No.	Moisture %	pH	CEC meq/100g	Swelling Index %	Residue on US sieve No.200 %
DYL-01G	05.01	7.82	72	125	03.00
DYL-02G	04.48	7.70	65	110	10.00
DYL-03G	04.75	8.20	63	115	05.00
DYL-04G	04.95	8.23	59	112	05.00
DYL-12G	02.03	8.35	46	60	02.50
DYL-13G	02.05	8.68	44	45	01.00
DYL-21G	04.25	8.13	47	65	04.00
DYL-09W	02.18	8.38	53	65	01.00
DYL-15W	01.75	8.34	43	40	03.20
DYL-21W	01.32	8.02	39	35	02.00

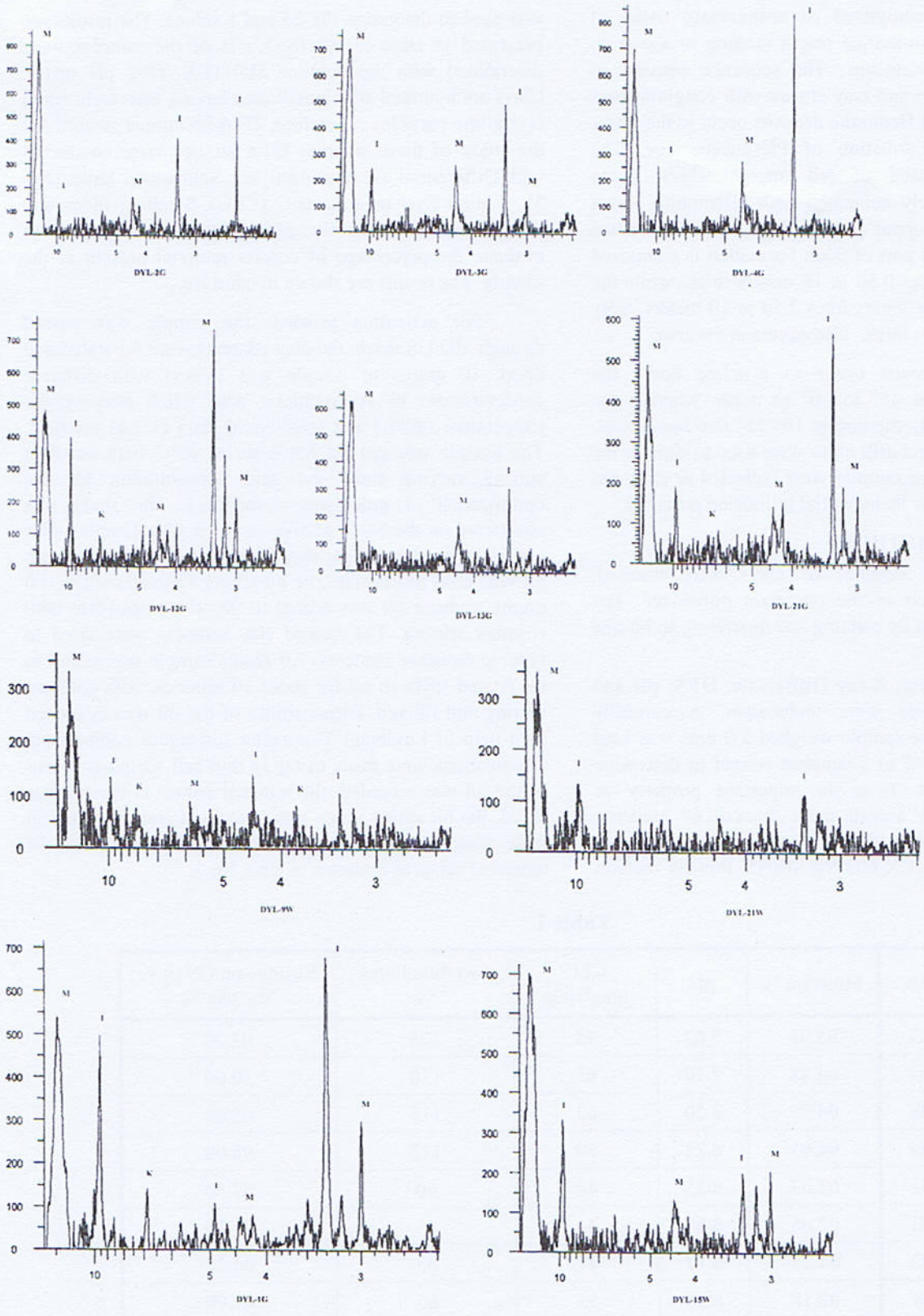

Fig.2. Showing XRD of the samples.

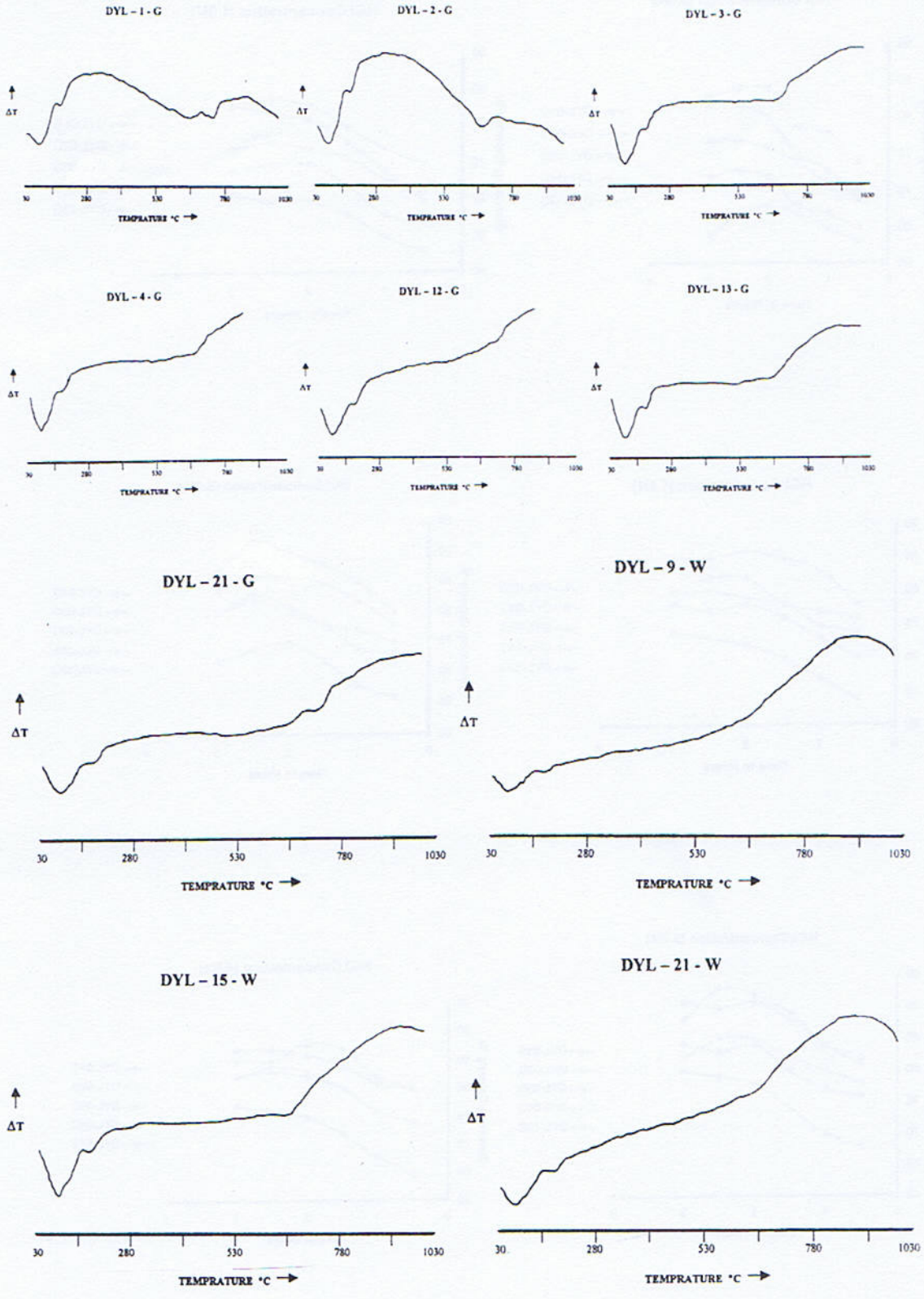

Fig. 3. Showing DTA of the samples.

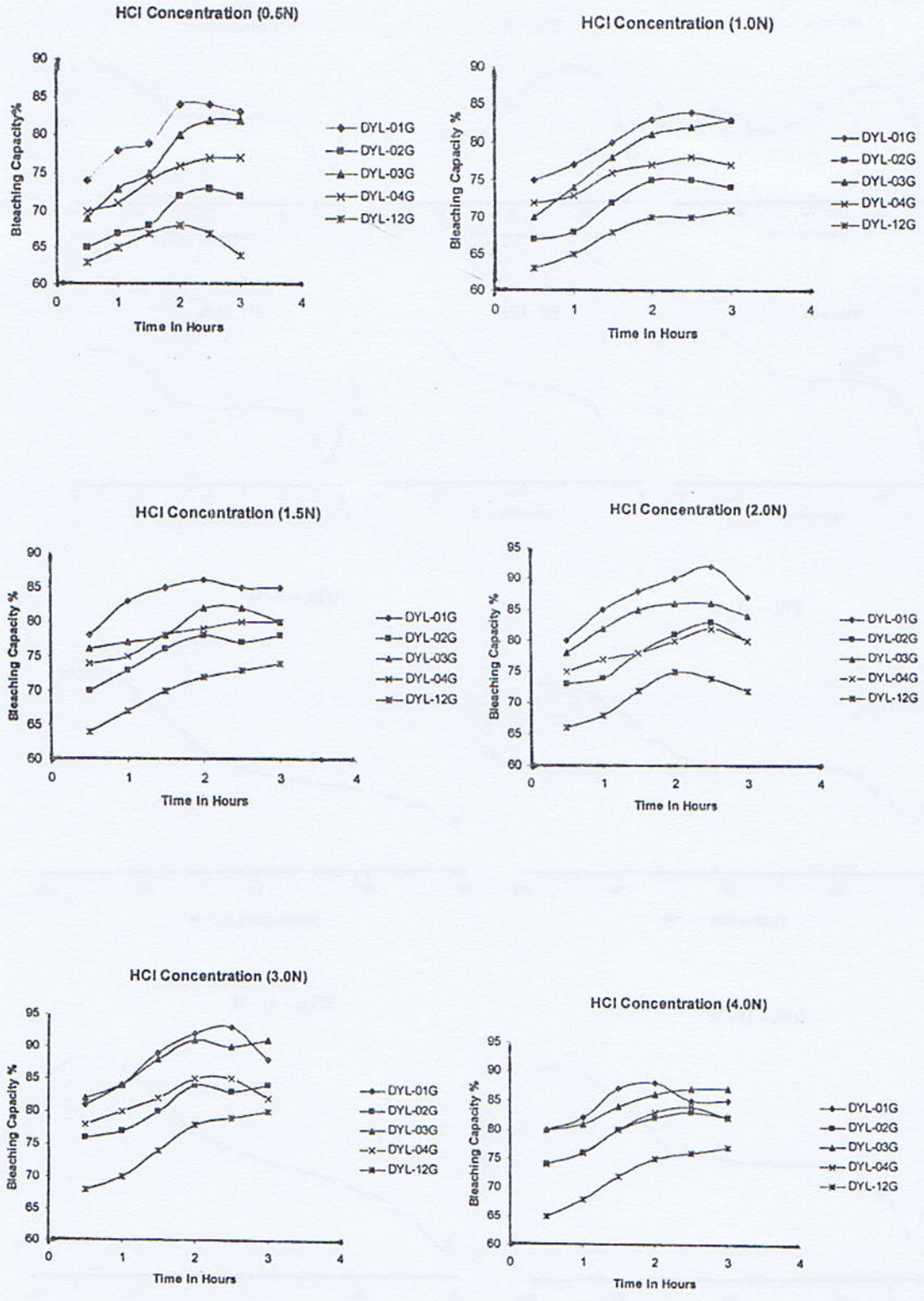

Fig-4. Showing variation in Bleaching capacity with different processing parameters.

Table 2
X-ray Diffraction

Sample No.	Montmorillonite	Kaolinite	Illite
DYL-01G	+++	+	+
DYL-02G	++	+	+
DYL-03G	+++	+	++
DYL-04G	+++	+	++
DYL-12G	++	++	++
DYL-13G	++	+	++
DYL-21G	++	+	++
DYL-09W	++	++	++
DYL-15W	++	+	+
DYL-21W	+	+	++

+++ Major ++ Medium + Minor

Table 3
Untreated clay samples

Sample No.	Bleaching Capacity %
DYL-01G	50
DYL-02G	42
DYL-03G	45
DYL-04G	44
DYL-12G	39

Table 4a
Treated clay samples

Time Hours	Bleaching Capacity (%) at HCl conc. 0.5 N				
	DYL-01G	DYL-02G	DYL-03G	DYL-04G	DYL-12G
0.5	74	65	69	70	63
1.0	78	67	73	71	65
1.5	79	68	75	74	67
2.0	84	72	80	76	68
2.5	84	73	82	77	67
3.0	83	72	82	77	64

Table 4b

Time Hours	Bleaching Capacity (%) at HCl conc. 1.0 N				
	DYL-01G	DYL-02G	DYL-03G	DYL-04G	DYL-12G
0.5	75	67	70	72	63
1.0	77	68	74	73	65
1.5	80	72	78	76	68
2.0	83	75	81	77	70
2.5	84	75	82	78	70
3.0	83	74	83	77	71

Table 4c

Time Hours	Bleaching Capacity (%) at HCl conc. 1.5 N				
	DYL-01G	DYL-02G	DYL-03G	DYL-04G	DYL-12G
0.5	78	70	76	74	64
1.0	83	73	77	75	67
1.5	85	76	78	78	70
2.0	86	78	82	79	72
2.5	85	77	82	80	73
3.0	85	78	80	80	74

Table 4d

Time Hours	Bleaching Capacity (%)at HCl conc. 2.0 N				
	DYL-01G	DYL-02G	DYL-03G	DYL-04G	DYL-12G
0.5	80	73	78	75	66
1.0	85	74	82	77	68
1.5	88	78	85	78	72
2.0	90	81	86	80	75
2.5	92	83	86	82	74
3.0	87	80	84	80	72

Table 4e

Time Hours	Bleaching Capacity (%) at HCl conc. 3.0 N				
	DYL-01G	DYL-02G	DYL-03G	DYL-04G	DYL-12G
0.5	81	76	82	78	68
1.0	84	77	84	80	70
1.5	89	80	88	82	74
2.0	92	84	91	85	78
2.5	93	83	90	85	79
3.0	88	84	91	82	80

Table 4f

Time Hours	Bleaching Capacity (%)at HCl conc. 4.0 N				
	DYL-01G	DYL-02G	DYL-03G	DYL-04G	DYL-12G
0.5	80	74	80	74	65
1.0	82	76	81	76	68
1.5	87	80	84	80	72
2.0	88	82	86	83	75
2.5	85	83	87	84	76
3.0	85	82	87	82	77

DISCUSSION

X-ray Diffraction studies (Table 2) indicate that these are mixed type clays having predominant montmorillonite contents with subordinate amounts of Kaolinite and illite. Kaolinite contents are minor in nature. However Illite is almost invariably associated as medium contents. The clay can be regarded as Bentonite. Values of CEC and swelling index correspond with the montmorillonite contents in the samples (Table 1).

Differential Thermal Analysis shows that most of the clay samples have dehydroxilation temperature in the range of 600-700 °C exhibiting the presence of montmorillonite. Low temperature endotherms depict the association of Kaolinite along with other clay minerals.

Activation studies revealed that the behaviour of the sample vary with montmorillonite contents. It is evident from the results that sample Nos. DYL-01G to DYL-04G responded relatively more favourably to the activation process as compared with other samples (Table-3). Moreover, the value of bleachability increases from 0.5 hours to 2.0 hours treatment, attaining maximum value at 2.5 hours at 80°C (Table 4a-4f). The bleaching capacity increases up to 3N and again decreased afterwards. This indicates that the optimum value of bleachability is attained at 3N acid concentration, 80°C heating time 2.5 hours. Lower values of residue on US mesh No. 200 indicate that the samples do not require complicated process of removal of grit for the activation process.

CONCLUSION

X-ray diffraction, differential thermal analysis, cation exchange capacity and swelling index indicate that most of the clay samples from Dudial area are bentonitic in character. These samples responded well to the activation process and the bleaching capacity was considerably enhanced as compared with raw clays. Keeping solid/liquid ratio 1:2.6, optimum bleaching capacity of 94% can be achieved by heating at 80°C for 2.5 hours at 3.0 N hydrochloric acid concentration. So, these clays can be used as decolorizing agent for edible oil/ghee industry. However, further studies are required to explore the potential of these clays for their other industrial utilization.

REFRENCES

Griffiths, J., 1990. Acid activated bleaching clays. What's cooking in the oil industry. *Ind. Miner.* **276,** pp.55-67.

Grim, R.E., 1962. *Applied Clay Mineralogy.* McGraw-Hill, New York, 422 pp.

Hashmi, S.J., and Pervez, S, 2004. Detailed exploration and evaluation of Sadiqabad-Kathar-Dudial Bentonite deposits, district Mirpur, Azad Kashmir. *Azad Kashmir Mineral & Industrial Development Corporation, Muzaffarabad.* pp. 15-19.

James, O.O., Mesubi, M.A., Adekola, F.A., Odebunmi, E.O., Adekeye and Bale, R.B. 2008. Bleaching performance of a Nigerian (Yola) Bentonite. *Latin American Applied Research.* **38,** pp.45-90.

Kardy, N, Sediek and Ashraf M. Amer. 2007. Sedimentaological and Technical studies on the Montmorillonitic clays of Abu Tartur Plateau, Western Desert, Egypt. *Physiochem. Prob. of Min. Proc.* **41,** pp.89-99.

Kaviratna, H., Pinnavaia, T., 1994. Acid hydrolysis of octahedral Mg 2+ sites in 2:1 layered silicates: An assessment of edge attack and gallery access, mechanisms. *Clays Clay Miner.* **42,** pp.717-723.

Rhodes, C.N., Brown, D.R., 1992. Structural characterization and optimization of acid-treated montmorillonite and high-porosity silica supports for $ZnCl_2$ alkylation catalysts. *J. Chem.Faraday Trans.* **88 (15),** pp.2269-2274.

Salawudeen, T.O, Dada, E.O, and Alagbe, S.O. 2007. Performance evaluation of acid treated clays for palm oil bleaching. *Jour, of Eng, and Appl, Sci,* **2(11),** pp. 1677-1680.

Srasra, E., Bergaya, F., Van Damme, H., Arguib, N.K., 1989. Surface properties of an activated bentonite. Decolorization of rape-seed oil. *Appl. Clay Sci.* **4,** pp.411-421

Shah, S.M.I. 1977. *Stratigraphy of Pakistan*, Geological Survey of Pakistan, Quetta, **12,** 138 pp.

Siddiqui, M.K.H., 1968. *Bleaching earths. Pergamon* Press, Oxford, pp. 32-55.

Tiwari, R.N., Chatterjee, R.N., and Naidu, S.R., 1996. Chemistry of acid activation of Kaolinite Clays and economization of the process. *Chem. Engin. World,* **31,** pp.59-66.

Zaki, I., Abdel-Khalik, M., Habashi, G.M., 1986. Acid leaching and consequent pore structure and bleaching capacity modifications of Egyptian clays. *Colloids Surf.* **17,** pp.241-249.

Geol. Bull. Punjab Univ. 43, 2008.

A-TYPE GRANITES FROM THE NAGARPARKAR COMPLEX, PAKISTAN: GEOCHEMISTRY AND ORIGIN

BY

SYED ALIM AHMAD
Institute of Geology, University of the Punjab, Quaid-i-Azam Campus,
Lahore-54590 Pakistan
Email: syedalim21@hotmail.com

AND

MOHAMMAD NAWAZ CHAUDHRY
Postgraduate Centre for Earth Sciences, University of the Punjab, Quaid-e-Azam Campus,
Lahore-54590, Pakistan

Abstract: *The Neoproterozoic Nagarparkar Complex is characterized by isolated semicircular hillocks of outcrops of "withinplate" A-type peralkaline to peraluminous granites. Geochemically the granites/rhyolites of the Nagarparkar Complex are characterized by high SiO2, Na2O+K2O, K2O, Fe/Mg, Al2O3, Zr, Nb and Y and low CaO and Sr. Majority of samples show moderate iron enrichment. The rocks show the characteristic trend of alkali enrichment and depletion of Ti, Fe, Mg and Ca, which are comparable with the rift-related mildly alkaline suites worldwide. Another characteristic feature of the alkaline/mildly alkaline felsic volcanoplutonics of the Nagarparkar area is their enrichment in incompatible trace elements similar to other peralkaline rocks of the Basin. High values of incompatible trace elements like Zr, Nb, Ce, and Y are characteristic of the granites/rhyolites under study. The multielement primitive mantle normalized spidergrams show that the granites/rhyolite from Nagarparkar Complex are enriched in Rb, Y, U and Zr, a characteristic of A-type granitoids. These granites are also strongly depleted in Ti and Sr. Negative Ti anomaly can be interpreted as reflecting ilmenite fractionation. Nb shows low negative anomaly, which is typical of crustal material. The negative anomaly shown by Ba and Sr can be attributed to low-pressure felspar fractionation and are typical of A-type granitoids. Primitive mantle normalized spider diagrams show that the Nagarparkar granites/rhyolites are enriched in Rb, La, Ce, Zr and Y and depleted in Sr, Ba, Ti, P and show negative Nb anomaly, which is typical of upper crust (hypersolvus). The Chondrite normalized spidergrams show that LREE are enriched as compared with HREE. A wide variation in Eu/Eu*values suggest felspar fractionation. P.I Index of majority of samples varies from .87 to 1. A/CNK versus ANK plots clearly confirm peralkaline to peraluminous nature of the rocks. The presence of Na-amphibole in the granites further confirms the alkaline nature of the granites. Granites/rhyolite plot as "alkali granite" in the QAP diagram. The normative appearance of acmite and nepheline in some samples further supports the alkaline nature of these rocks. The granites/rhyolites of the Nagarparkar Complex exhibit "within plate" setting on plotting in different discrimination diagrams.*

INTRODUCTION

The peralkaline rock complexes of the West Indian Shield at Thar and Rajasthan areas on the both sides of the Indo-Pakistan border, has isolated hillocks of magmatism represented by the Nagarparkar, Malani, Kirana, Siwana, Tosham, Mount Abu and Gurapratapsingh, complexes (Kochhar, 1973, 1974, 1984; Bushan.1985, Naqvi. 1987; Eby, 1990; Rathore et al., 1991; Butt et al., 1992 and Ahmad et al., 2000). This study consists of geochemistry of the peralkaline granites of the Nagarparkar Complex constitutes a distinct anorogenic igneous cratonic rift assemblage of the widespread magmatic activity and is a part of widespread Late Proterozoic Malani Igneous suite extending from western Rajasthan (India) to Sindh Province in Pakistan. The Complex constitutes two distinct magma

series; the older series represents the plutonic subalkaline association of gabbro, diorite, granodiorite and granites, while the younger volcanoplutonic magma series represents pulses of bimodal suites comprising alkali dolerite and alkali rhyolite/granite. These intrusions of tholeiitic and subalkalic mafic dykes and coeval magmas in the Nagarparkar Complex are related to the Neoproterozoic rifting of NE Gondwanaland, and are therefore, fundamental in understanding the interaction between magma genesis and the geodynamics of sub continental lithospheric mantle beneath the Northwestern margin of the Indo-Pakistani plate.

The Nagarparkar Complex is a multi-intrusion mildly alkaline magma association of gabbro, alkali-granite, emplaced probably as a horseshoe shaped ring dyke complex. Such complexes are exclusively confined to the rift-valley system of extensional environment worldwide (Le Bas, 1986 and Woolly, 1992). It is generally believed that such alkaline complexes are formed as a result of continental rifting, characterized by alkaline differentiates.

This paper presents the geochemistry of the granites alongwith crystallization history from the Nagarparkar Complex based on major and trace element geochemistry and microprobe analyses.

GEOLOGICAL SETTING

The Nagarparkar Complex is situated at the extreme southeast of Thar Desert of Sindh near the Runn of Kutch (24° 15' to 24° 30' latitude, 70° 37' to 71° 07' longitude) and covers an area of about 450 sq km (Fig.1). The earliest accounts of the geology of the Nagarparkar rocks are recorded in Geological Survey of India (Wynne, 1867 and Fermor, 1932). A map of the area and description of the basic intrusions and granitic rocks were presented by Kazmi and Khan (1973) who defined the Nagarparkar Complex as Precambrian basement. Description of geology and petrographic data of various rock units of the Nagarparkar Complex are presented by several workers (Shah, 1973; Butt et al., 1989, 1992; Muslim et al., 1997 and Jan et al., 1997). These workers are of the opinion that the Nagarparkar Complex is a part of Precambrian fragment of the Western Indian Shield. The granites of the complex are considered to be the extension of the post-Aravalli magmatism in the Late Proterozoic. They may have been generated as a consequence of sinistral shear along the Narmada-Son lineament and crustal anataxis in the continental anorogenic environment (Butt et al., 1997 and Jan et al., 1997). The basement may have undergone a tectono-metamorphic event before the emplacement of the granites.

The gabbroic intrusions occur near Dhedvero, Karai, Karki, Parodhra and Ramji-Ka-Vandi areas. They are dark green massive and generally coarse to medium-grained. At places, particularly around Dhedvero, they are highly weathered, sheared and show foliation. Present field investigations and petrographic studies clearly indicate that the gabbroic intrusions locally have been subjected to variable alteration and weathering. Near Dhedvero, chloritization and epidotization is generally observed.

Typical adamellites are exposed in Wadlai area. Jan et al (1997) coined the term 'Mottled' pink granite for this adamellite rock found NE of Mokrio village. Petrographic and geochemical studies shows that the rock is a medium to coarse-grained alkali adamellites rather than adamellite as believed earlier (Muslim et. al, 1997).

The Nagarparkar Granite occurs near Nagarparkar town along the northeastern margin of Karunghar Hill. Other exposures of this unit are found in Bhodisar, Dinsy, Waravai Dhedvero and NE of Kharsar. The granite is medium to coarse grained, mostly homogenous and leucocratic. It exhibits spheroidal weathering surfaces. The granite in the Nagarparkar and Bhodisar is intruded by aplites, acid porphyry dykes and doleritic dykes (Kazmi and Khan, 1973; Butt et al., 1992 and Muslim et al., 1997).

Several small dykes of felsic composition are found intruding the older lithologies, particularly in Dhedvero and Nagarparkar localities. They range from rhyolite porphyry to aplite and microgranite. Best exposures of acid porphyry and microgranite dykes occur in Dhedvero, Chanida, Dhanagam Ghantiari and Dinsy areas.

Major outcrops of rhyolite and microdiorite occur near Sadarous and Dungri-in the form of domal shape plugs. Small bodies of rhyolite unit are also found associated with the Grey Granite and the granitic stocks in Dinsy and near Mokrio. The rhyolite unit is homogeneous, dark grey and dark brown in colour, fine-grained, subporphyritic at places glassy-looking and apparently banded.

Grey Granite covers the major portion of Karunghar Hill, forming a large plutonic body striking in the NW-SE direction. The exposures of this unit are found at many places including Karai, Dungri, Ghantiari, Rarko, Karai, Adhigam and Mau. The Grey Granite is undeformed; medium to coarse grained, contains xenoliths of dolerite and is characterized by peralkaline mineralogy (Na-amphiboles are present in most of the samples studied)

Churio Granite occurs as isolated outcrops in Churio and Virawah. It is coarse grained, off-white to light pink in colour, leucocratic and shows alkaline character. This type of granite is also exposed at Mokrio, Sadarous and Dungri.

GEOCHEMISTRY

The major and trace element analyses are given in Table. 1. The chemistry of the Nagarparkar Complex is

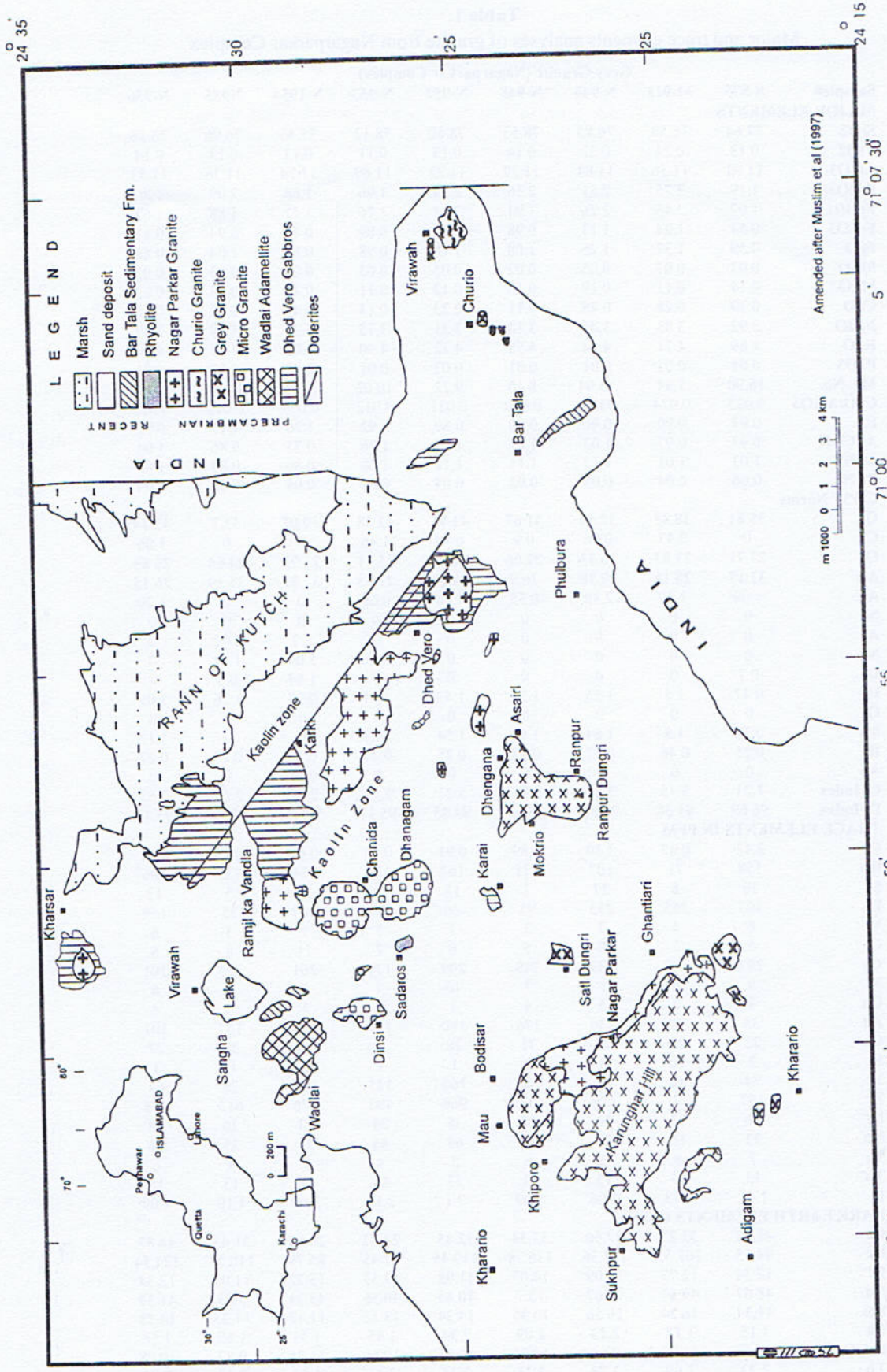

Fig. 1.. Geological map of Nagar Parkar area

Table 1.

Major and trace elements analyses of granite from Nagarparkar Complex

	Grey Granite (Nagarparkar Complex)								
Sample#	**S-875**	**M-913**	**N-946**	**N-948**	**N-952**	**N-953**	**N-1954**	**N955**	**N-956**
MAJOR ELEMENTS									
SiO2	77.64	76.59	76.83	78.53	78.50	78.12	75.46	76.96	78.18
TiO2	0.13	0.24	0.22	0.14	0.13	0.11	0.13	0.13	0.14
Al2O3	11.93	11.56	11.84	11.29	11.22	11.69	11.74	11.36	11.53
Fe2O3(t)	1.19	2.75	2.51	2.16	2.34	1.96	1.68	2.09	1.80
FeO(t)	1.07	2.48	2.26	1.94	2.11	1.76	1.51	1.88	1.62
Fe2O3	0.54	1.24	1.13	0.98	1.06	0.89	0.76	0.94	0.81
FeO	0.59	1.37	1.25	1.08	1.16	0.98	0.84	1.04	0.89
MnO	0.03	0.07	0.05	0.02	0.05	0.03	0.04	0.03	0.03
MgO	0.14	0.11	0.19	0.10	0.12	0.11	0.17	0.13	0.12
CaO	0.39	0.28	0.48	0.11	0.23	0.14	0.45	0.14	0.26
Na2O	3.92	3.83	3.46	3.18	3.31	3.73	6.31	5.09	3.49
K2O	4.69	4.71	4.54	4.58	4.22	4.30	4.05	4.17	4.54
P2O5	0.01	0.02	0.01	0.01	0.02	0.01	0.05	0.02	0.01
Mg. No.	18.90	7.34	13.04	8.40	9.22	10.02	16.70	10.97	11.67
CaO/Al2O3	0.033	0.024	0.041	0.010	0.021	0.012	0.039	0.012	0.023
P.I.	0.97	0.99	0.90	0.90	0.89	0.92	1.26	1.13	0.92
Al/CNK	0.97	0.97	1.03	1.09	1.07	1.06	0.75	0.86	1.04
Al/NK	1.03	1.01	1.12	1.11	1.12	1.08	0.80	0.88	1.08
Pk No.	0.06	0.04	0.08	0.02	0.04	0.02	0.06	0.02	0.04
CIPW Norms									
Q	35.81	38.37	37.52	41.67	41.91	42.38	30.02	33.7	42.14
C	0	0.47	0.36	0.9	0.78	1.46	0	0	1.06
Or	27.71	27.83	26.83	27.06	24.94	25.41	23.93	24.64	26.83
Ab	33.17	28.18	29.28	26.9	28.01	27.33	37.81	35.19	26.15
An	1.09	1.39	2.38	0.55	1.14	0.69	0	0	1.29
Ne	0	0	0	0	0	0	0	0	0
Ac	0	0	0	0	0	0	2.2	2.72	0
Ns	0	0	0	0	0	0	3.04	1.11	0
Di	0.7	0	0	0	0	0	1.64	0.6	0
Hy	0.47	1.5	1.56	1.23	1.43	1.21	0.98	1.76	1.09
Ol	0	0	0	0	0	0	0	0	0
Mt	0.78	1.8	1.64	1.42	1.54	1.29	0	0	1.17
Il	0.25	0.46	0.42	0.27	0.25	0.21	0.25	0.25	0.27
Ap	0	0	0	0	0	0	0.11	0	0
C. Index	2.21	3.75	3.62	2.91	3.21	2.71	2.87	2.61	2.53
D. Index	96.69	94.38	93.63	95.63	94.85	95.12	91.76	93.54	95.12
TRACE ELEMENTS IN PPM									
Cs	2.42	0.47	3.30	0.89	0.91	0.44	0.69	0.49	0.41
Rb	158	71	107	171	164	184	134	139	106
Sr	19	8	27	7	13	7	34	5	12
Ba	103	365	233	95	28	39	307	25	154
V	6	4	7	3	7	5	7	3	6
Cr	5	7	8	5	6	7	11	8	6
Co	197	149	233	248	209	179	261	205	201
Ni	9	6	5	7	10	7	1	8	6
Cu	7	0	5	4	3	5	1	0	4
Zn	35	79	130	176	180	141	76	157	101
Ga	22	25	26	31	28	33	23	30	27
Sc	2	10	4	0	1	1	2	0	1
Y	74	48	81	131	160	115	120	78	64
Zr	157	271	600	1021	960	492	376	613	428
Hf	16	13	16	15	38	24	13	20	18
Nb	23	16	33	59	68	44	34	35	26
Ta	7	8	5	6	8	4	7	4	6
Th	13	17	13	21	23	19	18	13	15
U	1.41	1.13	3.06	1.09	7.1	2.12	3.09	1.19	1.09
RARE EARTH ELEMENTS IN PPM									
La	48.23	33.23	37.66	33.34	32.45	28.87	20.98	31.43	44.87
Ce	93.55	102.55	153.56	136.78	110.45	67.45	85.78	110.55	124.54
Pr	12.34	12.77	13.09	14.07	11.98	12.55	13.22	11.99	12.34
Nd	48.67	49.67	72.67	73.7	80.45	40.56	45.34	59.3	41.37
Sm	11.34	16.34	16.56	13.35	14.34	13.12	11.12	11.23	14.55
Eu	1.15	1.78	2.13	2.09	2.34	1.45	1.34	1.67	1.56
Gd	10.45	11.23	9.56	10.34	10.55	10.66	11.55	9.87	10.08
Tb	2.23	1.69	2.78	2.34	2.34	2.61	1.54	3.18	3.05
Dy	10.89	9.94	11.34	9.89	10.66	9.93	10.66	11.12	10.34
Er	3.67	4.56	4.88	5.46	4.99	5.58	6.45	5.98	5.36
Yb	6.67	4.65	5.67	5.28	5.38	4.45	5.09	4.67	4.15
Lu	1.33	1.09	1.12	0.98	0.89	1.13	0.99	1.13	0.89

Table 1.

Major and trace elements analyses of granite from Nagarparkar Complex

	Churio Granite and Wadlai Adamellite (Nagarparkar Complex)										
Sample#	1902	1907	1936	1937	1940	1880	1884	1885	1892	1893	1911
MAJOR ELEMENTS				Granite				Adamellite			
SiO2	76.50	74.99	76.96	75.50	75.83	76.25	75.05	74.38	74.75	76.87	76.29
TiO2	0.27	0.30	0.25	0.34	0.27	0.26	0.27	0.32	0.29	0.16	0.22
Al2O3	10.99	12.72	11.56	12.16	12.20	12.96	13.92	13.59	14.11	13.12	13.04
Fe2O3(t)	3.15	2.48	2.49	2.57	2.43	1.63	1.85	2.03	1.93	1.36	1.55
FeO(t)	2.84	2.23	2.24	2.31	2.19	1.47	1.67	1.83	1.74	1.22	1.40
Fe2O3	1.43	1.12	1.12	1.16	1.10	0.74	0.84	0.92	0.87	0.61	0.70
FeO	1.57	1.23	1.24	1.28	1.21	0.81	0.92	1.02	0.96	0.68	0.77
MnO	0.11	0.05	0.05	0.05	0.05	0.03	0.07	0.07	0.08	0.04	0.08
MgO	0.13	0.21	0.20	0.36	0.23	0.36	0.35	0.28	0.35	0.17	0.39
CaO	0.42	0.57	0.50	0.74	0.66	0.99	1.06	1.21	0.99	0.44	1.09
Na2O	3.51	3.25	3.08	3.36	3.17	2.66	3.75	4.83	3.90	3.82	3.53
K2O	5.07	5.49	5.02	5.13	5.26	4.68	3.73	3.34	3.66	4.09	3.86
P2O5	0.01	0.06	0.01	0.04	0.02	0.24	0.03	0.04	0.03	0.01	0.04
Mg. No.	7.56	14.36	13.73	21.63	15.79	30.43	27.26	21.46	26.43	19.85	33.26
CaO/Al2O3	0.038	0.045	0.043	0.061	0.054	0.077	0.076	0.089	0.070	0.034	0.083
P.I.	1.02	0.89	0.91	0.91	0.89	0.73	0.73	0.85	0.74	0.82	0.77
Al/CNK	0.91	1.03	1.01	0.98	1.01	1.15	1.15	0.99	1.16	1.14	1.09
Al/NK	0.98	1.13	1.10	1.10	1.12	1.37	1.36	1.18	1.36	1.22	1.31
Pk No.	0.07	0.09	0.09	0.12	0.11	0.19	0.19	0.19	0.17	0.08	0.20
CIPW Norms											
Q	35.53	33.29	38.02	37.55	35.12	40.66	35.95	30.33	35.18	37.55	37.89
C	0	0.53	0.17	0.67	0.13	2.29	1.85	0	2	1.6	1.16
Or	29.96	32.44	29.67	29.72	31.08	27.66	22.04	19.74	21.63	24.17	22.81
Ab	28.28	27.5	26.06	23.35	26.82	22.51	31.73	40.87	33	32.32	29.86
An	0	2.44	2.42	4.1	3.14	3.35	5.06	5.52	4.72	2.18	5.15
Ne	0	0	0	0	0	0	0	0	0	0	0
Ac	1.25	0	0	0	0	0	0	0	0	0	0
Ns	0	0	0	0	0	0	0	0	0	0	0
Di	1.81	0	0	0	0	0	0	0.18	0	0	0
Hy	1.2	1.45	1.53	2.16	1.53	1.4	1.55	1.32	1.58	0.98	1.59
Ol	0	0	0	0	0	0	0	0	0	0	0
Mt	1.45	1.62	1.62	1.68	1.59	1.07	1.22	1.33	1.26	0.88	1.01
Il	0.51	0.57	0.47	0.65	0.51	0.49	0.51	0.61	0.55	0.3	0.42
Ap	0	0.13	0.02	0.09	0.04	0.52	0.07	0.09	0.07	0	0.09
C. Index	4.97	3.65	3.63	4.49	3.64	2.96	3.28	3.44	3.39	2.16	3.02
D. Index	93.77	93.23	93.75	90.63	93.02	90.83	89.72	90.93	89.81	94.04	90.56
TRACE ELEMENTS IN PPM											
Cs	1.23	1.28	2.48	2.59	2.60	3.50	1.82	2.66	2.66	3.12	2.98
Rb	95	86	112	110	103	146	111	69	95	87	101
Sr	12	40	27	64	44	90	96	111	100	29	135
Ba	307	450	122	218	99	454	684	661	705	796	879
V	6	4	7	3	5	6	5	7	6	4	6
Cr	9	19	12	26	7	22	12	13	8	17	34
Co	146	185	222	121	151	140	239	158	221	257	150
Ni	3	5	7	6	2	5	6	5	6	3	4
Cu	4	2	2	1	0	6	3	2	0	3	2
Zn	126	59	102	75	83	38	161	68	56	32	29
Ga	25	22	25	21	24	19	20	20	20	20	16
Sc	4	8	4	7	5	4	6	7	3	4	3
Y	94	58	72	57	77	50	47	45	50	37	24
Zr	532	387	440	321	380	160	249	292	269	189	110
Hf	21	15	16	10	12	6	8	8	8	8	9
Nb	23	13	33	23	24	15	13	12	14	10	10
Ta	7	4	9	4	5	4	6	4	7	5	7
Th	10	7	13	14	10	12	14	15	10	13	7
U	3.18	1.45	1.1	1.22	0.67	2.74	3.44	1.21	2.24	2.56	3.52
RARE EARTH ELEMENTS IN PPM											
La	25.66	24.45	31.21	48.87	32.12	45.34	39.78	35.44	34.55	36.66	33.24
Ce	118.78	130.6	172.34	154.23	115.65	113.12	102.45	76.66	99.89	96.13	88.12
Pr	13.09	12.98	12.44	12.55	12.99	11.98	14.78	12.34	12.55	12.33	11.13
Nd	64.35	45.2	63.35	65.25	57.28	27.34	30.75	44.34	30.34	32.56	21.35
Sm	11.67	12.45	13.09	13.14	11.23	6.91	7.67	13.45	15.15	13.12	12.54
Eu	2.27	1.66	1.66	1.89	1.15	1.18	1.57	1.28	1.34	1.18	1.65
Gd	9.35	10.34	10.09	10.35	9.45	9.67	10.12	10.15	9.55	9.05	10.12
Tb	2.58	1.17	2.28	2.14	1.89	1.77	1.54	1.35	1.34	1.07	1.37
Dy	10.55	9.55	11.33	10.12	10.44	10.14	11.22	9.22	11.09	11.12	9.77
Er	5.76	4.87	5.79	5.45	6.06	3.17	3.73	0.62	6.25	6.38	5.66
Yb	5.35	5.55	4.45	5.89	4.76	6.78	6.79	5.65	5.34	6.88	6.56
Lu	0.87	1.09	1.24	1.22	0.89	0.93	1.14	1.21	1.23	1.14	1.15

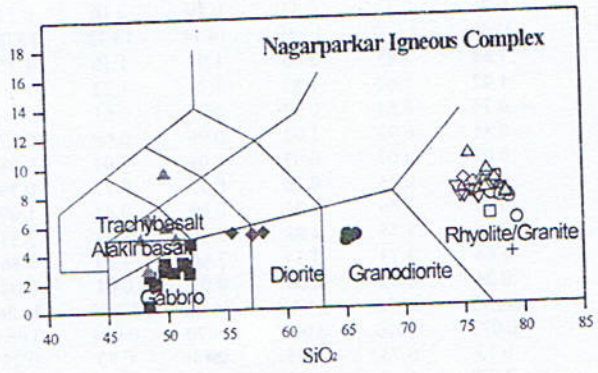

Fig. 2.

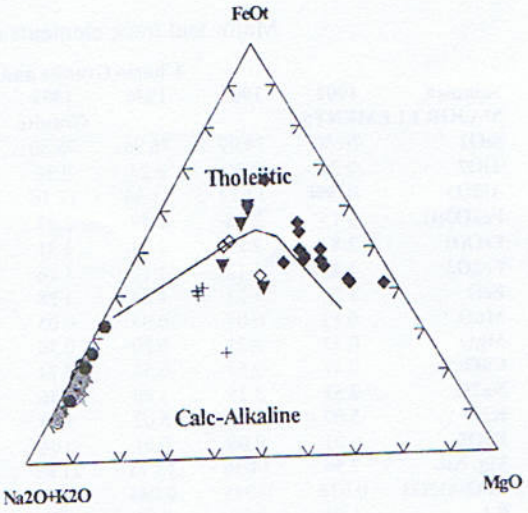

Fig. 3.

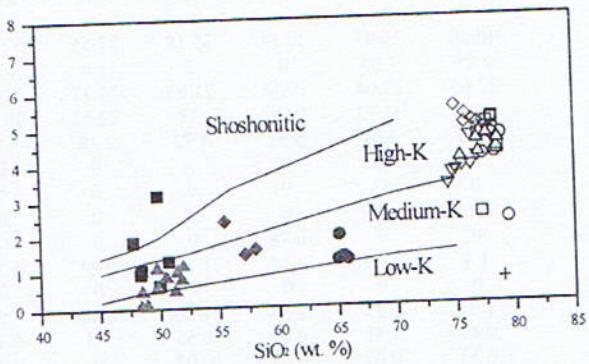

Fig. 4.

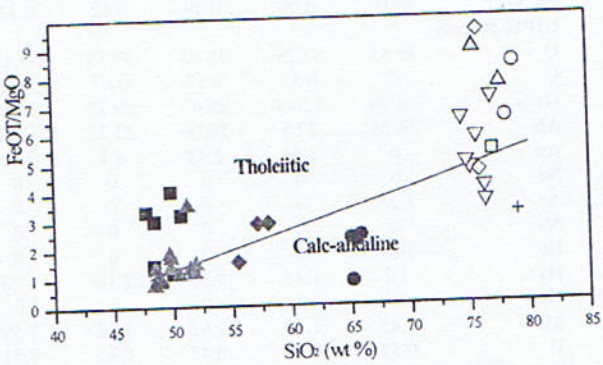

Fig. 5.

Fig. 2. The total alkali-silica classification (TAS) diagram (Le Bas et al 1986; Le Maitre et al, 1989) for the Nagarparkar Complex (Gabbros = square, Alkali basalt = filled triangle, Diorite = filled diamond, Granodiorite = filled circle, Rhyolite = open triangle, Nagarparkar Granite = inverted open triangle, Grey Granite = open diamond, Churio Granite = open circle).

Fig.3. AFM Diagram after Irvine and Baragar (1971), showing the major element compositional diversity in the mafic and felsic rocks from the Nagarparkar Complex. Gabbro (filled diamond), dolerite (inverted filled triangle) and diorite (open diamond) fall within tholeiitic field. On the left are, Grey granite (filled circle), Churio Granite (filled triangle), Nagarparkar Granite (cross), rhyolite (open circle) and diorite (plus).

Fig. 4. Classification of Tholeiitic and Calc-alkaline series within igneous rocks of the Nagarparkar Complex. The dividing line between the two series is taken from Miyashiro (1974).

Fig. 5. K2O versus SiO2 (wt%) diagram for the igneous rocks of the Nagarparkar Complex with boundaries for the division into compositional fields of the low-K Tholeiite (low-K), Calc-alkaline (medium-K), high-K Calc-alkaline (High-K) and Shoshonitic suits (after Peccerillo and Taylor 1976; Rickwood 1989).

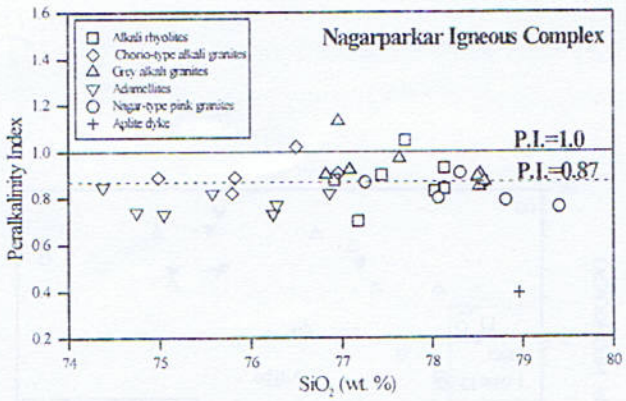

Fig. 6.

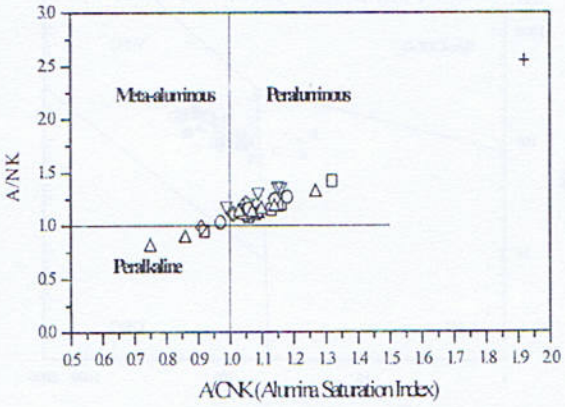

Fig. 7.

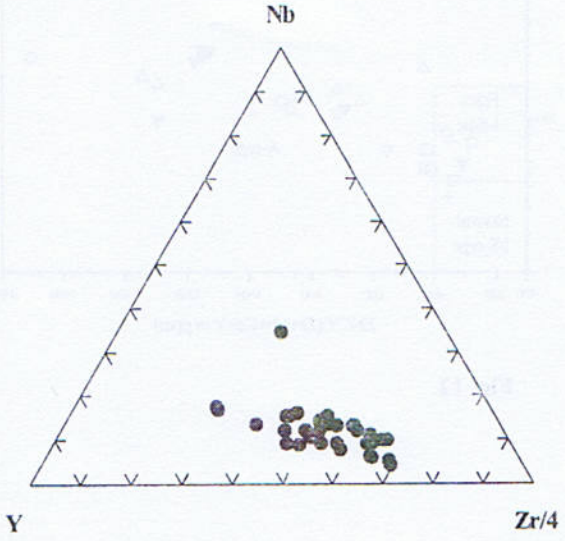

Fig. 8.

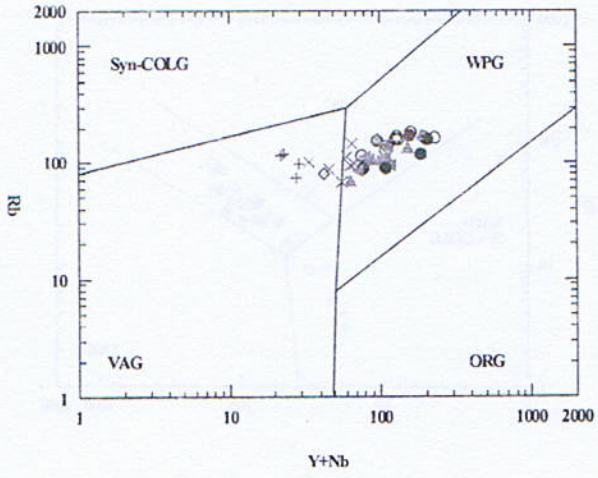

Fig. 9.

Fig. 6. Plot of Peralkalinity Index [mol% ($Na_2O+K_2O)/Al_2O_3$] versus SiO_2 for the Nagarparkar Felsic rocks. The limit at P.I. = 0.87 (minimum value for alkaline granites) is after Liegeois and Black (1987).

Fig.7. Plots of A/NK [(mol.% of Al2O3/(Na2O+K2O)] Versus A/CNK [(mol.% of Al2O3/Cao+Na2O+K2O)], Shand Diagram for granite/rhyolite of the Nagarparkar Complex. Fields after Maniar and Piccolli (1989).

Fig. 8. Plots of granite from the Nagarparkar Complex on the Nb-Y-Zr diagram (after Eby, 1992), Almost all the samples fall in "A2" i.e. A-type granites derived from continental crust or underplated crust. "A1" is allocated for A-type granites derived from sources like those of oceanic island basalts.

Fig. 9: Plots of granite from the Nagarparkar Complex on Y+Nb versus Rb discrimination diagram of Pearce, 1984 (Pearce, 1996) indicating "continental rifting origin".

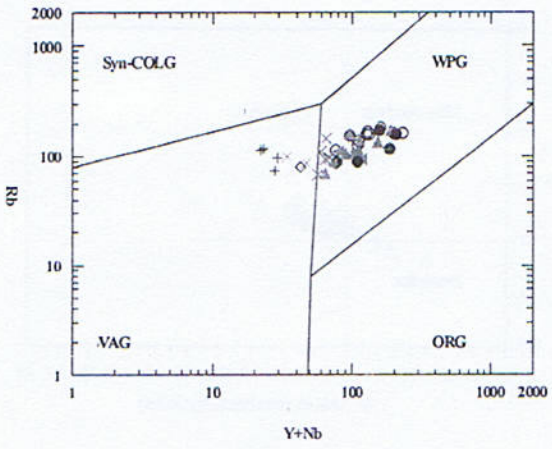

Fig. 10.

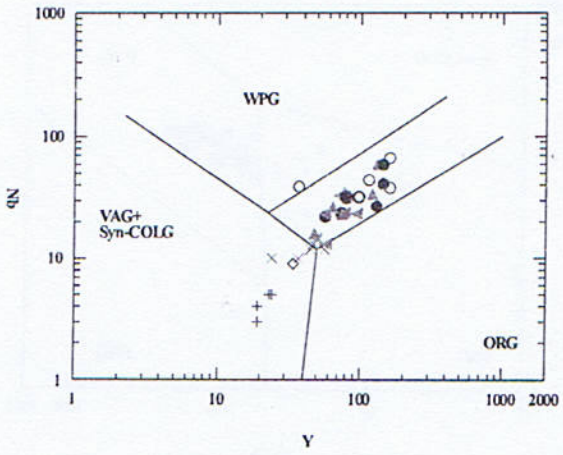

Fig. 11.

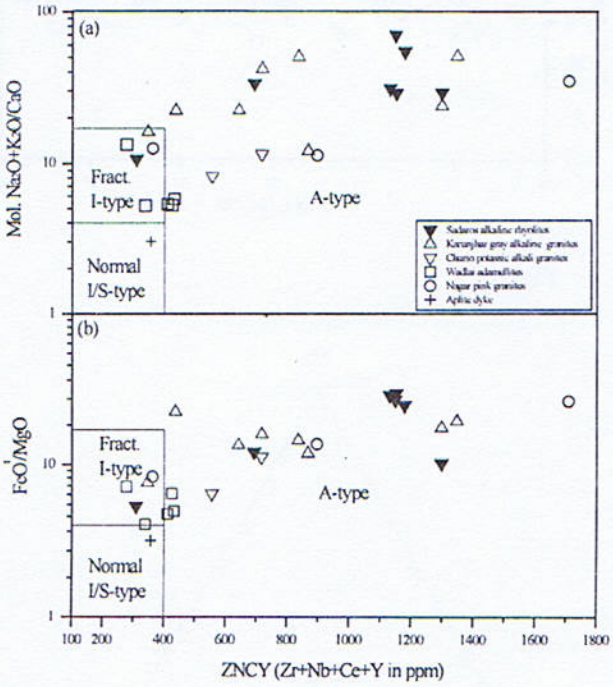

Fig. 12.

Fig.10. Plots of granite from the Nagarparkar Complex on Y+Nb versus Rb discrimination diagram of Pearce, 1984 (Pearce, 1996) indicating "continental rifting origin".

Fig. 11. Plots of representative felsic rocks from the Nagarparkar Complex, on the Y versus Nb discrimination diagram (after Pearce et al, 1984) indicating "within plate setting".

Fig. 12: Plots of FeO^t/MgO and Na_2O+K_2O/CaO versus Zr+Nb+Ce+Y discrimination diagram (after Whalen et al, 1987) for the Nagarparkar Complex. All the granite/rhyolite are indicating "A-type" (anorogenic) environment.

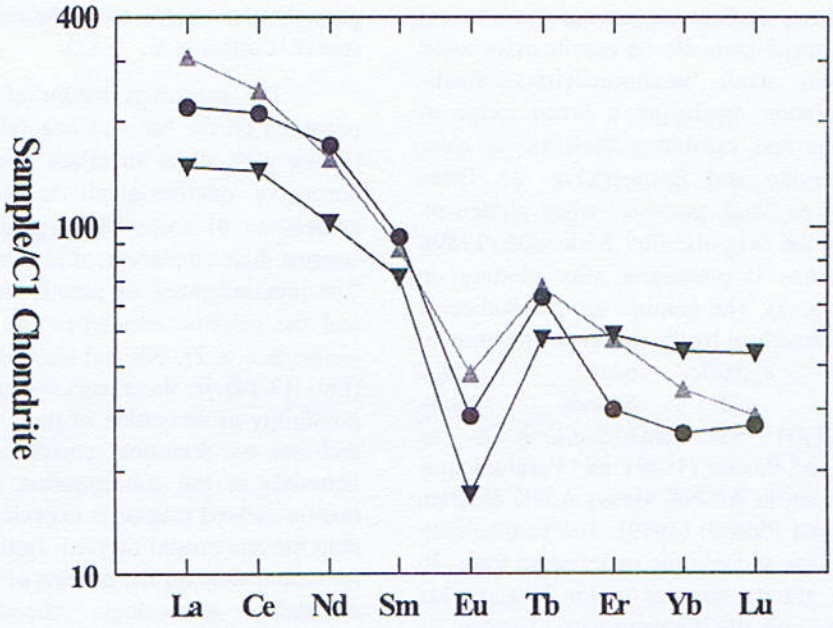

Fig. 13.

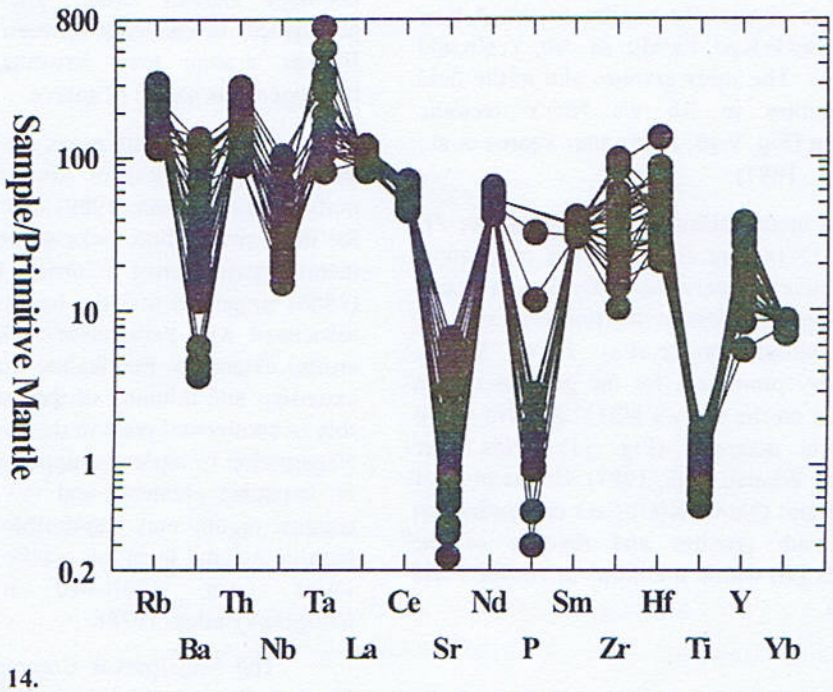

Fig. 14.

Fig.13. Chondrite normalized (after McDonough and Sun, 1995) REE plots of the representative Nagarparkar Granite (circle) Kirana Rhyolite (triangle) alongwith Sankara Granite (Pandit and Deep, 1999) (inverted triangle).

Fig.14. Primitive mantle normalized (after McDonough and Sun 1995) trace element plots of representative granite from the Nagarparkar Complex.

described in terms of two distinct magma associations: (a) Sub-alkaline gabbro-diorite-granodiorite-granite association (Fig. 2) (b) Bimodal alkali basalt/trachybasalt–alkali-rhyolite/granite association displaying a broad range of chemical compositions and exhibiting tholeiitic to calc-alkaline character (Irvine and Barager)(Fig. 3) These granites are classified as "high potassic" when plotted on K_2O versus SiO_2 diagram (Fig. 4), after Rickwood (1989). Tholeiitic to calcalkaline is prominent after plotting on Myashiru diagram (Fig. 5). The granites are peralkaline in nature (Fig. 6) as characterized by the presence of acmite in their norms and agpaitic index > 1[Mol $(K_2O+Na_2O)/Al_2O_3$] and Shands Index $[Al_2O_3/(CaO+Na_2O+K_2O)$ vs $Al_2O_3/(Na_2O+K_2O)$ as proposed by Manier and Piccoli (1989). and Peraluminous to peralkaline on plotting in A/CNK versus A/NK diagram (Fig.7) after Maniar and Piccolli (1989). The peralkalinity Index (P.I) in the rhyolite and granitic rocks range from .70 to 1.1 (Fig. 6). The granite samples of the Nagarparkar Complex, when plotted on the discrimination diagram Y-Zr-Nb (after Eby, 1996), fall in the limit of "A2" indicating A-type granites derived from continental or underplated crust (Fig.8). They are chemically similar to the A-type granitoids with high Na_2O+K_2O, Fe/Mg, Zr, Nb, Y, Zn and low Al_2O_3, CaO and Sr. The study granites plot in the field of within plate granites in Rb v/s Nb+Y tectonic discrimination diagram (Fig. 9,10, fields after Pearce et al., 1984 and Whalen et al., 1987).

High values of incompatible trace elements like Zr, Nb, Ce and Y (Fig. 13-14) are characteristics of granites under study. The negative anomaly shown by Ba and Sr can be attributed to low-pressure felspar fractionation and are typical for A-type granitoids (Pearce et al., 1984). "Within plate" character is very prominent for the granites of the complex when plotted on the Rb v/s Nb+Y and Nb v/s Y tectonic discrimination diagrams (Fig. 11) fields after Pearce et al., 1984 and Whalen et al., 1987). On the plots of ZNCY vs FeO^t/MgO and $(Na_2O+K_2O)/CaO$ discrimination diagram (Fig 12) both granites and rhyolite of the Nagarparkar Complex fall within the limits of A-type Field (Whalen et al., 1987).

DISCUSSION

The extensional tectonic environment is generally represented by peralkaline rock suites. In fact peralkaline rocks of anorogenic occurrences have been reported globally (Currie, 1989), are the products of a complex set of processes and no petrogenetic model can satisfactorily explain their origin (Eby, 1990). Any petrogenetic model must account for the relatively anhydrous and incompatible HFS element enriched character of the magma. The models proposed include partial melting of relatively anhydrous lower crustal source rocks (Collins et al., 1982), tonalitic to granodioritic source rock (Anderson, 1983) and granulite source (Collins et al., 1982).

The subsolvus nature of these granites has been proposed on the basis of one felspar dominance (perthitic texture with albite lamellaes forming core), abundance of normative quartz, alkali felspar and albite alongwith association of volcanics in granite under study, strongly suggest their emplacement at relatively high crustal levels. The preponderance of peralkaline rocks over basic rocks and the extreme enrichment of some incompatible trace elements i. e. Zr, Nb and Ce and depletion of Sr and CaO (Fig. 13-14) in these rocks (Currie, 1989), suggests the possibility of derivation of these granites by crustal source and not by fractional crystallization of mantle derived materials as the concentration of these elements in the mantle-derived magma is expected to be significantly lower than the one crustal derived. Both crust and mantle sources are responsible for the genesis of Nagarparkar granites. The correlative mineralogy, chemical characteristics and tectonic setting of the peralkaline granite from the Nagarparkar Complex indicate their generation under a common thermal event. The difference in absolute abundances of elements between Nagarparkar, Siwana and Barmer granite may however, be attributed to the heterogeneous nature of source.

Continental rift zones are generally associated with the peralkaline rocks of low abundance with associated mafic rocks (Wilson, 1989) and the most probable source for these peralkaline rocks seems to be partial melting of metasomatised crust (Currie, 1989). Leat and Thorpe (1986) suggested that the basalts of withinplate character associated with peralkaline rocks represent the zones of crustal extension. Peralkaline magma is generated by the extension and thinning of the continental lithosphere. The role of continental crust in the evolution of granite from the Nagarparkar Complex is supported by high concentration of incompatible elements and low Sr contents. Extensional tectonic regime may responsible to generate heat by rising basaltic magma from the mantle to promote melting of the lower crust. (Enriched in LILE, HFSE and halogens)(Bailey, 1978).

The Nagarparkar Complex alongwith Mount Abu, Siwana, Barmer, Malani and Jodhpur complexes of the western Rajasthan marks an important late Proterozoic thermal event in the continental evolution of this part of the subcontinent. This Trans-Aravalli Block is unique in the geological evolution of the "Indian Shield" (Kirana-Malani-Basin after Chaudhary and Ahmad, 1999) as it is characterized by a major period of anorogenic (A-type), "Within Plate" magmatism represented by the Nagarparkar, Kirana, Malani, Siwana, Jaswantpura, Tusham, Mount Abu and Gurapratapsingh, complexes (Kochhar, 1973, 1974,

1984; Naqvi, 1987; Bushan, 1985; Eby, 1990; Rathore et al., 1991; Bhushan and Chittora, 1999; Bhushan, 1989; Butt et al 1992; Maheshwari et al, 2001, 2002 and Ahmad et al., 2000). The Pan-African tectonothermal event (900-450 Ma) has resulted in crustal accretion in the Gondwana land prior to its fragmentation and plate tectonic movements (Kennedy, 1964). Stern (1984) has described six magmatic episodes from 780 to 540 Ma from eastern Egypt. This late Proterozoic magmatic event "hot spot" in the Kirana-Malani Basin representing at least four magmatic episodes from 780 Ma to 680 Ma (Rathore et al., 1996, 1999) is therefore correlatable to this global thermal event. A-type rocks of similar age (750 to 550 Ma), formed under extensional tectonic regime have also been reported from southern India (Santosh and Drury, 1988; Rajesh and Santosh, 1996; Rajesh et al., 1996) indicating the fact that these wide apart occurrences of A-type rocks have resulted through a common thermal event during the Pan-African.

A-type, within plate peraluminous to peralkaline granites/rhyolite alongwith "within plate" alkali mafic rock associations are among the most distinctive igneous suites, and these are generally characteristic of extensional tectonic environment, forming high-level plutons. The anorogenic peralkaline complexes have not been studied in detail by researchers in the past but with the discovery of mineralization in these rocks, a number of peralkaline anorogenic occurrences have been reported globally in the last couple of years (Currie, 1989). The peralkaline rocks are the products of a complex set of processes and no petrogenetic modal can satisfactorily explain the origin of these rocks (Eby, 1990).

CONCLUSION

The A-type, within plate granites and rhyolite of the Nagarparkar Complex marks Neoproterozoic rifting in the Kirana-Malani Basin. Peraluminous to peralkaline granite association is a typical rock suite represented by the complex.

AKNOWLEDGEMENTS

This research work was carried out under financial support of the Punjab University research grant. Geological Survey of Pakistan is highly acknowledged for providing facilities at the Nagarparkar.

REFERENCES

Ahmad, S. A., 2000. Geology and geochemistry of the Neoproterozoic Kirana Volcanics, Sargodha district, Pakistan. *Geol. Bull. Punjab Univers.* **35:** 59-71.

Bailey, D.K., 1978. Continental rifting and mantle degassing. In: Neumann, E.R and Ramberg, I.B. (Eds.) Petrology and geochemistry of continental rifts. *Reidel.* Holland 1-13.

Bushan, S.K., 1985. Malani volcanism in the Western Rajasthan. *Indian.Jour.Earth.Sciences.* **12, 1:** 58-71.

Bhushan, S.K., 1989. Mineral chemistry and petrogenetic aspects of the Malani Volcanics, Western Rajasthan. *Indian Minerals.* **43: 3&4.** Dec, 89. 325-338.

Bhushan, S.K., Chittora, V.K., 1999. Late Proterozoic bimodal volcanic assemblage of the Siwana subsidence structure, Western Rajasthan, India. *J. Geol. Soc. India.* **53:** 433-452.

Butt, K.A., Nazirullah, R., Syed, S.A., 1989. Geology and Gravity interpretation of the Nagarparkar area and its potential for surfacial uranium deposits. *Kashmir. Jour. Geol.* **6&7:** 41-50.

Butt, K.A., Jan, M.Q., Karim. A., 1992. Late Proterozoic rocks of Nagarparkar, Southeastern Pakistan. A preliminary petrologic account. In: Ahmad, R and Sheikh, A, M. (Eds). *Geology in South Asia-1*, Islamabad. 106-109.

Collins, W.J., Beam, S. D., White, A. J.R., Chappel, B.W., 1982. Nature and origin of A-type granites with particular refrence to Southeastern Australia. *Contrib. Min. Pet.* **80. 2:** 189-200.

Chaudhry, M.N., Ahmad, S.A., Mateen, A., 1999. Some postulates on the tectonomagmatism, tectonostratigraphy and economic potential of Kirana-Malani-Basin, Indo-Pakistan. *Pakistan. Jour. of Hydrocarbon. Res.* Islamabad, Pakistan **11:** 52-68.

Currie, K.L., 1989. New ideas on the old problem: the peralkaline rocks. *Geol. Soc. India, Mem.* **15:** 117-136.

Collins, W.J., Beam, S. D., White, A. J.R. and Chappel, B.W., 1982. Nature and origin of A-type granites with particular refrence to Southeastern Australia. *Contrib. Min. Pet.* **80. 2:** 189-200.

Eby, G.N. and Kochhar., 1990. Geochemistry and petrogenesis of the Malani igneous suite, north penisular India.*Jour.Geol.Soc.India.* **36:** 109-130.

Eby, G.N., 1990. The A-type granitoids: A review of their occurrence, and chemical characteristics and speculation on their petrogenesis. *Lithos,* **26.** 115-134.

Fermor, L. L., 1932. General report of the Geological Survey of India for the year 1931. *Records: Geological Survey of India.* **LXVI (1):** 1-150.

Jan, M.Q., Laghari, A., Khan, M.A., 1997. Petrography of the Igneous Complex, Tharparkar, Sind, Pakistan. *Geol, Bull, Uni. Peshawar.* **30:** 227-249.

Kazmi, A., Khan, R.A., 1973. The report on the geology, mineralogy and mineral resources of Nagar-Parkar, Pakistan. *Geol. Surv. Pakistan, Information release.* **64:** 44-56.

Kochhar, N., 1973. On the occurrence of a ring dyke in the Tosham igneous Complex, Hisar (Haryana). Jour. *Geol. Soc. India.* **14-2:** 190-193.

Kochhar, N., 1974. The age of the Malani series. *Jour. Geol. Surv.India.* **15:** 316-317.

Kochhar, N., 1984. Malani igneous suite: Hotspot magmatism and Cratonization of the northern part of Indian Shield. *Jour. of Geol. Surv. India* **25-3:** 155-161.

Leat, P.T., Thorpe, R.S., 1986. Geochemistry of an Ordovician basalt-trachybasalt-sub-alkaline/peralkaline rhyolites provinces within the Southern British Caledonides. *Jour. Geol. Soc. London.* **143:** 259-276.

Maheshwari, A., Sial, A. N., Massimo, C., Chittora, V.K. and Manoel, J.M 2001. Geochemistry and Petrogenesis of Siwana Peralkaline Granites, West of Barmer, Rajasthan, India. *Gondwana Research.* **4-1:** 87-95.

Maheshwari, A., Garhia, S.S., Sial, A.N., Ferreira, V.P., Dwivedi, V., Chittora.V.K., 2002. Geology and geochemistry of granites around Jaswantpura, Jalor District, Southwestern Rajasthan, India. *Gondwana Research.* **5-2**: 373-379.

Maniar, P.D., Piccoli, P.M., 1989. Tectonic discrimination of granitoids. *Geol. Soc. Amer. Bull.* **101:** 635-643.

Muslim, M., Akhtar, T., Khan, Z.M., 1997. Geology of Nagar Parkar area, Thar Parkar District, Sindh, Pakistan. *G.S.P. Release.* **605.**

Naqvi, M.S. and Rogers, J.J.W., 1987. Precambrian Geology of India. *Oxford University press. New York.* **1:** 234-270.

Pearce, J. A., Lippard S. J., Roberts, S., 1984. Characteristics and tectonic significance of supera-subduction zone ophiolites. In: KoKelaar, B. P and Howells, M. F., (eds.), *Marginal basin geology. Blackwell, Oxford.* 77-94.

Rathore, S.S. Trivedi, J.R. and Venkateshan, R., 1991. Rb/Sr age of Jalore and Siwana granites: Resolution of Thermal Events by Ar40-39 study. *5th National Symposium on Mass Spectroscopy, Ahmadabad,* **10- 3.**

Rathore, S. S., Venkatesan, T. R., Srivastava, R. K., 1996. Rb-Sr and Ar-Ar systematics of Malani volcanic rocks of southwest Rajasthan: Evidence for a younger post-crystallization thermal event. *Proc. Indian Acad. Sci. (Earth Planet. Sci.* **105:** 131-141.

Rathore, S. S., Venkatesan, T. R. and Srivastava, R. K. 1999. Rb-Sr isotope dating of Neoproterozoic (Malani Group) magmatism from southwest Rajasthan, India: Evidence of younger Pan-African thermal event by ^{40}Ar-^{39}Ar studies. *Gondwana Research.* **2:** 271-281.

Rajesh, H. M., Santosh, M. and Yoshida, M., 1996. The felsic magmatic province in East Gondwana: Implications for Pan-African tectonics. In: Yoshida, M., Santosh, M and Arima, M (Eds.), Precambrian India within East Gondwana. *special issue, J. Southeast Asian Earth Sci.***14:** 275-292.

Rajesh, H. M. and Santosh, M., 1996. Alkaline magmatism in Pennisular India. *Gond. Res. Mem.* **3:** 91-115.

Rickwood, P.C., (1989). Boundary lines within petrologic diagrams, which use oxides of major and minor elements. *Lithos.* **22:** 247-263.

Santosh, M. and Drury, S.A., 1988. Alkali granites with Pan-African affinities from Kerala, South India. *J.Geol.* **96:** 616-622.

Shah, S.M.I (1973). Occurrence of Gold in the Kirana group, Sargodha (Punjab) Pakistan. *Inform. Release, GSP, Quetta, Pakistan.* **68:** 1-14.

Stern, R.J (1994). Arc assembly and continental collision in the Neoproterozoic east African Orogen: Implications for the consolidation of Gondwanaland. *Annu. Rev. Earth&Planet. Sci* **22:** 319-351.

Tauson, L. V., 1967. Geochemical behaviour of rare earths during crystallization and differentiation of granitic magma. *Geochemistry Intrernational.* **4:** 1067-1075.

Wilson, M., (1989). Igneous Petrogenesis: A Global Tectonic Approach. *Unwin Hyman*, London, 466.

Wooley, A. R. and Jones, G.C (1992). The alkaline peralkaline syenite granite complex of Zomba-Malosa, Malavi: mafic mineralogy and genesis. *J. African Earth Sci.* **14-1:** 1-12.

Wynne, A.B (1867). Memoir on the Geology of Kutch. *Geological Survey of India, Memoir.* **9:** 293.

Whalen, J.B., Currie, K. L. and Chappel, B. W., (1987). A-type granites: Geochemical characteristics, discrimination and petrogenesis. *Contrib. Mineral. Petrol.* **95:**.407-419.

Geol. Bull. Punjab Univ. 43, 2008.

PALYNOLOGY OF THE MESOZOIC SUCCESSION OF THE KALA CHITTA RANGE PAKISTAN

BY

KHAN RASS MASOOD, KALEEM AKHTER QURESHI
Department of Botany, University of the Punjab, Quaid-i-Azam Campus, Lahore 54590, Pakistan

AFTAB AHMAD BUTT AND SHAHID GHAZI
Institute of Geology, University of the Punjab, Quaid-i-Azam Campus, Lahore-54590 Pakistan

ABSTRACT:-*A total of one hundred six samples of the Mesozoic succession of the Kala Chitta Range were processed for the palynological analysis out of which only twenty one samples proved to be productive. Palynoflora recovered from the productive samples comprise thirty one form genera belonging to the thrity three form species. Eighteen triletes, two monoletes, eight bisaccates, two acritarchs and one monosaccates constitute eighteen genera. Palynoflora is less diverse exhibiting little compositional change. Lundbladispora willmotti and L. microconata are age diagnostic for the Upper Triassic Kingriali Formation. Aequitriradites triangulatus is typical of the Upper Jurassic-Lower Cretaceous Chichali Formation. Palynoflora are abundant in the Lower Cretaceous Lumshiwal Formation containing Succinctisporites grandior, Gordodinium alberti, Leptodineum eumorphum, Faveosporites subtriangularis, Densoisporites nejburji, Enzonalasporites vigens, Minutosaccus crenulatus, Ovalipollis ovalis, Podocarpites ellipticus and Aequitriradites triangulates. The Upper Cretaceous Kawagarh Formation contains Ptrospermella australliensis of Campanian age. The present contribution is the first comprehensive study of its kind.*

INTRODUCTION

The Kala Chitta Range is a part of the foreland-fold and thrust belt which forms the northern border of the adjoining hydrocarbon bearing Potwar Basin (Fig. 1). The sampled localities have been shown in Fig. 2. The abstract of this paper forms part of the abstract volume of the 33rd International Geological Congress, Oslo, Norway. (Butt et al. 2008).

The Mesozoic succession of the Kala Chitta Range as formalized by the Stratigraphic Committee of Pakistan (Fatmi, 1973) has been tabulated here as follows.

	Nomenclature of the Stratigraphic Committee of Pakistan (Fatmi 1977)	Nomenclature after Cotter (1933)
Upper Paleocene	Lockhart Limestone (Thanetian) Sequence Boundary (Absence of Maastrichtian-Danian)	Hill Limestone
Upper Cretaceous	Kawagarh Formation (Coniacian to Campanian) Sequence Boundary (Absence of Cenomanian-Turonian)	Kawagarh shales
Lower Cretaceous	Lumshiwal Formation	Giumal sandstone
Upper Jurassic- Lower Cretaceous	Chichali Formation Sequence Boundary (Lateritic Crust)	Spiti shale
Middle Jurassic	Samana Suk Limestone	Kioti Limestone
Lower Jurassic	Datta Formation	Ferruginous beds in the kiotos
Triassic	Kingriali Formation Chak Jabbi Limestone Mianwali Formation	Kioto Limestone

Base not exposed by virtue of the Thrust Fault

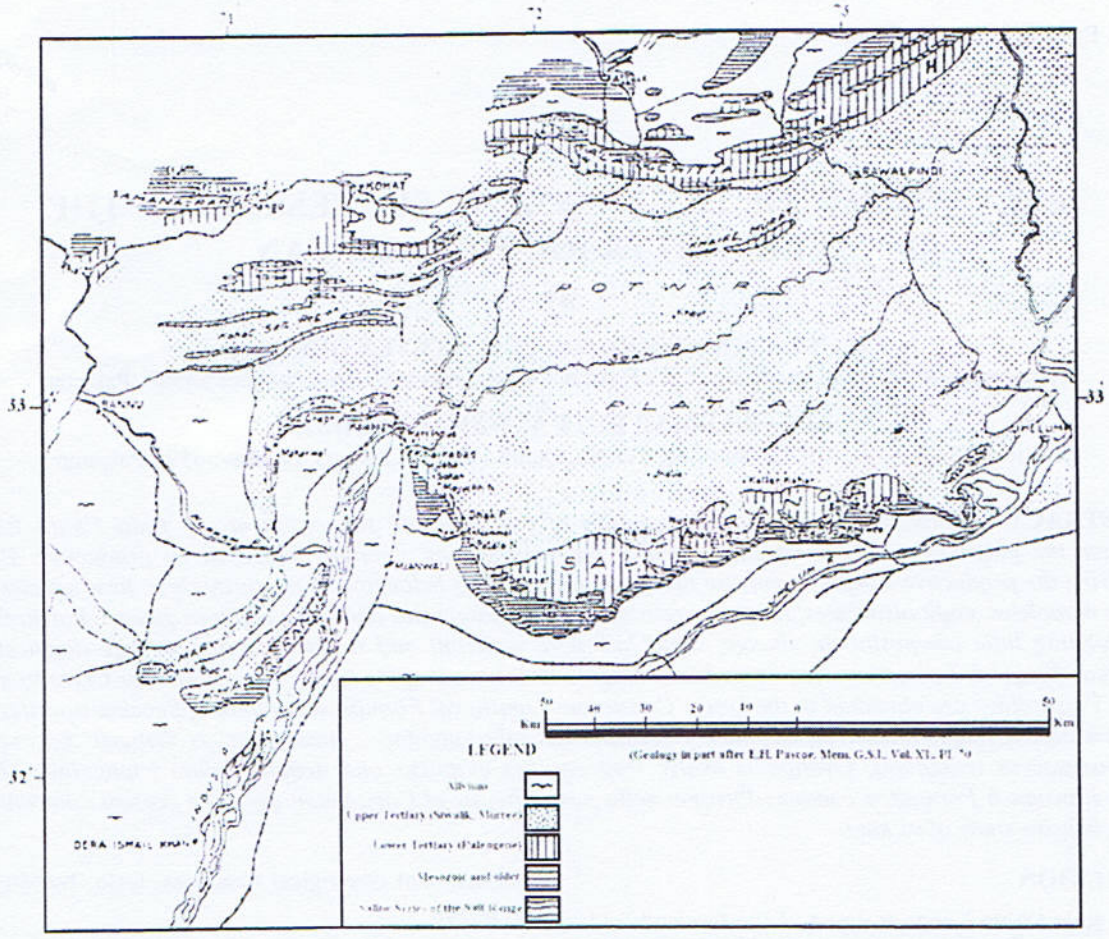

Fig. 1. Location map of the Kala Chitta and Samana Ranges (after Davies and Pinfold,1937)

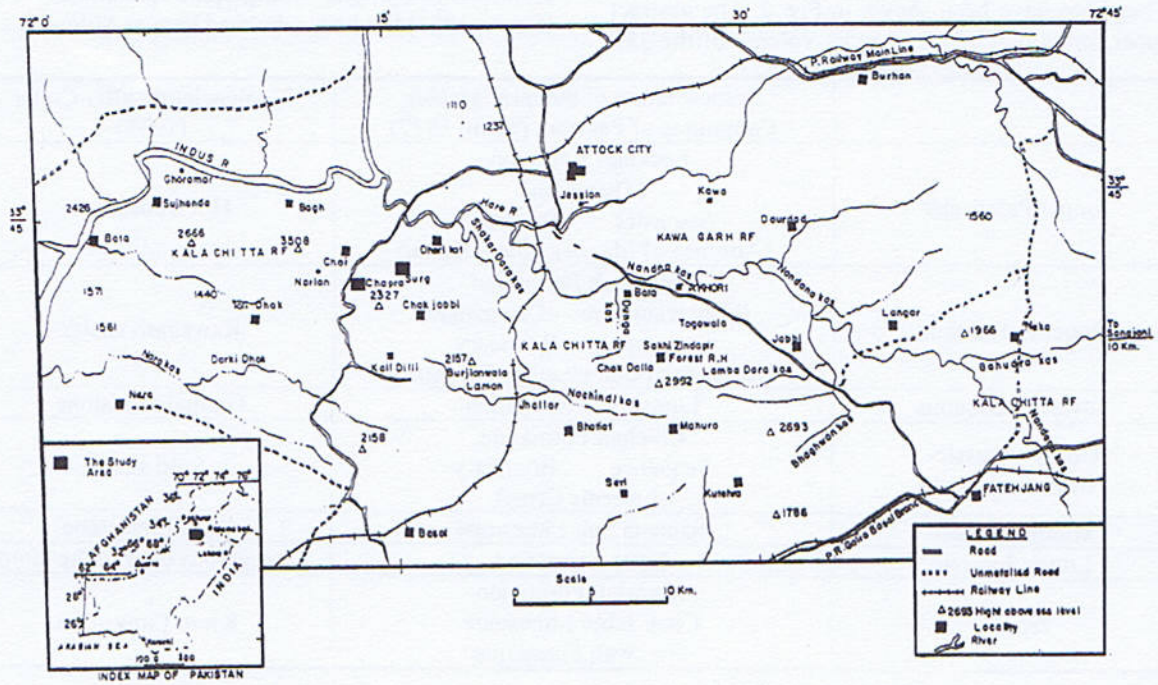

Fig. 2. Location map of the study area of Kala Chitta Range.

Palynomorphs are preserved in sediments under great variety of environments. During sedimentation they behave as very small particles like fine sand and silt. Coarse sandstones, oxidized and weathered sediments, dolomites and sometimes even limestones are poor containers of these microfossils. But some workers have reported well preserved palynomorphs in carbonate environments (Scott et al., 1985b; Masood et al., 1995, Blome and Albert, 1985).

Palynomorphs recovered during the present investigation are poorly preserved. In most cases it was difficult to apply correct identification beyond generic level. However, only those palynomorphs are included in this dissertation that were to some extant moderately preserved. Systematic section includes technical description of only selected palynomorphs most of which also appear in table No. 1.

A total of one hundred and six samples of the Mesozoic succession of the Kala Chitta Range were processed for palynological analysis. Only twenty one samples proved to be productive. The details are shown in table No. 1. It is quite evident from this table that the most productive samples belong to the Lumshiwal Formation, whereas, the Samana Suk Limestone and the Kingriali Formation were least productive.

METHODOLOGY

Special strew mount preparations were made (sandwich mounts between two cover slips) to allow morphographic examination of palynomorph from two angles i.e., proximal and distal. Descriptive features of each palynomorph species encompassing morphographic characters appearing in the systematic palynology were registered as they appeared in the actual specimen under oil immersion objective upon careful L-O analysis. Such features, however, may not be properly depicted in the photomicrographs provided due to poor state of preservation (e.g. crumpling, variously folding, differential decay).

REMARKS

Very few specimens allowed identification up to genus or species level. All palynomorphs posing problems regarding correct identification due to poor preservation were excluded from the study.

Palynoflora recovered from the productive samples comprise thirty one form genera belonging to thirty three form species. Of the thirty one genera 18 belong to triletes 2 to monoletes 8 to bisaccates 2 to acritarchs and one to monosaccates. Palynoflora is less diverse exhibiting little compositional change across the respective formation. Most miospores were of restricted origin, occurring only in one or two formations and very few long ranging types were encountered.

Consideration of Table No. 1 reveals that *Leiotriletes* and *Laevigatotriletes* are the only two long ranging genera occurring almost in all samples, whereas, *Alisporites grandis*, *Pinuspollenites sp.*, *Affropollis jordinus*, *Inaperturopollenites sp.* and *Pterospermella australiensis* were the next long ranging types commonly shared by two or more formations. *Punctatisporites* which otherwise is a long ranging form genus (Devonian to Neogene) was found to be restricted only to the basal part of the Lumshiwal Formation.

PALYNOSTRATIGRAPHY

Kingriali Formation (Upper Triassic)

The Kingriali Formation contains four palynospecies of restricted origin, viz., *Lundbladispora willmotti*, *L. microconata*, *Goubinispora sp.* and *Indotriletes korbaensis*. The first three are age diagnostic, mostly restricted to later part of the Middle Triassic (Jansonius and Hills, 1976).

Samana Suk Limestone (Middle Jurassic)

No age diagnostic or the palynomorph of restricted origin was found in this formation. Apart from the general long ranging types *Leiotriletes* and *Laevigatosporites* only few *Mycorrhizae* were found here.

Chichali Formation (Upper Jurassic-Lower Cretaceous)

This formation is slightly more productive than the Kingriali and the Samana Suk Formations. It contains *Leptolepidites eparcornatus* as the restricted form. *Impardecispora cf. parvelentus* (Plate No. 1c) may be another such type, but extending to the lower most part of the overlying Lumshiwal Formation. Age diagnostic palynomorphs for this formation are *Aequitriradites triangulatus* and *Frangospora sp.* that are peculiar for Early Cretaceous or some time Latest Jurassic (Jansonius and Hills, 1976).

Lumshiwal Formation (Lower Cretaceous)

The Lumshiwal Formation is palynologically the richest horizon investigated during the present study. Palynoflora recovered from this formation is most abundant and diverse as compared to other formations. *Punctatisporites sp.* (Plate No. 4e), *Succinctisporites grandior* (Plate No. 4a), *Gordodinium alberti* (Plate No. 4c), *Leptodineum eumorphum* (Plate No. 2e), *Foveosporites subtriangularis* (Plate No. 2f), *Densoisporites nejburji* (Plate No. 2a), *Enzonalasporites vigens* (Plate No. 4d), *Minutosaccus crenulatus* (Plate No. 2g), *Ovalipollis ovalis* (Plate No. 3c) and *Podocarpites ellipticus* (Plate No. 4a) are of restricted origin, whereas, *Frangospora sp.* (Plate No. 4f) and *Aequitriradites triangulatus* (Plate No. 1a) are age diagnostic.

Table 1

The frequency of occurrence of the palynomorphs in the Mesozoic sucession of the Kala Chitta Range.

AGE		TRIASSIC	JURASSIC		JURASSIC/ CRETACEOUS				CRETACEOUS													
FORMATION		KINGRIALI	SAMANA SUK		CHICHALI				LUMSHIWAL										KAWAGARH			
S.No	Sample No. PALYNOMORPH	576	703	1029	658	669	754	181	148	149	209	210	661	665	666	756	187	188	1236	1237	170	171
1	*Affropollis jordinus*												13.5	2		28		10	4	3.5		
2	*Densoisporites nejburgii*										10.5	15	6.5	1	13	4.5						
3	*Alisporites grandis*							8	5	8	4	10	3	3.5	9	19	21.5	4.5	8	1	2.5	2
4	*Alisporites bilateralis*							2	18	1.5	6.5	10.5	3.5	19	2.5	2.5	5	31	2	3.5	1	1
5	*Enzonalasporites vigens*								3	1.5	11						4.5					
6	*Frangospora sp.*							*51	1	1.5	1.5	9.5	2	16	10		21					
7	*Inaperturopollenites sp.*														1.5	2.5		3.5	2	1.5	1.3	
8	*Leptolepidites eparcornatus*				4.5	2.5	6	10														
9	*Leiotriletes sp.*		85	90	69	43	29	10	10	17	2.5	3.5	9.5	2	8.5	1.5	6	9	2.5	2	4	19
10	*Laevigatosporites sp.*		10	8	18	39	51	8	3	2	7	8.5	17	19	1	16	4	4.5	1	1	3	20
11	*Minutosaccus crenulatus*								2	3	4	4	8.5				5					
12	*Ovalipollis ovalis*								16	4.5	3.5						4					
13	*Podocarpites ellipticus*								8	5.5	1	2	7	16	8	2.5	1.5	19				
14	*Punctatisporites sp.*									28	11.5	6.5	2				1.5					
15	*Succinctisporites grandior*								12	2	9						4.5					
16	*Valiasaccites validus*													2	19	55		1.5				
17	*Leptodineum eumorphum*								2		13						9.5					

Table No. 1:Continued from pre-page.

S.No	Sample No. PALYNOMORPH	576	703	1029	658	669	754	181	148	149	209	210	661	665	666	756	187	88	1236	1237	170	171
18	*Gordodinium alberti*								9	2.5	2.5						2.5					
19	*Foveosporites subtriangularis*											18	8.5	1.5	1	11.5						
20	*Crybelosporites pannuceus*					7	4	3.5	1	3.5							3					
21	*Verrucosisporites narmianus*																		34	29		
22	*Verrucosisporites densus*																		20	14		
23	*Cyclobaculisporites minutus*																		15	23	56	49
24	*Inferopollenites sp.*																		5	4		
25	*Densipollenites densus*																		1.5	2	10	5
26	*Pinuspollenites sp.*								1.5	1	1.5	3	10	1.5	19	1.5	1	10	2	2.5	1	3
27	*Aequitriradites triangulatus*					4	5	2	1	2							1					
28	*Lundbladispora willmotti*	53																				
29	*Lundbladispora microconata*	2																				
30	*Indotriletes korbaensis*	34																				
31	*Impardecispora cf. parvelentus*				3.5	1	1.5	2.5	1.5													
32	*Pterospermella australiensis*																		3	12	9	
33	*Goubinispora sp.*	9.5																				
34	*Mycorrhiza*		4.5	2	4.5	1.5	1	1	2	4	6	7.5	1.5	13	4.5		1.5					
35	*Acritarchs*							1	4	3	1.5	1	1	1.5	1	3	1	5				
36	*Dinoflagellate*					2	1					1	2	1	2		1	0.5				
37	*Algal remnants*									1.5	2	1	2	1	1	1	1.5	0.5				

PLATE 1

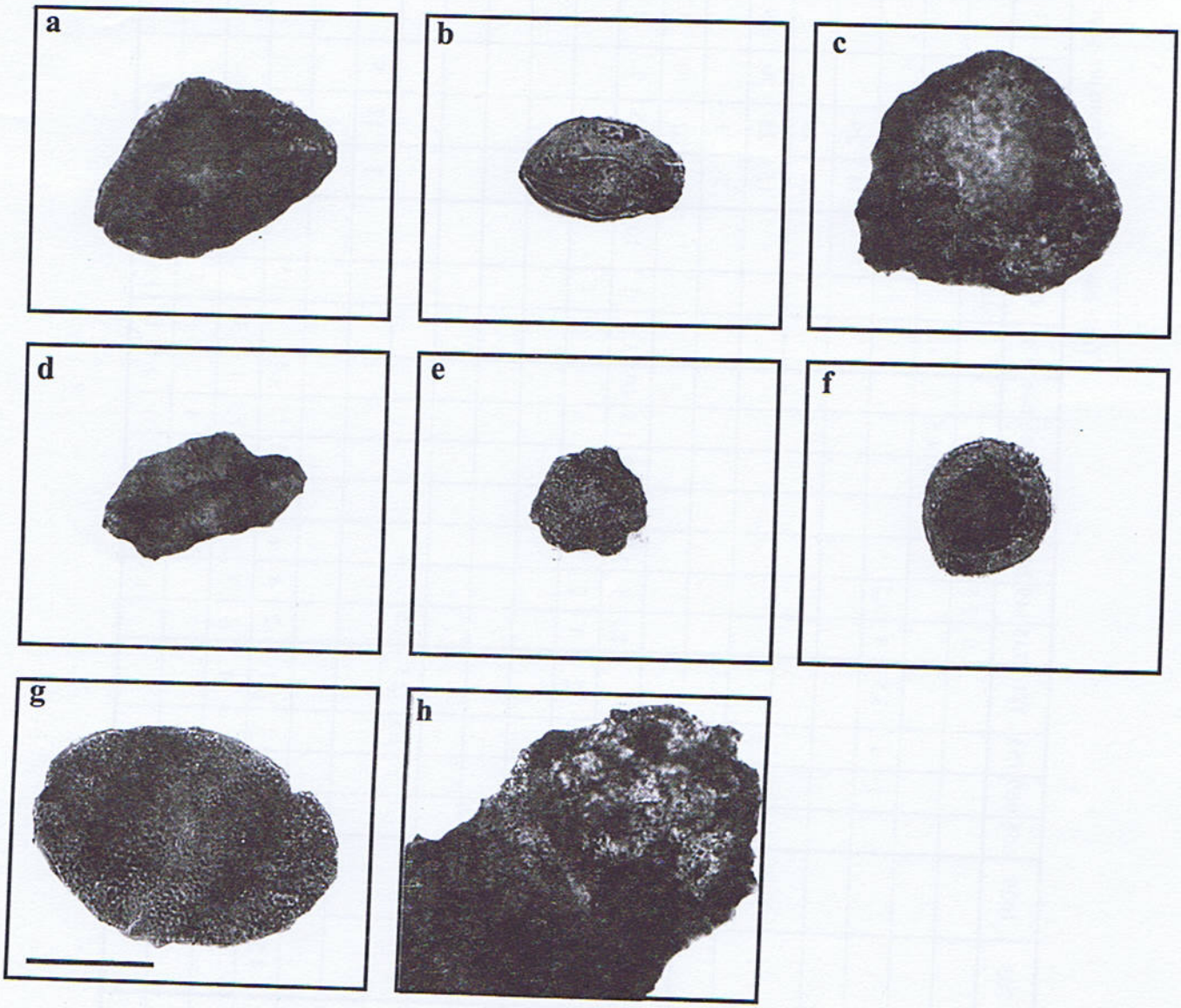

Fig. a *Aequitriradites triangulates*, Lumshiwal Formation. KQ. 188, Dheri Kot

Fig. b *Laevitriletes sp.*, Chichali Formation. KQ. 669, Burjianwala Laman

Fig. c *Impardecispora cf. parvelentus*, Chichali Formation. KQ. 754, Chapra

Fig. d *Bisaccate*, Lumshiwal Formation. KQ. 188, Dherikot

Fig. e *Indotriletes korbaensis*, Chichali Formation. KQ. 754, Chapra

Fig. f *Pterospermella australiensis*, Kawagarh Formation. KQ. 170, Choi

Fig. g *Alisporites grandis*, Chichali Formation. KQ. 669, Burjinwala Laman

Fig. h *Podocarpites sp.*, Chichali Formation. KQ. 754, Chapra

PLATE 2

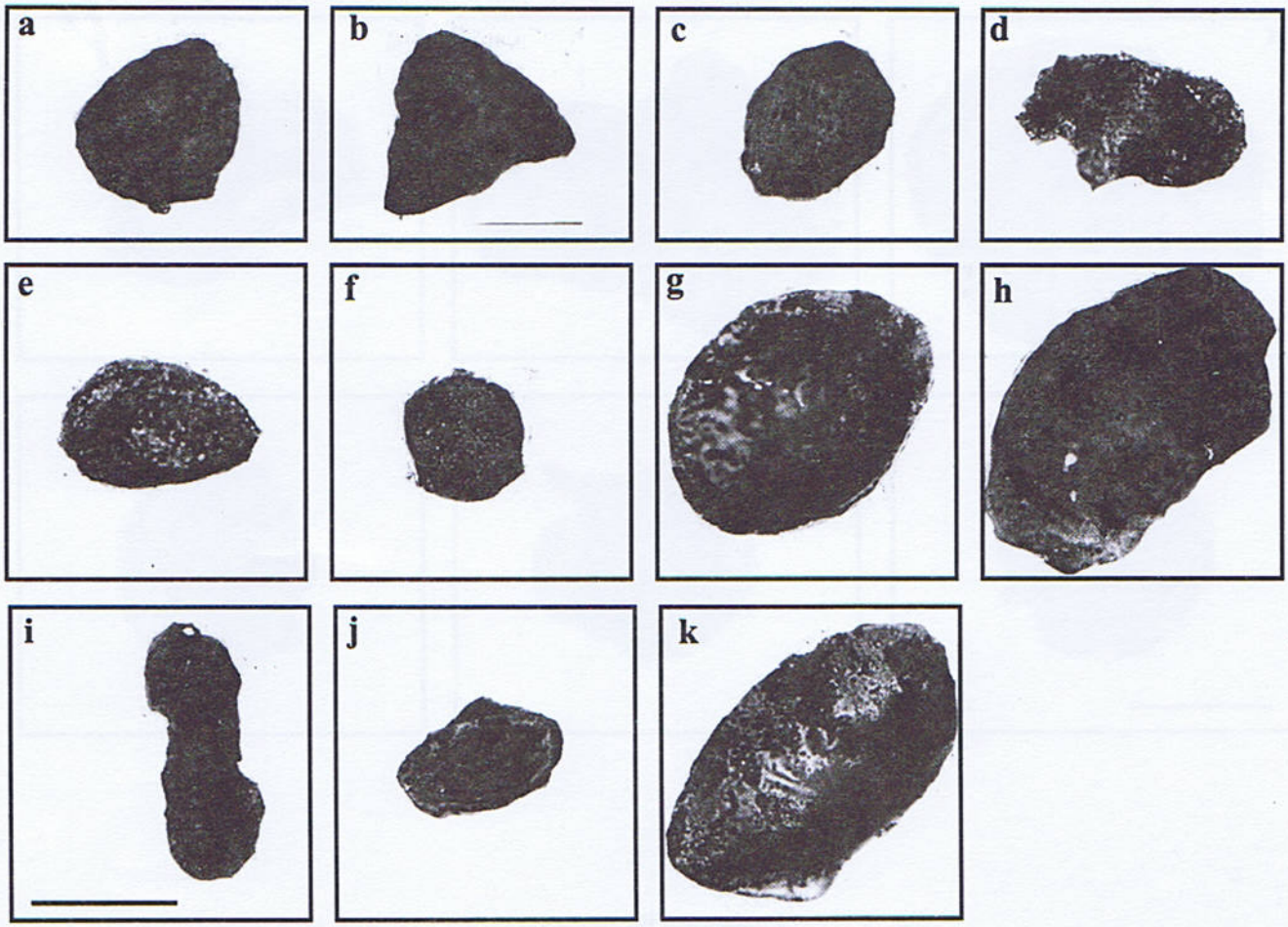

Fig. a *Densoisporites nejburji*, Lumshiwal Formation. KQ. 665, Burjianwala Laman

Fig. b *Leiotriletes sp.*, Lumshiwal Formation. KQ. 208, Daurdad

Fig. c *Leptolepidites eparcornatus*, Lumshiwal Formation. KQ. 187, Dherikot

Fig. d *Alisporites grandis*, Chichali Formation. KQ. 181, ½, F 2/7, Bata

Fig. e *Leptodineum eumorphum*, Lumshiwal Formation. KQ. 148, 6/3 F 3/24a, Togowala

Fig. f *Foveosporites subtriangularis*, Lumshiwal. KQ. 208, 1/1, F 1/35, Daurdad

Fig. g *Minutosaccus crenulatus*, Chichali Formation. KQ. 669, 4/1, F 3/2a, Burjianwala Laman

Fig. h *Alisporites bilateralis*, Chichali Formation. KQ. 181, 4/3, F 2/8, Bata

Fig. i *Valiasaccites validus*, Lumshiwal Formation. KQ. 147, 1/1, F 3/14, Togowala

Fig. j *Laevigatosporites sp.*, Lumshiwal Formation. KQ. 148, 3/3, F 3/20a, Togowala

Fig. k *Laevigatosporites sp.*, Lumshiwal Formation. KQ. 148, 6/3, F 3/23a, Togowala

PLATE 3

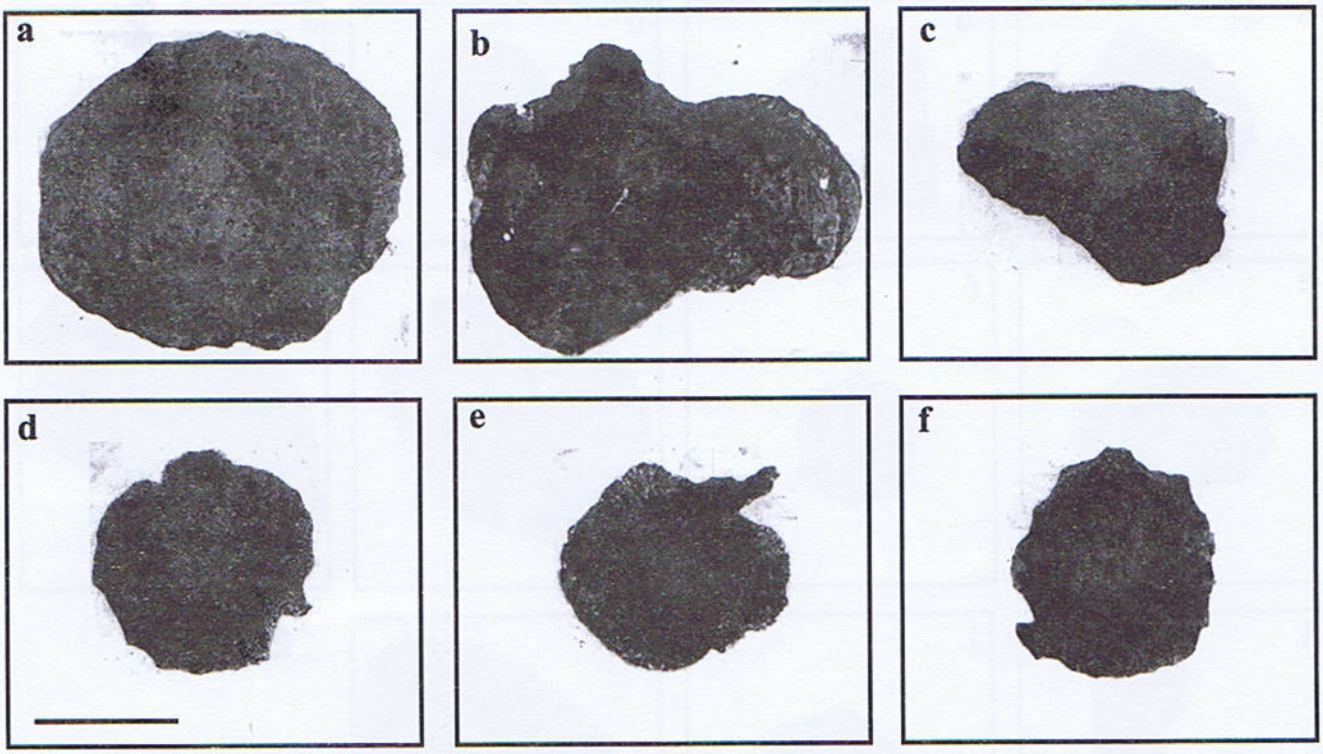

Lumshiwal Formation

Fig. a *Succinctisporites grandior*. KQ. 149, Togowala

Fig. b *Inaperturopollenites sp.* KQ. 148, Togowala

Fig. c *Ovalipolis ovalis*. KQ. 149, Togowala

Fig. d *Crybelosporites sp.* KQ. 209, Daurdad

Fig. e *Crybelosporites pannuceus*. KQ. 149, Togowala

Fig. f *Afropollis jardinus*. KQ. 756, Chapra

PLATE 4

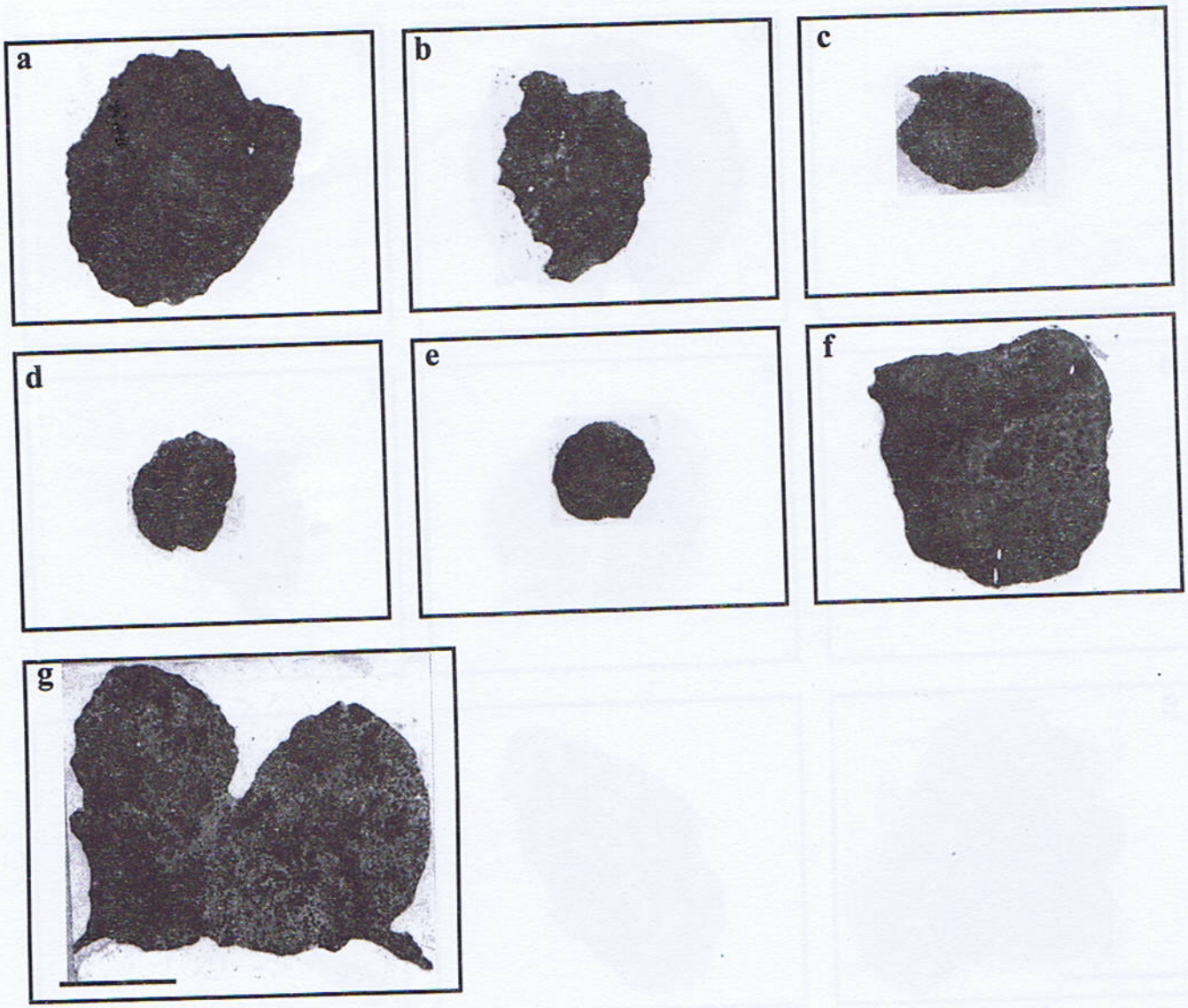

Lumshiwal Formation

Fig. a *Podocarpites ellipticus.* KQ. 148, Togowala

Fig. b *Palambages sp.* KQ. 149, Togowala

Fig. c *Gordodinium alberti.* KQ. 149, Togowala

Fig. d *Enzonalasporites vigens.* KQ. 148, Togowala

Fig. e *Punctatisporites sp.* KQ. 149, Togowala

Fig. f *Frangospora sp.* KQ. 148, Togowala

Fig. g *Endogone sp.* KQ. 149, Togowala

PLATE 5

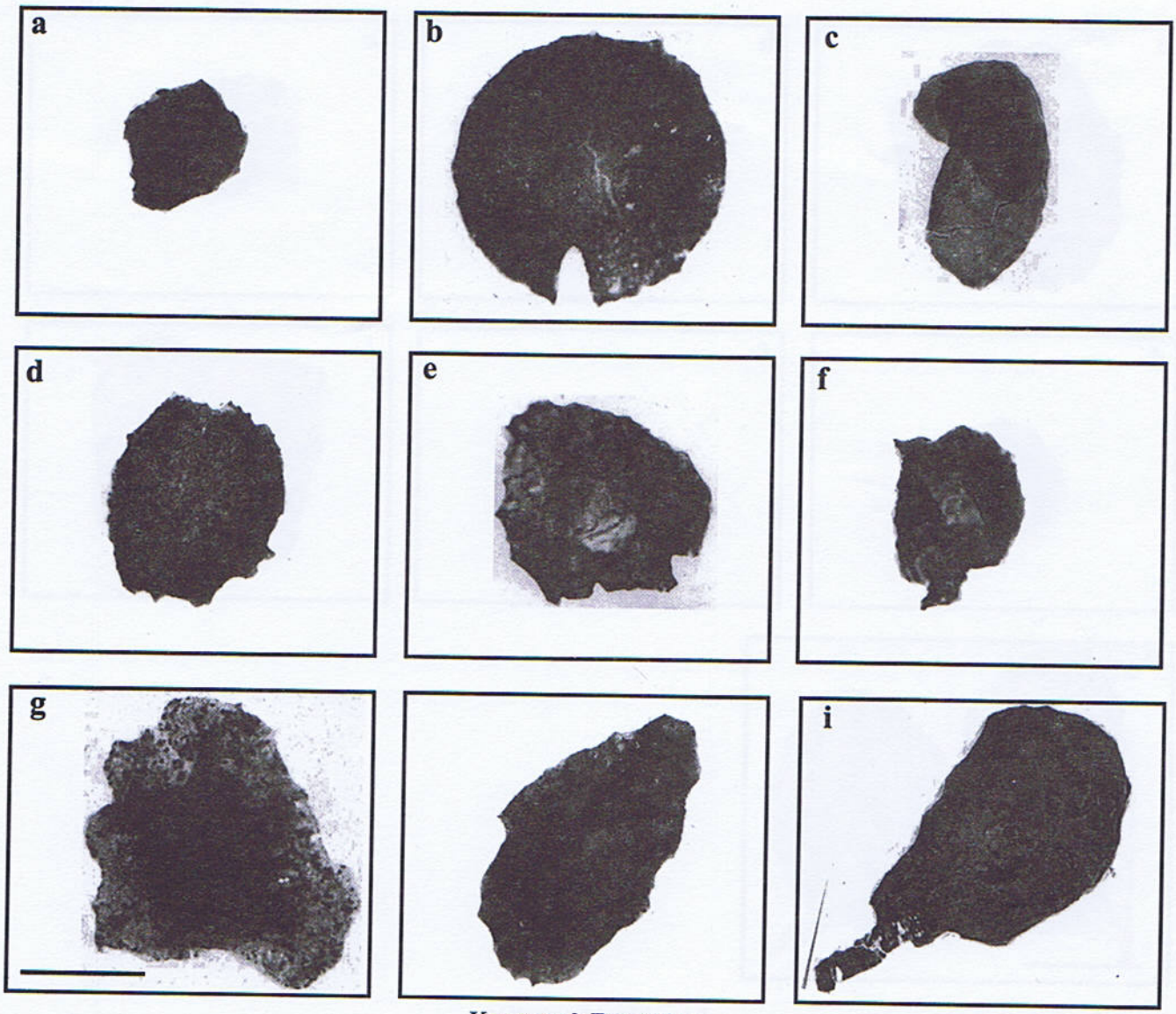

Kawargarh Formation

Fig. a *Cyclobaculisporites minutes.* KQ. 170, Choi

Fig. b *Verrucosisporites narmianus.* KQ. 1236, Surg

Fig. c *Pinuspollenites sp.* KQ.1225, Dherikot

Fig. d *Verrucosisporites densus.* KQ. 170, Choi

Fig. e *Palambages sp. (Acritarch).* KQ. 1237, Surg

Fig. f *Leiotriletes sp.* KQ. 170, Choi

Fig. g *Densipollenites densus.* KQ. 1237, Surg

Fig. h *Infernopollenites sp.* Kq. 170, Choi

Fig. i *Sclerocystis sp.* KQ. 158, Daurdad

Kawagarh Formation (Late Cretaceous)

Kawagarh Formation was poorly productive. Apart from *Leiotriletes* and *Laevigatotriletes* that are the general long ranging types for all the formations only four palynomorphs species are encountered here. These are also commonly shared by the Lumshiwal Formation, viz., *Affropollis jordinus* (Plate No. 3f), *Alisporites grandis*, *Inaperturopollenites sp.* (Plate No. 3b) and *Pinuspollenites sp.* (Plate No. 5c). Apart from these commonly shared types, the Kawagarh Formation also contains *Ptrospermella australiensis* (Plate No. 1f) that is age diagnostic for Campanian.

Considerations of table No. 3 reveal that three palynomorph genera (recovered during the present study) deviate considerably from their already established stratigraphical range of occurrence. *Leptolepidites* was found in the Lumshiwal Formation (Lower Cretaceous) which otherwise is only restricted to the Jurassic strata. *Densipollenites* has a restricted range of occurrence between Early Permian to Late Jurassic, but in the Kala Chitta Range it was identified in the Kawagarh Formation (Upper Cretaceous), whereas, *Lundbladispora* (purely a Triassic genus) was also isolated from the Samana Suk Limestone (Middle Jurassic). All these exceptions might be due to the reworking/stratigraphical leak or the contamination of the palynomorphs. If further studies reconfirm such instances in the same outcrops of adjoining areas, the stratigraphical occurrences of these genera (*Leptolepidites Densipollenites*, *Lundbladispora*) might be revised.

SYSTEMATIC PALYNOLOGY

Anteturma SPORITES H. Potonie, 1893
Turma TRILETES (Reinsch) Dettmann, 1963
Suprasubturma ACAVATITRILETES Dettmann, 1963
Subturma AZONOTRILETES (Luber) Dettmann, 1963
Genus *Leiotriletes* Naumova ex Isohchenko 1952
Type species *Leiotriletes sphaerotriangulatus* (Loose) Potonie and Kreump 1954
Leiotriletes sp.
Plate No. 2b, Plate No. 5f

Description: Miospore, trilete, amb triangular or subrounded, distorted due to compression, "Y" marking not very clear, longer than ½ radius. Exine faintly infrapunctate, up to 1 µm.

Genus *Punctatisporites* Ibrahim 1933
Type species *Punctatisporites punctatus* (Ibrahim) Ibrahim 1933
Punctatisporites sp.
Plate No. 4e

Description: Miospore, trilete, amb ± circular, trilete rays relatively short, may or may not be reaching equator. Exine punctate or finely reticulate up to 1 µm thick.

Genus *Frangospora* Venkatachala and Kar 1968
Type species *Frangospora fracta* Venkatachala and Kar
Frangospora fracta Venkatachala and Kar
Plate No. 4f

Description: Miospore, trilete, amb circular to subcircular rays ¾ radius, tapering, exine laevigate, sometimes infra-structured, unevenly thickened, outer exine splitting up by irregularly distributed cleavages giving the spore a mud crack like appearance, exine 2 µm.

Genus *Foveosporites* Balme 1957
Type species *Foveosporites canalis* Balme 1957
Foveosporites subtriangularis (Brenner) Doring
Plate No. 2f

Description: Miospore, trilete, amb rounded or elongate triangular, angles broadly rounded sides straight to convex. "Y" marking extending ¾ radius. Exine infraverrucate to foveolate ± 3 µm thick.

Genus *Verrucosisporites* Ibrahim, 1933
Type species *Verrucosisporites verrucosus* Ibrahim
Verrucosisporites narmianus Balme, 1970
Plate No. 5b

Description: Miospore, trilete, amb circular to subcircular, exine verrucose, verrucae closely set, height equal to or less than their breadth, apex truncate, average diameter of verrucae 3-4 µm, exine up to 3 µm thick.

Genus *Leptolepidites* Couper, 1953
Type species *Leptolepidites verrucatus* Couper
Leptolepidites eparcornatus
Plate No. 2c

Description: Miospore, trilete, amb subtriangular, sides convex to concave, biconvex in equatorial view. "Y" marking usually well developed, but not discernable in present specimen due to poor preservation. Exine very thick (up to 3 µm). Sculptured with large irregularly shaped rounded verrucae.

Subinfraturma NODATI Dybova and Jackovicz (1957)
Genus *Cyclobaculisporites* Bharadwaj 1955

Type species *Cyclobaculisporites grandiverrucosus* (Kosanke) Bharadwaj

Cyclobaculisporites minutus Kar 1968
Plate No. 5a

Description: Miospore, trilete, amb circular to subcircular, trilete rays indistinct, less than _ radius, exine surface thickly set with baculae of uniform length but

Table 2

Relationship between various chemical compounds and palynomorph occurrence in the Mesozoic sucession of the Kala Chitta Range.

Age	Formation	Sample	SiO_2	Fe_2O_3	FeO	P_2O_5	TiO_2	Al_2O_3	CaO	MgO	MnO	Na_2O	K_2O	H_2O^+	H_2O^-	CO_2	S	C	Total	Pal/g
Triassi c	Kingriali	576	0.48	1.55	1.18	-	0.15	0.80	42.62	8.06	0.04	1.54	1.25	0.10	0.20	41.74	0.24	0.10	99.99	164
Jurassic	Samana Suk	703	3.91	1.13	0.42	4.41	3.02	0.47	43.88	0.20	0.04	2.45	1.28	0.10	0.02	35.59	0.87	2.21	100	1050
		1029	10.92	1.59	0.16	0.04	0.30	0.37	28.04	16.13	0.04	1.62	0.68	0.10	0.12	37.62	0.06	2.21	100	54
Jurassic / Creta-ceous	Chichali	658	50.70	1.04	0.12	0.02	0.30	6.63	20.50	2.94	0.07	1.65	0.68	0.10	0.09	14.61	0.15	0.40	100	800
		669	16.22	4.82	0.10	0.80	0.20	6.98	35.89	2.42	0.01	0.21	0.26	0.10	0.09	31.73	0.06	0.10	99.99	482
		754	34.74	1.30	0.42	0.02	0.30	7.69	30.44	5.53	0.04	1.35	0.50	0.10	0.10	17.26	0.29	0.10	100	150
Lower Creta-ceous	Lumshiwal	148	28.74	0.30	0.02	0.02	0.30	6.59	36.44	0.35	0.04	1.35	0.50	0.10	0.10	23.20	0.29	0.10	98.56	4080
		149	44.67	1.09	0.24	0.02	0.30	8.08	21.86	1.81	0.05	2.45	1.28	0.10	0.13	17.77	0.06	0.10	100	2400
		187	15.04	2.79	0.10	1.91	0.10	8.43	38.13	2.36	0.02	0.86	0.23	1.51	0.62	26.26	0.15	1.30	99.99	1000
		188	47.40	8.16	2.42	0.05	1.50	8.99	12.33	1.61	0.04	1.53	1.96	0.10	3.30	10.30	0.19	0.10	99.98	9000
		209	20.42	5.71	0.44	0.09	0.42	9.83	33.94	5.91	0.09	1.53	3.01	0.10	2.00	16.35	0.06	0.10	100	6200
		210	14.61	9.00	2.78	0.17	0.97	12.58	39.11	3.22	0.01	3.45	4.20	1.68	1.29	6.17	0.03	0.20	99.52	10100
		661	45.19	5.15	0.32	0.09	0.20	1.33	21.16	1.35	0.06	2.22	2.41	0.10	3.30	16.90	0.04	0.20	100	8000
		665	29.00	1.30	0.32	0.02	0.30	5.69	28.00	5.60	0.04	1.32	0.06	0.10	0.20	27.10	0.26	0.10	99.94	2000
		666	20.20	1.23	0.32	0.09	0.08	5.20	33.25	2.31	0.06	1.35	0.68	0.10	0.08	33.31	0.06	0.10	98.42	4200
		756	9.33	0.09	1.80	0.11	0.71	10.15	48.82	6.15	0.05	3.36	3.89	0.93	2.92	6.62	0.20	2.21	99.34	7100
Upper Creta-ceous	Kawagarh	170	24.70	1.30	0.42	0.01	0.20	2.69	38.45	6.35	0.04	2.17	2.56	0.10	0.32	19.30	0.07	1.30	99.98	400
		171	16.74	1.24	0.10	0.02	0.38	1.24	40.72	2.97	0.06	2.22	2.65	0.10	0.14	30.41	0.87	1.30	100	192
		1236	20.15	3.25	2.17	0.05	0.20	4.30	35.77	1.64	0.02	2.11	2.71	0.10	0.11	27.02	0.16	0.20	99.96	1000
		1237	18.20	2.20	0.17	0.04	0.20	4.60	38.40	2.02	0.04	2.05	1.51	0.10	0.13	30.08	0.06	0.20	100	984
r-values (Co-efficient of correlation)			+0.39 ns	+0.66 **	+0.60 **	-0.22 ns	+0.24 ns	+0.56 **	-0.02 ns	-0.23 ns	-0.20 ns	+0.50 *	+0.61 **	+0.11 ns	+0.83 **	-0.70 **	-0.30 ns	-0.20 ns	-	-

Legend: ns= not significant at α 0.05 Pal/g = Palynomorph per gram of sample

*= significant at α 0.05

**= highly significant at α 0.05 (significant at α 0.01)

Table 3
Tentative range of occurrence of some stratigraphically important palynomorph genera recovered from the Mesozoic Rocks of the Kala Chitta Range.

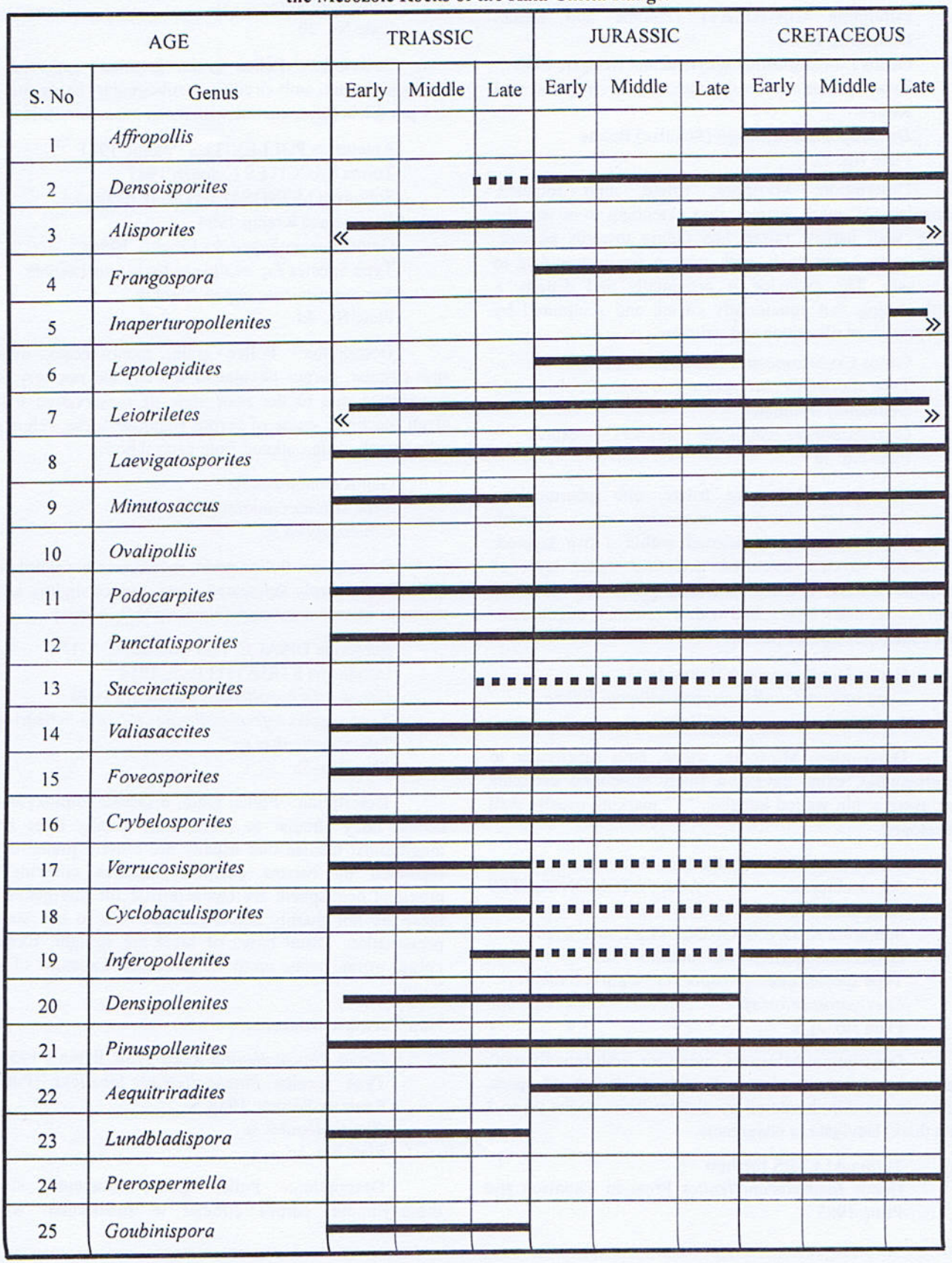

■ ■ ■ ■ ■ Age not clearly established.

« Extending into older rocks

» Extending into younger rocks

widely ranging width, interbacular spaces very narrow, discernable only under oil immersion objective.

Infraturma CINGULATI (Potonie and Klaus) Dettmann, 1963
Genus *Densoisporites* Weyland and Krieger, 1953
Type species *Densoisporites velatus* Weyland and Krieger
Densoisporites nejburgii (Schulze) Balme
Plate No. 2a

Description: Miospore, trilete, amb rounded, triangular, "Y" mark distinct, rays extending to or into the flange, with narrow raised lips fading towards equator. Exine up to 2 µm thick, with surface finely granulate to chagrenate. The exoexine is proximally and distally ± tightly fitting, but equatorially cavate and sculptured by numerous short plications and wrinkles.

Genus *Crybelosporites* Dettmann 1963
Type species *Crybelosporites striatus* (Cookson and Dettmann) Dettmann
Crybelosporites pannuceus (Brenner) Srivestava
Plate No. 3e

Description: Miospore, trilete, amb spheroidal to ellipsoidal, exine stratified consisting of a smooth homogenous inner layer enclosed within a two layered, proximally cavate, structured 'sculptine', outer layer of sculptine without a trilete aperture, proximally detached from trilete, inner layers; and with a reticulate, rugulate, or foveolate (OL) surface pattern.

Genus *Lundbladispora* Balme 1963
Type species *Lundbladispora willmotti* Balme
Lundbladispora willmotti Balme

Description: Miospore, trilete, amb subcircular to subtriangular, exine cavate, a finely structured exoexine enclosing a thin walled intexine, "Y" marking usually well developed.

Turma MONOLETES Ibrahim 1933
Suprasubturma ACAVATOMONOLETES Dettmann, 1963
Subturma AZONOMONOLETES Luber, 1935
Genus *Laevigatosporites* Ibrahim, 1933
Type species *Laevigatosporites vulgaris* Ibrahim
Laevigatosporites sp.
Plate No. 2j, k

Description: Miospore, monolete, amb broadly oval, tetrad scar distinct, alete extending ¾ length of spore, commissure thin, bordered by distinct labra. Exine up to 3 µm thick, laevigate to chagrenate.

Turma ALETES Ibrahim
Genus *Inaperturopollenites* Pflug in Thomson and Pflug 1953
Type species *Inaperturopollenites dubius* (Potonie and Venkatachala) Thomson and Pflug 1953
Inaperturopollenites sp.
Plate No. 3b

Description: Pollen grain, germinal apparatus or suture indistinct, amb circular or subcircular. Exine thin up to 1 µm thick, infrapunctate with many secondary folds.

Anteturma POLLENITES Potonie 1931
Turma SACCITES Erdtman 1947
Subturma MONOSACCITES (Chitaley) Potonie and Kremp 1954
Genus *Enzonalasporites* Leschik 1956a
Type Species *Enzonalasporites vigens* Leschik
Enzonalasporites vigens Leschik
Plate No. 4d

Description:- Pollen grain, monosaccate, overall amb circular, corpus circular to sub circular not very well demarcated due to the poor state of preservation in the given specimen, exine of corpus rugulose, alete, velum not very sharply differentiated from central body.

Genus *Goubinispora*
Type species *Goubinispora*
Goubinispora sp.

Description: Pollen grain, monosaccate, central body diffuse, not sharply delineated, alete, saccus slightly lobed, exoexine of saccus infrareticulate, up to 2µm thick.

Subturma DISACCITES Cooksoon, 1947
Infraturma STRIATITI Pant, 1954
Genus *Infernopollenites* Scheuring 1970
Type species *Infernopollenites sulcatus* Scheuring
Infernopollenites sp.
Plate No. 5h

Description:- Pollen grain, bisaccate, diploxylonoid, central body circular to subcircular, usually three broad longitudinal taeniae that usually are closely joined or are separated by narrow ectexinal fissures covering the proximal hemisphere are characteristic for this genus, but these are not sharply delineated here due to bad state of preservation. Distal bases of sacci are straight. Exine of corpus infrapunctate up to 1.5 µm thick. Exoexine of sacci 2 µm.

Non Taeniate Bisaccate

Genus *Pinuspollenites* Raatz 1938, Potonie 1958
Type species *Pinuspollenites labdacus* (Potonie) Raatz ex Potonie 1958
Pinuspollenites sp.
Plate No. 5c

Description:- Pollen grain, bisaccate, slightly diploxylonoid, corpus circular to subcircular, without

germinal suture, exine of corpus laevigate up to 1.5 μm thick. Sacci small, attachment ventral , exoexine of sacci 2 μm thick.

Genus *Valiasaccites* Bose and Kar 1966
Type species *Valiasaccites validus* Bose and Kar
Valiasaccites validus Bose & Kar
Plate No. 2i

Description:- Pollen grain, bisaccate, haploxylonoid, overall amb ± oval, central body oval, usually with two longitudinal lateral ridges which are not detectable in the present specimen. Exine of corpus infravermiculate to infrareticulate. Monolete mark on corpus absent. Proximal saccus attachment zone along equator, distally subequatorial and associated with a semilunar body. Sacci semicircular, coarsely intrareticulate (makes up to 2 μm), attachment of sacci lateral with slight ventral displacement. Exoexine of sacci up to 2 μm thick.

Genus *Podocarpites* Bolkhovitina 1956
Type species *Podocarpites flacciformis* (Malj.) ex Bolkhovitina
Podocarpites sp.
Plate No. 1h

Description:- Pollen grain, bisaccate haploxylonoid to slightly diploxylonoid. Central body circular to subcircular, alete. Exine of corpus infrapunctate up to 1.5 μm thick. Attachment of sacci lateral with slight ventral displacement. Exoexine of sacci up to 2 μm thick.

Genus *Ovalipollis* Krutrch 1955
Type species *Ovalipollis ovalis* Krutrch
Ovalipolis ovalis Krutrch
Plate No. 3c

Description:- Pollen grain, bisaccate, overall amb slender or broadly oval, in part rhombic, usually a major fold runs longitudinally on one face from one end to other, the pointed ends of oval central body are capped by weakly developed sacci that possess a pronounced rodlet structure and have a smooth surface. Exine of central body up to 1.5 μm thick whereas that of sacci up to 2 μm thick.

Genus *Minutosaccus* Madler 1964
Type species *Minutosaccus acutus* Madler 1984
Minutosaccus crenulatus Dobly
Plate No. 2g

Description:- Pollen grain, bisaccate, haploxylonoid, overall amb broadly fusiform, central body circular to subcircular, strongly cutinized and small, sacci distally displaced, usually with sharply delineated sulcus which is detectable in actual specimen under oil immersion objective upon careful L-O analysis but not in the photomicrograph provided. Exine of corpus laevigate up to 2 μm thick, exoexine of sacci up to 1.5 μm thick.

Genus *Alisporites* Daugherty emend Nilsson, 1958
Type Species *Alisporites opii* Daugherty
Alisporites grandis (Cookson) Dettman
Plate No. 1g

Description:- Pollen grain, bisaccate, haploxylonoid, central body circular to subcircular. Exine of corpus 1 μm thick laevigate. Sacci attached laterally with slight distal inclination. Exoexine of sacci infra reticulate up to 1.5 μm thick.

Non-Vesiculate Tectate Pollen

Genus *Afropollis* Doyle, Jardine and Doerenkamp 1982
Type species *Afropollis Jardina* (Brenner) Doyle
Afropollis jardina (Brenner) Doyle
Plate No. 3f

Description:- Pollen grain, overall amb spheroidal, radially symmetrical, coarsely reticulate to ruguloreticulate, semitectate. Due to corrosion and poor preservation, differentiation of tectum is not so sharp in the photomicrograph provided. It was however, discernable under oil immersion objective upon careful L-O analysis in the actual specimen. Lumina on most of the grain surface 2-5 μm maximum dimension.

GEOCHEMISTRY AND PALYNOMORPH PRODUCTIVITY

During the present study an attempt has been made to investigate whether or not the chemical composition (or any change in it) of the parent sediment affects productivity and preservation of palynomorphs in the Mesozoic rocks of the Kala Chitta Range. However, if a particular sediment is not productive (containing no palynomorphs) no method is devised to date to judge whether it originally contained palynomorphs or not, or the microfossils disappeared later due to some postdepostitional hazard(s). The author has personally observed that if a zone of a particular formation is highly productive at one level, it may become poorly productive or totally barren at another horizon. As indicated by several workers it may be due to the changes in depositional environments (Darrell and Hart, 1979), thermal effects (Dow, 1977) or other post depositional hazards (Bonny, 1976, 1978).

Some other sedimentological factors in combination with the associated vegetational pattern on nearby land and the differential rate of transportation of various palynomorphs to the depositional site may affect occurrence and preservation of palynoflora in rocks (Smith, 1962; Chaloner and Muir, 1968; Phillips et al., 1974; Scott and King, 1981). But the possibility of the fact that any change(s) in the chemical composition of the parent sediment may affect palynomorph productivity cannot be ruled out totally.

Twenty rock samples viz KQ 575 (Kingriali Formation); KQ 703, KQ 1029 (Samana Suk Limestone); KQ 658, KQ 669, KQ 754 (Chichali Formation); KQ 148, KQ 149, KQ 187, KQ 188, KQ 209, KQ 210, KQ 661, KQ 665, KQ 666, KQ 756 (Lumshiwal Formation); KQ 1236, KQ 1237, KQ 170, KQ 171 (Kawagarh Formation) were randomly selected to study such phenomenon.

Chemical analysis

The contents of SiO_2, H_2O+, H_2O- were determined gravimetrically. Al_2O_3, MnO, CaO and MgO were determined by atomic absorption and spectrophotometry.

The amounts of TiO_2 and P_2O_5 were determined by spectrophotometry. FeO and inorganic carbon were determined volumetrically. The alkalies and organic carbon were determined by C and S analyser.

Statistical analysis

Coefficient of correlation (r-values) were calculated between percentages of an elemental oxide and number of palynomorphs/g in different samples to check whether any relationship exists between the two independent variables viz: percentage of an elemental oxide and number of polynomorphs per gram of samples (productivity).

Table No. 2 shows the sample wise percentage of elemental oxides and number of palynomorphs/g of different samples and the r-values.

It has been observed that FeO, Fe_2O_3, Al_2O_3, K_2O show highly significant positive correlation between the two independent variables indicating a highly favourable chemical environment for palynomorph preservability. Na_2O also shows significant positive correlation. Negative correlation is also observed in P_2O_5, CaO, MgO, MnO, though not significant at 5% level of significance. However, it may indicate that oxidizing environments such as that of P_2O_5 are highly unfavourable for palynomorph preservation. Similarly, CaO and MgO, which are components of dolomites, are also unsuitable for palynomorph preservability. Similar observations have also been made by Masood et al. (1995) on the samples from the Amb Formation (Permian) of the Salt Range.

The above study indicates that the higher amounts of FeO, Fe_2O_3, Al_2O_3, K_2O, Na_2O, SiO_2 TiO_2 favour higher palynomorph occurrence whereas P_2O_5, CaO, MgO and MnO_2 impart low productivity.

PALEOCLIMATOLOGY AND DEPOSITIONAL ENVIRONMENTS

The climate experienced by an area at a particular time depends upon its continentality and latitudinal position. Fossil spores and pollen exhibit various morphographic characters with specific configurations and structures, each with a precise function. These morphographic features transcend taxonomic delimitations of the dispersed spores and pollen. The behaviour pattern of significant morphographic events are evaluated for their sensitivity to climate. The combination of characters in a given palynoflora is diagnostic for that period and it has been considered for climatic interpretation. Since the palynoflora recovered during the present investigation was not well preserved, it was not possible in most cases to interpret morphographic features associated with palynomorphs correctly, and hence accurate climatic interpretation at various stratigraphic levels was not possible.

Considering Bharadwaj scheme (1966) it is possible to some extent to comment on vegetational history and then to elucidate the depositional environment on a broad scale. According to Bharadwaj scheme -- trilete and monolete miospores represent Cryptogams striated bisaccates, Glossopteroids; non-striated bisaccates, Conifers, trilete monosaccates, Gangamopteroids, monosulcates, Cycadoginkops and alete monosaccates represent Cordaitales.

Absence of monosaccate in all samples except in the Kingriali Formation (i.e. *Goubinispora*) is noteworthy (Table No. 1), indicating that none of the members of *Pteridospermaeles* existed within the close vicinity of the depositional site from Jurassic to Upper Cretaceous periods.

CONCLUSION

Assemblages from Kingriali Formation, the Samana Suk Limestone and the Chichali Formations are characterised by poor preservation, lack of diversity and the presence of enormous small spinose acritarch and indistinctive leiospheres. The Kingriali Formation also contains few species of *Lundbladispora* and *Goubinispora*. Both these types indicate tropical to subtropical hot climate with medium to high humidity in closely located land area, whereas, the palynoflora of the Samana Suk Limestone and the Chichali Formation include great abundance of cryptogams, which must be present very near to shore in an upland area with typical temperate to subtemperate (low cooling) with medium to high humidity.

Assemblages of the Lumshiwal Formation are much more diverse than those recovered from any other formation. The distributional heterogeneity is evident from consideration of Table 1. Several pollen species were found only in the Lumshiwal Formation and the diversification of spore and pollen assemblage is due mainly to an increase in the variety of trilete and bisaccate palynomorphs.

Taken in its entirety a strongly regressive phase, which may of course have been associated with wide climatic changes, have been observed. Regression would be

expected to manifest itself by an increase in the number of plant microfossils reaching the depositional area. A decrease in the number and veriety of the acritarchs and the diversification of the assemblages associated with large number of pollen and spores derived from subordinate or locally restricted floral elements are the characteristics of the assemblages from the Lumshiwal Formation.

There is a marked decline in this trend in the Kawagarh Formation. However, the Kawagarh Formation is palynologically more rich as compared to the Kingriali Formation or the Samana Suk Limestone.

REFERENCES

Bharadwaj, D.C. 1966. Distribution of Spores and Pollen grains dispersed in the Lower Gondwana Formations of India. *Symp. Florist. Strat. Gondwanaland. Spec. Session Publ*: 69-84.

Blome, C.R. and Albert, N.R. 1985. Carbonate Concentrations: an ideal Sedimentary Host for Microfossils. *Geology* **13**: 212-215.

Bonny, A.P. 1976. Recruitment of pollen to the sesten and sediment of some English Lade Distrct lakes: *Jour. Ecol.* **64**: 859-87.

Butt, A.A., Qureshi, M.K.A., Masood, R. and Ghazi, S. 2008. Palynology of the Mesozoic Succession of the Kala Chitta Range, Pakistan. Abstract Volume *33rd Internat. Geol. Congr.* Oslo, Norway.

Chaloner, W.G., Muir, M. 1968. Spores and Floras in coal and coal bearing strata, D.G. Murchinson & T.S. Westall (eds.), 127-146 Oliver & Boyd Edinburgh.

Cotter, G. De. P. 1933. The Geology of the part of the Attock District, West of Long. 72°45′ E. *Mem. Geol. Surv. India* **55**: 63-161.

Darrell, J.H. and G.F. Hart. 1979. Environmental determinations using absolute miospore frequency, Mississippi River delta. *Geol. Soc. Amer. Bull.* **81**: 2513-18.

Dow, W.G. 1977. Kerogen studies and geological interpretations. *Jour. Geochem. Explor.* 7: 79-99.

Fatmi, A.N., 1973. Lithostratigraphic units of Kohat-Potwar Province, Indus Basin, Pakistan, *Mem.Geol. Surv: Pakistan* **10**:1-80.

Jansonius, J. and Hills, H. 1976. Fossil genera file of Palynomorphs, *Univ. Calgary, Spec. Publ.*

Masood, K.R., Qureshi, K.A., Hussain, Z. and Parveen, M. 1995. Palynomorph occurrence in relation to geochemistry, in the Amb Formation (Artiiskian), Zaluch Gorge, Salt Range, Pakistan. *Pak. Jour. Hydrocarbon Research* 7(1): 61-70.

Phillips, T.L., R.A. Peppers, M.J. Avcin and P.F. Langhnan. 1974. Fossil plants and coal: patterns of chang in Pennsylvanian coal swamps of Illinois Basin. *Science* **187**(4144), 1367-1369.

Scott, A.C., J. Galtier and G. Clayton. 1985. A new late Tournaisian (lower carboniferous) Flora from the Kilpatrich Hills, Scotland. *Rev. Paleobot. Palynol.*: **44**: 81-89.

Smith, A.H.V. 1962. The palaeoecology of Carboniferous peats based on miospores and petrography of bituminous coals. *Proc. Yorkshir Geol. Soc.* **33**: 423-474.

Geol. Bull. Punjab Univ. 43, 2008.

EVALUATION OF SHAKI SARWAR AND RAJAN PUR AGGREGATES FOR CONSTRUCTION IN SOUTHERN PUNJAB PROVINCE, PAKISTAN

BY

MUHAMMAD MUNAWAR IQBAL GONDAL
Road Research and Material Testing Institute, New Campus, Lahore-54590

NAVEED AHSAN
Institute of Geology, University of the Punjab, Quaid-i-Azam Campus, Lahore-54590 Pakistan

AND

AHMAD ZIA JAVID
Road Research and Material Testing Institute, New Campus, Lahore-54590

ABSTRACT: *Colossal quantity of performance bound and economical aggregate is required for in progress and planned mega projects in southern Punjab. The aggregates from established area along with two new sources were sampled and geotechnically and petrographically evaluated for their suitability as valuable aggregates. Girdu Limestone exposed along Multan-Quetta road, N-70, showed the best results as potential aggregate source for asphalt and cement concrete. It will not only drastically trim down the cost but will enhance performance life of buildings, bridges, barrages and roads.*

Besides this source, aggregates deposited in alluvial fans of ephemeral streams like Kaha/Khalgari, Pitok and Zungi is good quality aggregate for road sub base and base course. However, the presence of quartz wackes imparts this aggregate hydrophilic character that proscribes its use in asphalt and cement concrete.

INTRODUCTION

In southern Punjab, from Khanewal to Sadiqabad many national and provincial mega projects are under executions that require huge quantity of aggregates. The public and private sector is thriving to search out good quality aggregate for such projects to substantially reduce the cost of projects. In order to explore physiochemically durable and economically cheap crushed aggregates this study was taken up in Sulaiman Range.

A variety of aggregates for road construction are available in the Punjab province. Crushed rock aggregate is mainly derived from limestone outcrops of Margalla Pass (e.g. Ahsan et al., 2000), crushed gravel and sand (e.g. Chaudhry et al., 1999) is mined from river deposits and alluvial terraces. Other mineable deposits for aggregates are situated near Attock (Indus gravel and sand), Taraki-Dina quarries near Jhelum and a number of small crushers and gravel pits situated at various locations through out the Punjab province (e.g. Ahsan et al., 2000; Gondal et al., 2004a, 2004b). Besides these sources, Neoproterozoic outcrops of Kirana Hills in Sargodha and Chiniot area are the major quarries of aggregates (Alam, 1987; Alam et al., 1988; Khan and Chaudhry, 1991; Khan, 2004) for road construction, ordinary Portland cement concrete, railway ballast and riprap, etc.

In the southern Punjab (Gondal et al., 2006a, b), Sakhi Sarwar quarries (D. G. Khan) are considered the third longest quarry site where approximately 70 crushers have been installed since long and they are crushing boulders/gravels retrieved from Shaki Sarwar gravel complex. Each crusher is producing 6 to 7 trucks of aggregate per day with average capacity of 750 cft per truck. In order to meet demands of mega projects 10 crushing plants are supplying crushed rock aggregate (about 7500 cft /day) for sub base and base course in highway projects in Muzzafar Garh, D. G. Khan, Layyah, Vehari, Bahawal Pur, Bahawal Nagar, Multan and Rahim Yar Khan districts. Besides mechanical crushing facilities, base course aggregate is also produced by manual stone breaking

process in Sakhi Sarwar area. Another extensive source of aggregates are alluvial fan complex along Sulaiman Range from which coarse and fine aggregate is mined through open pit excavation and transported to construction sites in southern Punjab for sub base and base course aggregates. All these quarry sites are approved sources for Punjab Communication and Works Department for base. However, crushed rock aggregate from Shaki Sarwar is not approved for cement and asphalt concrete.

It is therefore imperative to evaluate the sources whose crush can safely be used in asphalt and cement concrete work. In this context, the present study was carried out to find and evaluate such rocks that meet the following requirements. 1) Extensive source is available for aggregate crushing, 2) show good bitumen adhesion, 3) free from deleterious effects like alkali aggregate reaction in cement concrete through its performance period and 4) located near to end users so that transportation cost and other taxes may be reduced. The rock outcrops along Multan-Quetta road (N-70) district D. G. Khan, Kaha/Khalgari, Pitok and Zungi Nullahs aggregates from Sakhi Sarwar and Girdu of district Rajanpur in Sulaiman Range were sampled for evaluation of their engineering properties.

SAKHI SARWAR AND GIRDU AREAS

Sakhi Sarwar and Girdu areas (lat. 29°50'-29°30' N and long. 70°00' - 70°30' E, in District DG Khan) dominantly comprises gravel terraces and outcrops of various rock types (Iqbal and Shah,1980) that are accessible through recently widened Multan-Quetta road. The Sulaiman Range in this area exhibits NS trending Fort Munro anticline. The outer hills of this range comprises gravel beds, sandstone and shale (Siwaliks) which rise abruptly from plains (372m) to about 1939m at Fort Munro. Immediately in the back, older tertiary formations comprising variegated shale and sandstones with thin layers of limestone (Shah, 1977, Iqbal and Shah, 1980; Malkani, 2004, 2006) are exposed. In Girdu area dark grey, hard and thick bedded limestone with intercalated marl beds is exposed (Shah, 1977; Kazmi and Jan, 1997) along both sides of the highway N-70. It is overlain by thin to massively bedded, off white to brownish quartzose sandstone. At places argillaceous limestone and shale horizons also outcrop (Hunting Survey Corporation, 1961; Malkani, 2004, 2006). The outcrop of limestone with distinct dark gray colour is exposed between 62+500 km and 67+900 km on the N-70 and extends upto village Girdu.

In addition to limestone exposures, numerous terraces occur in alluvial fans that are composed of granular material in the size which ranges from boulders to sand. These gravels and sand is transported by various stream originating from the adjacent rising Sulaiman Range. These clasts comprise off-white to brownish quartzite, hard and tough sandstone with subordinate limestone pieces. The rock fragments are generally rounded. The exposed surface of the fragments indicates effects of desert varnish.

KAHA/KHALGARI, PITOK AND ZUNGI NULLAHS

Pitok, Zungi, Khalgari and Kaha Nullahs are ephemeral streams. In these areas rainfalls are erratic and likely to occur in several brief torrential showers. Locally these torrents are known as Rud Kohi and their discharge produce uncontrolled flood, extensive erosion and loss of property and life in some cases. These torrents transport rock blocks/boulders to sand and clay sized material from hills onto the piedmont to develop gravel fans. The flow of the ephemeral streams gradually dissipated through distributaries on gravel fans/piedmont slopes and develops terraces.

Pitok Nullah Quarry

Pitok Nullah is a potential quarry of the area (lat. 29° 09' to 29°15' N; long. 69° 54' to 70° E). Nullah Pitok drains a large sedimentary area of the Sulaiman Range. Its drainage pattern is structurally controlled and many second order streams join it. The nullah cut across the range at Pitok and deposits its load forming a 1km wide terraced gravel fan. This source is 49 km from Rajanpur inclusive of 27 km Katcha track. The height of these terraces varied between 20ft to 150ft from nullah bed. Presently, Kachhi Canal contractors are using its aggregate but it had never been used by Highway Department due to inaccessibility to the alluvial fan area. The material mainly comprises limestone and sandstone.

Zungi Nullah Quarry

The aggregate source area of Nallah Zungi (lat. 28°54' to 29°00' N; long. 69°43' to 69°55' E) is situated 33 km from Rojhan Chowk at Indus Highway (N-55). This Nullah traverses through various sedimentary rocks of Dera Bugti hills. In down slope areas, fine sediments are abundant and toward plain area gravelly bed comprising limestone boulders and gravel occurs. This gravelly bed extends many kilometers in length. The width of Nullah was more than 300 meter whereas its terraces are wider.

Khalgari and Kaha Nullahs Quarry

Khalgari and Kaha nullahs (lat. 29°21' to 29°36 N and long. 69°56' to 70°04' E) are the potential quarry area of gravel and sand deposits that is accessible through existing road network. A metalled road traverses through the fan area. The road passes through fan area that starts from Indus Highway at Jampur and after crossing Fazilpur, Lalgarh, Lundi Saiyidan and Shahzadgor, it terminates at Mari in Sulaiman Range. These nullahs originate from severely dissected anticlinal area where olive

green, greenish grey, grey and brownish coloured shales, reddish brown to brown and grey sandstones are exposed. Close to Shahzadgor thick beds of offwhite to creamish coloured limestone about than 300 feet thick is present. It is underlain by dark grey marl and overlies whitish to grey coloured gypsum bed. Khalgari and Nullah Kaha nullahas form a 3 to 4 kilometers wide gravel fan that has been uplifted and dissected. Neotectonis has developed four terraces at different levels. The boulders exposed on the terraces indicate effects of desert varnish.

SAMPLING

In the present study gravel deposits and outcrop samples from Tahli Wala Pull-Girdu area comprising quartzite and limestone samples were taken to assess its suitability for surfacing and asphalt concrete work. However, the crush and pit run gravel deposits of Sakhi Sarwar area have already been approved for use as base course and sub base course material.

In Pitok, Zungi, Khalgari and Kaha Nullahs areas, samples of pit run gravels were collected from nullah beds and gravel fan area. Crush samples were collected from crushing plant located close to Uzman Fort in Mazari area which was operating to produce crush.

ENGINEERING PROPERTIES

A number of factors control behaviour of aggregates in mortar, concrete and unbound and bound pavements, etc (Fookes et al. 1988; Yoon and Tarrer, 1988; Lafrenz, 1997; Wu et al., 1998; Dewar, 1999; Hudson, 1999; Kandhal et al., 2000; Neville, 2000). Over a period of time the researchers have come up with a number of aggregate tests that can help them to anticipate in-service performance of aggregates being used in construction works. It is common practice to use durable and strong aggregate that can resist abrasive wear and disintegration, give an excellent bond with cementing materials, resistant to rapid impacts and sound enough to resist extreme weathering conditions (e.g. Smith and Collis, 2001; Sherard et al., 1984; Ahsan et al., 2000; Neville, 2000; Chaudhry et al., 1999, 2006).

The present study deals with selection of suitable aggregate resources, mainly for roads and highways and partly for cement concrete in southern Punjab. In this context gradation (AASHTO T-27), specific gravity and water absorption (AASHTO T-85), soundness test (AASHTO T-104), Los Angeles abrasion value (AASHTO T-96), modified proctor test (AASHTO T-180), California Bearing Ratio (CBR, AASHTO T-193), plasticity index of fines (AASHTO T-88), and coating and stripping test with 60/70 and 80/100 bitumen (AASHTO T-182) were conducted for the determination of engineering properties of aggregates ensure selection of best quality aggregates for future use.

Following the test procedures the calculated specific gravity (AASHTO T-85) of the test samples ranges from 2.61 to 2.69 with an average of 2.65 whereas the water absorption 0.57% to 1.65% giving a mean of 0.74%. Although there are no specified limits for specific gravity in the standards (e.g. AASHTO T-85-88) however values of specific gravity and water absorption are comparable with the available aggregates of Punjab (e.g. Ahsan et al., 2000; Khan, 2004). The above mentioned specifies a maximum limit of 2% for water absorption aggregates.

Many workers (e.g. Fookes and Collis, 1975; Wu, et al., 1998) suggested for durability evaluation of the material that is an important requirement of rock aggregates. Fookes et al., (1988) considered that the aggregate should be sound enough to resist intense mechanical and chemical weathering conditions (Wu, et al., 1998; Navilli, 2000). In present work, Los Angeles abrasion test and soundness of the aggregate were carried out to compare durability of the materials with the standards. Soundness by using Na_2SO_4 solution indicates an average value of 3.07% with a minimum value of 1.80% and highest value is 3.77%. These values are suggestive that the aggregate is very sound and can perform well under severe conditions. In the standard specifications (AASHTO T-104) permissible limit of degradation of the aggregate is taken as 12% for base course and 10% for ordinary Portland cement concrete. Similarly, Los Angeles abrasion values for these aggregates range from 17.9% to 30.6% with an average value of 22.6%. Specified values for sub base, base course, asphalt and cement concrete are 50%, 40% and 30%. As such the achieved values are within specified limits, but it in case of blends in asphalt and cement concrete the values are much closer to maximum specified limits in the literature (ASTM Designation C-131; Gondal et al., 2004a, 2004b). Therefore, some precautionary measures must be observed in order to use the aggregate in asphalt and cement concrete (Smith and Collis, 2001; Navilli, 2000).

Modified Proctor compaction test is a procedure to calculate the maximum dry density and moisture content of soils and aggregates (AASHTO T-180). All the samples were subjected to modified Proctor procedure to evaluate the maximum dry density and optimum moisture content on the 65% of coarse and 35% fine. The value of maximum dry density ranged from 143.7pcf to 144.9pcf with an average of 143.95pcf. Where as the optimum moisture content varied from 5.2% to 5.4% and showing average value of 5.3%.

California Bearing Ratio (CBR) is an extensively used test to assess strength of the material under load. CBR test in this study was carried out at 100% compaction level under soaked conditions (AASHTO T-193). The coarse and fine ratios were combined as they were available in natural deposits. The values range from 84.4% to 99.2% (mean is

94.32) at 100% compaction. Normal requirement for base course is 80% and for sub-base course is 30% at 100% compaction level.

Plasticity index of fines present in the gravels of Pitok Nullah were determined.. Plasticity index is the numerical difference between liquid limit and plastic limits in accordance with AASHTO T-88. Plasticity Index value of these two samples are 5% and 6% whereas the liquid limit of the samples is 24 and 22. According to values given in literature these values are less and should not exceed 25%. The maximum values of liquid limit and plasticity index are 4% for base course 6% for sub base and in case of cement and asphalt concrete, the fines should preferably be non plastic.

The collected samples of crush were evaluated to determine their ability to retain bituminous film (AASHTO T-182) in case of 80/100 and 60/70 immersion in water (16-18 hrs) grade bitumen. Six out of fifteen samples at 25°C qualified the test requirements with bitumen adhesion values (Table 1).

PETROGRAPHIC ANALYSIS (ASTM C-295)

Limestones are generally hydrophobic in nature and show good affinity with bitumen whereas quartzitic sandstone/quartizites are hydrophilic in nature and show poor affinity with bitumen (Smith and Collis, 2001; Bell, 2007). The samples from Girdu Formation, Zungi nullahs and Uzman quarry are hydrophobic in nature therefore they may make good bond with bitumen. Whereas samples from Pitok Quarries 1, 2 and 3, Sakhi Sarwar (Hussain Cotex crusher), off white to white quartzite, Khalgeri Nullah/Kaha Nullah Quarry 7 and 8 are hydrophilic and they are not suitable aggregate sources for asphaltic concrete. In addition to this microscopic analysis of Khalgeri Nullah/Kaha Nullah aggregate indicates that it may not form good bond with bitumen as it contains 57.5% quartz, 35.5 % clay and microcrystalline quartz.

In the presence of certain types of aggregates (e.g. quartzite, greywacke, strained quartz, etc) alkali hydroxides originating from the Portland cement form a gel that induces cracks in concrete thereby deteriorating the civil structures (Gillot, 1969; Hobbs, 1978, 1988; Hudec, 1989; Chaudhry and Zaka, 1998; Chaudhry et al., 2004). Besides modal analysis, for precise assessment of such deleterious constituents present in aggregates, mineralogical composition under the microscope is a pre-requisite to predict the in-service behaviour of aggregates. In this regard, microscopic evaluation of aggregates indicates the presence of 2.5% carbonate and 35.5% clay and microcrystalline quartz in Khah/Khalgeri nullah samples that may induce alkali aggregate reaction. Similarly, some rock fragments in Zungi Nullah also contain microcrystalline quartz and clay.

Petrographic modal analysis of crushed aggregate of Khah/Khalgeri and Zungi nullahs shows the presence of 55% and 1.0% quartzwackes that may cause alkali aggregate reaction when used with high alkali and ordinary Portland cement. However, to predict the alkali aggregate reaction behaviour of aggregates of this area a detailed study is required.

DISCUSSION AND CONCLUSIONS

Dark grey limestone of Girdu Formation exposed along N-70 from Tahli Wala Pull to Girdu revealed low water absorption (0.57% to 1.65%, mean is 0.74%) and is hydrophobic in nature. Other properties (e.g. LAV) indicate that the limestone under study is hard, tough to hammer, durable and its physical properties are comparable with Margila Hills crush (one of the best aggregate resources in Pakistan). It is an excellent resource for surface treatment, asphalt and cement concrete work.

Girdu Formation is exposed along both the sides of the road (N-70). The Girdu valley is quite wide at number of places that may be suitable for open pit mining and installation of pit face crushers where haulage distance is about 100 to 150 meters. Tahlli Wala Pull is approximately 18 km from Sakhi Sarwar where as Girdu is at 23 km distance and locally it could be a market for the crushed stone. The area in general is barren as it receives scarce precipitation and population of this area has limited economic resources. In case, this quarry is developed as a potential resource for construction material, it will definitely elevate the economic conditions of local populace.

Nullah Khalgeri/Kaha

Khalgeri/Kaha Nullah gravel fan is considerably of large extent and if observed through satellite imagery, it is one of the largest gravel fans of Sulaiman Range. One crushing unit located at the crest of this fan for which large pieces are picked up manually from terraces and transported to crusher located on the road side of the fan. However open pit mining material is transported to the crusher installed for Kachhi Canal at Harand. These crushers crushed predominately quartzite/sand stone material of light brown to reddish brown colour.

Off white to light gray coloured limestone outcrops close to Shazadgore. The test results of the limestone bed indicate that limestone is suitable for use in sub base, base course, asphalt concrete and cement concrete. In addition to this terrace deposits comprising predominantly of sandstone/quartzite are hydrophilic in nature that can be used as sub base and base course material while the same did not qualify for use in asphalt concrete and cement concrete.

Table 1

Physical properties of crushed rock and gravel of Shaki Sarwar and Rajan Pur areas

No.	Description	Specific Gravity	Water Absorption %	Sodium Sulphate Soundness %	Los Angles Abrasion Value%	Max. Lab. Density(pcf) S/Base (max)	Optimum Moisture Content%	CBR Value % 100% compaction	Area coated 60/70 Grade Bitumen Immersion in water (16-18 hrs)	Area coated 80/100 Grade Bitumen Immersion in water (16-18 hrs)
1	Dark grey Girdue limestone	2.67	0.58	3.77	21.9	144.9	5.2	98.7	Above 95%	Above95 %
2	Dark grey Girdue limestone	2.66	0.61	3.59	22.4	144.7	5.3	96.2	Above 95%	Above 95%
3	Dark grey Girdue limestone	2.68	0.57	3.59	22.3	143.7	5.2	96.3	Above 95%	Above95 %
4	Dark grey Girdue limestone	2.67	0.58	3.65	21.8	144.2	5.2	96.4	Above 95%	Above95%
5	Off white to white quartzite	2.66	0.66	3.65	19.2	144.6	5.3	95.3	Below 95%	Below 95%
6	Off white to white quartzite	2.67	0.67	3.44	19.8	144.6	5.4	95.4	Below 95%	Below 95%
7	Sakhi Sarwar (Hussain Cotex crusher)	2.65	0.64	3.68	21.8	144.5	5.4	94.2	Below 95%	Below 95%
8	Pitok Quarry 1	2.69	0.72	2.85	20.9	143.7	5.3	96.2	Much below 95%	Much below 95%
9	Pitok Quarry 2	2.65	0.71	2.93	30.6	144.2	5.2	96.3	Below 95%	Below 95%
10	Pitok Quarry 3	2.61	0.69	3.20	25.1	144.5	5.2	94.8	Much below 95%	Much below 95%
11	Pitok Quarry 4	2.65	0.89	1.80	24.6	143.7	5.3	95.1	Below 95%	Below 95%
12	Uzman Quarry (Nullah Zungi) 5	2.65	0.70	2.56	26.2	144.9	5.3	99.2	Above 95%	Above 95%
13	Uzman Quarry (Nullah Zungi) 6	2.63	0.76	2.44	17.9	144.7	5.4	91.0	Above 95%	Above 95%
14	Khalgeri Nullah/Kaha Nullah Quarry 7	2.65	1.65	2.56	24.2	143.7	5.4	84.4	Much below 95%	Much below 95%
15	Khalgeri Nullah/Kaha Nullah Quarry 8	2.67	0.67	2.36	21.2	144.2	5.3	85.4	Much below 95%	Much below 95%
AVERAGE		2.65	0.74	3.07	22.66	143.95	5.3	94.32		

Nullah Pitok

The material comprises limestone and sandstone. Installation of material separator was observed in Nullah bed. The material of the Nullah qualified only for use as sub base and base. The presence of olive green fines material was suggestive that it should be removed from coarse fraction due to its potential for higher plasticity index value. The coarse fraction is suitable to be used as base and sub base but its use in asphalt concrete and cement concrete may not be suitable.

Nullah Zungi

The test results of these rocks and their hydrophobic characteristics revealed that gravels/boulders bed of Nullah Zungi are suitable for use in sub base, base course, asphalt concrete and cement concrete. If this deposit is developed, it will serve not only Tehsil Rojhan and Kashmore area of Sind. But after construction of Ichha Bunglow high level bridge over the River Indus, it will also meet the requirement of District Rahim Yar Khan and Ghotki area of Sind being the nearest source.

REFERENCES

Ahsan, N., I.H. Baloch, M.N., Chaudhry,Ch M. Majid, 2000. Strength Evaluation of Blends of Lawrencepur, Chenab and Ravi Sands with Lockhart and Margala Hill Limestones for use in Concrete. *Special Issue Pak. Muse. Nat. Hist.* Pakistan Science Foundation, pp. 213-240.

Ahsan, N., M.N. Chaudhry, and M. Muzaffar, Ch.2000a, Mineralogy, Engineering Properities and Alkali Aggregate Reaction Potential of Maira Sand, Thakot, Pakistan. *Third South Asia Geological Congress*, Lahore, Pakistan Sept. 23-26, 2000, pp. 150-151.

Alam, G.S. 1987, Geology of Kirana Hills District Sargodha, Punjab, Pakistan. *Geological Survey of Pakistan*, Quetta, Pakistan. Pp.1-37.

Alam, G.S., Jaleel, A. and Ahmad, R. 1992. Geology of the Kirana area, District Sargodha Punjab, Pakistan. *Acta Mineralogica Pakistanica*, Vol. **6**, pp.93-100.

Barksdale, R. D. 2001. The Aggregate Handbook. National Stone, Sand, and Gravel Association, Arlington, Virginia, pp. 3-74.

Bell, F. G., 2007. Engineering Geology. Butterwotth-Heinemann, Oxford, UK, 581pp.

Chaudhry, M. N., and Zaka, K. J., 1998 "Petrographic Evaluation of Alkali Aggregates Reaction in Concrete Structures of Warsak Dam, N.W.F.P- A Case Study", *Proceedings Eighth International Congress Association of Engineering Geology and Environment*, pp. 2841-46, 1998.

Chaudhry, M.N., I.H. Baloch, N. Ahsan, and Ch. M. Majid, 1999. Engineering properties, Mineralogy, Alkali Aggregate Reaction Potential and Provenence of Lawrencepur Sand Pakistan, *Special Issue Pak. Muse. Nat. Hist.* Pakistan Science Foundation, pp. 241-254.

Dewar, J. D., 1999. Computer Modelling of Concrete Mixtures, E & FN Spon, London.

Fookes, P. G., Gourley, C. S., and Ohikere, C. (1988). Rock Weathering in Engineering Time. In *Quarterly Journal of Engineering Geology*, vol. **21**, pp. 33-57.

Fookes, P.G. and Collis, L., 1975, "Problems in Middle East", *Concrete*, Vol. **9**, No. **7**, pp. 12-17.

Fookes, P.G., Gourley, C.S., and Ohkere, C., 1988 "Rock Weathering in Engineering Time," *The Quarterly Journal of Engineering Geology* (British), Vol. **21.**

Gillot, J.E. and Swenson, E.C (1969) Mechanism of Alkali-Carbonate Rock Reaction. *Qart. Jour. Eng. Geology*, **2**, pp.7-23.

Gondal, M.M.I., Javaid, A.Z., Chaudhry, M.N. and Ahsan, N. 2006a. Geotechnical Investigation of Nullah Sanghar Gravel Deposits, District Dera Ghazi Khan, Punjab, Pakistan. Geological Material & Aggregates of Pakistan. Publ: National Geological Society of Pakistan.

Gondal, M.M.I, Javaid, A.Z., Ahsan, N. and Chaudhry, M.N. 2006b. Engineering Evaluation of Gravel Deposits from Mauza Kalary District Dera Ghazi Khan. Geological Material & Aggregates of Pakistan. Publ: National Geological Society of Pakistan.

Hobbs, D.W. (1988) Alkali-silica reaction in concrete. Thomas Telford Ltd., London, UK.

Hobbs., D.W. (1978) Expansion of concrete due to the alkali-silica reaction: an explanation. *Mag. Concr. Res.*, **30**, pp. 215-220.

Hudec, P.P. (1987) Deterioration of aggregates - the underlying causes. Concrete durability. Katharine and Bryant Mather Int. Conference, *Amer. Conc. Inst.* SP-**100, 2**, pp. 1325-1342.

Hudson, B., 1999. Modification to the Fine Aggregate Angularity Test," *Proceedings, Seventh Annual International Center for Aggregates Research Symposium, Austin, TX.*

Hunting Survey Corporation, Ltd., 1961, Reconnaissance geology of part of West Pakistan by the Govt. of Canada, Toronto, Canada.

Kandhal, P.S., Mallick, R.B., and Huner M., 2000. Measuring Bulk Specific Gravity of Fine Aggregates: Development of a New Test Method. *Transportation Research Board, Transportation Research Record,* **1721**.

Kazmi, A.H. and Jan, M.Q., 1997. Geology and Tectonics of Pakistan. Graphic Publishers, Karachi, pp. 1 – 554.

Khan, Z.K. 2004. Classification of base and sub-base of road aggregates in Kirana area, districts Jhang and Sargodha, Punjab. *Workshop on Geological Materials/Aggregates of Pakistan,* June 10, 2004, Islamabad. National Geological Society of Pakistan & Pakistan Museum of Natural History (Pakistan Science Foundation).

Khan, Z.K. and Chaudhry, M.N., (1991). Engineering Geological and Petrographic Evaluation of Metadolerites of Buland Hill and Chak 123 Quarries of Kirana Hills, District, Sargodha, Pakistan: *Kashmir Journal of Geology*, Volume **8-9**, pp.181-184.

Lafrenz, J.L., 1997, "Aggregate Grading Control for PCC Pavements: Improving Constructability of Concrete Pavements by Assuring Consistency of Mixes," Proceedings, *Fifth Annual International Center for Aggregates Research Symposium*, Austin, Texas.

Malkani, M. S. (2004), Stratigraphy and Economic potential of Sulaiman, Kirthar and Makran-Siahan Ranges, Pakistan. In Hussain, S. S., and Akbar, H. D., eds., Fifth Pakistan Geological Congress , 14-15 April, Islamabad, Abstracts volume, *National Geol. Soc. Pak.*, Pakistan Museum of Natural History (Pakistan Science Foundation), Islamabad. Pp.63-66.

Mielenz, R. C. (1994). Petrographic Evaluation of Concrete Aggregates. In Significance of Tests and Properties of Concrete and Concrete-Making Materials. Klieger, P., and Lamond, J.F. (eds.) ASTM STP 169C, 341-364.

Mikani, S. M., 2006. Lithofacies and lateral extension of latest Cretaceous dinosaur beds from Sulaiman foldbelt, Pakistan. *Sindh University Research Journal (Science series)*, 38:1, pp. 1-32.

Neville, A.M. 2000. Properties of Concrete 4th ed. Pearson Education Asia Pte. Ltd. Edinburgh, U.K. 844p.

Shah, S.M.I., 1977, Stratigraphy of Pakistan: *Geol. Surv. Pakistan*, Quetta, Mem. No. **12**, pp. 138.

Sherard, J.L., Dunnigan, L.P. and Talbot, J.R. (1984), "Basic Properties of Sand and Gravel Filters", *Journal of Geotechnical Engineering*, **110(6)**, 684-701.

Smith, M. R. and Collis, L. 2001. Aggregates – Sand, Gravel and Crushed Rock Aggregates for Construction Purposes (3rd edition). The Geological Society London. 339p.

Wu, T., F. Parker, and P.S. Kandhal. 1998, Aggregate Toughness/Abrasion Resistance and Durability/Soundness Tests Related to Asphalt Concrete Performance in Pavements. *Transportation Research Board, Transportation Research Record* : **1638**.

Yoon, H. H., and A. R. Tarrer. 1988. Effect of Aggregate Properties on Stripping. *In Transportation Research Record* **1171**, TRB, *National Research Council*, Washington, D.C., pp. 37–43.

Geol. Bull. Punjab Univ. 43, 2008.

SEISMIC MICROZONING OF UPPER HAZARA REGION: BASED ON IMPACT ANALYSIS OF RECENT EARTHQUAKES

BY

TALAT IQBAL, ZAHID ALI, TARIQ MAHMOOD AND M. QAISAR
Mciro Seismic Studies Programme, Ishfaq Ahmed Research Laboratories
P. O. Nilore, Islamabad, Pakistan.
E-mail: talatiqbal@hotmail.com

AND

NASIR AHMAD
Institute of Geology, University of the Punjab, Quaid-i-Azam Campus,
Lahore-54590 Pakistan

ABSTRACT: *Microzoning of the strong ground motion hazard for the Upper Hazara region based on expected Peak Ground Acceleration (PGA) is carried out through deterministic approach by using the Maximum Credible Earthquakes (MCE) along faults and recent microintensity distribution data of 4 significant local earthquakes. The seismogenic faults are identified and MCE is estimated along each fault through considering its longest rupture segment. The microintensity data of significant earthquakes was used to estimate PGA through empirical relationships and correlated with locally recorded strong motion data. Attenuation relationships between seismogenic fault and distances on hanging and foot walls are developed by utilizing estimated PGA data. Finally, these relationships are applied to each seismogenic fault segment to estimate PGA value at 200m grid by assuming that the geomorphology of the region is same. The compiled seismic microzoning map indicates that most of the part of Balakot city area lies in high PGA value (0.5g) zone. Similarly, some areas of Muzaffarabad, Garhi Habib Ullah, Mansehra and Shinkiari cities are placed in high PGA zones, primarily depending on the closest distance to local seismogenic faults of the region. However, local instrumental strong motion data for different geological conditions is required to obtain more realistic microzoning.*

INTRODCUTION

Damage is caused due to ground shaking, which is generally stronger by the earthquake close to the seismogenic structure and gradually decreases away. Damage owes to the region indicate that the geological and geomorphologic conditions of top few tens of meters accompanied by the tectonic and seismic setup of area. Various studies have shown that the earthquake impacts also vary greatly within a few square kilometer of an area, depending upon the source geometry and site conditions (Schwartz et. al., 1986, Abrahamson et. al., 1996). It is, therefore, important to consider appropriate ground motion parameters that correlate well with the observed structural damage during strong ground motions and that can also be implemented in engineering design of structures.

The goal of this research is to delineate seismic zones in the Upper Hazara region and to prepare a realistic strong motion hazard map of the area.

METHODOLOGY

The methodology adopted for seismic microzonation of Upper Hazara region is based on the following steps:

I. Seismic analysis of recent instrumental seismicity performed to investigate seismic nature and its spatial distribution. Seismic, geologic and geomorphic studies of the region are carried through seismic data analysis, field surveys, GIS and remote sensing based geospatial data analysis.

II. Identification of seismogenic structures through spatial data sensing analysis, field observations of active seismogenic structures, distribution of seismicity pattern and focal mechanism studies of significant seismic events. In addition to demarcation of surface traces of seismogenic structures, their geospatial geometry and continuous rupture segments are also studied.

III. Maximum credible earthquake estimation on seismogenic faults using largest single continuous rupture segment identified by physical boundaries.

IV. The microintensity distribution data of the four major recent earthquakes in and around the region was collected from both hanging and foot wall sites of seismogenic faults, used to determine expected PGA by correlating the "Revised peak ground motion versus intensity relations" as given by Dave Wald 1999.

V. The attenuation relationships between PGA and horizontal distance away from surface trace of the seismogenic fault are developed for both hanging and foot wall sites.

VI. To develop seismic microzonation map of Upper Hazara region, attenuation relationships with local site amplification factors are utilized to estimate PGA on grid point bases.

SEISMOGENIC ANALYSIS

Tectonic Environment

The Upper Hazara region is a part of lower Himalayas and the seismicity of the area is associated with densely populated thrust fault systems that have generated a number of low to moderate earthquakes with shallow focal depths (Seeber and Armbruster 1979). The region has undergone tectonic compression resulting in various faults and fold systems (Baker et al. 1964). The seismicity in the area is mainly associated with tectonic faults.

Identification of Seismogenic Structures

The seismogenic structures are the main source of seismic activity in the region. It is observed that the strong ground motion distribution is strongly influenced by the spatial geometric character of its causative fault. Therefore, for deterministic seismic microzonation, identification of seismogenic structures is most significant, special care and reliable spatial, seismic and geologic, data are required to identify their geometric distribution. The analysis was made to observe general tectonic trend of the region and it was found that most of the fault systems are thrust in nature, which are directly or indirectly associated strike slip faults.

Special consideration is made to observe features related to thrust movements that include (a) monocline structure across strike of fault, (b) linear presence of continuous thrust born slides along the surface trace of fault, (c) significant lineation in surface geomorphology, (d) surface cracks parallel to fault strike, (e) presence of fault fluvial deposits on foot wall side, (e) discontinuities in rock formations, and (f) sharp change in stream patterns orientations along active fault.

In addition to geologic and seismic studies, analysis of the presence of these features in the region is more critically made by utilizing satellite imageries and digital elevation models of 0.5 arc second ground resolutions. However, more critical studies are still required to identify presence and nature of these seismogenic structures more accurately.

Critical Seismogenic Structures

The major seismogenic structures identified (Fig. 1) through study of tectonic setup, surface geology, seismic and spatial data include Main Boundary Thrust (MBT) structure, the Kashmir Thrust, the Panjal Thrust, the Oghi Thrust and the Mansehra Thrust structure.

Main Boundary Thrust Structure

The Main Boundary Thrust (MBT) is a regional thrust dipping northward and oriented sub-parallel to the MMT (Treloar et al. 1989a). It is located at the northern margin of Indian Plate and is younger to MMT in age. It comprises a set of north-dipping faults and forms a boundary between the Sub-Himalayas and the Lesser Himalayas (Calkins et al. 1975). It has generated low to moderately high and frequent seismicity, with characteristically shallow focal depths. The various sections of MBT are locally named by different workers as Hazara Fault, Parachinar Fault, Kala Chita Fault and Murree Fault. It forms an intensely deformed and tectonised belt with isoclinal folds and several thrust sheets.

a. Kashmir Thrust Structure

The Kashmir Thrust structure comprises a series of parallel thrust faults including Kashmir Thrust, Garhi-Batgram Thrust and Rawalkot-Besham Thrust. The Kashmir Thrust is an active fault structure dipping northward and passing just beneath the city of Balakot (MSSP 2005). This Thrust has generated disastrous earthquake (M_L=7.0) of October 8, 2005 followed by 341 aftershocks of magnitude greater than 4.0 (M_L) (MSSP 2005).

b. Panjal Thrust Structure

The Panjal Thrust structure is sited parallel to MBT on the eastern limb of the Syntaxis. The Panjal Thrust probably separates from MBT about 6 km south of Balakot and continues beneath Kaghan Valley alluvium up to Ghari Habib Ullah. Panjal Thrust is an active fault and represents southeastern tectonics of the area. Panjal Fault appears as reverse fault with strike-slip component, in the south of Abbottabad (Calkins et al. 1975).

c. Mansehra Thrust Structure

This is an arc shaped small active fault structure present in the south of Mansehra Basin. The local seismic data analysis indicates that this fault has produced numerous and frequent earthquakes of low to moderate magnitude of very shallow depths.

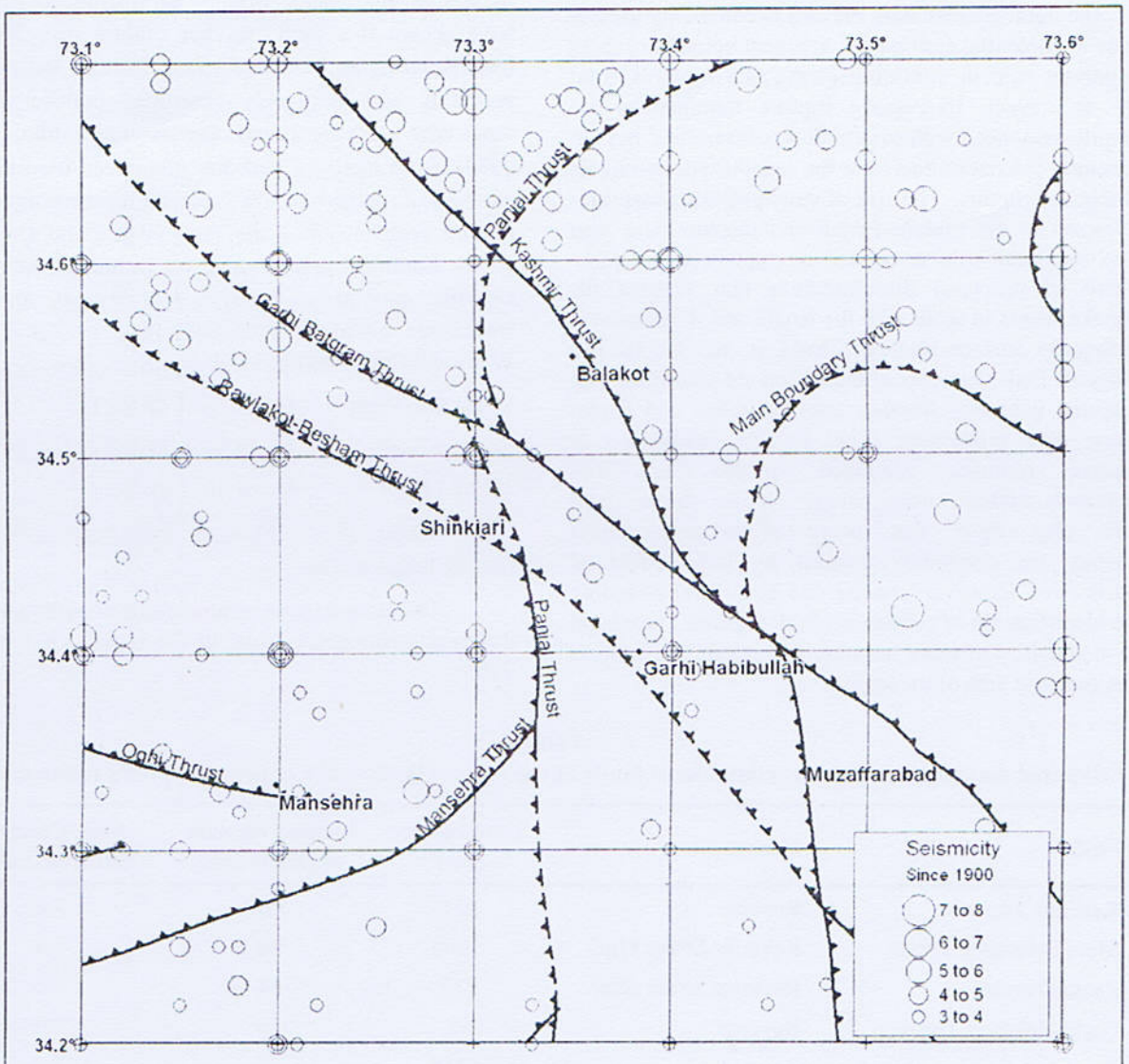

Fig. 1: Map showing seismogenic structures (dashed lines with possible presence) and instrumental seismicity of the study area (Since 1900).

d. Oghi Fault Structure

The Oghi Fault structure strikes northwest to southeast direction and is sited near the Oghi Fort in Mansehra district. The nearest surface trace of Oghi Fault is about 30km west of Balakot city.

Seismogenic Fault Segment Determination

The fault-segmentation method is commonly used to estimate the potential earthquake. Segment boundaries play an important role in confining earthquake ruptures from event to event. Earthquake rupture terminations are commonly associated with structural discontinuities, but not all-structural discontinuities have the capability to terminate an earthquake rupture. The size of structural discontinuities with respect to the rupture length and displacement may play an important role in controlling rupture termination. The size of structural discontinuities that stopped the earthquake seems to scale with the length and displacement of earthquake surface rupture (Zhang et. al., 1998). The seismogenic fault segments of the region are identified with their spatial geometry through satellite image and digital elevation data processing (Fig. 1). In addition to earthquake ruptures examined in this study, fault segmentation studies along major active thrust fault systems also show that many of the segmentation boundaries are commonly marked by large structural discontinuities. However, precise and better understanding for the identification of continuous fault segments is subject to the availability of more accurate and reliable seismic as well as geologic data of the region.

MAXIMUM MAGNITUDE POTENTIAL

The analysis of recorded instrumental seismicity of the region shows that the thrust fault systems are mainly responsible for the significant seismic events. The maximum credible earthquake on seismogenic faults can be estimated through the study of geology and physical nature of seismogenic faults. Studies of worldwide earthquakes have shown that faults do not rupture over their entire lengths during an individual event. Instead, individual fault segments with physically controlled boundaries rupture repeatedly (Schwartz and Coppersmith 1986, Schwartz 1988). Fault rupture length has often been used to estimate earthquake magnitude by considering maximum single rupture segment along the fault (Wells and Coppersmith 1994). Empirical relationships for estimation of maximum credible earthquake based on statistical analyses of worldwide historical earthquake data are developed by Wells and Coppersmith, 1994 as

Strike Slip Fault	M_w=5.16+1.12 log L
Reverse Fault	M_w=5.00+1.22 log L
Normal Fault	M_w=4.86+1.32 log L

Where M_w is Moment magnitude and L is the rupture length in km.

The estimated maximum credible earthquakes on the different seismogenic faults of the region are listed in the Table 1.

Table 1.
Estimated maximum credible earthquake of faults of the region (Wells and Coppersmith, 1994 relationships)

Fault	Movement	Total Length (km)	Longest Rupture Segment (km)	Max. Credible Earthquake (M_w)
Kashmir Thrust	Reverse	224	112	7.6
Main Boundary Thrust	Reverse/ Strike Slip	> 300	98	7.4
Panjal Thrust	Reverse/ Strike Slip	225	64	7.2
Garhi-Batgram Thrust	Reverse	53	53	7.0
Rawlakot-Besham Thrust	Reverse	> 250	78	7.2
Havailian Thrust	Reverse	44	22	6.6
Oghi Thrust	Reverse/ Strike Slip	54	27	6.7
Mansehra Thrust	Reverse	29	15	6.4

MICROINTENSITY ANALYSIS

The seismicity of the region shows a number of low to moderate earthquakes with only a few of magnitude greater than 5.0 (M_L). The distribution of the recorded instrumental seismicity in the region by local seismic network is shown in figure 1. The significant earthquakes that have been used in present study are the Muzaffarabad Earthquake (M_L=7.0) of Oct. 8, 2005 (MSSP 2005), the Kaghan Valley Earthquake (M_L =5.2) of Feb. 14, 2004

(Khan et. al., 2004, Mahmood et. al., 2004), the Astor Valley Earthquake (M_L=6.2) of Nov. 20, 2002 (Mahmood et. al., 2002) and the Mangla Earthquake (M_L=5.0) of March 10, 2006 (Talat, et. al. 2008). The microintensity distributions of each earthquake are investigated with determination of seismogenic fault through the focal mechanism solutions and geospatial data analysis. Observations indicate that the microintensity decreases away from the seismogenic ruptures of the earthquake as shown in table 3. The seismic data analysis shows that the region comprises shallow seismogenic clusters of shallow depth range. Therefore, these seismic events may produce almost maximum possible strong ground motion impacts at surface. These impacts may be of localized nature extended over a few tens of kilometers away from the seismogenic structure.

Table 2.
PGA values during Oct. 8, 2005 earthquake recorded by MSSP strong motion network

Recording Station	Closest Distance from Rupture (km)	PGA (g) East-West	PGA (g) North-South	PGA (g) Vertical
Abottabad	43	0.231	0.197	0.087
Cherat	144	0.042	0.037	0.021
Fateh Jang	126	0.051	0.053	0.032
Murree	60	0.076	0.078	0.069
Nilore	92	0.023	0.026	0.030
Peshawar	190	0.054	0.051	0.022
Thamewali	245	0.019	0.014	0.009

Table 3.
Intensity distribution of four major recent earthquakes in the region

Seismic Rupture Distance (Km)	Intensity (MMI)							
	Muzaffarabad Earthquake of Oct. 8, 2005 (M_L 7.0)		Mangla Earthquake of Mar. 10, 2006 (M_L 5.0)		Kaghan Valley Earthquake of Feb. 14, 2004 (M_L 5.6)		Astor Valley Earthquake of Nov. 20, 2002 (M_L 6.2)	
	Hanging Wall Region	Foot Wall Region	Hanging Wall Region	Foot Wall Region	Hanging Wall Region	Foot Wall Region	Hanging Wall Region	Foot Wall Region
0	XI	X	VII	VII	VIII	VIII	VIII	VIII
5	X	VIII	VII	VI	VIII	VII	VIII	VII
10	IX	VIII	VI	V	VII	VI	VII	VI
15	IX	VII	VI	V	VII	VI	VII	VI
20	VIII	VII	V	IV	VI	V	VI	V
25	VIII	VI	V	IV	VI	V	VI	V
30	VII	VI	IV	IV	VI	V	VI	V
35	VI	V	IV	<IV	V	IV	V	IV
40	VI	V	IV	<IV	V	IV	V	IV
45	VI	V	IV	<IV	V	IV	V	IV
50	V	IV	IV	<IV	IV	<IV	V	IV
55	V	IV	<IV	<IV	IV	<IV	IV	<IV
60	V	IV	-	-	<IV	<IV	IV	<IV
65	V	IV	-	-	-	-	IV	<IV
70	IV	<IV	-	-	-	-	<IV	<IV

Muzaffarabad Earthquake of Oct. 8, 2005

The Muzaffarabad Earthquake of Oct. 8, 2005, magnitude (M_L) 7.0 (Ms=7.7, M_w=7.6, m_b=6.8 USGS), occurred at 03:50:38 GMT near the city of Muzaffarabad at a focal depth of about 13km (Qaisar et. al 2007). The main shock was followed by more than 6400 aftershocks within one month with 296 having magnitude (M_L) greater than 4. The maximum net slip of 4.2m±0.5m mainly between Muzaffarabad and Balakot areas and surface features of thrust fault were observed at a number of places along the fault structure, named Kashmir Thrust (KT). Earthquake caused a death toll of more than 95,000 with 100,000 people injured and about 4 million people in the affected area were left homeless. The maximum intensity, XI on Modified Mercalli Intensity (MMI) scale, was observed along the strike of causative seismogenic fault where as maximum horizontal strong ground motion was 0.231g (Table 2). It was found that the ground shaking was not symmetrical around the epicenter, but was intensive along the strike of KT and on the hanging wall areas, mainly due to fault rupture directivity and near-fault effects. The microintensity distribution and respective strong ground motion generated by the main shock was believed to be the function of the 3-dimentional spatial geometry of the causative fault i.e. KT and the closest distance to seismogenic fault plane. Some significant local variations in microintensity were also observed due to site effects like thin soil amplification, ridge effect, basin edge and basin trapping etc (Qaisar et. al 2007).

Kaghan Valley Earthquake of Feb. 14, 2004

The Kaghan Valley Earthquake (M_L=5.6) of February 14, 2004 was located in Mansehra district near the town of Paras with shallow focal depth (Khan et. al., 2004, Mahmood et. al., 2004). The focal mechanism solution shows thrusting on the fault plane with strike ENE-WSW and dip in the NNW direction. The event struck near the northern margin of Indian Plate on the Main Boundary Thrust (MBT) with scattered aftershock distribution. The main shock was followed by more than 30 aftershocks, 6 of which had magnitude greater than (M_L) 4. The seismic as well as geological data suggest that the tectonic movement was concentrated in upper crust down to a depth of about 18 km. The observations made during the field work indicated that the intensity contours converged around the town of Paras in Kunhar Valley in an elongated shape trending NW-SE. The isoseismal map shows that the lateral extent of the intensity contours did not extend significantly far from peak intensity (MMI VIII) point near Paras. Most of the damage took place along the strike of seismogenic fault. Sharp relief and loose/thin fluvial filled narrow valleys contributed more to the damage in the affected area. The Earthquake was felt over an area of about 8000 sq. km whereas the damage occurred over an area of about 1200 sq. km. Damage and other surface evidence indicated a sharp decrease in the intensity away from the causative fault i.e. MBT. The Earthquake caused deaths of 26 persons, 43 injured, about 95 houses collapsed and 186 houses received damage.

Astor Valley Earthquake of Nov. 20, 2002

The Astor Valley Earthquake (M_L=6.2) of Nov. 20, 2002 occurred about 60 km southeast of Gilgit near Bunji in northern areas of Pakistan (Mahmood et. al., 2002). The estimated seismic moment of the November 20, 2002 main shock is 9.4×10^{17} Nm which gives M_w=5.9. The focal mechanism solution indicates normal faulting with a small component of strike slip on source fault whose strike is parallel to the local trend of MMT. The results indicate that the Astor Valley Earthquake may be considered to have occurred in an uncoupled region, in response to the gravitational pull due to internal tensional environment.

Mangla Earthquake of March 10, 2006

The Mangla Earthquake magnitude 5.0 (M_L) occurred at 12:50 PST (07:50 GMT) on March 10, 2006, near Mangla Lake about 95 km south-east of Islamabad (Talat et. al.,. al., 2008). One person was killed, and 22 injured in Mirpur District. The epicenter was located in the area of Mangla anticline near the town of Kalial on Kalial Thrust with the fault plane oriented in NW-SE direction with strike 293°, dip 20° and rake 117° respectively. The focal mechanism solution determined predominantly as thrust with a slight strike slip component, striking northwest and dipping northeast, coincides well with the slip nature of the fault and also supported by surface evidences. The intensity survey indicated maximum intensity along Kalial Thrust with some higher intensity values on hanging wall sites. The intensity contours are found elongated in the direction parallel to the strike of the observed fault.

MICROZONATION PARAMETERIZATION

The effects of earthquake are controlled by earthquake magnitude, wave propagation from source to site region, site distance and site characteristics. The other important influence on strong motion are near fault rupture directivity effects, basin response effects, rock edge effects, hanging wall effects, style of faulting, focal depth, basin edge effects and valley front effects.

Seismogenic Characteristics

he moment magnitude of the earthquake generated by the seismogenic fault is the measure of the energy released and thus directly sets the levels of strong ground motion. However, it has been observed during a number of catastrophic seismic events that the ground shaking was not symmetrical around the epicenter. The spatial geometry of

the seismogenic rupture was found responsible for the surface distribution of the strong ground motion. During the study of Oct 8, 2005 earthquake, the high damage in Balakot and Bagh, located about 28km and 40km respectively from the epicenter, was the result of near seismogenic fault effect. Similarly, microintensity levels of the earthquake were considerably high along and near the Kashmir Thrust, i.e. the causative seismogenic fault. This phenomenon gives importance to evaluate 3-dimensional characteristics of the seismogenic fault in terms of nature, sense, movement and depth.

3D Definition and Nature of Faulting

The variability in the earthquake microintensity has long been recognized and taken into account in engineering applications. There is a large amount of variability in ground motion due to effects that are more complex than the simple parameterization using magnitude, epicenter distance, and site category. In addition to magnitude, the additional parameters like faulting style, near surface rupture, hanging wall etc. cause spatial variation in the ground motion around a fault. There is a well established difference in ground motion amplitudes between reverse and strike-slip faulting mechanism for crustal earthquakes where ground motion for reverse earthquakes typically exceed those for strike-slip earthquakes by a factor ranging from about 1.3 to 1.4 (Somerville and Sato 1998).

The pattern and focal mechanism study of the Oct 8, 2005 earthquake accompanied with seismic microintensity surveys, utilized to identify 3-dimensional geometry of the Kashmir Thrust. Based on the surface evidence and rapid decrease in the microintensity, it was observed that the seismic attenuation was considerably high in the direction perpendicular to the strike of seismogenic fault or rupture zone.

Strong Motion Relationship to Seismogenic Structure

The ground motion amplitude in near-fault region is strongly influenced by the fault geometry (Abrahamson and Somerville 1996). For vertical strike slip faults, rupture directivity effects cause a strong spatial variation in ground motion for given close distance to the fault. For a dipping fault, there are two prominent effects; the rupture directivity effect and the hanging wall effect. The effects of the hanging wall on strong motion were previously analyzed by Abrahamson and Somerville (1996). They found larger short period ground motions for sites on hanging wall compared with those on the foot wall at equivalent distance. The effect is greatest (a factor of 1.45) in the closest distance range of 8 to 18 km, and is significant (larger than a factor of 1.2) in the distance range of 6 to 22 km (Abrahamson and Somerville 1996). The rupture directivity effect is due to rupture propagation and damping of seismic wave along rupture plane (Archuleta and Hartzell 1981, Somerville et al. 1997).

During the study of Oct. 8, 2005 earthquake, it was found that the ground shaking was not symmetrical around the epicenter, but was intensive along the strike of KT and on areas on the hanging wall side, mainly due to fault rupture directivity and near-fault effects respectively. It was also observed that the intensity levels were considerably high at and near the causative faults and sharply decreased perpendicularly away from the causative fault plane. During the earthquake of Oct. 8, 2005, seismic intensity and associated damage was observed at near-fault areas in Balakot, Jabbori, Baso, which were located about 28km, 35km, and 43km respectively from the epicenter of the earthquake (Ali et. al., 2008).

The microintensity variations of the earthquakes at various places across the strike of causative faults are used to determine respective peak ground motion by correlating the "Revised peak ground motion versus intensity relations" as given by Dave Wald 1999.

$$I_{(MMI)} = 3.66 \text{ Log } (PGA_{(g)}) - 1.66 \quad \ldots\ldots 1$$

After assessment of peak ground acceleration ($PGA_{(g)}$,) distribution, the empirical relationship between $PGA_{(g)}$ and closest distances from causative fault plane was determined for both hanging and foot walls. The polynomial regression analysis method applied to draw graphs of PGA - fault distance (Fig. 2a, 2b) for maximum recorded earthquake of magnitude 7.0 (M_L), using the following empirical relationships;

$$PGA_{(g)} = 1.59 + 6.0\times10^{-4} D_{hw} - 6.35\times10^{-4} D_{hw}^{0.2} \quad \ldots\ldots 2$$

$$PGA_{(g)} = 1.59 + 2.4\times10^{-3} D_{fw} - 7.20\times10^{-1} D_{fw}^{0.2} \quad \ldots\ldots 3$$

Where "D_{hw}" and "D_{fw}" are the closest distance in kilometers from the seismogenic fault plane on hanging wall and foot wall, respectively.

From comparison of microintensity distribution of earthquake of Oct. 8, 2005, it was observed that these regression relationships are more appropriate between the intensity range of MMI≥IV and MMI≤XI with up to a distance of 100km.

SEISMIC MICROZONING

Expected peak ground acceleration (PGA) microzonation map of Upper Hazara region (Fig. 3) is compiled on the basis of maximum credible earthquake along seismogenic structures where the PGA is determined by applying equation 2 and 3 on the largest rupture segments of Kashmir Thrust, MBT, Panjal Thrust, Mansehra Thrust, Manshera Thrust and Oghi Fault at 200m horizontal surface grid spacing. For estimation of expected strong ground motion, percentage impact factors to these

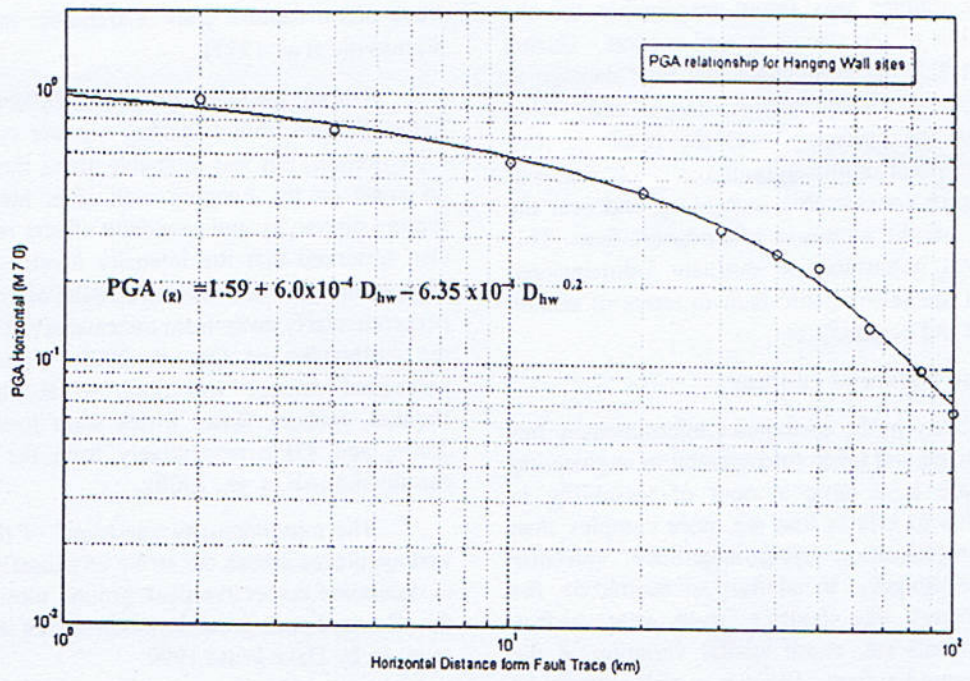

Fig. 2a: PGA relationship to distance from fault on hanging wall sites for max. recorded magnitude 7.0 (M_L).

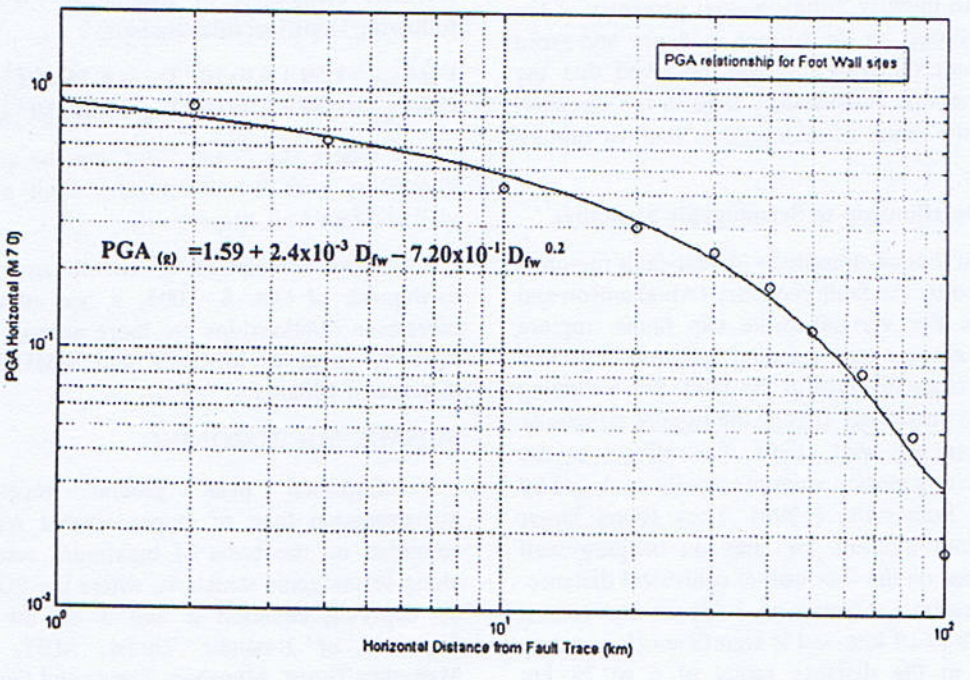

Fig. 2b: PGA relationship to distance from fault on foot wall sites for max. recorded magnitude 7.0 (M_L)..

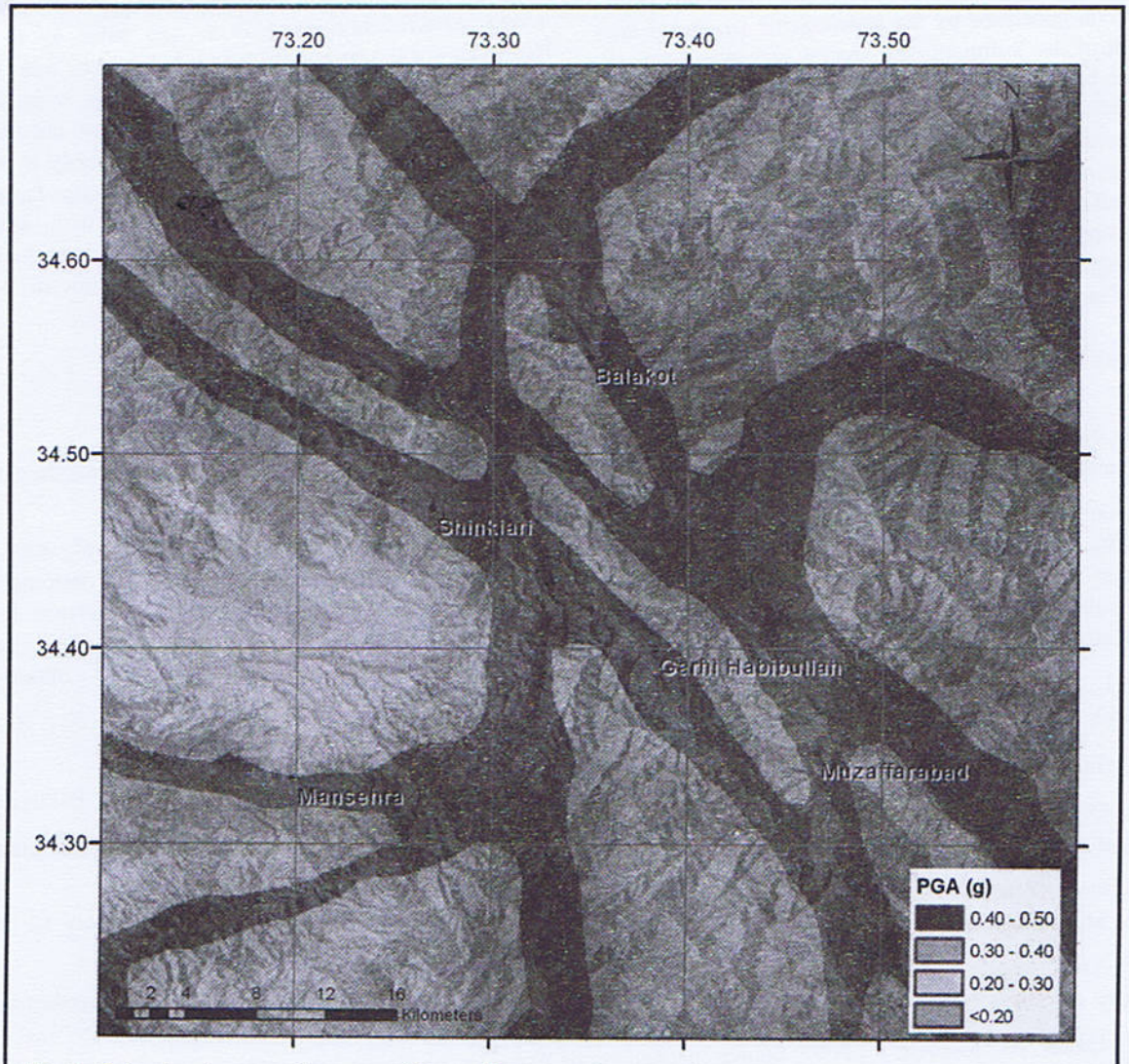

Fig. 3: Seismic microzonation map of Upper Hazara and surrounding regions showing zones of expected peak horizontal acceleration (PGA).

parameters are assigned at 200m grid spacing on ground. In the zoning map, following 4 strong ground motion hazard zones are defined.

PGA 0.40 – 0.50 - Zone of very high seismic hazard
PGA 0.30 – 0.40 - Zone of high seismic hazard
PGA 0.20 – 0.30 - Zone of moderate seismic hazard
PGA < 0.20 - Zone of low seismic hazard

CONCLUSION

The microintensity distribution and expected peak ground motion generated by the seismogenic structures are the function of the 3-dimentional spatial geometry of their seismogenic faults. It is found that the ground shaking was not symmetrical around the epicenter, but was intensive along the strike of causative fault and on area on the hanging wall side, mainly due to fault rupture directivity and near-fault effects, respectively. Therefore, in addition to seismic potential and tectonic setup of an area, understanding the spatial spreading and orientation of seismogenic structures are essential to determine PGA. In addition to seismic and geologic data, the advance techniques of Geographic Information System (GIS) and Remote Sensing (RS) are very helpful tools to identify seismogenic structures. These tools greatly facilitate to analyze geoscientific data to investigate earthquake source parameters and their impacts on grounds at different site conditions. Based upon the maximum credible earthquakes along the seismogenic structures of the area and PGA-distance attenuation relationships, the most part of the Balakot city fall in the zone of very high seismic threat where expected horizontal PGA may raise up to 0.50g. However, local site conditions and distances may modify the PGA up to about a factor 1.45. Similarly, some areas of Muzaffarabad, Garhi Habib Ullah, Mansehra and Shinkiari cities are placed in high PGA zones, primarily depending upon the closest distance to local seismogenic faults. The local instrumental strong motion data with sufficient geospatial coverage and different site and geological conditions is required for more realistic microzoning at small scale.

REFERENCES

Abrahamson, N.A. and Somerville, P.G., 1996. Effects of the hanging wall and foot wall on ground motion recording during the Northridge *Earthquake. Bull. Seism. Soc. Amer.*, **86:** S93-S99.

Ali, Z., Qaisar, M., Mahmood, T., Shah, M. A., Iqbal, T., Serva, L., Michetti, A.M. and Burton, P. W. 2009. The Muzaffarabad, Pakistan, earthquake of 8 October 2005: surface faulting, environmental effects and macroseismic intensity. Palaeoseismology: Historical and Prehistorical Records of Earthquake Ground Effects for Seismic Hazard Assessment (Reicherter, k., Michetti, A.M. & Silva, P.G. editors). The Geological Society, London, Special Publications, 316, 155-172. DOI: 10.1144/SP316.9 0305-8719/09/$15.00 © The Geological Society of London 2009

Archuleta, R.J., and Hartzell, S.H., 1981. Effects of fault finiteness on near source ground motion. *Bull. Seism. Soc. Am.* **71:** 939-957.

Baker, M.A., and Jackson, R.O., 1964. Geological Map of Pakistan (1:2,000,000): *Geol. Surv. Pakistan, Quetta,* Pakistan.

Calkins, J.A., Offield, T.W., Abdullah, S. K. N. and Ali, S.T., 1975. Geology of Southern Himalaya in Hazara, Pakistan and adjacent areas. *U.S. Geol. Surv., Prof. Pap.* 716-C, C1-29.

Khan, S.A., Khan, K., Iqbal, Z., Mahmood, T., and Ali, Z., 2004. The Kaghan Valley Earthquakes of February 14, 2004: Source Mechanism and Regional Neotectonics. PAEC Report No. MSSP-71/2004.

Mahmood, T. Ali, Z., Khan, K., Iqbal, T., Hakim, A., Khan, S.A. and Qaisar, M., 2004. The Kaghan Valley Earthquake of February 14, 2004: *Intensity Survey and Geotectonics. PAEC Report No. MSSP-72/2004.*

Mahmood, T., Qaisar, M., and Ali, Z., 2002. Source mechanism of Astor Valley Earthquake of November 20, 2002 inferred from teleseismic body wave. *Geol. Bull. Peshawar Univ.*, 35: 2002.

Qaisar, M. Shah, D. Ali, Z. Mahmood, T., 2007. Muzaffarabad Earthquake of October 08, 2005: Seismological Aspects. Natural Cataclysms and Global Problems of the Modern Civilization, *Special edition of Transaction of the International Academy of Science. H&E. ICSD/IAS,* Baku-Innsbruck, Azerbiajan. p: 332-337.

Schwartz, D.P. and Coppersmith, K.J., 1986. Seismic Hazards: New trends in analysis using geologic data. in R.E. Wallace, ed., Active tectonics, Academic Press, Orlando, Florida. p 215-230.

Schwartz, D.P., 1988. Geology and seismic hazards: Moving into the 1990s. Proceedings, Earthquake Engineering and Soil Dynamics II: Recent Advances in Ground Motion Evaluation, *Geo-technical Special Publication* **20,** ASCE, New York, p 1-42.

Seeber, L. and Armbruster, J., 1979. Seismicity of the Hazara Arc in Northern Pakistan: Decollement versus Basement Faulting. In Geodynamics of Pakistan. Farah, A. and DeJong. K. A. (Eds.), *Geol. Surv. Pakistan, Quetta,* p131-142.

Somerville, P.G., and T. Sato, 1998. Correlation of Rise Time with the Style-of-Faulting factor in Strong Ground Motions. Abstract, 1988 *Annual Meeting of the Seis. Soc. America.*

Somerville, P.G., N.F. Smith, R.W. Graves, and N.A. Abrahamson, 1997. Modification of the empirical strong ground motion attenuation relations to include the amplitude and duration effects of rupture directivity. *Seismological Research Letters* **68:** p199-222.

Talat Iqbal, Khan, K., Qaisar, M., Mahmood, T., Ahmad, N., 2008. Mangla Earthquake of March 10, 2006: Source parameters and nature of the derived fault. Submitted for publication in the *Geol. Bull. Punjab Univ.* (in press).

Treloar, P. J., Broughton, R. D., Williams, M. P., Coward, M. P. and Windly, B. F., 1989a. Deformation and imbrication of the Indian Plate south of the Main Mantle Thrust, *North Pakistan. Jour. Met. Geol.,* **7:** p 111-125.

Wald, D.J., Quitoriano, V., Heaton T.H., Kanamori, H., 1999. "Relationships between Peak Ground Acceleration, Peak Ground Velocity and Modified Mercalli Intensity in California", *Earthquake Spectra,* **15, (3):** p557-564.

Wayne, P.D., 1979. A summary of field and seismic observations of the Pattan Earthquake – 28 December 1974 in Geodynamics of Pakistan edited by A. Farah and K. Dejong, *Geol. Surv. Pakistan, Quetta, Pakistan 1979,* p 143-147.

Wells, D.L., and Coppersmith, K.J., 1994. New empirical relationships among magnitude, rupture length, rupture width, rupture area, and surface displacement, *Bull., Seis., Soci., America,* **84 (4):** p 974-1002.

Geol. Bull. Punjab Univ. 43, 2008.

FRACTURE ANALYSIS OF EOCENE SAKESAR LIMESTONE AT MARDWAL ANTICLINE, SOAN-SAKESAR VALLEY, WESTERN PART OF CENTRAL SALT RANGE, DISTRICT KHUSHAB, PAKISTAN.

BY

A. H. BAITU
Pakistan Petroleum Limited, Karachi

RIAZ A. SHEIKH, NAZIR AHMAD
Institute of Geology, University of the Punjab, Quaid-i-Azam Campus, Lahore-54590 Pakistan

AHSAN JAVED DEO
Petroleum Exploration (Pvt.) Limited, Islamabad

ATIQ UR REHMAN
Baker Hughes, Pakistan

AND

ABDUL WAHAB
Nespak, Lahore

ABSTRACT:-*By using circle inventory method, fracture density at different part of Mardwal Anticline was calculated. It is preceded by estimation of fracture porosity as well as permeability of Sakesar Limestone exposed at Mardwal anticline which is present at flattened part of Ramp-Flat-Ramp geometry of Salt Range Thrust (SRT). Anticline is formed under flexure slip folding mechanism which creates offset between fractures across the beds and slikensides on bedding plane as well. That offset disconnects the continuity of fractures across the bedding plane and results in elimination of permeability for inter-bedded migration of fluid. Crest of the anticline as well as local shear zones at places, where axial trace of the anticline turns, are characterized by more fractures.*

INTRODUCTION

Mardwal Anticline is present on left side of the main road while going from Naushahra to Jaba near Mardwal village (Long. 72°09'55": Lat.32°36'25") Fig.1. It lies on topo-sheet no. 43D/2 of Survey of Pakistan and has extension from Long. 72°08'35" to 72°10'05" and from Lat. 32°35'56": to 32°36"30". It is mainly E-W trending anticline with asymmetric geometry (Plate 1). It has steeper northern limb while gentler southern limb. The anticline also shows the effect of flexure slip folding mechanism which is evident from slickensides on bedding planes and presence of offset between fractures across the bedding plane (Plate 4). There is bending in the axis from WNW to ENE because of shear zones one of these was observed at vicinity of Mardwal Anticline (Plate 4&5). Development of fractures, at Mardwal fractures Anticline, is very pronounced and sparking for analysis (Plate 2&3). Sakesar Limestone of Early Eocene is exposed through out the anticline. Here, main purpose of fracture analysis is to calculate density of fractures at different part of fold; and it is to estimate porosity and permeability of Sakesar Limestone.

TECTONIC SETUP

The mighty Himalayan mountain chain is a geological expression of collision of Indian Plate with Eurasian Plate (Tahirkheli, 1979). The ongoing northwards movement of Indian Plate caused crustal shortening that gave rise to fold and thrust belts (Lillie, et. al 1987). Since the collision in Eocene, deformation progressively shifted from the collision zone in north to the frontal fold and thrust belt in the south (Powel, 1979) (Table 1). About 2 M.Y. ago, major deformation front shifted to the present day frontal fold and thrust belt named as Salt Range – Potwar (Yeats et al., 1987) . It is an active fold and thrust belt that emerged in response to the underthrusting of

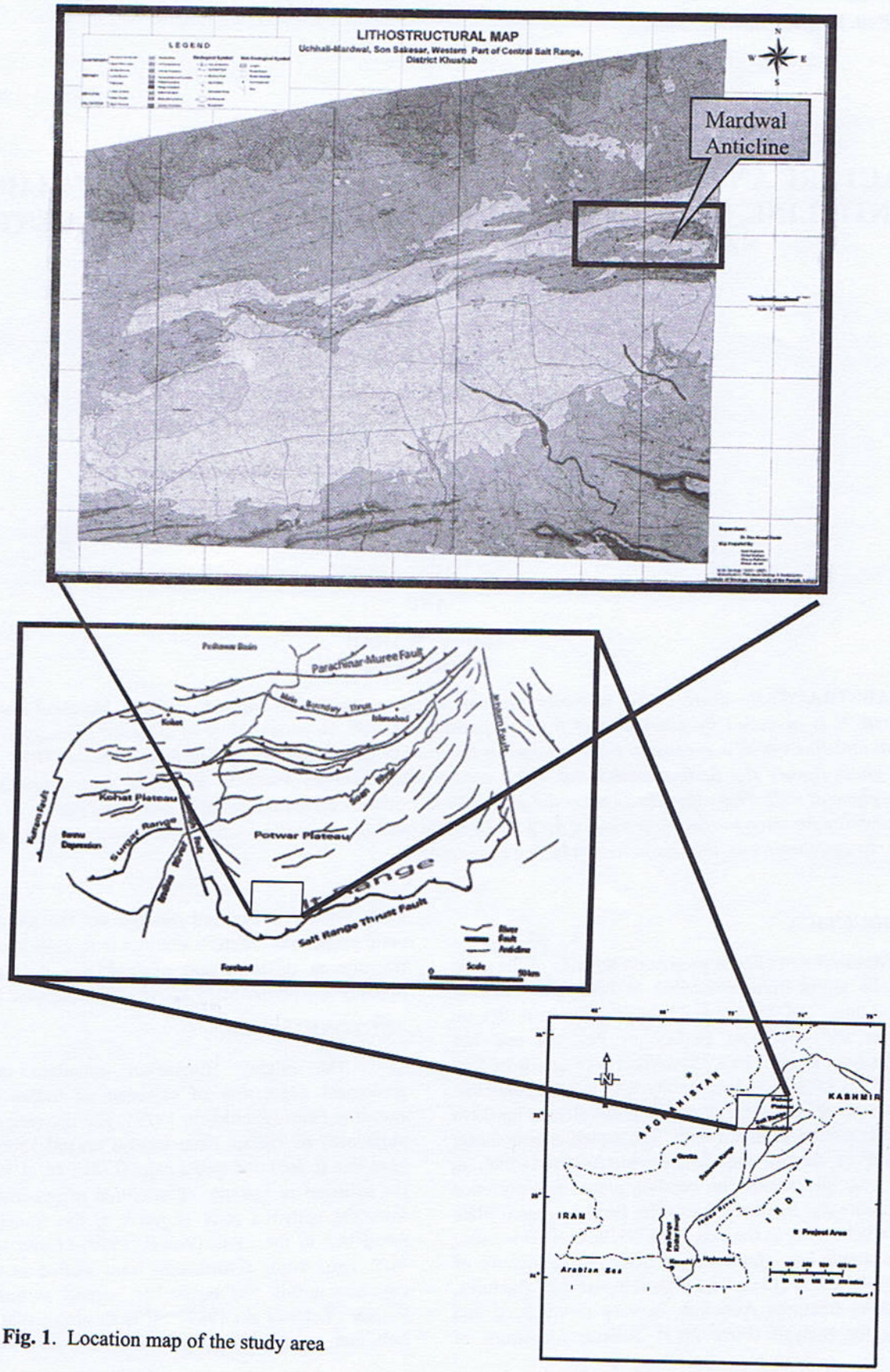

Fig. 1. Location map of the study area

cratonic Indian Plate beneath its own sedimentary cover. The main difference between the Salt Range and the region just in the north is that the Salt Range has undergone strong folding and uplifting in narrow zone (Farah et al., 1977). The Eocambrian rocks of Salt Range Formation are composed of thick evaporates and these low strength evaporites constitute the lubricated zone of decollement and Salt Range is the surface expression of the leading edge of decollement thrust in which the crystalline basement is not involved (Crawford, 1974). At Salt Range Front, the evaporites and overlying strata over-ride syn-orogenic fanglomerate of Punjab plains along Salt Range Thrust (SRT) (Yeats et al., 1987). The strongly emergent Salt Range forms an escarpment along the SRT in south, while northwards it extends as a gentle monocline that merges into Potwar Plateau (Yeats et al., 1984).The northern monocline is a surface expression of a foot wall ramp. It is a basement normal fault down to north. It may be confirmed from seismic reflection data (Lillie, 1987) (Baker, 1988).

Table 1
Fracture Density, Porosity and Permeability of Sakesar Limestone at Mardwal Anticline

Sr. No.	circle No	Density cm-1	Porosity %	Permeability 107 darcy
1	5	0.144	13.2	6.9
2	6	0.16	12.6	7.5
3	8	0.08	10.4	10.1
4	4	0.104	9.9	6.08
5	15	0.109	7.2	4.4
6	9	0.07	7	6.7
7	10	0.063	6.4	3.5
8	11	0.055	5.8	4.7
9	13	0.065	4.64	0.15
10	14	0.098	4.4	0.16
11	7	0.03	3.4	2.9
12	12	0.062	2.23	0.13

As for as Mardwal Anticline is concerned; tectonically, area falls in Western central Salt Range (WCSR). Western Central Salt Range is differentiated from Eastern Central Salt Range (ECSR) on the basis of deformational style as it is dominated by folding while in Eastern Central Salt Range (ECSR), faulting is prominent. This interpretation is made by using maps of Gee (1980) and satellite data. Shortening in ECSR is compensated by conjugate strike slip faults with reverse slip movement i.e. Kalar Kahar & Vasnal Faults. On the other hand in WCSR, shortening is compensated by folding.

STRUCTRAL SETUP OF NEAR BY AREA

Structural features, present near by vicinity of Mardwal anticline, show that there was initially NNE to NNW lateral compressional forces that resulted in formation of WNW to ENE trending major folds with minor thrust faults. Later on, gravity tectonics prevailed which was caused by release provided by the propagation of SRT to the surface and build up of salt in anticlines. It may result in the formation of extensional fractures and cross-folding of the pre-existing folds.

METHODOLOGY

(CIRCLE INVENTORY METHOD)

Circle Inventory Method was used for fracture analysis. Total 12 sampling stations were selected which represented different parts of anticline. In this method, a circle of known as well as predetermined radius is traced on surface hosting fracture (Davis, 1996) --- in our case, it was bedding plane all the time --- and it requires measuring of all the fractures that is occupied by circle (Plate 2). The orientations, lengths and widths of the each fracture within the circle were measured. Circles, having radius ranging from 40cm-100cm, were traced out on bedding plane by the

help of chalk and measuring tape; orientation of fractures were measured in terms of strike by using Brunton; length and width were measured by the help of simple ruler and measuring tape. To avoid repetition, each fracture was traced with chalk after measuring (Plate 2). Accuracy is very good for length measurement but it is satisfactory for width measurement in our case. For measuring orientation, only the straight lines traces of the fractures were evident at bedding plane due to that, only strikes of the fractures were measured.

FRACTURES

The term fracture is typically used to emphasize the notion that something is broken e.g. "any break in a rock; [Gary, 1872]. Fractures are the most commonly developed structures, since these are found in all competent rocks. Fractures increase porosity as well as permeability of the carbonate rocks.

The fractures, present on the Mardwal Anticline, are mainly controlled by fold stresses. Four sets of fractures are present on Mardwal anticline, which are open fractures with variable orientations (Plate, 3). Two of the four sets are related to extension while other two are associated to shear. On the basis of the relationship of fractures to the fold axis, fractures can be divided as under.

RELEASE FRACTURES

This fracture set is parallel to the fold axis and geometrically named as longitudinal fractures (Billings, 1972) (Fig. 3). These types of fractures are formed at the point of maximum curvature and are caused by tension on the upper side of the folded bed (Billings, 1972) (Nelson, 1985). Tangential longitudinal strain, in which outer part of folded competent layer is stretched, may develop release fractures (Billings, 1972) (Ramsay, 1988), Release fracture may also form when overburden load is removed or released (Billings, 1972). At Mardwal anticline, longitudinal fractures are common and are oriented at EW, WNW and ENE or simply have varying strikes from $N80^0E$ to $S70^0E$ (Plate, 3). The longitudinal fractures are dipping at high angle. Their width ranges from 0.1 to 1.5 cm. Their length within an inventory circle (50cm radius) ranges up to 95cm. Frequency of release fractures varies from 0% to 40% at different inventory circles, but these are 17% of total fractures measured at all sampling stations.

EXTENSION FRACTURES

This fracture set is oriented perpendicular to the fold axis and geometrically named as cross fracture (Billings 1972) (Fig. 6). These are resulted from slight elongation parallel to the axis of fold (Billings 1972). Cross fractures are mainly present at crestal part the Mardwal anticline. At Mardwal anticline, their orientations are NS, NNW and NNE or varied in strikes from N20°W to N30°E (Fig. 6). These fractures are also dipping at high angle. Their width ranges from 0.15cm to 1.9cm. Within the inventory circle of 50 cm radius their length ranges from 15cm to 95cm. Frequency of release fractures varies from 0% to 50% at different inventory circles, but these are 24% of total fractures measured at all sampling stations.

CONJUGATE SHEAR FRACTURES

There are two sets of fractures set-1 and set-2, conjugate sets, present at Mardwal Anticline (Fig. 6). These fractures are oblique to the fold axis and dipping at very high angle and named as vertical diagonal fracture (Billings, 1972) (Fig. 6) and these fractures are parallel to the intermediate stress direction (δ_2) (Jadoon, 2003).

Set-1 has orientation mainly NW, but ranging from N20W-N50W at different sampling inventory circle (Fig. 1). Their width ranges from 0.2cm to 2.1cm. Within the inventory circle of 50cm radius, their length ranges from 20cm to 100cm. Frequency of shear set-1 fractures varies from 0% to 56% at different inventory circles, but these are 26% of total fractures measured at all sampling stations.

Set-2 has orientation mainly NE, but ranging from N40E to N75E at different sampling inventory circle (Fig. 7). Within the inventory circle of 50cm radius, their length ranges from 20cm to 100cm and width ranges from 0.2cm to 2cm. Frequency of shear set-1 fractures varies from 10% to 67% at different inventory circles, but these are 33% of total fractures measured at all sampling stations. Their width ranges from 0.2 to 2.1 cm. Where as the length, within the inventory circle of 50cm radius, ranges from 25cm to 100cm.

FRACTURE DENSITY

The abundance of fractures at a given station is described through the evaluation of fracture density (Davis, 1996). Fracture density can be measured and described in a number of ways; total cumulative length of fracture within a given volume of rock divided by area of the circle (Jadoon et al., 2003). The measure of fracture density used in conjunction with the circle inventory method is the summed length of all fractures within an inventory circles, divided by the area of the circle (Davis, 1996).

$$FD = \sum L / \pi r^2$$

FD = Fracture density
$\sum L$= Cumulative length of all fractures
r = Radius of inventory circle

The fracture density on the Mardwal Anticline varies from $0.03cm^{-1}$ to $0.16cm^{-1}$ (Table, 1).

Iso fracture density map is prepared, which shows the fracture density variation at different part of the Mardwal Anticline. There is shear zone with maximum fracture density value of $16m^{-1}$ ($0.16cm^{-1}$) (Table 1). Maximum

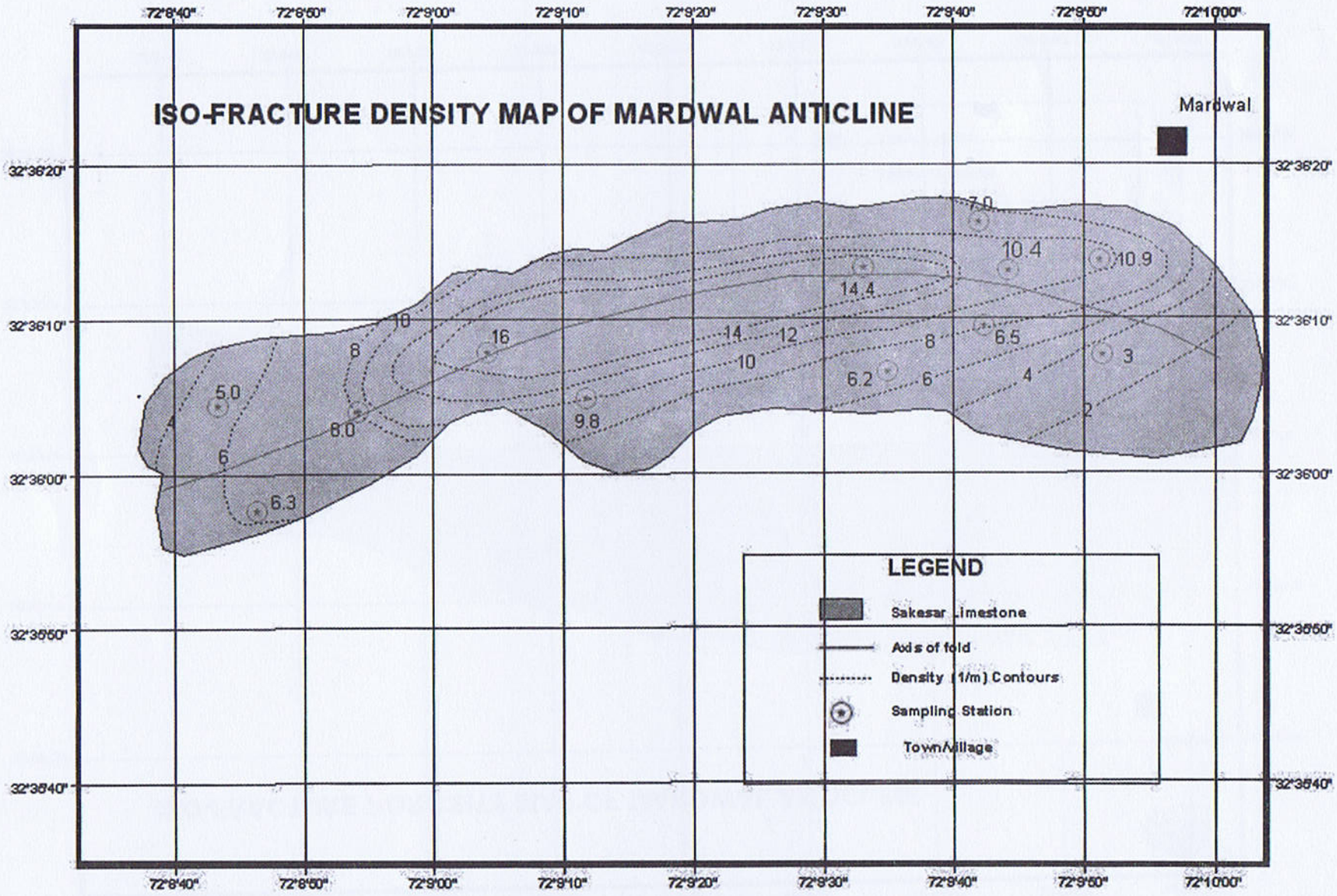
ISO-FRACTURE DENSITY MAP OF MARDWAL ANTICLINE
Mardwal
72°8'40"
72°8'50"
72°9'00"
72°9'10"
72°9'20"
72°9'30"
72°9'40"
72°9'50"
72°10'00"
32°36'20"
32°36'10"
32°36'00"
32°35'50"
32°35'40"
7.0
10.4
10.9
14.4
16
14
12
10
8
6.5
6.2
6
4
3
2
5.0
8.0
9.8
6.3
LEGEND
Sakesar Limestone
Axis of fold
Density (1/m) Contours
Sampling Station
Town/Village

Fig. 2.

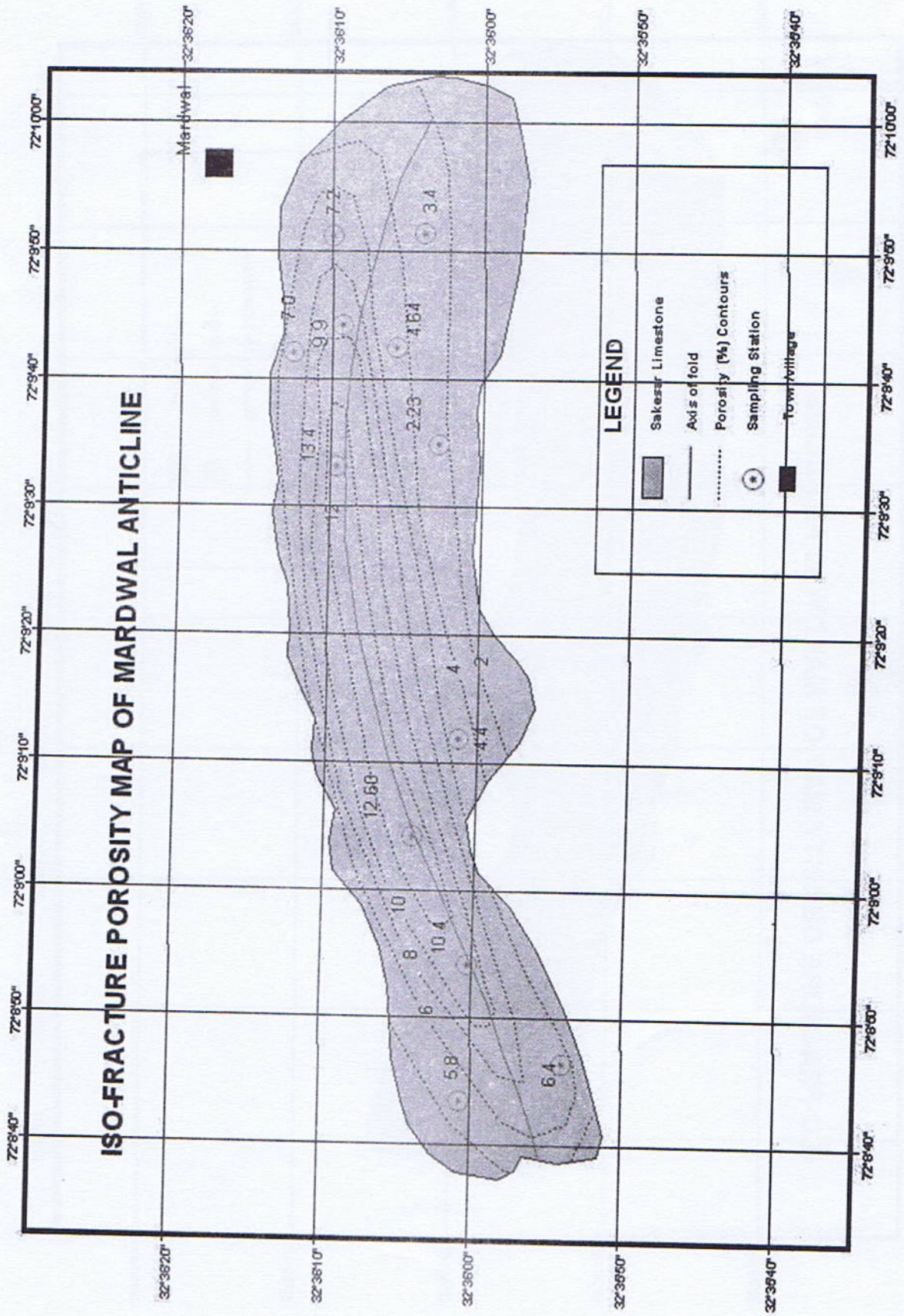
ISO-FRACTURE POROSITY MAP OF MARDWAL ANTICLINE
Mardwal
LEGEND
Sakesar Limestone
Axis of fold
Porosity (%) Contours
Sampling Station
Town/Village
72°8'40"
72°8'50"
72°9'00"
72°9'10"
72°9'20"
72°9'30"
72°9'40"
72°9'50"
72°10'00"
32°36'20"
32°36'10"
32°36'00"
32°35'50"
32°35'40"
7.0
9.9
13.4
7.2
12
3.4
4.64
2.23
4
2
4.4
12.60
10
8
10.4
6
5.8
6.4

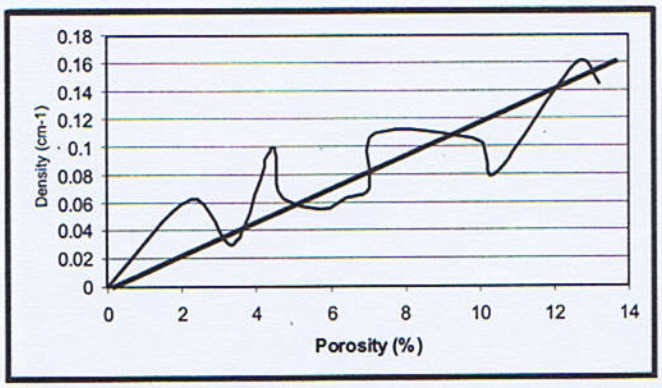

Fig. 4. Showing the Relationship between Fracture Density and Porosity of Sakesar limestone of Mardwal anticline.

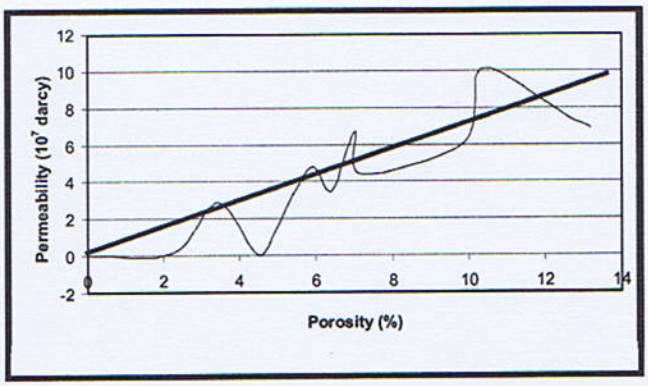

Fig. 5. Showing the Relationship between Fracture Porosity and Permeabilty of Sakesar limestone at Mardwal anticline.

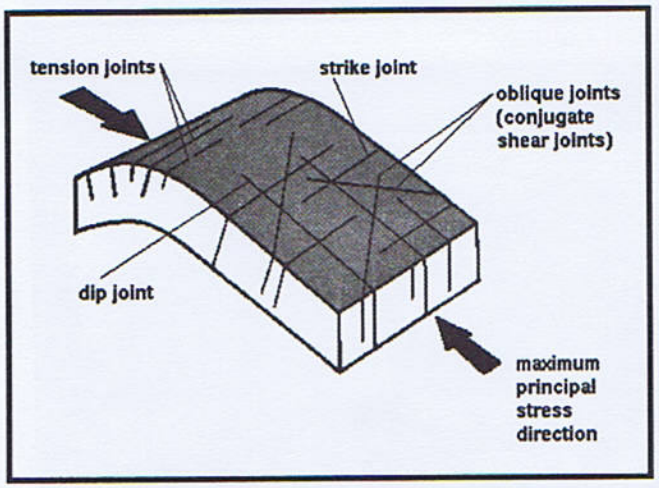

Fig. 6. Model shows orientation of fractures with respect to fold Axis

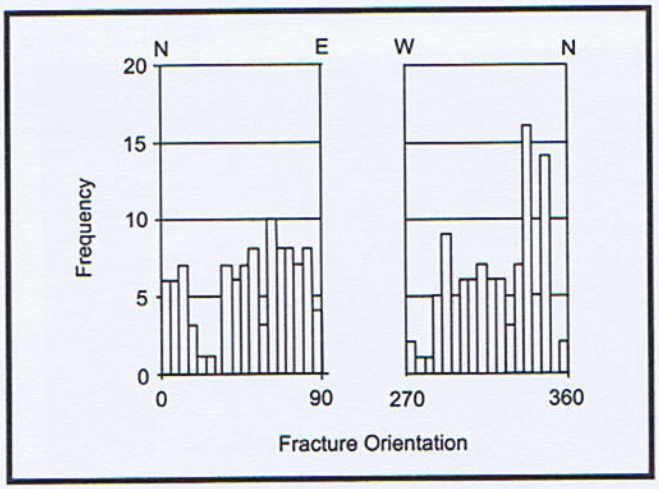

Fig. 7. Orientation strike Histogram of the fractures at Mardwal anticline.

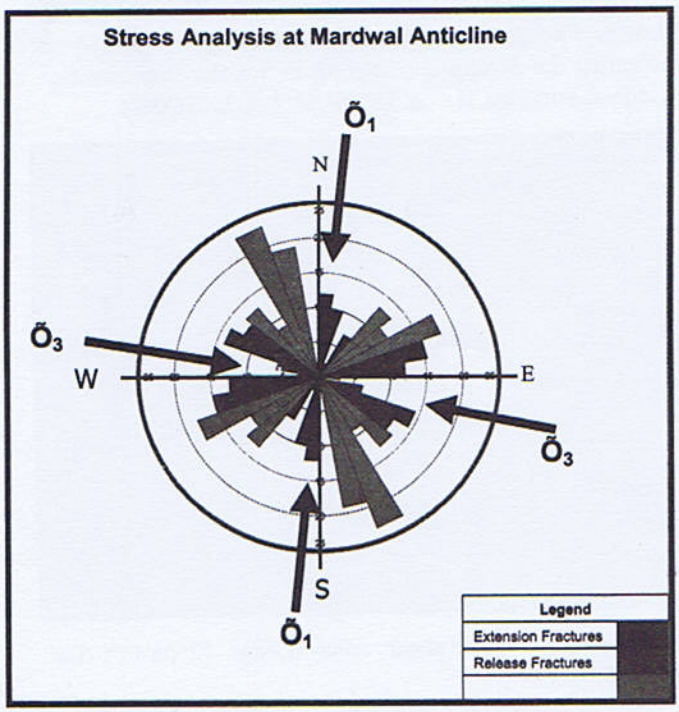

Fig. 8. Generalized direction of Principle Compressive Stress $\tilde{O}_1$ parallel to extensional fractures, while Minimum Principle stress $\tilde{O}_3$ is parallel to release fractures.

Fig. 3.

Plate 1. A view of Mardwal Anticline.

Plate 2. A traced circle with marked fractures for fracture analysis of Sakesar lime stone at Mardwal Anticline.(Long. 72°09'51": Lat. 32°36'03")

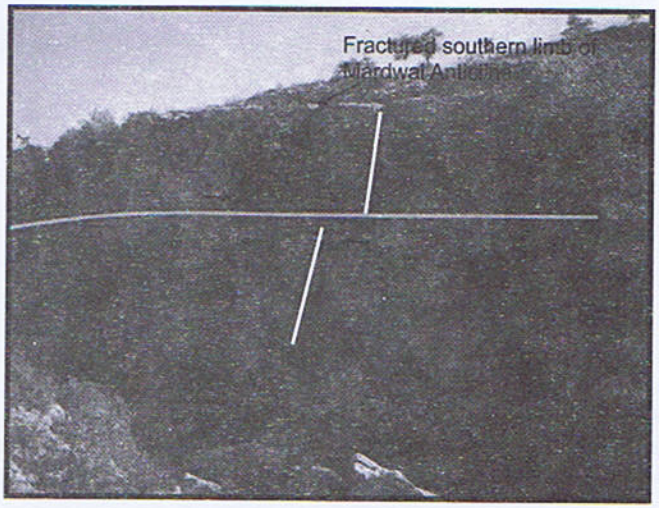

Plate 4. Facing toward NE, movement along bedding plane indicating the flexure slip folding in Sakesar lime stone at Mardwal Anticline. (Long. 72°09'06": Lat. 32°36'06").

Plate 3. Facing toward south, fractured northern limb of Mardwal Anticline (Long. 72°09'49"; Lat. 32°36'12").

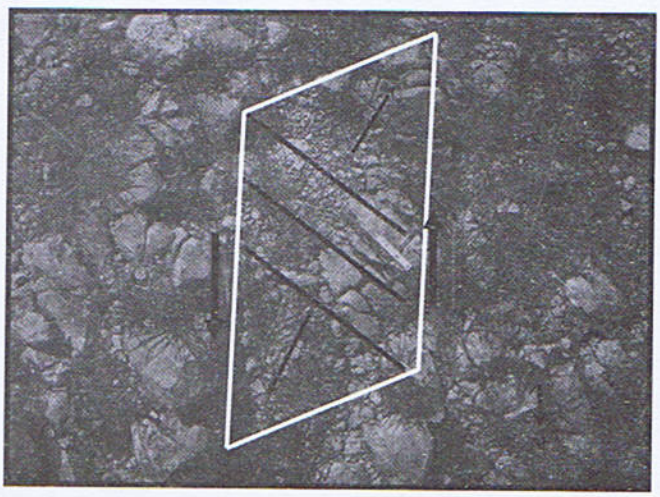

Plate 5. Left hand shear zone (Long. 72°08'40": Lat. 32°35'57")

density is present at crest of Mardwal Anticline and near shear zone (Fig. 2).

FRACTURE POROSITY

Porosity depends upon lengths, widths, and densities of fractures at sampling stations (inventory circles) (Jadoon et al., 2003). Through Monte Carlo techniques, these functions can be combined to yield fracture porosity. Lengths and widths, in fact, are the lengths and widths of segments of fractures captured in an inventory circle. As the fractures on the Mardwal Anticline have variable widths, so we took more then one reading of width for each fracture and then considered their average value. The fracture porosity in an inventory circle is determined by using following formula (Jadoon et al. 2003):

$$\text{Porosity} = (1/A) \sum_{i=1}^{N} (L_i \times W_i)$$

Where

i = Index to designate each fracture in an inventory circle

Li = Length of the i^{th} fracture

Wi = Width of the i^{th} fracture

N = Number of fractures in the inventory circle,

$A = \pi r^2$ = Area of inventory circle.

The fracture porosity for Sakesar Limestone, exposed at Mardwal Anticline, ranges from 2.23 % to 13.6 % (Table 1).

Iso Fracture Porosity map was prepared. It indicates the variation in porosity of Sakesar Limestone at Mardwal Anticline. Crest and Northern limb of the anticline have more porosity than less deformed southern limb (Fig. 3).

FRACTURE PERMEABILITY

The permeability within individual inventory circle, assuming no matrix, is estimated from the following equation (Muskat, 1949):

$$K = (3.5 \times 10^8)\ (1/A) \sum_{i=1}^{N} (L_i \times W_i^3)$$

Where

K = Permeability in darcy

i = Index to designate each fracture in a inventory circle

N = Number of fracture in the inventory circle,

Wi = Width of the i^{th} fracture,

Li= Length of the i^{th} fracture,

A= Area of the inventory circle, and

3.35×10^8= Factor to convert cm^2 to darcy.

This calculation is also based on a Monte Carlo approach and is similar to that carried out for estimating fracture porosity. The fracture permeability for Mardwal Anticline ranges from 1.3×10^6 to 10.1×10^7 Darcy (Table 1).

RELATIONSHIP BETWEEN FRACTURE POROSITY AND DENSITY

There is overall linear relationship between Fracture Porosity and Fracture density which are measured at different sampling stations on Mardwal Anticline (Fig. 4). But it is not smooth line, because fracture density represents cumulative length of the fractures within inventory circle, on the other hand, fracture porosity represents fractures opening area within inventory circle. So, opening of fractures may differ at different sampling stations having same cumulative fracture length. That creates fluctuation in cross plot.

RELATIONSHIP BETWEEN POROSITY AND PERMEABILITY

As we know, fracture porosity represents fractures opening area within inventory circle and permeability is a function of fractures inter-connectivity. But in our case, permeability, having no relation with connectivity, represents the multiplication of fracture length and cube of width (W^3), divided by area of inventory circle. So graph line is not smooth and has fluctuation, but overall linear relationship between Fracture Porosity and Fracture permeability is present (Fig. 5).

STRESS ANALYSIS

For stress analysis, the fracture orientation data is plotted on the rose diagram. Rose diagram provides an immediate visual estimation of stress orientation regarding any data. A standard rose diagram is constructed on a grid, composed of concentric circles superimposed on a set of radial lines (Fig. 8)

The principal stress direction (δ_1) is always parallel to the extensional fracture sets and normal to the Release/ Longitudinal fractures (Davis 1984) (Twiss, 1992) (Billings 1972). Shear fractures are always oblique to the Principle stress direction (δ_1) (Billings 1972). Fracture system of concerned anticline is analyzed under these particular rules.

CONCLUSION

On the basis of above facts, it is concluded that the general behavior of fractures in concerned area is as:

- Cross fractures have orientation NS/NNE/NNW (N20°W-N30°E)
- Release fractures have orientation EW/ENE/WNW (N80°E – S70°E)
- Shear Fracture set-1 have orientation NW (N20°W-N50°W)
- Shear Fracture set-2 have orientation NE (N40°E-N75°E)

Nearly orthogonal relationship of cross fractures and release fractures suggests that tensile force is normal to the principal stress (δ_1) direction, where as compressive force is parallel to the principal stress direction (δ_1). Hence on the basis of orientation of release and extension fractures, we can say the principal stress direction is from NNW-SSE to NNE-SSW (Fig. 8) and the fractures are formed due to the stress related to the formation of the Mardwal Anticline.

REFERENCES

Davis, G.H., 1984. *Structural Geology of Rocks and Regions,* New York. Willey. pp. 325-352.

Davis, G.H., and Raynolds, J.S., 1996. *"Structural Geology of Rocks and Regions"*, 2nd Ed. Published by John Wiley and Sons Inc., New York.

Davis, L.M., 1937. The Eocene Beds of the Punjab Salt Range, Indian *Geol. Surv. Mem. New Series.* **24,** pp. 1-79.

Gardezi, A.H., and Ashraf, A.M., 1974. Gravitative structures of the Katha Masral region of the Central Salt Range, Pakistan. *Geol. Bull. Punj. Univ.*, **11,** pp. 75-80.

Gee, E.R., 1980. Pakistan Salt Range Series Geological Maps, 1:50000, 6 sheets. Directorate of Overseas surveys, United Kingdom, for Government of Pakistan, and Geol. Survey of Pakistan.

Gee, E.R., 1989. Overview of the geology and structure of the Salt Range, with observations on related areas of Northern Pakistan. *Geol. Surv.* Spec. Paper **232,** pp. 95-111.

Gee, E.R., 1983. *Tectonic Problems of the Sub-Himalayan region of Pakistan.* pp. 308-328.

Jadoon, et al., 2003. Fracture analysis of Khaur anticline, *Proceeding of the Annual Technical Conference of PAPG*, pp. 235-249.

Lillie et al., 1987. Structural Development within the Himalayan foreland fold and thrust belt of Pakistan.

Lillie, R.J., Jaume, C.S., 1988. " Mechanics of the Salt Range Potwar Plateau, Pakistan: A Fold and Thrust Belt Underlain by Evaporites" Pub., Am. Geophys. Union, *Tectonics,* **7,** pp. 1-11.

Muskat, M., 1949. *Physical Principles of Oil Production:* New York, McGraw-Hill, 922 p.

Nakata, T., 1972. Geomorphic history and crustal movement of the foothills of the Himalaya: *Inst. Of Geog., Tohoku Univ., Sendai.*, pp. 39-77.

Nelson, R.A., 1985. *Geological Analysis of Naturally fractured reservoir.* Gulf Publishing Company, Texas.

Philip, K. and Frederick, J.V., 1996. *"Global Tectonics"*, 2nd Ed. Blackwell Science Ltd. U.K.

Pinfold, E.S., 1918. Notes on the structure and stratigraphy in the NW of Punjab: *Indian Geol. Surv.*, pp. 137-160.

Powell, C.M., and Conaghan, P.J., 1973. Plate Tectonics and the Himalayas: *Earth Planet. Sc. Letters*, **20,** pp. 1-12.

Raynolds, R.G.H., and Johnson., G.D., 1985. Rates of Neogene depositional and deformational process in the Himalayan foredeep, Pakistan: *Geol. Soci. London* Spec. Publ.

Yeats, R.S., and Lawrence, R.D., 1984. Tectonics of the Himalayan Thrust Belt in Northern Pakistan. In: Haq, B.U., and Milliman, J.D (eds), *Marine Von Nostrand,* New York, 177-198.

Yeats, R.S., and Hussain, A., 1987. Timing of structural events in the Himalayan foothills of north-western Pakistan. *Bull. Geol. Soci. Am.* **99,** pp. 161-175.

Zhang, Zh. M., et al., (in press.). An outline of plate tectonics of China.

Geol. Bull. Punjab Univ. 43, 2008.

GEOLOGY OF HETTANGIAN TO MIDDLE EOCENE ROCKS OF HAZARA AND KASHMIR BASINS, NORTHWEST LESSER HIMALAYAS, PAKISTAN

BY

NAVEED AHSAN
Institute of Geology, University of the Punjab, Quaid-i-Azam Campus,
Lahore-54590 Pakistan
e-mail: naveedahsan@ymail.com

AND

M. NAWAZ CHAUDHRY
College of Earth and Environmental Sciences, University of the Punjab, Lahore-54590. Pakistan

ABSTRACT:-*The Mesozoic to Eocene sedimentary succession of Hazara Basin dominated by carbonates is characterized by a distinct package of sediments punctuated by a number of diastems, hiatus and unconformities. The Hazara Basin evolved in Hettangian with the development of lagoonal to upper shoreface conditions on the northern margin of northward flying India. It was followed by a thick pile of middle Jurassic to upper Cretaceous sediments representing deposition in supratidal to outer ramp settings. During late Cretaceous the basin was exposed subaerially when the Indian Plate established its first contact at 67±2Ma with the Kohistan Island Arc. During this time the Kashmir Basin remained exposed.*

Sedimentation resumed in Hazara and Kashmir basins with the development of transgressive shoreline and Hangu Formation was formed in Danian. The Hazara and Kashmir basins and adjacent areas experienced the last marine incursion at the close of Danian in which a sequence of carbonates and siliciclastics represented by Lockhart Formation, Patala Formation, Margala Hill Formation and Chorgali Formation were deposited. This was followed by main collision between India and Asia sandwiching the Kohistan Island Arc at 40 to 50Ma. This collision was followed by retreat of sea, uplift of Himalayas, development of a foredeep and deposition of a fluvial package, by meandering river system, from Himalayan provenance namely Murree Formation.

INTRODUCTION

Fragmentation of the super-continent, Pangaea (e.g. Scotese et al, 1979; Condie, 1984), initiated in Carboniferous to Early Permian (300-250 Ma) resulted into the formation of several plates microplates and a new ocean, Neo Tethys (e.g. Angiolini et al. 2003). The Indian Plate, began its rapid northwards drift across the Indian Ocean from the Southern Hemisphere (Mattauer et al. 1977, 1978, 1986a, b; Farah and DeJong, 1979; Tapponnier, et al. 1986; Searle, 1991) and the Neo-Thethys that stretched from the Pacific to the Mediterranean started to shrink (Mattauer et al. 1977, 1978, 1986a, b; Farah and DeJong, 1979; Tapponnier, et al. 1986; Jaeger et al. 1988; Searle, 1991; Chaudhry et al. 1994b; Valdiya, 2002; Burlini et al. 2005). A series of volcanic arcs (e.g. Kohistan Island Arc) were generated due to intra-oceanic subduction of the Indian Plate in Cretaceous (Chaudhry et al. 1974a, b; Searle, 1991; Ghazanfar; 1993; Burg et al., 1996, 1997, 2005a, b, 2006, Ahsan, 2008). During Turonian the Kohistan Island Arc accreted to Eurasia. The suturing event is constrained at 102 Ma (Searle et al., 1991). The Indian Plate established its first contact with the Kohistan Island Arc at 67 ± 2 Ma (Bard et al., 1980; Jaeger et al. 1988; Spencer, 1993; Valdiya, 2002; Burlini et al. 2005). This conclusion is further substantiated by Chaudhry et al., (1994b) on the basis of biostratigraphic and sedimentological studies. Many workers (e.g. Dewey et al., 1988; Klootwijk, et al., 1979; Powell, 1979; Searle et al., 1987; Searle, 1991) have accepted that collision occurred at 55-45 Ma (in Eocene). However according to Chaudhry et al. (1994b) the Kohistan Island Arc sandwiched between

India and Eurasia at 55 Ma. The terminal collision between Indian and Asian Plates according to Spencer (1994) occurred between 45-40 Ma. The collision between Indian Plate and Kohistan Island Arc is recognized when the Neo-Tethys disappeared and the two continental masses tied up (Spencer, 1994).

The flight of India and its collision with the Asian continent has been studied from many different aspects, such as sea-floor spreading, paleomagnetisim, siesmicity, structure, stratigraphy, paleontology and sedimentology (e.g. Ahsan, 2008; Ahsan et al., 2001a; Chaudhry et al., 1998a; Chaudhry and Ahsan, 1999a,b; Klootwijk et al., 1985; Latif et. al., 1995; Powell, 1979; Patriat and Achache, 1984, etc). A series of benchmark papers published by Latif (e.g. 1970a and b, 1976, 1980, 1990, and 1995), Marks and Ali (1961), Gardezi and Ghazanfar (1965), Calkins et al. (1975), Latif (1980), Ghazanfar et al. (1987, 1990), Butt (1986, 1987, 1988, 1989), Baig and Lawrence (1987), Baig (1999), Chaudhry et al. (1992; 1994a and b; 1995; 1996a and b; 1998a, b and c; 2000) and Baloch et al., (2002) have contributed to the understanding of lithostratigraphy, tectonics and structure of the Hazara area and partly the Kashmir Basin.

Sedimentary rocks are believed to keep the record of relative sea level changes and provenance of sediments in relation to plate movement and reflect on the tectonic evolution of sedimentary basins (e.g. Pettijohn, 1957; Krumbein and Sloss, 1963; Tucker and Wright, 1990; Reading, 1996; Tucker, 1988). Sedimentological studies of the Hazara Basin with emphasis on microfacies investigations of numerous Mesozoic and Tertiary formations were carried out by Chaudhry et al. (1992, 1994a and b, 1996a and b, 1997a, 1998a, b and c, and 2000), Ahsan et al. (1993, 1994, 1998a and b, 1999a and b, 2000a and b, 2001b, c and d) and Ahsan and Chaudhry (1998 and 1999). Microfacies and palynological studies of Tertiary rocks in the adjoining Kashmir Basin permitted correlation with the Hazara Basin (Ahsan et al. 1998a and b, 1999a and b, 2001b, 2001a, b, c and d). Recently, Ahsan (2008) established microfacies, worked out environments of deposition and diagenesis and interpreted the inferred pathways of geochemical changes in the Kawagarh Formation of Hazara Basin.

This paper documents the geology of Hazara and Kashmir Basins in relation to tectonics of the India and Asia, timing of collision, provenance of the sediments and finally the development of foreland basin. In addition to this, in the last section of this paper, an over view of the tectonic has been presented to understand and constrain sedimentological variations in the area.

REGIONAL SETTING

The Northwest Himalaya is the meeting point of a number of tectonic elements and lines (Fig. 1). From north to south they can be enumerated (Ghazanfar, 1993) as the Asian plate (Desio, 1963, 1964, 1979; Tahirkheli et al. 1979; Bard et al. 1980; Ghazanfar, 1993;), the Shyok Suture Zone (Main Karakoram Thrust, MKT; Tahirkheli, et al. 1979; Ghazanfar, 1993; Heuberger et al. 2007), the Kohistan Island Arc Complex (Tahirkheli et al. 1979; Bard et al. 1980; Chaudhry et al. 1984; Treloar et al. 1989a, b, 1991; Ghazanfar et al. 1991; Anckiewicz et al. 1998 a,b; et al. 1996, 1998, 2005a,b; Arbaret et al. 2000; Zeilinger et al. 2000; Llana-Fúnez et al. 2005; Garrido et al. 2006, 2007), the Indus Suture (Tahirkheli et al. 1979; Ashraf et al. 1991; Zeilinger et al. 2000) and the Indian Plate margin (Chaudhry and Ghazanfar, 1987, Ghazanfar, 1993) with its cover sequence as the major tectonic elements of northern Pakistan.

The Northwest Himalayas in Pakistan (Bard et al. 1980; Ghazanfar et al. 1991; Ghazanfar, 1993) extends from Main Frontal Thrust (MFT) to Main Mantle Thrust (MMT). Internally they are divided into Outer, Lesser, Higher and Tethyan Himalayas. Each unit is demarcated by a major boundry thrust. The existence of Tethyan Himalaya is being debated (Bard et al. 1980; Tahirkheli et al. 1979; Chaudhry et al. 1983; Fletcher et al. 1986 and Ghazanfar, 1993). Two major rock sequences of the Indian plate comprise the Proterozoic basement and the Phanerozoic cover rocks (Chaudhry and Ghazanfar, 1987, 1993; Ghazanfar, 1993; Spencer, 1994; Chaudhry et al. 1974a, b and c; 1976; 1980; 1983a and b; 1984, 1986; 1987; 1993a, b and c, 1997b and c, 1999, Burg et al., (1996, 1997, 1998, 2005a, b, 2006). The Precambrian basement is subdivided into Salkhalas, Hazara slates and Tanols. The Main Central Thrust (MCT) demarcates two main tectonostratigraphic areas (Ghazanfar, 1993; Spencer, 1994; Chaudhry et al. 1997b and c). In Kaghan the High Himalaya basement composed of metaturbidites, migmatites, pelites, psammites, calc pelites, minor marbles and granitoids is designated as Purbi Nar Group. The Higher Himalayan cover is composed of marbles, dolomitic marbles, pelites, garnetiferous calc pelites, amphibolites and eclogites. Their equivalents in Swat are Manglaur Group (basement) and Alpurai Group (cover to basement). In the southern part the Precambrian rocks of the Lesser Himalaya are overlain by Palaeozoic to Neogene cover sequences in various basins like Kashmir, Muzaffarabad, Attock, Hazara, Peshawar and the Salt Range. Molassic sediments fill a wide trough in the extreme south. The Indian platform exposures, for the most covered by alluvium, can be recognized near Sargodha, Chiniot and Sangla Hill and again far to the south at Thar and Nagar Parker in southern Pakistan. These four zones namely Tethys Himalaya, High Himalaya, Lesser Himalaya and Sub-Himalaya in Northwestern and Western Himalayas represent an essential continuity of the geology of Central and Eastern Himalayas.

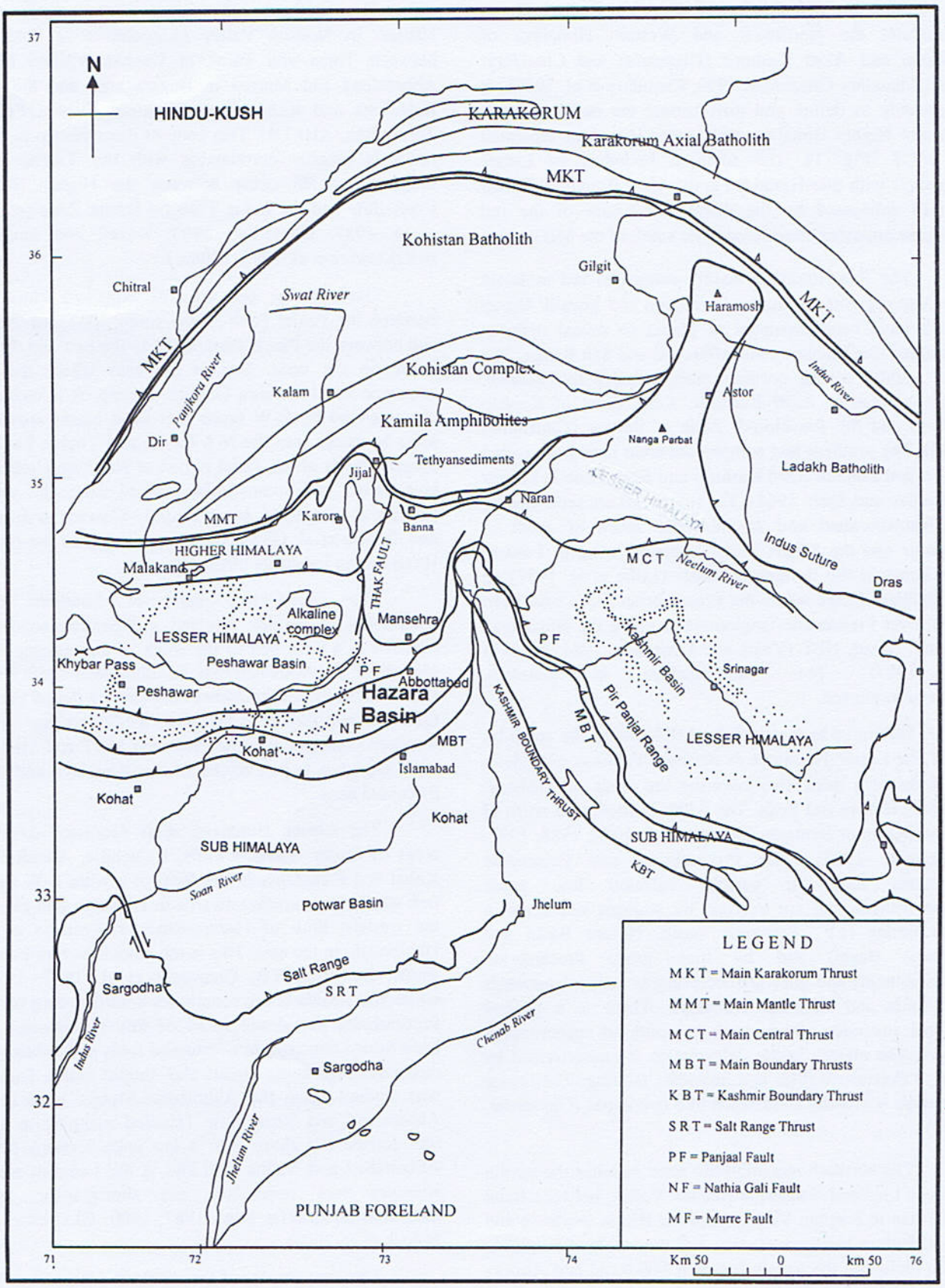

Fig.1. Tectonic map of Pakistan.

After the demarcation of the Main Central Thrust throughout the Northwest and Western Himalaya of Pakistan and Azad Kashmir (Ghazanfar and Chaudhry, 1987; Chaudhry Ghazanfar, 1990; Chaudhry et al. 1997b) it is possible to define and differentiate the major tectonic zones of Higher Himalaya and Lesser Himalaya separated by MCT (Fig. 1). The southern boundary of Lesser Himalaya with Sub-Himalaya is the Main Boundary Thrust (MBT) delineated by the distinctive nature of the red Neogene molasses considered to lie south of the MBT.

The Sub-Himalaya mainly comprises red molassic foredeep deposits of Murree Formation and Siwalik Group which have been disrupted at places to reveal upthrust structures like Balakot - Muzaffarabad and Salt Range. The more tightly folded northern part includes the Poonch, Patehka areas of Azad Kashmir, Kwai (area of Kaghan Valley) and the Rawalpindi Zone of Potwar (Ghazanfar, 1993). The southern less compressed areas have been called the Sialkot Zone in Azad Kashmir and Soan Zone in Potwar (Sokolove and Shah, 1966). The two zones are separated by the Muzaffarabad and Jammu/Riasi zones of uplift in Kashmir and the Khairi Murat anticlinal zone in Potwar. Salt Range is the limiting structure (Lillie et al. 1987) on the southern fringe where the Precambrian rocks have been thrust over Pleistocene fanglomerates along the Himalayan Frontal Thrust, HFT (Yeats and Lawrence, 1984; Lillie et al. 1987). The Sub-Himalaya is generally unmetamorphosed.

Delimited to the north by MCT and to the south by MBT the Lesser Himalaya in northern Pakistan extends in the form of a thick slab covering the areas of Kashmir, Kaghan, Hazara and Swat. The width is attenuated north of Hazara-Kashmir Syntaxis (Bossart et al. 1984, 1988, 1992; Ghazanfar, 1993). The Precambrian and Palaeozoic sediments have in general suffered low grade metamorphism and are overlain by younger sediments in large basins (e.g., Peshawar Basin, Hazara Basin and Kashmir Basin) and by high grade Precambrian metasediments and gneisses occurring as nappes eastwards in Shimla and Gharwal Himalaya. There is a general tectonic inversion, from north to south of metamorphic grades. The mainly brittle deformation is characterized by tight to overturned folds and imbricate faulting. The Lesser Himalaya is broadly subdivided into two zones (Ghazanfar, 1993).

The northern metamorphic zone includes the terrain between Luat and Nauseri in Neelum Valley, between Batal and Tutan in Kaghan Valley, between Banna sequence and Panjal fault in Northern Hazara, and the whole of Peshawar Basin including the terrain between Malakand and Attock-Cherat (Ghazanfar, 1993).

The southern sedimentary zone extends around Nauseri in Neelum Valley (Autochthonous Fold Belt), between Tutan and Paras in Kaghan Valley, between Abbottabad and Murree in Hazara area and the Cherat Kalachitta and Kohat Ranges (Attock Hazara Fold and Thrust Belt, AHFTB). This zone of Precambrian to Eocene rocks is broadly correlatable with the Tibetan Tethys sediments which occur between the Higher Himalaya Crystalline and the Indus Tsangpo Suture Zone (e.g. Burg et al. 1987; Ghazanfar, 1993; Kazmi and Jan, 1997; Anczkiewicz et al. 1995, 1998a, b).

Geologically, the area of Northern Hazara lies between the Panjal Fault in the south, MMT in the north and between the Panjal Fault/MBT in the east and the Indus River on the west. This is the area where the Tanol sequence and Mansehra Granite outcrop. It is tectonically characterized by E-W faults that bend northwards on the sides to merge into the N-S Panjal and Thakot Fault. The arcuate trends of the Tanol region of Northern Hazara have been noted and some faults marked since the work of Calkins et al. (1975). More recently Coward et al. (1988) and Treloar et al. (1989a, b) have interpreted the Northern Hazara as an imbricate thrust pile.

The sedimentary zone of Southern Hazara comprising of a thick foreland sedimentary sequence is exposed as a wide belt to the south of the metamorphosed hinterland. The wide belt may be subdivided into a northern Cambrian to Eocene sequence between the Panjal Fault and the MBT and further to the south a Miocene and younger foredeep molasses sequence between MBT and MFT. This shelf sequence is part of the Lesser Himalaya and will be discussed here.

The Lesser Himalaya shelf sequence covers the areas of Galiat, Margala Hills, Kalachitta, Attock-Cherat, Kohat and Parachinar in the form of a wide E-W trending belt which turns northeastwards to converge and close into the western limb of Hazara-Kashmir Syntaxis at Garhi Habibullah, in the east. This is the Attock Hazara Fold-and-Thrust Belt (AHFTB; Ghazanfar et al. 1987, 1990) of which the Hazara Basin constitutes a northeastern part. The Precambrian to Eocene rocks of this synclinorium have been folded into tight to overturned folds and imbricated by numerous high-angle thrusts and normal faults. This basin was studied along the Abbottabad-Murree road between Abbottabad and Kuza Gali. Detailed mapping at 1:9500 was carried out along 3 to 8 km wide sections between Abbottabad and Nathia Gali and in the Langrial area, the structure was unravelled and stratigraphic sections measured (Ghazanfar et al. 1987, 1990; Ghazanfar, 1993; Baloch et al. 2002).

The stratigraphy of the southern Hazara i.e., Galiat including the Margala Hills to the south has been

summarized by Wadia (1975) and Shah (1977). It was worked out by Waagen and Wynne (1872), Middlemiss (1896), Latif (1970a, b), Calkins et al. (1975), Ghazanfar et al. (1990) and Ghazanfar (1993). Ghazanfar (1993) carried out large-scale mapping including section measurement and worked out the structure and tectonics of the area. Ghazanfar et al. (1987) correlated the stratigraphy of southern Hazara with Muzaffarabad and Pir Panjal areas of Kashmir to the north.

HETTANGIAN TO MIDDLE EOCENE GEOLOGY

Rocks of the study area belong to Paleozoic to Eocene strata (Table 1) exposed in Attock Hazara Fold and Thrust Belt and Azad Kashmir that itself is a part of Northwest Lesser Himalaya (Fig. 1). Many workers (e.g. Waggen, 1872; Waagen and Wyne, 1872, Wadia, 1931; Gardezi and Ghazanfar, 1965; Fatmi, 1973; Latif, 1970a, b, 1980; Shah, 1977; Butt, 1986, 1987, 1988, 1989; Ghazanfar et al., 1986, 1987, 1990; Baig and Lawerence, 1987; Kadri, 1995; Chaudhry et al., 1998a; Baig, 1999; Ahsan et al., 2001d; Ahsan, 2008, etc) have discussed the geology of the area. Their work shows that internal, lateral and vertical thickness and facies variations are common in these sediments. A comprehensive description and comparison of lithostratigraphic units of Hazara, Khanpur Dam area, Fauji Cement Factory located near Brahama Bhater and Neelum Valley in Azad Kashmir is given below. The measured section representing Tertiary formations exposed in Neelum valley, Azad Kashmir (Lat 34° 23' 25"N; Long 73° 28' 25" E) have been presented whereas references for the lithostratigraphic units that belong to Hazara Basin have been cited in the text.

Datta Formation

During upper Hettangian, after a break (Cambrian to Early Jurassic) in deposition, the Hazara landmass again changed into a marine basin (Chaudhry et. al., 1998a; Chaudhry and Ahsan, 1999a; Ahsan, 2008) with the development of a transgressive shoreline marked by the deposition of the siliciclastic Datta Formation. It overlies either Upper Proterozoic Hazara Formation or the Cambrian Hazira Formation (Chaudhry et. al., 1996a; Manzoor et al., 1996) or Sanghar Gali Formation of Ghazanfar (1993). In the northern part of the Hazara Basin the Datta Formation rests directly on the Cambrian sequence of the Hazira Formation but southwards the Datta Formation rests successively on older Formations until south-east of Thandiani it onlaps directly on the Precambrian Hazara Formation. In the Salt Range the Datta Formation (e.g. Shah, 1977) is of much thickness (about 150m thick) and of continental origin containing plant remains and carbonaceous matter and giving a variegated color. In the Hazara area, today 100 km, to the north of the Salt Range the thickness of the Datta Formation is greatly reduced (2.6m near Thai) and it changes to a marine facies. It is not exposed in Khanpur Dam section.

In the southeast Hazara the best-developed outcrop (18.40m thick) of the formation is exposed at Jaster Gali (Chauhan et. al. 1992) on the Abbottabad Nathiagali Road. It generally represents all the lithological variations in the Datta Formation in Hazara Basin. According to Chaudhry and Ahsan (1999a), at Thai further north the Datta Formation is poorly developed and only 2.6m thick. Thus from south in the Salt Range to north at Thai, the Datta Formation progressively thins.

The Datta Formation in the south-east Hazara is composed (Chaudhry and Ahsan, 1999) of gritty sublithic arenites, gritty arenites, arenaceous limestones, bioclastic wackestone, oolitic and pelletoidal wackestones – packstones with occasional dolomitic, marly and shaly horizons. The sandstones are cross-bedded at places. Microconglomerate occurs in the basal portion and contains slate clasts derived from the underlying Hazara Formation. Laterite bands and coaly layers occur at places. Fireclay is also intercalated at places.

Chaudhry and Ahsan (1999a) grouped the above mentioned microfacies of Datta Formation under four standardized lithofacies that include carbonate facies, argillaceous facies, arenaceous facies and ferruginous hardground facies. In all, this predominantly clastic shoreface lithostratigraphic unit is intercalated with the lagoonal shale beds, carbonate shoals, lagoonal pelletoidal limestone horizons, glauconitic subtidal sandstone, minor shallow tidal channels and barriers which indicate cyclic deposition. The study of heavy mineral suits, their quantities, and shapes suggest a recycled origin of the clastic part of the Datta Formation from metamorphic sialic part of the Indian continental Plate (Chaudhry et al. 1998a). The average lithified rates of sedimentation were 2mm/1000 years. The very low rates of sedimentation are due mainly to frequent breaks in sedimentation.

Contrary to the description of Shah (1977) the Shinawari Formation can hardly be identified as a distinct lithostratigraphic unit in Hazara. In Bagnotar section, Shah (1977) reports 25 m thick Shinawari Formation, whereas study by Chaudhry and Ahsan (1999a) does not support this observation. Moreover, the formation does not outcrop in Khanpur and Fauji Cement Factory area.

Samana Suk Formation

The Samana Suk Formation (Shah, 1977) generally represents an epicontinental intertidal environment. The formation is generally medium grey on fresh surface. However, fine-grained horizons give darker shades of medium grey. At places, the limestone shows a brownish tinge on weathered surface. It is well bedded and the

Table 1
Stratigraphic Table of Hazara Basin, Margala Pass, Fauji Cement Factory and Nelum Valley

Age	Hazara Basin		Margala Pass	Fauji Cement Factory, Brahama Bhater	Neelum Valley Azad Kashmir
	Galiat	Khanpur Dam Area			
Middle Eocene to Miocene	Not Exposed	Not Exposed	Not Exposed (?)		Murree Formation
Early to Middle Eocene	Kuldana Formation	Kuldana Formation			Kuldana Formation
Early Eocene	Chor Gali Formation	Chor Gali Formation			Chor Gali Formation
Early Eocene	Margala Hill Formation	Margala Hill Formation	Margala Hill Formation	Margala Hill Formation	Margala Hill Formation
Late Paleocene	Patala Formation	Patala Formation	Patala Formation	Patala Formation	Patala Formation
Middle Paleocene	Lockhart Formation	Lockhart Formation	Lockhart Formation	Lockhart Formation	Lockhart Formation
Early Paleocene	Hangu Formation	Hangu Formation	Hangu Formation	Hangu Formation	Hangu Formation
	UNCONFORMITY				
Late Cretaceous	Kawagarh (Jabri) Formation	Kawagarh (Jabri) Formation	Lumshiwal Formation	Lumshiwal Formation	UNCONFORMITY
Early Cretaceous to Middle Cretaceous	Lumshiwal Formation	Lumshiwal Formation			
Late Jurassic to Early Cretaceous	Chichali Formation		Chichali Formation	Chichali Formation	
Middle Jurassic	Samana Suk Formation	Samana Suk Formation	Samana Suk Formation	Samana Suk Formation	
Early Jurassic	Datta Formation	Datta Formation	Datta Formation	Not Exposed (?)	
	UNCONFORMITY				

individual beds being generally 40 cm to 60 cm in thickness. Some parts show thick intercalations of thinly bedded marl or shale between massive beds. The bedding planes of some massive beds in south at Kundla are particularly irregular with pits and protuberances. The limestone is medium grained but fine-grained horizons towards top break with conchoidal fracture. The occasional fine-grained texture and lighter grey weathering may be confused with Kawagarh limestone. Yellow dolomitic patches, streaks, and bands are present especially towards the lower and middle parts. Oolites, pellets and intraclasts are common alongwith or without bioclasts. They are generally difficult to recognize in the Ayubia area. Oolites are well developed near the base and top.

At places, medium grained quartz bearing beds are exposed. A 30 cm thick bed composed of flat pebble conglomerate occurs near Thai. The pebbles are generally 4 cm to 5 cm long. The matrix contains sub-rounded to subangular detritial quartz grains. Gastropods and pelecypods oyster-bearing beds occur frequently. Horizontal, inclined, vertical and U-shaped burrows are common. Burrow infill has been dolomitized and shows positive relief. Other sedimentary structures such as ripple marks and cross bedding are common. Laterite encrustations are dark brown to blackish brown and occur at most places. Scours are now filled with dolomite and are augen shaped. Towards the top, near Neil Gadri, Khanpur Dam area, Margala Pass section and Fauji cement factory belemnites are pricked in the beds. Flat pebble conglomerate beds occur in Thai and Khanpur Dam areas. Some carbonaceous layers also occur at places. The formation is highly folded. Its estimated thickness is about 160m near Biran Gali.

As described earlier the formation contains oolites, pellets, intraclasts and bioclasts. These allochems occur in many combinations in the formation. Thus, this limestone, of all the limestones exposed in the Hazara Basin, contains maximum number of microfacies (Chaudhry et al. 1998a). Besides this, angular to subrounded detrital quartz occurs in association with pellets, ooides and intraclasts in some cases in the in the Samana Suk Formation. The oyster topped beds and hard grounds represent slow rates of deposition and subareal exposures (Latif, 1970a). The average lithified rates of sedimentation according to Chaudhry et al., (1998a) were about 6mm/1000 years. The low rates of sedimentation may be due to frequent breaks in deposition. On the basis of fauna it ranges in age from Toarcian to Collovian. The lower contact of the Samana Suk Formation with Datta Formation is sharp but normal. The upper contact with Chichali Formation shows minor disconformity and lateritization. One such horizon is exposed around Thandiani.

In the Kashmir Basin the Samana Suk Formation is absent.

Chichali Formation

It is separated by Callovian disconformity (Shah, 1977) in the Hazara Basin from the underlying Samana Suk Formation. The unit is exposed at a number of places in the studied area as thin bands. However, near Kundla the exposure is fairly wide. The formation is composed of blackish grey to grey splintery shale. It weathers to brownish black to rusty grey shades. However, khaki colored shale belonging to this formation is exposed near Harno. Ferruginous concretions, silver yellow pyrite nodules with rusty brown to rusty black weathering are also present. At places, shale contains rounded or elliptical variegated clayey nodules with concentric layers. At places, subordinate beds of sandstone are present. Petrographically, sandstone is composed of arenites that are cemented with quartz, calcite, clay or glauconite. Quartz is fine to coarse grained. Glauconitic horizons are also present at places. Parts of Chichali Formation are fossiliferous (Iqbal and Shah, 1980) and in Hazara Basin it hardly contains fossils. However, near Margalla Pass and Brahama Bhater it contains belemnites. Because of its incompetent nature, the shale is commonly squeezed and forms topographic depressions. Its thickness may vary from 33 m to 64 m (Shah, 1977; Iqbal and Shah, 1980).

The formation was deposited in a restricted anoxic environment during Oxfordian to Kimmeridgian time (Shah, 1977). The lithified sedimentation rates are 2.3mm/1000 year (Chaudhry et al., 1998a).

The Chichali Formation has not developed in the Kashmir Basin and Khanpur Dam area. In Khanpur Dam area, Lumshiwal Formation rests unconformably over Samana Suk Formation.

Lumshiwal Formation

Being absent in the Kashmir basin, the Lumshiwal Formation comprises four principal lithologies that include sandstone/quartzite, marl/shale, arenaceous limestones and arenaceous dolomite in the Hazara basin. Some impure glauconitic sandstone, brownish grey on fresh surface and yellowish brown on weathered surface alongwith some shales occur also. Towards the base, where the formation has gradational contact with the underlying formation (at Borian and Kundla) belemnite, ammonite and brachiopod rich horizons occur at places. The shaly/marly horizons are rusty brown to maroon purplish and black in colour. At places, intraformational breccias and conglomerate with angular monocrystalline and polycrystalline quartz clasts occour that range in size from a few millimeters to 20 cm or even more in size. One such horizon is exposed in Toot Gran village on Abbottabad Nathia Gali Road. The conglomeratic zone is followed towards the top by siltstones and shales. The siltstones and shales are dark grey

on fresh surface and yellowish brown on weathered surface. The shales are splintery while the siltstones occur as relatively massive beds, some of which are lenticular and grade into shale.

In the Kahnpur Dam area, the formation is about 1m thick and is composed of coarse grained ferruginous quartz arenites. It contains paleo-channels at the base and elsewhere elongated clasts of Samana Suk Formation are embedded in coarse grained sandy matrix. Here, this unit appears to show time transgression. In Margalla Pass area the formation contains a number of hard grounds marked by intact and abraded pelecypod shell lags that occur at the top of every bed. The formation here is composed of medium to coarse grained quartz arenites cemented with silica and iron oxides. The beds vary in thickness from 30cm to more than 1m. Minor shaly horizons also occur at places.

Chaudhry et al. (1998b) and Ali et al. (2000) described twelve lithofacies from Kundla that include lower grey sandstone facies, fossiliferous limestone facies, phosphatic glauconitic sandstone facies, sandy shale/carbonaceous sandstone facies, lower grey sandstone facies, silty sandstone facies, green sandstone facies, light grey sandstone facies, carbonaceous sandstone facies, hard-ground facies, upper grey sandstone facies and grey arenaceous carbonate facies. Ahsan et al., (1999a) described fourteen microfacies from Jhameri Village section. They grouped these microfacies into three facies on the basis of grain size. According to Chaudhry et al. (2000), the Lumshiwal Formation is composed mainly of quartz arenites at Karlan Bazar. Fine-grained quartz arenites are represented by 57% of samples. Fine to medium grained quartz arenites were minor and represented by 14% of the samples. Remaining samples were medium grained.

Ahsan and Chaudhry (1999) presented a comprehensive study of the Lumshiwal Formation of Hazara Basin. According to them the formation is composed of glauconitic arenite, quartz wackes, arenaceous limestone, arenaceous dolomites and oolitic limestones. Shales/marls are minor. Diastems at places are marked by submarine hard-grounds. These horizons are cemented with iron oxides and may occasionally contain collophanite or dahalite. Heavy mineral suit indicates derivation from a low relief area on the Indian Shield to the south.

Strongly reducing conditions changed to mildly reducing environment with better circulation in the Thithonian to deposit the Lumshiwal Formation (Ahsan et al. 2001c). The ubiquitous glauconite indicats slow rates of deposition. The average lithified rates of deposition were about 0.96mm/1000 years (Chaudhry et al. 1998a). Frequent breaks in deposition are responsible for low rates of sedimentation. The age of the formation is Thithonian to Lower Turonian. In Khanpur Dam area it can be recognized as a time trangressive unit.

Kawagarh (Jabri) Formation

One of the tectonically significant formations of the Hazara Basin, the Kawagarh Formation, shows two distinct facies (Ahsan and Chaudhry, 1998) north and south of the Nathiagali Fault. The northern facies are exposed near Giah (Chaudhry et al., 1992a), Borian (Ahsan et al., 1993a) and Kala Pani (Ahsan et al., 2001a) whereas the southern facies outcrop at Changla Gali (Ahsan et al., 1994) Jabri (Ahsan et al., 1993b) and Khanpur Dam area. In Kashmir basin and Margala Pass (Ahsan et al. 2000) section and Fauji Cement factory setion at Brahama Bhater the formation has not developed.

The Kawagarh Formation in the sections north of the Nathiagali Fault is mainly thick bedded, fine gained and medium to dark grey limestone. The basal part is relatively coarse grained on fresh surface. It is whitish grey or yellowish grey on weathered surface. The middle part is medium to thick bedded, medium to dark grey and breaks generally with conchoidal fracture. The basal portion at Kala Pani is nodular. The upper part of the Kawagarh Formation at Giah is generally coarse grained and somewhat arenaceous. A few yellow dolomitic bands are also present within Kawagarh Formation. In the Khanpur Dam area the formation contains centimeter sized solution holes that indicate the effects of subareal weathering at Cretaceous Paleocene boundary. In this area the top portion of the formation is dolomitized and shows sugary texture with distinctive brownish to blackish weathering coloures whereas base is marly.

South of the Nathia Gali Thrust the upper part of Kawagarh Formation is marly and intercalations of marl are also present. This part is especially well developed on the Dunga Gali pipeline road and at Changla Gali. The marly part is dark grey to yellowish grey on fresh surface and relatively more yellowish on the weathered surface. The marly part has a dark grey colour on the fresh surface. Near Kundla the base of the Kawagarh Formation has a slightly irregular surface with some pebbles and few inches to about one foot long worm tracks.

In the Khanpur area the formation contain cleaved marls at the base. The topmost beds of the formation that underlie the Cretaceous Tertiary unconformity contain iron stained solution holes. These holes are 5 to 6cm in radius and penetrate downwards in the underlying beds. The Kawagarh limestones contain millimeter sized burrows that can easily be recognized on the outcrop. It contains dolomite beds at the base and at places top beds are also dolomitized.

Plankton foraminifera, shelly fauna and calcispheres are the major skeletal components of the Kawagarh Formation. Filaments, echinoids, ostracods, bryozoans and textularia constitute the shelly fauna that occur as skeletal debris. Three genera, *Pithonella sphaerica, Pithonella ovalies and Pithonella perlonga*, of calcispheres are recognized (Ahsan, 2008).

The study of the Kawagarh Formation in the Hazara Basin shows that it is generally composed of seven microfacies (Ahsan, 2008) that include Planktonic foraminiferal-calcispheres wackestone (and Packstone), Planktonic foraminiferal-shelly faunal wackestone (and packstone), Shelly faunal mudstone and wackestone (and packstone), Calcispheres-planktonic foraminiferal wackestone (and packstone), Dolostone, Planktonic foraminiferal wackestone (mudstone and packstone) and Marl.

The Kawagarh Formation, according to Ahsan (2008) needs a new nomenclature as existing type locality and division into two members (Shah, 1977) is indistinct. By itself, the designated type section is structurally disturbed and the two members indicated by Shah (1977) could not be recognized in Hazara Basin. Two lithologies, carbonates and marls occur in parts of the study area. The Jabri section (73° 10' 1.5" E; 33° 5' N, 43G/1) with good lithological contacts may be preferred as type section in Hazara Basin with a new nomenclature as Jabri Formation (Paper in preparation by Ahsan and Chaudhry) instead of Kawagarh Formation. Moreover all the 7 established microfacies outcrop at Jabri.

The petrographic analyses indicate that the Kawagarh Formation carbonates have undergone a complex diagenetic history encompassing compaction, minor cementation and dolomitization (Ahsan, 2008). Depletion in $\delta^{18}O$and $\delta^{13}C$ as well as Sr and Na and elevated Fe and Mn content confer a meteoric diagenetic environment with minor contribution from an outside source (Ahsan, 2008). Ambient sea surface temperature of about 27°C to 33°C is estimated for warm tropical waters in which Kawahgarh Formation was deposited. Trace elemental variations and stable isotopes compositions are interpreted to reflect meteoric and burial diagenetic processes for the precipitation of dolomite at 38°C to 54°C temperature (Ahsan, 2008).

According to Ahsan (2008) the base of the Kawagarh (Jabri) Formation is marked by the occurrence of *Globotruncana helvetica* followed by *Globotruncana sigali* at Turonian, at Giah, Borian and Kala Pani sections. Lower Coniacian is recognised by the presence of *Globotruncana sigali* in Jabri and Changla Gali sections. Last zone of the Kawagarh (Jabri) Formation is *Globotruncana gansseri* in the Lower Maastrichtian. On the basis of paleoecological information rendered by planktons, shelly fauna (especially filaments) and calcispheres the formation was deposited on a homoclinal ramp, (middle to outer ramp settings) at about 23°S (Ahsan, 2008). The average lithified rates of sedimentation were about 9mm/1000 years that compares favorably with the American and European chalks (Chaudhry et al. 1998a).

Hangu Formation

Laterite and fireclay are predominant lithologies of the Hangu Formation. However, subordinate carbonaceous shales and sandstones are also present at places. The laterite is reddish brown to reddish black or reddish grey or even grayish on fresh surface and reddish brown, dark grey and rusty brown on weathered surface. The fire clay is pale white and earthy grey on fresh surface and yellowish brown to rusty brown on weathered surface. Horizons of ball clay are present near Khaira Gali. Well-developed pisolites also occur in laterites. Carbonaceous shales are dark grey to black. Quartzites are dominantly white but variegated coloured quartzite may occur also.

In the Kashmir area the basal microfacies, black shale, marks the on set of a transgression that deposited 227 cm thick black shale. The formation consists of coarse to fine grained clay/iron oxides cemented quartz arenites at the base which grades to silty coal to the top. The top of the Hangu Formation contains bauxitic clays that vary in color from off-white to black and weathers to rusty grey to orange.

In Khanpur Dam area, the Hangu Formation is maroonish to red coloured laterites and khaki to grey coloured shales. Poorly developed pisolites can be recognized associated with laterites. At places, it contains about 35cm thick coarse grained sandstone beds. The laterites are mined for use in nearby cement factories.

The upper and lower contacts of the formation are unconformable. It does not contain fossils however some plants remains are present. The Lockhart Formation unconformably overlies the Hangu Formation. The lithified rates of sedimentation were 1.77mm/1000years (Chaudhry et al., 1998a).

Lockhart Formation

The formation is light grey, pale grey, bluish grey and blackish grey on fresh surface while the weathering colours are generally dirty grey with dark patches but pale grey and rusty grey patches are also seen. On the outcrop it is fine to medium grained and gives foeted smell on freshly broken surface. The limestone has a fair amount of marly intercalations. These marly intercalations are generally upto 8 cm thick and weather pale grey. Southeast of the Nathiagali Fault, in the section between Kuza Gali and Changla Gali, the limestone is found frequently intercalated with marls. Shales have not developed.

In the areas northwest of the Nathiagali Fault, the limestone is dark grey and weathers to bluish grey. At the base the limestone is massive (upto 2m thick), coarse grained and does not contain marly intercalations. The middle part is medium bedded and marly horizons are absent. However, towards the top the formation is highly nodular and contains marls around the nodules. Limestones are composed of foraminiferal mudstones, wackestones and packstones. The lithified rates of sedimentation were 30mm/1000years (Chaudhry et al., 1998a). Ahsan et al. (2000a) have described one such outcrop near Ghumawan.

Lockhart Formation, according to Ahsan et al., (2001e), near Chahla Bandi, in Neelum Valley Azad Kashmir, is light grey, pale grey to khaki grey, bluish grey and blackish grey on weathered surface and dark grey on fresh surface. It is about 72.80 m thick nodular limestone with intercalations of marl/shale. Nodules vary in size and are poorly developed. These nodules are smaller than that of Margala Hill Limestone. At places the intercalations of grey colored carbonaceous material occur within the limestone. Lithologically, the formation can be divided into two parts: i) Nodular limestone that contains marl and shale intercalations. The nodules vary in size. The calcite veins occur in the marl between the poorly developed nodules; and ii) Massive to thick-bedded limestone having no intercalations of shale or marl. In this part the nodules are not clearly visible. At the contact with the Hangu Formation the formation is splintery and contains orange patches, and upward it grades into thin-bedded limestone.

Patala Formation

In the Hazara and Kashmir Basins the conditions changed from carbonate shelf to siliciclastic depositional environment that deposited Patala Formation. The formation is composed of shale and occasional limestone bands with abundant larger benthic foraminifera of upper Paleocene to lower Eocene age. The shales are khaki, yellowish brown to yellowish grey on weathered surface and on the fresh surface they are khaki to grey. At other places, the shales are greenish brown or greenish grey on fresh surface and brown to dark brown on the weathered surface. They have been called khaki shales after their colour (Latif, 1970). Pyrite nodules 1 to 2 cm across are present at some horisons. The shales are splintery and some marly bands near the contact with the Lockhart limestone are present. Some times splinters take on the shape of small brittle flakes. Within the body of the shales subordinate lithologies, both arenaceous and calcareous, occur in the form of thin bands. In the Khanpur area it contains various hard grounds. The lithified rates of sedimentation were 30mm/1000years (Chaudhry et al., 1998a).

Margala Hill Limestone

During Ypresian the siliciclastic basin developed into a carbonate platform and deposition of the Margala Hill Formation took place. The formation (Shah, 1977) is mainly a fossiliferous, medium grained to fine grained nodular limestone with marly horizons. It is bluish grey and yellowish grey on the weathered surface and on the fresh surface is generally dark to blackish grey. The lower part may contain frequent marly horizons. The nodularity of Margala Hill Limestone is more prominent as compared to the Lockhart limestone. Generally the limestone is medium grained but fine-grained horizons occur which may break with sub-conchoidal fracture. Some pyritic nodules are observed which contain weathered limonitic powder. Sometimes they show hollow cavities. Ahsan et al. (1998a, 200b) described the Margala Hill Limestone from Khaira Gali that contains twelve lithofacies units, separated by eleven marly horizons. These lithofacies contain 45% foraminiferal wackestone facies, foraminiferal mudstone and foraminiferal packstone facies (19% each) and 17% marly facies. The entire formation is free of oolites and pellets. Sedimentary structures like ripple marks and cross bedding are absent. Basal beds are bioturbated. The lithified rates of seimentation were 62.5mm/1000years (Chaudhry et al., 1998a).

The Margala Hill Limestone at Chahla Bandi, Azad Kashmir (Chaudhry et al., 2001) is composed of light grey to dark grey limestone. The formation at the base is thinly bedded. It is overlain by calcirudite that contains abundant pelecypode shells. Some shells are reworked. Highly fissile dark grey shale overlies the shelly beds and contains marcasite nodules. The shale is followed by highly nodular limestone. The nodules are upto 30 cm x 50 cm x 13 cm and contain very thin shale partings. This zone is 29m thick. It is very dark grey in color and gives very strong fetid smell. An argillaceous marly limestone that is 28 meters thick overlies the dark grey limestone. It is overlain by medium bedded to highly nodular limestone towards the top of the formation. This zone is grey and weatheres to light grey. On the basis of petrographic and field observations the formation is divided into six facies.

Chorgali Formation

The Margala Hill formation passes upwards with a gradual change of facies into the Chorgali Formation. The formation outcrops near Khaira Gali and Rati Gali, south of the Nathiagali Fault in the Hazara Basin. The formation comprises of limestone, marls and shales. The shale is khaki to off-whitish grey. The limestones are light grey on fresh surface, weather to pale grey and are nodular. The size of the nodules is smaller than that of Lockhart limestone or Margala Hill formations. They generally contain marl around the nodules. The nodule size is generally 2 cm x 4 cm at places. The limestone is rarely massive and generally shows a flaggy habit. The beds are usually less than 8 cm in thickness. The flaggy habit is due to the increasing marly

intercalations. At places, the limestones are fine grained and break with conchoidal fracture. Occasionally, these limestones weather to a chalky appearance. The marls are generally cream to off-white in color and sometimes give light shades of grey. The argillaceous content increases upwards, which may range from argillaceous limestone to calcareous mudstone.

The Chorgali Formation in Neelum valley, Azad Jammu and Kashmir (Ahsan et al., 1998b) is 60.75m thick. It is mainly composed of medium grey shale and silty shale, light grey to dark grey foraminiferal mudstone to packstone, dolomitic limestone and dolomite. No grainstone was observed. The limestone is thin to thick bedded and contains occasional nodules.

According to Ahsan et al. (1998b) this formation can be divided into 3 facies. The lower unit is composed of intercalated limestone and shale. This unit is 31.04 m thick. The shale of this unit is medium grey to grey splintery and fissile. The limestone is thin to thick bedded and nodular. Nodules are poorly to well develop. The middle unit is composed entirely of thin to very thin-bedded limestone. Limestone is grey poorly nodular and the nodules are generally small and elongated. The upper unit is composed of intercalated dolomite, calcareous shale and shale. The dolomite horizons are fine grained and greenish in color. The shale and calcareous shale are light grey to greenish grey and splintery. This unit is 19.51 m thick. The lithified rates of sedimentation were 83.3mm/1000years (Chaudhry.et.al., 1998a).

Kuldana Formation

The formation (Shah, 1977) is exposed in the southeast of Hazara Basin from Kalabagh Cantonment to Islamabad. The formation consists of crimson, brown, purple, chocolate, green, grey and khaki shales interbedded at places with khaki to pale grey marl and marly limestone bands and lenses. The clays are gypsiferous near Bansara Gali and Kalabagh (Latif, 1976). The formation is generally calcareous at the base and arenaceous towards the top.

Chaudhry et al. (1998a) measured the Kuldana Formation at Ratri Gali on Murree Ayubia Road and reported 17 lithofacies. According to them it is composed of splintery marl, calcareous shale, sandstone, sandy shale, sandy marl, clayey sandstone, oolitic grainstone, pisolitic limestone, bioclastic wackestone to grainstone and intraclasts bearing wackestone. Some lithic arenites contain clasts of limestone and abundant haematitic specks. Clayey siltstones contain stylolites.

In the Khanpur area the formation is composed of maroonish red to greenish grey shales. Here, the formation contains grey to white gypsum bands that are being mined for use in cement industry. At places, the formation contains maroonish red to greenish beds of coarse grained sandstone that are about 30cm to 90cm in thicknesss. At Jab, these beds contain mm to cm sized angular limestone clasts. Generally, in the Khanpur area, the Kuldana Formation outcrops along the Nathia Gali Thrust (in contact with the Pre-Cambrian Hazara Formation).

The Kuldana Formation in Neelum Valley is composed of greenish to maroonish coloured shales with occasional limestone and calcirudite facies.

According to Chaudhry et al. (1998a) the upper contact of Kuldana Formation with Murree Formation is transitional and they place the contact between the Kuldana Formation and the Murree Formation at the base of a sandstone bed, which has a Himalayan (northern) rather than Indian Shield (southern) provenance in the Murree area. As a whole the contact is either transitional or slightly disconformable but the break, if present, is likely to be minor. The formation contains macrofossil and microfossils. Latif (1976) on the basis of fossils assigned middle Eocene age to the formation. The lithified rates of sedimentation were 71.1mm/1000years (Chaudhry et al., 1998a).

Murree Formation

The Murree Formation consists (Chaudhry et al., 1998c) of a monotonous sequence of dark red, purple and maroon coloured shales and purple grey and greenish grey sandstone with subordinate intraformational conglomerate. The shales are characterized by a splintery nature, presence of fracture cleavage and tension gashes. The sandstones are maroon and show green tinge.

Sandstones, though very abundant, are never-the-less subordinate to shales. Sandstones are cross-bedded or have episilon cross bedding. The predominant type are lithic arenites, and wackes are rare and when they do occur it is not certain whether the matrix is primary or diagenetic in origin. The sandstones are predominantly medium to fine grained, coarse grained and gritty sandstones are minor. The grains in general are sub-angular to sub-rounded. Distinctly angular and rounded grains are minor. The stable minerals/rock fragments are subangular to subrounded and include quartz and chert. Feldspar is generally less than 5%. The unstable rock fragments are represented by limestone, argillite/meta-argillite that includes slate, phyllite and shale.

Shales and claystones are the most common lithologies of the Murree Formation. These rocks are massive to moderately well laminated. They represent over bank or abandoned channel fill deposits. In some cases they represent the complete soil profile. These rocks are composed predominantly of clay minerals with subordinate silt sized and fine sand sized quartz and some carbonates. The clay is composed predominantly of illite. However,

some kaolinitic and mixed layered clay with smectitic components are also present. Other ordered phyllosilicates like muscovite, biotite and chlorite generally occur as accessories. Silt to fine sand sized quartz grains constitute essential components of these rocks. Chaudhry et al., (1998c) have measured section from base of the Murree Formation from Murree area and Neelum valley.

Conglomerates/breccias occur repeatedly along the paleo-channels. The fragments are generally subangular. The conglomerates may be either clast supported or matrix supported. They have a limited number of lithologies represented in them. The matrix is often grit or coarse gritty sand. The fragments include argillites, sandstone, carbonate fragments, re-worked calcareous concretions, calcareous fossils mainly larger foraminifera. The fragments are mainly of granule or pebble size. Quartzite and volcanic rock fragments are rare.

According to Shah (1977) the basal strata of the formation consists of sandstone and conglomerate and it has been designated as Fatehjang Member after "Fatehjang Zone". *Fatehjang Member* present in other areas at the base of Murree Formation is absent in Galiat Area.

Chaudhry et al. (1998a) reported a couple of limestone and shale horizons at the base of the Murree Formation near Ratri Gali. These horizons are fossiliferous and contain foraminifera (e.g. *Nummulites striatus).* On this basis and palynoflora recovered they assigned an upper Eocene to Oligocene age to Murree Formation.

It is doubtful that Swaliks were deposited in the Hazara Basin.

TECTONO-SEDIMENTARY EVOLUTION OF HAZARA AND KASHMIR BASINS

In the following a brief account of evolution of Hazara Basin and Kashmir Basin is presented to explain the relationship between tectonic activity and sedimentation.

Paleozoic

The Tethys (e.g. Angiolini et al. 2003) stretched from the Pacific to the Mediterranean encompassing India and the northern borders of Arabia and Africa and formed through the process of rifting and successive fragmentation of Gondwanaland (Kazmi and Jan, 1997). The process started in Middle to late Paleozoic while the assembly of Pangaea was still in progress (Sengor et al., 1988; Tikku, 2002). In middle Carboniferous, the ocean between Laurasia and Gondwanaland has been universally known as Paleo-Tethys. From early Permian to late Triassic the northern passive continental margin of Gondwana was covered by a thick pile of sediments, most of which comprised thick carbonate platform deposits (Shah, 1977; Spencer, 1993). In late Permian, rifting along northern margins of the Gondwanaland formed a Cimmerian microcontinent (Sengor et al., 1988) and several back arc basins of Paleo-Tethys had evolved followed by the opening of Neo-Tethys (Patriat and Achache, 1984; Scotese et al. 1988; Van der Voo et al. 1999). By the late Triassic, most of the Cimmeride blocks had collided with Laurasia and the Paleo-Tethys closed by the early Jurassic times. During this complex interplay of opening and closing of oceans Paleozoic sequence in Hazara and Kashmir was deposited followed by a period of uplift and metamorphism during Pan African Orogeny (Baig and Lawerence, 1987).

Mesozoic

Throughout much of the Mesozoic, the Hazara Basin (Chaudhry et al. 1998a) was an important depocenter at the Northern margin of the Neo-Tethys resulting in the deposition of Mesozoic pile of sediments upto 1000m thick (Latif, 1970a; Shah, 1977). However Kashmir was a positive area throughout the Mesozoic. With the development of a transgressive shoreline of Neo-Tethys during upper Hettangian, the Datta Formation was deposited (Chaudhry and Ahsan, 1999a) that overlies either upper Proterozoic Hazara Formation or Cambrian Hazira Formation (Table 1). The Datta Formation represents open marine, lower to upper shore face, lagoonal to subareal regimes of deposition (Chaudhry et al., 1995, 1996a, 1997, 1998a;). The sediments were derived from metamorphic sialic Indian Plate to the south.

The Neo-Tethys shoreline changed to a shallow carbonate platform containing oolitic - pelletoidal shoals in Toarcian all over the Indus Basin (Shah, 1977) and Hazara (Chaudhry et al., 1998a) and to deposit several hundred metres thick carbonates of Samana Suk Formation from Toarcian to Callovian (Shah, 1977; Jadoul et al. 1989; Kemal et al., 1992). Many workers (e.g. Bernoulli and Jenkyns, 1974; Bosellini, 1989) have reported such platforms along the other Neo-Thethyan margins. The Hazara carbonate platform was stable until Bathonian (Shah, 1977, Chaudhry et al., 1998a; Ahsan, 2008) after which it remained exposed till Callovian with the separation of the Indo-Pakistan continent from Gondwanaland and then started to collapse (Garzanti, 1993). This separation started with the late Mid-Jurassic (Callovian) opening of the Somali and Mozambique basins (Scotese et al., 1988).

After the deposition of Samana Suk Formation a restricted anoxic environment (Chaudhry et al. 1998a) prevailed and a condensed, pyrite rich and belemnite bearing black shale siltstone sequence represented by Chichali Formation was deposited on mid-outer shelf. Similar conditions may have prevailed at the time of deposition of the Chichali Formation as in the Black Sea (Demaison and Moore, 1980). The base of the time equivalent Spiti Shale in the Zanskar is late middle Jurassic

(Gaetani, et. al. 1986), while that of Chichali Formation in the upper Indus Basin is early late Jurassic, whereas in lower Indus Basin it is late upper Jurassic to basal Early Cretaceous (Shah, 1977; Dolan, 1990). Therefore the middle Jurassic carbonate platform lasted longer in the southern Pakistan. Latif et al. (1995) have correlated this event with the break up of Indo-Pakistan from Gondwanaland. The Chichali Formation pinches out towards the Kashmir Basin that was a positive area.

According to Katz (1979) and Norton and Sclater (1979) by the basal early Cretaceous, the subcontinent had separated from Madagascar and the West Coast Fault was formed and probably the Sargodha horst also started to rise (Latif et al., 1995). In early Cretaceous the Indo-Pakistan passed over the Niney East-Kerguelen hotspot, the Rajmahal Traps of northeast India erupted (Mahoney et. al., 1983; Baksi et. al., 1987) while the Bela volcanism was active in the Axial Belt (Shah, 1977). In Valangnian, the seafloor spreading began in the Indian Ocean and the subduction of the Neo-Tethys oceanic crust started in Aptian to Albian towards end of Early Cretaceous (Garzanti, 1993). According to Latif et al., (1995), South Asia experienced a domal uplift in the early Cretaceous and due to craton erosion, sands were wide spread in all the Indo-Pakistan sedimentary basins from Berriasian to Aptian stages (Sastri et al., 1981; Garzanti, 1993). In Tithonian the Lumshiwal Formation composed mainly of glauconitic quartz arenite (Ahsan and Chaudhry 1999; Ahsan et al. 2001c; Chaudhry, et al. 1994a, Chaudhry, et al. 2000) with submarine hardgrounds was deposited. The formation contains pelecypods, brachiopods, ammonites and belemnites (Shah, 1977). They indicate improved circulation conditions compared to Chichali Formation for the deposition of the Lumshiwal Formation at a depth of less than 80m (Ahsan and Chaudhry; 1999). Slightly reducing conditions, at least below water – sediment interface, were indicated by the ubiquitous presence of organic matter, glauconite and pyrite. According to Ahsan and Chaudhry (1999) plagioclase, microcline, schrol, indicolite, zircon, epidote and sphene are the accessory minerals that indicate sialic basement with minor basic component as the ultimate source from a low relief area on the Indian shield to the south.

However, to the southwest of Hazara Basin the Lumshiwal Formation in the Surghar Range was deposited under terrestrial conditions (Danilchick and Shah, 1987). Warwick et al. (1995) considered the basal part of the Formation in the Surghar Range a shallow marine deposit in the lower part and deltaic in the upper part. However, Frederiksen (1992) suggested a brackish to marine environment of deposition for the upper part of the formation. Gradational contact of the Lumshiwal Formation with Hangu Formation led Danilchick and Shah (1987) to suggest a late Cretaceous age for the upper part of the formation.

In Cenomanian due to rapid northwards flight of India from near Madagascar, the Hazara Basin started to sink gradually to deposit Kawagarh Formation (Ahsan and Chaudhry, 1998). The formation is composed of pelagic limestones and marls. The Kawagarh Formation, of upper Cretaceous age, in the Hazara Basin (Ahsan and Chaudhry, 1998; Ahsan et al., 1993a, b, 1994, 2001a, c,) overlying the Lumshiwal Formation was deposited in a homoclinal ramp settings (Ahsan, 2008). This setting is further substantiated by the presence of effects of abrasion in the grains, sharp crested wave ripple cross-lamination and cross-lamination and waviness, tubular tempestites and alternations of micrite and skeletal grains laminae (Ahsan, 2008). Moreover, contrary to previous interpretations (e.g. Ahsan et al, 1998) these features indicate a water depth of not more than 100m for the deposition of Kawagarh Formation. In the Kashmir Basin Cambrian to Cretaceous strata is absent (Table 1).

The top of the Kawagarh Formation exposed sub-aerially when the Indian Plate established its first contact with the Kohistan Island Arc at about 67± 2 Ma. This reworked the Maastrichtian (top of Kawagarh Formation) sediments into pisolitic laterites, bauxites and fireclays now represented by Hangu Formation of Danian age (Ahsan et al., 2001a; Chaudhry, et al., 1994b, 1998a).

Tertiary

There is a large gap of about 505 million years after the deposition of Precambrian Abbottabad Formation in Azad Kashmir Area (Ahsan et al., 2001b, d). At the advent of early Paleocene the Kashmir and Hazara Basins changed into a transgressive shoreline with the deposition of sub-areal / laogonal / supratidal (marshy) / middle shoreface sediments represented by the Hangu Formation (Ahsan et al., 1999b, 2001b, d). The beds underlying the Danian Hangu Formation (Ahsan et al., 1999b) belong to Abbottabad Formation (Shah, 1977)/Sirban Formation (Ashraf et al., 1983) of Cambrian age. The Hangu Formation unconformably overlies the upper Cretaceous Kawagarh Formation in the Hazara Basin. Whereas in the areas around Rawalpindi, the Hangu Formation lies over Lumshiwal Formation (Ahsan et al., 2000a, Williams, 1994) or reduced Kawagarh Formation. The rocks belonging to middle Paleocene-Eocene strata are represented by Lockhart Formation, Patala Formation, Margala Hill Limestone and Chorgali Formation. These units were deposited in lagoonal to inner ramp settings in Hazara-Kashmir Basin (Chaudhry et al., 1998a, Ahsan et al., 2001d).

At about 45-50Ma (upper Eocene), the main collision between India and Kohistan Island Arc took place due to which during Lutetian the sea retreated. Continental conditions prevailed in the Salt Range while marginal marine and evaporitic environment occurred in the Hazara area under which Kuldana Formation was deposited followed immediately by the deposition of Murree Formation. On the basis of micropalaeontological and palynological studies the Murree Formation started deposition in the upper most Eocene (Chaudhry et al., 1998a). This age is contrary to the general thinking that Murree Formation was deposited in Miocene in the area. In addition to this the Murree Formation represents fluvial deposition by meandering river system.

Quantitative XRD analysis (Ahsan et al., 1998b) has been used in the determination of clay minerals of Chorgali Formation while tourmaline, zircon, hematite and pyrite were determined petrographically. The clay mineral assemblages in the Chorgali Formation consist of illite, chlorite and kaolinite. Illite (38%) is the chief clay mineral and its relative abundance through out is persistent. It is detrital in origin and is due to the abundant supply from the source area. Illite remains stable during burial (Abassi, 1994). The chlorite (24%) and kaolinite (29%) are subordinate to illite. However a minor contribution from the south cannot be ruled out. This conclusion is further substantiated by the findings of Chaudhry et al. (1998c) in the case of Kuldana Formation and molasse sediments of the Murree Formation (Chaudhry and Ashraf, 1978) of NW Himalayas that were derived from the north. Earlier, Calkins et al. (1975) have suggested that rising Himalayas went under intense chemical weathering and the Murree sediments of Hazara Kashmir Syntaxis were derived. Moreover, Latif (1970a), Fatmi (1973) and Tahirkheli (1982) consider these sediments of continental origin.

REFERENCES

Abbasi, I. A., 1994. Clay Minerals in the Himalayan Foreland Basin Sediments: Implications for Progressive Unroofing of an Orogenic Belt. In: *Geology in South Asia-I, Proceedings of the First South Asia Geological Congress Islamabad, Pakistan: February 23-27, 1992. Eds., Ahmed, R. and Sheikh, A.M.*, 280-284.

Ahsan, N., 2008. Facies Modeling, Depositional and Diagenetic Environments of Kawagarh Formation, Hazara Basin, Pakistan. *Unpublished Ph.D. thesis. Punjab University, Lahore, Pakistan.* 235P.

Ahsan, N. and Chaudhry, M.N., 1999. Sedimentology of Lumshiwal Formation, Attock Hazara Fold and Thrust Belt, NW Lesser Himalayas Pakistan. In: *Terra Nostra, 14th Himalaya-Karakoram-Tibet Workshop*, Germany. 4-5.

Ahsan, N., and Chaudhry, M.N., 1998, Facies and Microfacies analysis of Kawagarh Formation of Hazara Basin, Pakistan. 13th *Himalaya-Karakoram-Tibet Workshop*, Abstract Vol. **31**, Geol. Bull. University of Peshawar, 5-6.

Ahsan, N., Chaudhry, M.N., Sameeni, S.J. and Ghazanfar, M., 1993. Reconnaissance microfacies studies of Kawagarh Formation Jabri area, Hazara. *Pak. Jour. Geol.*, 1 No.**2**, 32-49.

Ahsan, N., Baloch, I.H., Chaudhry, M.N. and Majeed, Ch. M., 2000a. Strength evaluation of blends of Lawrencepur, Chenab and Ravi sands with Lockhart and Margalla Hill Limestones for use in concrete. In: *Economic Geology of Pakistan*, Pakistan Museum of Natural History, Islamabad, 194-213.

Ahsan, N., Iqbal, M. A. and Chaudhry, M.N., 1994. Deposition and Diagenesis of Kawagarh Formation, Changla Gali, Murree-Ayubia Road, Hazara, *Pakistan. Pak. J. Geol.*, V. 2 & 3 No.1, . 41-52.

Ahsan, N., Chaudhry, M N. and A.A. Khawaja, 2001c. Tithonian to Danian Sedimentation in Hazara Basin, Northern Pakistan. Abstract Vol. *Third Nepal Geological Congress,* Sept. 26-28, 2001

Ahsan, N., Chaudhry, M.N. and Masood, K.R., 2001d. Sedimentology and palynology of Paleocene – Eocene sediments of lower Neelum valley, Northwest Lesser Himalayas, Azad Jammu and Kashmir. Abstract Vol. *Third Nepal Geological Congress*, Sept. 26-28, 2001

Ahsan, N., Chaudhry, M., N., and Rehman, Z., 2000b. Lithofacies and Microfacies study of Margala Hill Limstone at Kharia gali Muree-Ayubia Road, Hazara, Pakistan. *Third South Asia Geological Congress, Lahore, Pakistan.* Sept. 23-26, 2000. 150.

Ahsan, N., Chaudhry, M.N., Ghazanfar, M. and Sameeni, S.J., 1993b. Microfacies analysis of Kawagarh Formation of Borian Area, Southern Hazara. *Geol. Bull. P.U.*, V. **28**, 30-40.

Ahsan, N., Chaudhry, M.N., Sameeni, S.J., and Ghazanfar, M.,1993a. Reconnaissance Microfacies Studies of Kawagarh Formation Jabri area, Hazara. *Pak. Jour. Geol.*, V.1 No.2, 32-49.

Ahsan, N., Chaudhry, M.N., Mahmood, T. and Masood, K.R., 2001b. Microfacies and Environment of Deposition of Hangu Formation at Chahla Bandi, Azad Kashmir, North West Himalayas. In: *4th Pakistan Geological Congress. Pakistan Museum of Natural History, Islamabad.*

Ahsan, N., Ahmed, N., Chaudhry, M. N. and Hameed, A., 1999a. Petrology and Environment of Deposition of Lumshiwal Formation, Jhamiri Village, Haripur-Jabrian Road, Hazara Basin, Pakistan. *Pak. Jour. Geol.* Vol. **10 & 11**, No. **1 & 2**, 9-19.

Ahsan, N., Ahmed, N., Nadeem, M. and Chaudhry, M. N., 1998b. Sedimentological Studies of Chorgali Formation at Chahla Bandi on the western limb of Hazara Kashmir Syntaxial region in Azad Jammu and Kashmir. *Pak. Jour. Geol.* Vol. **8 & 9**, No. **1 & 2**, . 18-28.

Ahsan, N., Ahmed, N., Chaudhry, M.N., Mahmood, T. and Masood, K.R., 1999b. Microfacies Analysis and Environment of Deposition of Hangu Formation at Chahla Bandi, Azad Kashmir, NW Lesser Himalayas. *Pak. Jour. Geol.* Vol. **10 & 11**, No. **1 & 2**, . 34-40.

Ahsan, N., Ahmed, N., Rehman, Z., Chaudhry, M. N., Ghazanfar, M. and Masood, K.R., 1998a. Lithofacies Studies of Margala Hill Limestone at Khaira Gali, Murree-Ayubia-Road, Hazara Basin, Pakistan. *Pak. Jour. Geol.* Vol. **8 & 9**, No. **1 & 2**, . 7-17.

Ahsan, N., Naveed, N., Khawaja, A.A. and Chaudhry, M.N., 2001a. A preliminary account of facies and determination of Ca, Mg, Sr, Mn, Fe and Na in Kawagarh Formation, Kala Pani, Abbottabad-Thandiani road, Hazara, Pakistan. In: *4th Pakistan Geological Congress. Pakistan Museum of Natural History, Islamabad.*

Ali, R., Ahsan, N., Chaudhry, M. N. and Masood, K. R., 2000. Lithofacies, Microfacies, diagensis, Environment of Deposition and Palynology of Lumshiwal Formation at Kundla, Hazara Basin, Pakistan. *Third South Asia Geological Congress, Lahore, Pakistan.* Sept. 23-26, 2000, . 155.

Anczkiewicz, R., Burg, J. P., Hussain, S. S., Dawood, H., Ghazanfar, M., Chaudhry, M. N., 1998b. Stratigraphy and structure of the Indus Suture in the Lower Swat, Pakistan, NW Himalaya. *Jour. Asian Earth Sciences*, **16; 2-3**, . 225-238.

Anczkiewicz, R., Oberli, F., Burg, J. P., Meier, M., Dawood, H. and Hussain, S. S., 1998a. Magmatism south of the Indus Suture, Lower Swat, Pakistan. *Geological Bulletin, University of Peshawar*, **31**, . 7-9.

Anderson, C.B., 1995. Provenance of Mudstones from two Ordovician foreland basins in the Aalachians. *In:* Stratigraphic Evolution of Foreland Basins. Eds., Dorobek, S.L., and Ross, G.M., Scholle, P.A. SEPM Special Publication No. **52**.

Angiolini, L., Balini, M., Garzanti, E., Nicora, A., and Tintori, A., 2003. Gondwanan deglaciation and opening of Neotethys: the Al Khlata and Saiwan formations of interior Oman. *Palaeogeography, Palaeoclimatology, Palaeoecology*, **196**, . 99-123.

Arbaret, L., Burg J-P., Zeilinger, G., Chaudhry N., Hussain S. and Dawood H. 2000. Pre-collisional anastomosing shear zones in the Kohistan arc, NW Pakistan. In: Tectonics of the Nanga Parbat Syntaxis and the Western Himalaya. M.A. Khan, P.J. Treloar, M.P. Searle & M.Q. Jan Editors. *Geological Society of London, Special Publication*, **170**, . 295-311.

Ashraf, M., Khan, M.S., Awan, M.A., Yasir, A., Warraich, M.Y., Khan, A. and Awan, M.S., 1991. Geology and petrology of Jijal and Pattan layered ultramafic-mafic complexes in the vicinity of Jijal, Duber and Pashto, NWFP, Pakistan. *Kashmir J. Geol.*, **8 & 9**, .193-195.

Ashraf, M., M.N. Chaudhry, and K.A. Qureshi, 1983. Stratigraphy of Kotli Area of Azad Kashmir and its correlation with Standard type Areas of Pakistan. *Kashmir Jour. Geol.* **1/1**, . 19-29.

Auden, J.B. 1974. Afghanistan-West Pakistan, in A.M. Spencer, ed., Mesozoic-Cenozoic Belt, Data for Orogenic Studies: *Geological Society London Special Publication*, **4**, p.235-253.

Baig, M. S. and Lawrence, R. D., 1987. Precambrian to Early Paleozoic Orogenesis in the Himalaya. Kashmir. *Jour. Geol.* No. **5**, . 1-21.

Baig, M.S. 1999. Geochronology of Pre-Himalayan and Himalayan Tectonic Events, Northwest Himalaya Pakistan: *Kashmir J. Geol.*, **8 & 9**, p. 196-197.

Baloch, I., H., Ahsan, N., Ghazanfar, M., Chaydhry, M. N. and Khan, Z. K., 2002. Geology and deformation in lesser Himalayan sedimentaries, Bagnotar-Bara Gali section, District Abbottabad, NW Lesser Himalaya, Pakistan. *Geol. Bull. P. U.* **37**, . 27-34.

Bard, J.P., Maluski, H., Matte, P.H. and Proust, F. , 1980. The Kohistan sequence, Crust and mantle of an obducted Island arc. Special *Issue, Geol. Bull. Univ. Peshawar*, **13**: p.87-93.

Baski, A. K., Barman, T. R., Paul, D. K. and Farrar, E., 1987. Widespread Early Cretaceous flood basalt volcanism in eastern India: Geochemical data from the Bengal-Rajmahal-Sylhet Traps: *Chemical Geology*, **63**, p. 133-141.

Bernoulli, D. and Jenkyns, H., 1974. Alpine, Mediterranean, and Central Atlantic Mesozoic facies in relation to the early evolution of the Tethys. *In*: Modern and Ancient Geosynclinal evolution. R.H. Dott and R. H. Shaver, eds., SEPM Special Publication, **19**, . 129-160.

Bosellini, A., 1989. Dynamics of the Tethyan carbonate platforms, *In* P.D. Crevello, J. L. Wilson, J. Frederick Sarg, and Read, J.F. eds., Controls on Carbonate Platform and Basin Development: S.E.P.M. Special Publication, **44**, p. 3-13.

Bossart, P., Chaudhry, M. N., Dietrich, D., Ghazanfar, M., Greco, A., Meir, A., Ottiger, R., Papritz, K., Ramsay, J.G., Rey, R., Spencer, D. and Wahrenberger, C.H., 1992. A review of the geology of the Northern Indian Plate, Kaghan Valley, NE Pakistan. *In*: 7th Himalaya-Karakoram-Tibet Workshop, Abstracts, Oxford, England, .6.

Brown, G., and G.W. Brindley, 1980. X-ray diffraction procedures for clay mineral identification, In G.W. Brindley and G. Brown eds., Crystal Structures of Clay Minerals and their X-ray Identification: *Mineralogical Society Monograph* no. **5**, p. 305-360.

Burg, J.-P., Arbaret, L., Chaudhry, N. M., Dawood, H., Hussain, S. S, and Zeilinger, G., 2005b. Shear strain localization from the uer mantle to the middle crust of the Kohistan Arc Pakistan. *In*: High-Strain Zones: Structure and Physical Properties. Geological Society Special Publication, **245**, . 25-38.

Burg, J.-P., Bodinier, J.-L., Chaudhry, M.N., Hussain, S. and Dawood, H. 1998. Infra-arc mantle-crust transition and intra-arc mantle diapirs in the Kohistan Complex Pakistani Himalaya: petro-structural evidence. *Terra Nova*, **10 :2**, . 74-80.

Burg, J.-P., Chaudhry, M. N., Ghazanfar, M., Anczkiewicz, R., and Spencer, D., 1996. Structural evidence for back sliding of Kohistan arc in the collisional system of north west Pakistan. ***Geology*, 24:8**, . 739-742.

Burg, J.P., Davy, P., Nievergelt, P., Oberli, F., Seward, D., Diao, Z., and Meier, M., 1997. Exhumation during crustal folding in the Namche Barwa syntaxis. *Terra Nova*, **9**, . 117-123.

Burg, J.-P., Jagoutz, O., Dawood, H., and Hussain, S. S., 2006. Precollision tilt of crustal blocks in rifted island arcs: Structural evidence from the Kohistan Arc. *Tectonics*, 25.

Burg, J.-P., Leyreloup, A., Girardeau, J. and Chen, G. M., 1978. Structure and metamorphism of tectonically thickened continental crust, Yalu Tsangpo Suture Zone Tibet. Phil. Trans., *R. Soc. Lond.*, **A-321**, . 67-87.

Burg, J-P., Bodinier, J.-L., Chaudhry, M.N., Hussain, S. and Dawood, H. 2005a. Infra-arc mantle-crust transition and intra-arc mantle diapirs in the Kohistan Complex Pakistani Himalaya: petro-structural evidence. *Terra Nova*, 10 2, . 74-80.

Burlini, L., Arbaret, L., Zeilinger, G., and Burg, J.-P., 2005. High-temperature and pressure seismic properties of a lower crustal prograde shear zone from the Kohistan Arc, Pakistan. In: High-Strain Zones: Structure and physical properties. *Geological Society Special Publication*, **245**, p. 187-202.

Butt, A.A., 1986. Cretaceous Biostratigraphic Synthesis of Pakistan. *Acta Mineralogical Pakistanica*, **2**:p.60-64.

Butt, A.A., 1987. The Ranikothalia sindensis zone in late Palaeocene biostratigraphy. *Acta Mineralogical Pakistanica*, **3**: p.111-115.

Butt, A.A., 1988. Some Geological aspects of the Hazara Arc Northern Pakistan. *Acta Mineralogica Pakistanic*, **4**: p.146-150.

Butt, A.A., 1989. An overview of the Hazara Arc Stratigraphy. *Geol. Bull. Punjab University*, **24**: p.1-11.

Calkins, J.A., Offield, T.W. and Abdullah, S.K.M., 1975. Geology of the Southern Himalayas in Hazara, Pakistan and adjacent areas. *Geological Investigation in Pakistan*.p.124

Caroll, D., 1970. X-ray identification of clay minerals: *U.S. Geological Society, Special paper* **126**, p. 1-67.

Chaudhry, M.N. and Ghazanfar, M., 1987. Geology, Structure and Geomorphology of Uer Kaghan Valley Northewst Himalaya, Pakistan. *Geol. Bull. Punjab University*, **22**, . 13-57.

Chaudhry, M.N. and N. Ahsan, 1999a. Reservoir Potential of Datta Formation, Hazara Basin, *Pakistan. Jour. Hydrocarbon Res*. **11**, . 15-28.

Chaudhry, M.N., A. Manzoor, N. Ahsan, and M. Ghazanfar, 1996a. Sedimentology of Datta Formation from Kalapani, District Abbottabad. *Geol. Bull. P.U.*, No. **29**, . 11-28.

Chaudhry, M.N., Ahsan, N., and Ghazanfar, M., 1998a. A Preliminary Account of Sedimentology of Hazara Basin from Jurassic to Eocene: Abstract volume 13th Himalaya – Karakorum-Tibet Workshop, Peshawar, 41-43.

Chaudhry, M.N., and Ashraf, M., 1978. Preliminary Mineral Survey in Kotli and Poonch Districts of Azad Kashmir Vol. I – Kotli, Engineers Combine Limited, Lahore. 1-249.

Chaudhry, M.N., Ashraf, M. and Hussain, S.S, 1983b. Lead Zine Mineralisation of lower Kohistan District, Hazara Division, N.W.F.P., Pakistan, Kashmir Jour. Geol., 1, 31-42.

Chaudhry, M.N., Ashraf, M. and Hussain, S.S., 1980. Preliminary study of nickel mineralization in Swat District, N.W.F.P., *Congr. Geol. Pakistan*, **1**, 9-26.

Chaudhry, M.N., Ashraf, M., and Hussain S.S., 1976. Geology and Petrolgoy of Malakand and a part of Dir. *Geol. Bull. Punjab Univ*., **1**, 17-40.

Chaudhry, M.N., Chaudhry, A.G. and Aftab, M., 1974b. The ortho-amphibolites and the paraamphibolites of Dir District, N.W.F.P., *Geol. Bull. Punjab University*, **11**, 80-86.

Chaudhry, M.N., Ghazanfar, M. and Ashraf, M., 1983. A Plate tectonic Model for Northwest Himalaya, *Kashmir Jour. Geol*., **1**, 109-112.

Chaudhry, M.N., Ghazanfar, M. and Ashraf, M., 1983a. A Plate tectonic Model for Northwest Himalaya, *Kashmir Jour. Geol.*, **1**, 109-112.

Chaudhry, M.N., Ghazanfar, M. and Walsh, J.N., 1993a. The Panjal Sea, Kashmir Hazara Microcontinent and Hercynide Geology of Northwest Himalaya, Pakistan: *Pakistan Jour. Geol.* **5**, 10-25.

Chaudhry, M.N., Ghazanfar, M., Ahsan, N., 1994b. Rates of Sedimentation of Kawagarh Formation at Giah and Timing of Uplift at K-T boundary. *Pakistan Jour. Geol.*, V. **2 & 3**, No.**1**, 29-32.

Chaudhry, M.N., Ghazanfar, M., Ashraf, M. and Hussain, S.S., 1984. Geology of the Shewa-Dir-Yasin Area and its Plate Tectonic Interpretation. *Kashmir Jour. Geol.*, **21**, 53-64.

Chaudhry, M.N., Hussain, S.S. and Dawood, H., 1993b. The Lithostratigraphic Framework of Northwest Himalaya, south of the Main Mantle Thrust, along Mingora-Daggar Section, Swat, Pakistan. *Pakistan Jour. Geol.*, **1**, 23-43.

Chaudhry, M.N., Hussain, S.S. and Dawood, H., 1993c. Position of Main Central Thrust and subdivision of Himalaya in Swat. *Pakistan Jour. Geol.*, **1**, 10-18

Chaudhry, M.N., Jafferi, A.A. and Saleemi, B.A, 1974c. Geology and petrology of malakand granite and its environs, *Geol. Bull. Punjab University*, **10**, . 43-58.

Chaudhry, M.N., M. Ghazanfar, I.H. Baloch, M. Adil, N. Ahsan and F.A. Chuhan. 1995. Sedimentology, Depositional Environment and Economic Potential of Datta Formation of Early Jurassic Age of Attock Hazara Fold and Thrust Belt. *Jour. Nepal Geol. Soc*., **12**, 25.

Chaudhry, M.N., M. Ghazanfar, N. Ahsan, 1994b. Rates of Sedimentation of Kawagarh Formation at Giah and Timing of Uplift at K-T boundary. *Pak. Jour. Geol.*, . **2 & 3**, No.1,29-32.

Chaudhry, M.N., M. Ghazanfar, N. Ahsan, and K.R. Masood, 1998c. Age, Stratigraphic Position and Provenance of Murree Formation of North West Sub-Himalayas of Pakistan and Azad Kashmir. In Third Geosas Workshop on Siwalik GSP, Islamabad. *Bull. Geol. Surv. Pak.*,81-91.

Chaudhry, M.N., M.A. Iqbal and N. Ahsan, 1994a. Petrology of Lumshiwal Formation from Gulagah Nala near Chinali Bridge, Abbottabad-Nathiagali Road, Hazara, Pakistan. *Pak.Jour. Hydrocarbon, Res.* **6, No.1 & 2**, . 41-52.

Chaudhry, M.N., Mahmood, A. and Shafiq, M., 1974a. Geology of Shahidabad-Bibior area, Dir District, N.W.F.P. *Geol. Bull. Punjab Univ.*, **10**, 78-89.

Chaudhry, M.N., Mahmood, T. Ahmed, R. and Ghazanfar M., 1992a. A Reconnaissance Microfacies Study of Kawagarh Formation Near Giah, Abbottabad-Nathagali Road, Hazara, *Pakistan. Jour. Hyd. Res.* **4/2**, 19-32.

Chaudhry, M.N., N. Ahsan, 1999b. Sedimentological constraints on India-Asia Collision. In: *Terra Nostra, 14th Himalaya-Karakoram-Tibet Workshop*, Germany, 22-23 sep, 1999.

Chaudhry, M.N., N. Ahsan, K.R. Masood., I.H. Baloch, A.D. Spencer, 1997. Facies, Microfacies, Palaeontology, Depositional Environment and Economic Potential of Datta Formation of Early Jurassic Age from Attock Hazara Fold and Thrust Belt, Lesser Himalayas and a part of Salt Range, Pakistan. *Abstract Volume, 12th Himalaya – Karakorum-Tibet Workshop*, Roma, Itlay, **16-18**, April 1997.

Chaudhry, M.N., N. Ahsan, N. Ahmed and F. Ahmed, 2000. Petrology of Lumshiwal Formation, Karlan Bazar, Nathiagali – Abbottabad Road, Hazara Basin, Pakistan. *Pak. Jour. Geol.* **12 & 13, No. 1 & 2**,1-12.

Chaudhry, M.N., N. Ahsan, N. Ahmed and K.R. Masood, 1998b. Lithofacies, Microfacies, Diagenesis and Environment of deposition of Lumshiwal Formation at Kundla, Hazara Basin, Pakistan. *Pak. Jour. Geol.* **8 & 9, No. 1 & 2**, . 29-39.

Chaudhry, M.N., N. Ahsan, T. Mahmood and K.R. Masood, 2001. Sedimentology of Margala Hill Limestone Neelum Valley Azad Kashmir, Northwest Himalayas. In: *4th Pakistan Geological Congress. Pakistan Museum of Natural History, Islamabad.*

Chaudhry, M.N., R.A. Chaudhry, N. Ahsan, and M. Ghazanfar, 1996b. Microfacies, Diagenesis, and Environment of Deposition of Lumshiwal Formation from Thub Top Ayubia. Abbottabad. *Pak. Jour. Hydrocarbon Res.*, **9**, . 57-66.

Chauhan, F.A., Chaudhry, M.N., and Ghazanfar, M., 1992. Microfacies, diagenesis and environment of deposition of Datta Formation from Jaster Gali, Abbottabad, Hazara, Pakistan, *Geol. Bull. Punjab University*, **27**, 47 – 62.

Condie, K.C., 1989. Plate tectonics and crustal evolution. Pergamon Press inc. New York, . 1- 476.

Coward, M.P., Butler, R.W.H., Chambers, A.F., Graham, R.H., Izatt, C.N., Khan, M.A., Knipe, R.J., Prior, D.J., Treloar, P.J. and Williams, M.P., 1988. Folding and imbrications of the Indian Crust during the Himalayan collision, Phil. Trans. *Royal Soc., London*, **A326**, 89-116.

Danilchik, W. and Shah, S.M.I. 1987. Stratigraphy and coal resources of the Makarwal area, Trans-Indus Mounains, Mianwali District, Pakistan: *U.S. Geol. Surv. Professional Paper*, **1341**, 1-38.

Demaison, G.J. and Moore, G.T. 1980 Anoxic Environments and Oil Source Bed Genesis. *Am. Assoc. Pet. Geol. Bull.*, **64**, 1179-1209.

Desio, A., 1963. I raorti tettonici fra il Badakhshan ed il Pamir Asian Centrale, Giorn. *Geol. Ann. Mus. Geol. Bologna*, Ser. **2a, 31**: 163-170.

Desio, A., 1964. On the geology of central Badakhshan northeast Afghanistan: *Qurat. Jour. geol. Soc. Lond.*, **120,** . 127-151.

Desio, A., 1979. Geological evoluction of Karakoram. In: Farah, A. and De Jong, K.A. EDS, Geodynamics of Pakistan. *Geol. Surv. Pakistan, Quetta*, . 111-124.

Dewey, J.F., R.M., Shackleton, Change Chenfa, and Sun Yiyin, 1988. The tectonic evolution of the Tibetan plateau: *Philosophical Transactions of the Royal Society of London, Series A*, v. **327**, 379-413.

Dickinson, W.R. 1977, Tectono-stratigraphic evolution of subduction-controlled sedimentary assemblages, in Talwani, M., and Pittman, W. C., III, eds., Island Arcs, Deep Sea Trenches, and Back Arc Basins: Washington, D.C., *American Geophysical Union Maurice Ewing Series*, **1**, 33-40.

Dolan, P., 1990. Pakistan: a history of petroleum exploration and future potential, in J. Brooks ed., Classic Petroleum Provinces: *Geological Society Special Publication,* **50,** 503-524.

Fatimi, A.N., 1968. Lithostratigraphic units of the Kohat- Potwar Province, Indus Basin, Pakistan. *Pak. Geol. Surv., Mem* **10**, 80.

Fatmi, A.N., 1973. Lithostratigraphic units of Kohat Potwar Privince, Indus Basin. *Mem. Geol. Surv. Pakistan.* **10**, 1-80.

Fletcher, C.J.N., Leake, R.C. and Haslam, H.W., 1986. Tectonic setting, mineralogy, and chemistry of a metamorphosed stratiform base metal deposit within the Himalayas of Pakistan: *J. Geol. Soc., London,* **143**, . 521-236.

Frederiksen, N.O., 1992. Palynology of Mesozoic and lower Tertiary samples from northern, central, and southern Pakistan: *U.S. Geol. Surv. Open-File Report* **92-215**, 1-11.

Gaetani, M., Casnedi, R., Fois, E., Garzanti, E., Jadoul, F., Nicora, A. and Tintori, A. 1986. Stratigraphy of the Tethys Himalaya in Zanskar, Ladakh. *Riv. It. Paleont. Strat.,* **91: 4**, . 443-478.

Gardezi, A.H. and Ghazanfar, M., 1965. A change of facies at the base of the Jurassic in Distt. Hazara, West Pakistan, *Geol. Bull.P.U.* **5**, 53-56.

Garrido, C.J., Bodinier, J.L., Burg, J.P., Zeilinger, G., Hussain, S. S., Dawood, H., Chaudhry, N.M., Gervilla, F., 2006. Petrogenesis of Mafic Garnet Granulite in the Lower Crust of the Kohistan Paleo-arc Complex Northern Pakistan. Implications for Intra-crustal Differentiation of Island Arcs and Generation of Continental Crust. *Jour. Pet.* **4710**,1873-1914.

Garzanti, E. 1992. Stratigraphy of the Early Cretaceous Giumal Group Zanskar Range, Northern India. Riv. *It. Paleont. Strat.,* **97, 3-4**, . 485-510.

Garzanti, E., 1993. Sedimentary evolution and drowning of a passive margin shelf Giumal Group; Zanskar Tethys Himalaya, India: palaeoenvironmental changes during final break-up of Gondwanaland, in P.J. Treloar and M.P. Searle, eds., Himalayan Tectonics: *Geological Society Special Publication*, **74**, 277-298.

Ghazanfar, M. 1993. Petrotectonic Elements and Tectonic Framework of Northewest Himalaya. Ph.D thesis, University of the Punjab,1 & 2, . 1-380.

Ghazanfar, M. and Chaudhry, M.N., Perviz, K. and Quyyum, M.,1990. Geology and structure of a section of Attock Hazara Fold and Thrust and Thrust Belt, around Ayubia, District Abbottabad, Pakistan.

Ghazanfar, M., Chaudhry, M.N. and Hussain, M.S., 1991. Geology and petrotectonics of South East Kohistan, N.W. Himalayas Pakistan. *Kashmir Jour. Geol.*, **8 & 9**, 67-97.

Ghazanfar, M., Chaudhry, M.N., Latif, M.A., 1987. Three stratigraphic provinces at Hazara-Kashmir Boundary, Pakistan: *Kashmir Jour. Geol.,* **5**, 65-74.

Heuberger, S., Schaltegger, U., Burg, J-P., Villa, I.M., Frank, M., Dawood, H., Hussain, S.S., and Zanchi, A. 2007. Age and isotopic constraints on magmatism along the Karakoram-Kohistan Suture Zone, NW Pakistan: Evidence for subduction and continued convergence after India-Asia collision. *Swiss Journal of Geoscience,* **1001**, 85-108.

Iqbal, M.W.A., and Shah, S.M. I., 1980. A guide to the stratigraphy of Pakistan. *Geol. Surv. Pak. Quetta,* **53**1 – 34.

Jadoul, F., E. Garzanti, and E. Fois, 1989. Uer Triassic-Lower Jurassic stratigraphy and palaeogeographic evolution of the Zanskar Tethys Himalayas Zangla Unit: Riv. *It. Paleont. Strat.*, **95**, 351-396.

Jaeger, J-J., Courtillot, V., and Taonnier, P., 1989. Paleontological view of the ages of the Deccan Traps, the Cretaceous/Tertiary boundary, and the India-Asia collision. *Geology,* **17**, 316-319.

Jaeger, J-J., Courtillot, V., and Taonnier, P., 1989. Paleontological view of the ages of the Deccan Traps, the Cretaceous/Tertiary boundary, and the India-Asia collision. *Geology*, **17**, 316-319.

Valdiya, K. S., 2002. Emergence and evolution of Himalaya: reconstructing history in the light of recent studies. *SAGE Publications. Progress in Physical Geography*, **26**, No. **3**, 360-399.

Kadri, I.B. 1995. Petroleum Geology of Pakistan. Pakistan Petroleum Limited, Karachi. 275.

Katz, M. B. 1979. India and Madagascar in Gondwanaland based on matching Precambrian Lineaments: *Nature*, **279**, 312-315.

Kazmi, A.H. and Jan, M.Q., 1997, Geology and Tectonics of Pakistan. Graphic Publishers, Karachi, 54.

Kazmi, A.H. and M.Q. Jan, 1997. Geology and Tectonics of Pakistan. Graphic publishers Pakistan, 554.

Kemal, A., Balkwell, H. R., Stoakes, F.A. 1992. Indus Basin hydrocarbon plays, in Ahmad, G. Kemal, A. Zaman, A.S.H. and Humayun, M. eds. New Directions and Strategies for Accelerating Petroleum Exploration and Production in Pakistan: Proceedings International Petroleum Seminar Nov. 22-24, 1991, Ministry of Petroleum and Natural Resources, Government of Pakistan, 78-105.

Klootwijk, C., Sharma, M.L. Gergan, J., Tirkey, B., Shah, S. K. and Agarwal, V., 1979. The extent of Greater India, II. Palaeomagnetic data from the Ladakh intrusives at Kargil, Northwestern Himalayas. – *Earth and Planetary Science Letters, Amsterdam Elsevier*. **44**, 47-64.

Klootwijk, C.T. Conaghan, P. J. and Powell, C.Mc. A. 1985. The Himalayan arc: large scale continental subduction, oroclinal bending and back-arc spreading. – *Earth and Planetary Science letters, Amsterdam Elsevier*, **75**, .167-183.

Krumbein, W. C., and Sloss, L. L., 1963. Stratigraphy and Sedimentation: San Francisco, Freeman, 660.

Latif, M.A. 1970a. Explanatory Notes on the Geology of Southern Hazara, to accompany the revised Geological Map. *Wein Jb. Geol. BA; Sonderb*. **15**, 5-20.

Latif, M.A. 1970b. Micropalaeontology of the Chanali Limestone, Upper Cretaceous of Hazara West Pakistan. *Jb. Geol. B.A. Sonderband*, **15**, 25-61.

Latif, M. A. 1976. Stratigraphy of Micropalaeontology of the Galis Group of Hazara, Pakistan. *Geol. Bull. P.U.*, **13**, 1-64.

Latif, M.A., 1980. Overstep of Thandiani Group over older rock sequences in Hazara, *Geol. Bull. P.U.***20**,b11-32

Latif, M.A., Yasin, A.R., Shafique, N.A. and Ashraf, M. 1995. Late Mesozoic Sedimentary Megacycle in the Rifted Haro Trough, Hazara, Pakistan and its Hydrocarbon Impliations in the Northern Rim of the North West Himalayan Basin. *Jour. Hydrocarbon Research*, **7: 1**., 31-52.

Lillie, R.J., Johnson, G.D., Yousaf, M., Zamin, A.S.H. and Yeats, R.S., 1987. Structural development within the Himalayan Foreland fold and thrust belt of Pakistan. *In*: Beaumont, C. and Tankard, A.J. Eds, Sedimentary Basins and Basin-Forming Mechanism. Canadian Soc. *Petrol. Geol. Mem*., **12**, 379-392.

Llana-Fúnez, S., Burg, J-P., Hussain S. S., Dawood, H., and Chaudhry, M. N., 2006. Structural evolution of the footwall of the Indus Suture in Malakand N Pakistan during the Himalayan collision. *Journal of Asian Earth Sciences*, **27 :5**, 691-706.

Mahoney, J.J., MacDougall, J.D. Lugmair, G.W. 1983. Kerguelen hotspot source for Rajmahal Traps and Ninetyeast Ridge? *Nature*, **303**, 385-389.

Manzoor, A., Chaudhry, M.N., Ahsan, N. and Ghazanfar,M., 1996. Microfacies, Diagenesis and Environment of Deposition of Datta Formation, Near Batangi, Distt. Abbottabad. *Geol., Bull., Punjab Univ.*, **29**, . 11-28.

Marks, P., and Ali, C. M., 1961. The geology of Abbottabad area, with special reference to infra-Trias. Ibid., 1, . 47-55.

Mattauer, M., 1986a. Sur le mecanisme de formationde la schistosite dans l Himalaya, *Earth Planet. Sci. Lett.*, **28**, . 144-154.

Mattauer, M., 1986b. Intracontinental subduction, crust mantle decollement and crustal stacking wedge in the Himalayas and other collisional belts. *In*: Collision Tectonics. Coward, M. P. and Ries, A., eds. *Geol. Soc. London, Spec. Pub.* **19**, . 39-52.

Mattauer, M., Proust, F., and Taonnier, P., 1977. Some new data on India Eurasis convergence in the Pakistani Himalayas. Colloq. Inter'l. CNRS., Paris, 268, 209-220.

Mattauer, M., Proust, F., Taonnier, P., and Cassigneau, C., 1978. Ophiolites, obduction et technique globale dans Test de l' Afghanistan. CRAS, Paris, 278, . 983-985. Farah, A., and DeJong, K., A., Eds, 1979. Geodynamica of Pakistan, Geol. Surv. Pak. Quetta, . 1 – 361.

Middlemiss, C. S., 1896. The geology of Hazara and Mlack Mountains. India. *Geol. Surv., Mem.*, **26**, 1-302.

Norton, I.O. and J.G. Sclater, 1979. A model for the evolution of the Indian Ocean and the break up of Gondwanaland: *Journal of Geophysical Research*,**84**, 6803-6830.

Patriat, P. and Achache, J., 1984. India-Eurasia collision chronology and its implications for crustal shortening and driving mechanisms of plates. *Nature*, **311**: 615-621.

Pettijohn, F. J., 1957, Sedimentary Rocks [2nd ed.]: New York, John Wiley & Sons. 718.

Powell, C. McA., 1979. A speculative tectonic history of Pakistan and surroundings: Some constraints from the Indian Ocean. In: Farah, A. & DeJong, K.A. eds. *Geodynamics of Pakistan. Geol. Surv. Pak., Quetta*, . 5-24.

Reading, H.G. 1996. Sedimentary Environments: Processes, Facies and Stratigraphy. Blackwell Scientific Publications. 688.

Sastri, V.V., Venkatachala, B.S. and Narayanan, V. 1981. The evolution of the east coast of India: *Paleogeography, Paleoclimatology, Paleocology*, **36**, 23-54.

Chaudhry, M.N., Chuhan, F.A. and Ghazanfar, M., 1994c. Microfacies, Diagenesis, Environment of Deposition and burial history of Datta Formation from Bara Oter, Distt. Abbottabad. *Kashmir Jour. Geol.*, **11 & 12**, 43-58.

Sastri, V.V., Venkatachala, B.S. and Narayanan, V. 1981. The evolution of the east coast of India: *Paleogeography, Paleoclimatology, Paleocology*, **36**, 23-54.

Scotese, C.R. Gahagan, L.M. and Larson, R.L., 1988. Plate tectonic reconstructions of the Cretaceous and Cenozoic ocean basins. *Tectonophysics*, **155**, 27-48.

Searle, M.P., 1991. Geology and Tectonics of the Karamoram Mountains. Jhon Wiley and Sons. Sedimentol. Spec. Publ., 1, Blackwell, Oxford, 249-271.

Searle, M.P., Windley, B.F., Coward, M.P., Cooper, D.J.W., Rex, A.J., Rex, D., Tingdong, Li., Xudhang, X., Jan, M.Q., Thakur, C.C. and Kamar, S., 1987. The closing of Tethys and the tectonics of the Himalaya. *Geol. Soc. Amer. Bull.*, **98**: 678-701.

Sengor, A.M.C., Altiner, D., Cin, A., Ustaomer, T. & Hsu, K.J., 1988. Origin and assembly of the Tethyside orogenic collage at the expense of Gondwanaland. In: Audley-Charles, M.G. & Hallam, A. eds. Gondwana and Tethys. *Geol. Soc. Lond.*, Spec. Publ. **37**: 81-119.

Shah, S.M.I., 1977, Stratigraphy of Pakistan: Geol. Surv. Pakistan, Quetta, *Mem. Geol. Surv.* **12**,138.

Sokolove, B.A. and Shah, S.H.A, 1966. Major tectonic features of Pakistan, Part-I, Western Provience. *Jour. Sci. Ind. Res.*, **4**,175-199.

Spencer, D.A. 1993. Tectonics of the higher and Tethyan Himalaya, Uer Kaghan Valley, NW Himalaya, Pakistan: Implications of an early collisional, high pressure eclogite facies metamorphism to the Himalayan belt. Doctoral dessert. ETH, Zurich.

Spencer, D.A. 1994. Continental collision in the northwest Himalayan Tethyan region. In: Ahmed, R. and Sheikh, A. M. eds. Geology in South Asia-1. Proc. *Ist South Asia Geol. Cong. Hydrocarbon. Dev. Inst. Pak. Islamabad*, 185-202.

Tahirkheli, R.A.K., 1979. Geology of Kohistan and adjoining Eurasian and Indo-Pakistan continents, Pakistan. *Geol. Bull. Univ., Peshawar*, **11**, . 1-30.

Tahirkheli, R.A.K., 1982. Geology of the Himalaya, Karakoram and Hindukush in Pakistan. *Geol. Bull. Univ. Peshawar*, Spec. Issue,1-21.

Taonnier, P., Peltzer, G., Armijo, R., 1986. On the mechanics of the collision between Asia and India. *In*: Coward M.P. & Ries A.C. Eds., Collision tectonics. *Geological Society, London*, Special Publications, **19**,115-157.

Treloar, P.J., Broughton, R.D., Williams, M.P., Coward, M.P., Coward, M.P. and Windley, B.F., 1989a. Deformation, metamorphism and imbricatin of the Indian Plate, south of the Main Mantle Thrust, north Pakistan. *Jour. Met. Geol.*, 7,111-125.

Treloar, P.J., G.J. Potts, J. Wheeler, and D.C. Rex, 1991. Structural evolution and asymmetric uplift of the Nanga Parbat syntaxis, Pakistan. *Himalaya. Geol. Rund.*, **80** 411-428.

Treloar, P.J., Rex, D.C., Guise, P.G., Coward, M.P., Searle, M.P., Windley, B.F., Petterson, M.G., Jan, M.Q., and Luff, I.W., 1989b. K-Ar and Ar-Ar geochronology of the Himalayan collision in NW Pakistan: constraints on the timing of suturing, deformation, metamorphism, and uplift. *Tectonics*, **8**, 881-909.

Tucker, M.E. 1988. Techniques in Sedimentology, Blackwells, Oxford. 394.

Tucker, M.E., and Wright, V.P., 1990, Carbonate Sedimentology. Blackwell Scientific Publications, Oxford, London, 482 p.

Van der Voo, R., Spakman, W., Bijwaard, H., 1999. Tethyan subducted slabs under India. *Earth and Planetary Science Letters* ,**171**,7–20.

Velde, B., 1985. Clay minerals-A physio-chemical explanation of their occurrence, *In: Developments in Sedimentology*, **40**, 427p.

Waagen, W. and A.B. Wynne, 1872. The geology of Mount Sirban in uer Punjab: *Memoirs of the Geological Survey of India*, **9**,331-350.

Waagen, W., 1872. Rough section showing the relation of the rocks near Mari Muree Punjab: *Mem. Geol. Surv. India*, **5**, Part I.

Wadia, D.N., 1931. The syntaxis of the North-west Himalaya, its rocks, tectonics, and orogeny. *India Geol. Surv. Recs.*, **65**, Pt. **2**, . 189-220.

Wadia, D.N., 1931. The syntaxis of the North-west Himalaya, its rocks, tectonics, and orogeny. *India Geol. Surv. Recs.*, **65/2**,189-220.

Warwick, P.D., Javed, S. Tahir, S. Mashhadi, A. Shakoor, T. Khan, A.M. and Khan, A.L., 1995. Lithofacies and Palynosratigraphy of Some Cretaceous and Paleocene Rocks, Surghar and Salt Range Coal Fields, Northern Pakistan. *U.S. Geol. Surv. Bull.* Special Paper **2096**. 1-34.

Williams, V.S., Sheikh, I., Pasha, M.K., Khan, K.S.A. and Reza, Q. 1994. Preliminary Report on the Environmental Geology of the Islamabad-Rawalpindi Area, Pakistan. In: Geology in South Asia-I, Proceedings of the First South Asia Geological Congress Islamabad, Pakistan: February 23-27, 1992. Eds., Ahmed, R. and Sheikh, A.M., 358-377.

Zeilinger, G., Burg, J. P., Chaudhry, N., Dawood, H. & Hussain, S. 2000. Fault systems and paleo-stress tensors in the Indus suture zone NW Pakistan. *Journal of Asian Earth Sciences*, **185**, 547-559.

Geol. Bull. Punjab Univ. 43, 2008.

TEACHING STAFF LIST OF
THE INSTITUTE OF GEOLOGY, UNIVERSITY OF THE PUNJAB
2008

No.	Name and Qualifications	Designation	Field of Specialization
1	**Dr. Nasir Ahmed** M.Sc. (Pb), Ph.D (Leeds)	Professor (Director)	Environmental Science
2.	**Dr. Akhtar Ali Saleemi** M.Sc. (Pb), M.Sc. (Leicester), Ph.D. (Leicester)	Professor	Mineralogy, Petrology, Industrial Mineralogy
3.	**Dr. Riaz Ahmad Sheikh** B.Sc. (Hons), M.Sc. (Pb), D.I.C., Ph.D (Imperial College)	Professor	Structure & Petroleum Geology, Sedimentology, Regional Tectonics
4.	**Dr. Muhammad Saeed Farooq** M.Sc. (Pb), Ph.D. (Pb)	Professor	Engineering Geology, Geohydrology
5.	**Mr. Umar Farooq** M.Sc. (Pb), M.Sc., D.I.C. (Imperial College), GTC (Japan)	Associate Professor	Exploration Geophysics
6.	**Mr. Zahid Karim Khan** M.Sc. (Pb) PGD (Delft)	Associate Professor	Engineering Geology, Geohydrology, Aggregate Materials
7.	**Dr. Nazir Ahmad** M.Sc. (Pb), Ph.D. (Leicester)	Associate Professor	Structural & Petroleum Geology, Mapping, Sedimentology, Regional Tectonics
8.	**Dr. Syed Alim Ahmad** M.Sc. (Pb), Ph.D (Pb)	Associate Professor	Mineralogy, Petrology
9.	**Dr. Shahid Jameel Sameeni** M.Sc. (Pb), Ph.D. (Pb.), COMETT- EUCOR Micropal (Basel)., Post-Doc (Berkley)	Associate Professor	Biostratigraphy, Micropaleontology, Paleobiology, Paleoecology
10	**Dr. Muhammad Ashraf Siddiqui** M.Sc. (Pb), PGD (Leicester) UK, Ph.D (Pb)	Assistant Professor	Mineralogy, Petrology, Industrial Mineralogy
11	**Mr. Sajid Rashid** M.Sc. (Pb)	Assistant Professor (on leave)	Engineering Geology, Geohydrology
12.	**Syed Mahmood Ali Shah** M.Sc. (Pb)	Assistant Professor	Mineralogy, Petrology

13.	**Dr. Naveed Ahsan** M.Sc. (Pb), Ph.D. (Pb)	Assistant Professor	Structural & Petroleum Geology, Tectonics
14.	**Mr. Shahid Ghazi** M.Sc. (Pb)	Assistant Professor (on leave)	Petroleum Exploration Sedimentology & Sequence Stratigraphy
15.	**Mr. Mustansar Naeem** M.Sc. (Pb)	Assistant Professor	Engineering Geology
16.	**Mr. Abdus Sattar** M.Sc. (Pb)	Assistant Professor	Geochemistry, Mineralogy
17.	**Dr. Abdur Rauf Nizami** M.Sc. (Pb), Ph.D. (Pb)	Assistant Professor	Petroleum Geology, Remote Sensing, Sedimentology
18.	**Mr. Zia ud Din** M.Sc. (Pb)	Assistant Professor	Geophysics
19.	**Mr. Kamran Mirza** M.Sc. (Pb)	Assistant Professor	Micropaleontology, Stratigraphy, Sedimentology
20.	**Mr. Sohail Akram** M.Sc. (Pb)	Lecturer (on leave)	Engineering Geology, Geohydrology

25.	**Muhammad Rafi**	Lab. Attendant
26.	**Arshad Ali**	Attendant
27.	**Syed Sajid Hussain Shah**	Qulli
28.	**Muhammad Ramzan**	Naib Qasid
29.	**Shabbir Ali**	Naib Qasid
30.	**Muhammad Imran**	Naib Qasid
31.	**Asad Ahmad**	Lab. Attendant
32.	**Malik Muhammad Nasir**	Naib Qasid
33.	**Syed Asif Ali**	Machine Assistant
34.	**Muhammad Irfan**	Semi-Skilled worker
35.	**Sohail Iqbal**	Naib Qasid
36.	**Qudrat Ullah**	Lab. Attendant
37.	**Abdul Waqar**	Lab. Attendant
38.	**Javed Masih**	Lab. Attendant

NON TEACHING STAFF MEMBERS LIST OF THE INSTITUTE OF GEOLOGY, UNIVERSITY OF THE PUNJAB 2008

Sr. No.	Name of Employee	Designation
1.	Sharafat Ali Khan	Librarian
2.	Mr. Ghulam Nabi	Admin. Officer
3.	Basher ul Islam	Assistant Accounts
4.	Aurangzeb Bhatti	Store Supervisor
5.	Nadeem Younas	Private Secretary
6.	Sarfraz Ahmad	Office Assistant
7.	Khurshid Ali	Office Assistant
8.	Liaqat Ali	Junior Technician
9.	Sami Ullah Khan	Junior Technician
10.	Tasneem Ahmad Khan	Draftsman
11.	Muhammad Ilyas	Head Lab. Assistant
12.	Safdar Ali Bhatti	Sr. Clerk
13.	Liaqat Ali	Lab. Attendant
14.	Muhammad Farrukh Javed	Sr. Clerk
15.	Ali Akbar Sindhu	Sr. Clerk
16.	Muhammad Bashir	Junior Clerk
17.	Shaukat Ali	Junior Clerk
18.	Muhammad Jahanzeb	Driver
19.	Muhammad Riaz	Driver
20.	Hafiz Malik Muhammad Nazir	Lab. Attendant
21.	Haq Nawaz	Lab. Attendant
22.	Syed Qaim Ali Shah	Junior Clerk
23.	Ghulam Mustafa	Lab. Attendant
24.	Nazir Ahmad	Lab. Attendant